UNIVERSITY OF TROMSØ UIT

FACULTY OF HEALTH SCIENCES
DEPARTMENT OF CLINICAL MEDICINE

Targeted *MYCN* suppression and its effect on miRNA in neuroblastoma

Jørn Remi Henriksen

A dissertation for the degree of
Philosophiae Doctor

December 2010

Targeted *MYCN* suppression and its effect on miRNA in neuroblastoma

Jørn Remi Henriksen

A thesis submitted according to the requirements for the degree of Philosophiae Doctor

Paediatric Research Laboratory, Research group for Paediatrics,

Department of Clinical Medicine, Faculty of Health Sciences

University of Tromsø

Department of Paediatrics,

University Hospital of Northern Norway

December 2010

Acknowledgements

This work was conducted both at the Department of Paediatrics, University Hospital of Northern Norway, as well as at the Paediatric Research Laboratory / the neuroblastoma group, Department of Clinical Medicine, University of Tromsø. The financial support was from the Northern Norway Regional Health Authority (the Gene Therapy Program), The University of Tromsø, The Norwegian Cancer Society, Ragnvarda F. Sørvik and Håkon Starheims Foundation and the Erna and Olav Aakre Foundation for Cancer Research.

Team work is essential for the completion of a PhD, and many colleagues and friends deserve my gratitude for achieving this degree.

First I want to offer my thanks to my supervisors for guiding me through this process. To my main supervisor Trond: Thank you for believing in me and offering a never-ending amount of optimism and patience. Whenever I have needed something, you have offered it. To my supervisor Christer: Thank you for finding the intriguing projects that made this thesis possible. You have always been readily available for answering any questions I might have and offering any guidance I might need.

Thank you to my fellow PhD-students at the neuroblastoma group, Jochen and Bjørn Helge. Research has been much more efficient and fun when we have shared not only our experience and knowledge, but also when we have shared our frustrations over results that never seemed to emerge as desired as well as the uninhibited joy when they finally did. Without you I would probably be stuck in 2008-mode forever...

There are large amounts of experimental work behind this thesis. And much of it has been performed by present and former engineers and research assistants at our group. A great thank you goes to Cecilie, Ellen and Martin for offering not only your assistance, but also your pleasant company during countless lunches.

The co-authors not already mentioned have offered large and precious contributions to the papers presented in this thesis. My gratitude for this goes to Baldur Sveinbjörnsson, Tommy Martinsson, Pär Kogner, Dirk Geerts and Rogier Versteeg.

To Elizabeth, Hildegunn, Pauline and Merethe at the biofilm-group: Thank you for being such vital contributors to all shared social arrangements. To such bundles of joy as you I will gladly continue to offer my blood. I especially appreciate the patience shown by Elizabeth when awaiting my arrival at the office for several years, and for her unconditional support when writing this thesis.

At the MH-building there is a fine tradition for giving support, lending reagents and sharing expertise whenever anybody might ask. Thus there are numerous people that have offered small but important contributions during the years this thesis has been under its way. I am truly grateful to you all.

I also want to thank my family and friends for their support. You have all been essential for my well-being whenever I have felt the need to focus on other areas of life than my research.

Last but possibly most important I will express my gratefulness to Marte Beate. Thank you for offering your continuous and unrestricted support, affection and patience when I have been working on this thesis. I truly admire you for leaving and living alone in Spitsbergen for the last three years. And I especially respect your endurance when carrying out your entire pregnancy by yourself in exile without complaints. I am however ecstatic about your return, and the fact that we finally can start living together again.

Contents

1. LIST OF PAPERS 1

2. ABBREVIATIONS 2

3. INTRODUCTION 3

3.1. Small RNAs 3

3.1.1. The history of RNAi and miRNA – a summary 3

3.1.2. The miRNA pathway in animals 4

3.1.3. The natural functions of RNAi in animals 8

3.1.4. The natural functions of miRNA in animals 8

3.1.5. Targeted gene regulation using exogenous RNA 9

3.1.6. Efficiency of RNAi 12

3.1.7. Duration of RNAi-based gene suppression 13

3.1.8. Strategies for achieving stable shRNA expression 14

3.1.9. Conditional shRNA expression 16

3.1.10. Off-target effects 19

3.2. Neuroblastoma 22

3.2.1. Embryonal development and neoplasms 22

3.2.2. Development of the sympathetic nervous system 22

3.2.3. From neuroblasts to neuroblastic tumours 24

3.2.4. Neuroblastoma – the disease 25

3.2.5. Expression of MYCN in neuroblastoma 27

3.2.6. MYCN targets 28

3.2.7. Targeted MYCN downregulation 29

3.2.8. MiRNA in neuroblastoma 30

3.2.9. *DKK3* and neuroblastoma 31

4. AIMS 34

5. DISCUSSION 35

5.1. Papers I and II 35

5.1.1. Brief description of the studies 35

5.1.2. Discussion 35

5.2. Paper III 39

5.2.1. Brief description of the study 39
5.2.2. Discussion 39

5.3. Paper IV 41
5.3.1. Brief description of the study 41
5.3.2. Discussion 42

6. CONCLUSIONS 45

7. REFERENCES 46

1. List of papers

Paper I:

Comparison of RNAi efficiency mediated by tetracycline-responsive H1 and U6 promoter variants in mammalian cell lines

Henriksen JR, Løkke C, Hammerø M, Geerts D, Versteeg R, Flægstad T, Einvik C.

Nucleic Acids Research, 2007:35:e67

Paper II:

Conditional expression of retrovirally delivered anti-*MYCN* shRNA as an in vitro model system to study neuronal differentiation in *MYCN*-amplified neuroblastoma

Henriksen JR, Haug BH, Buechner J, Løkke C, Flægstad T, Einvik C.

Manuscript accepted pending minor revisions in *BMC Developmental Biology*

Paper III:

Inhibition of *mir-21*, which is up-regulated during *MYCN* knockdown-mediated differentiation, does not prevent differentiation of neuroblastoma cells

Buechner J, **Henriksen JR**, Haug BH, Tømte E, Flægstad T, Einvik C.

Differentiation 2010, In press. Doi:10.1016/j.diff.2010.09.184

Paper IV:

***MYCN*-regulated miRNAs inhibit secretion of the tumor suppressor *DICKKOPF-3* (*DKK3*) in neuroblastoma**

Haug BH, **Henriksen JR**, Buechner J, Kogner P, Martinsson T, Flægstad T, Sveinbjörnsson B, Einvik C.

Manuscript submitted.

2. Abbreviations

Ago	Argonaute
BMP	Bone morphogenetic protein
bp	Base pair
Cre	Cyclization recombination
DKK	Dickkopf
DNA	De-oxy ribonucleic acid
Dox	Doxycycline
dsRNA	Double stranded RNA
e.g.	*exempli gratia*
EFS	Event free survival
Endo-siRNA	Endogenous siRNA
Exp5	Exportin 5
FGF	Fibroblast growth factor
I	Intertmediate
i.e.	*id est*
INSS	International Neuroblastoma Staging System
Lef	lymphocyte enhancer factor
LOH	Loss of heterozygosity
Lox	Locus of X over P1
LRP	low-density lipoprotein receptor-related protein
miRNA	Micro RNA
MLV	Moloney Murine Leukemia Virus
MNA	MYCN Amplified
mRNA	Messenger RNA
MVD	Microvessel density
N	Neuroblastic
NGF	Neural growth factor
nt	nucleotide
P-body	Processing body
PNA	Peptide Nucleic Acid
Pre-miRNA	Precursor micro RNA
Pri-miRNA	Primary micro RNA
RIIID	RNase III domain
RISC	RNA-induced silencing complex
RNA	Ribonucleic acid
RNAi	RNA interference
S	Substrate adherent
shRNA	Short hairpin RNA
siRNA	Small interfering RNA
ssRNA	Single stranded RNA
TCF	T-cell factor
Tet	Tetracycline
TetO	Tetracycline Operator
TetR	Tetracycline Receptor
TLR	Toll-like receptor
UTR	Un-transcribed region

3. Introduction

3.1. Small RNAs

3.1.1. The history of RNAi and miRNA – a summary

In 1958, Crick presented the idea of the central dogma of molecular biology, which states that the information from DNA is passed in a one-way direction via RNA to proteins [1]. Since then, one of the most important questions in molecular biology has been how the expression of proteins is regulated. The first time RNA was proposed as a regulator of protein expression was in 1969, when Britten and Davidson proposed a theory in which RNA might regulate the expression of genes using standard Watson-Crick base-pairing rules [2]. However, the idea that RNA could govern the expression profile of each cell type was neglected when transcription factors were discovered, and for decades transcription factors (there is an estimate of ~1500 transcription factors in the human genome [3]) were seen as almost exclusive effectors for regulating the mRNA expression profile and the proteome of eukaryotic cells.

It was not until the early 1990s that hints of expressional regulation of one mRNA caused by another RNA started to emerge. In 1990, it was reported that the overexpression of exogenous DNA encoding an enzyme, producing a purple pigment in petunias, led to white flowers as a consequence of a reduced expression of both endogenously and exogenously introduced enzyme mRNA [4, 5]. The downregulation of mRNA levels by the introduction of antisense RNA was an established technique as early as 1984 [6], but it was shown in 1995 that both antisense and surprisingly the synthetically produced sense RNA induced the silencing of gene expression in *Caenorhabditis elegans* [7]. In 1998, Fire and Mello demonstrated that this silencing was triggered by dsRNA and that the sequence of the dsRNA determined which mRNA was targeted for silencing [8]. Three years later, the same method was also shown to be a functional tool in mammalian cells [9] and that the concept of RNA-based gene silencing is functional in all eukaryotic supergroups (with a few exceptions, including budding yeast, which seems to have lost this feature during evolution) [reviewed in 10]. This mechanism is called RNA interference (RNAi)

At the same time as the mechanism of RNAi was discovered, another small RNA started to make its appearance. In 1993, Ambros *et al.* described *lin-4* as the first micro RNA (miRNA) in the nematode *C. elegans*. Here, it was shown how the smaller RNA *lin-4* seemed to repress the translation of the larger mRNA *lin-14* and that this repression might be a result of multiple RNA-RNA interactions between *lin-4* and the 3' UTR structure of *lin-14* [11]. In 2001, miRNA was established as a large class of gene regulators in several species including humans [12-14], thereby suggesting that miRNA and the proteins involved in its regulation are a part of a conserved pathway.

In 2001, RNAi and miRNA were linked together when it was demonstrated that Dicer, a protein that sliced long dsRNAs into smaller effector RNAs called small interfering RNAs (siRNAs) [15, 16], also converted longer *lin-4* transcripts into smaller mature *lin-4* miRNAs [17-19]. As a result, it was now apparent that both RNAi and miRNA were regulatory tools conserved in most eukaryotes and that they both used the same pathway to exert their regulatory effect on mRNAs.

3.1.2. The miRNA pathway in animals

There are two main differences between miRNA and siRNA in animals:

1. MiRNAs are transcribed endogenously from non-protein-coding separate genes. There are no dedicated genes for siRNAs. Instead, they are degraded from larger dsRNA introduced to the nucleus exogenously (e.g. viral transcripts) or endogenously (e.g. transposons) [20].

2. SiRNAs have a full complementarity towards their targets, while miRNA show a limited complementarity.

The main features of the miRNA pathway are outlined in Figure 1.

MiRNA genes are primarily transcribed by RNA polymerase II to form primary miRNA (pri-miRNA), a structure which is usually several kilobases long, with local stem loop structures [21, 22]. They can be encoded in independent transcription units, in polycistronic clusters or within introns of protein coding or non-coding genes [reviewed in 23]. The pri-miRNA is further processed in the nucleus into a hairpin approximately 60-70 nucleotides long, which is known as the precursor miRNA (pre-miRNA) [24]. This processing is done by the

Ribonuclease III (RNase III) protein Drosha and its essential co-factor DiGerorge syndrome critical region 8 (DGCR8) [25-29]. After processing, the pre-miRNA hairpin contains a 3' 2 nt overhang and a 5' mono-phosphate group [25, 30, 31], a feature that is characteristic of all RNAs cleaved by an RNase III protein [32]. Polycistronic clusters are transcribed as a single transcript, which is processed into all the separate miRNAs within the cluster by Drosha [12, 13].

Pre-miRNA exits the nucleus through nuclear pore complexes since further processing of the pre-miRNA takes place in the cytosol. This transport is executed by the nuclear transport receptor exportin-5 (exp5), which recognises dsRNA hairpins with stems >16bp long [33-35]. The 3' overhang of 2 nt further facilitates this process [36].

Following release into the cytoplasm, the pre-miRNA is recognised by and bound to the RNase III enzyme Dicer, which cuts it to generate a mature miRNA [16-19]. Dicer contains both an RNase III domain (RIIID) responsible for slicing dsRNA and a highly conserved Piwi Argonaute Zwille (PAZ) domain which recognises and binds the 3' dinucleotide overhang on the 3' end of the pre-miRNAs [15, 37]. This suggests that the 3' dinucleotide overhang locks into the PAZ-domain, bringing the pre-miRNA into position for cleavage by the RIIID of Dicer [38]. Human Dicer then cuts the pre-miRNA stem approximately 22 nt from the 3' end docked in the PAZ domain [39]. A crystal structure of Dicer from the parasite *Giardia* reveals that the distance from the PAZ-domain to the RIIID matches the length of the *Giardia* Dicer cleavage products [40], thus suggesting that Dicer itself acts as a molecular ruler which generates products defined in length by the fixed distance between its PAZ domain and RIIID. The pre-miRNA is now reduced to an approximately 22 nt dsRNA, with a 3' dinucleotide overhang and a 5' phosphate group at both ends.

Dicer works together with several other proteins in order to execute its function. Dicer containing the sliced dsRNA is recruited by the trans-activation-response RNA-binding protein (TRBP) to form a structure known as the RNA-induced silencing complex (RISC) loading complex [41, 42]. Here, the mature miRNA is transferred from Dicer to the RISC where it binds to an Argonaute (Ago) protein, which is the catalytic entity of the RISC [43, 44]. Of the two Ago proteins encoded in humans, Ago2 is functioning in the RNAi pathway [43, 44]. Ago2 also contain a PAZ domain, which recognises the presence of a 3' dinucleotide overhang and a 5' phosphate group on dsRNA, both of which are facilitating the incorporation

of the miRNA to the RISC [45-47]. After the transfer of the RNA duplex, it is the strand with its 5' end at the least thermodynamically stable end that is preferentially kept bound to Ago2 [48]. This strand is known as the guide strand, while the complementary passenger strand is cleaved and degraded [49]. When bound to the RISC, the guide strand functions as a sequence-specific template that leads the RISC to complementary targets through base-pairing interactions.

MiRNAs does not usually have a full complementarity with its targets. When bound to RISC, only nucleotides numbered 2-6 of the guide strand (starting from the 5' end) are exposed to such a degree that base-pairing with target RNA is possible [50]. This is in accordance with the observation that animal miRNAs contains a seed region ranging from nt 2-8, which is critical for the specificity of target recognition [51-53]. MiRNAs usually exert their regulatory functions by binding to a complementary seed sequence in the 3'UTR of their target mRNA, although binding to the 5'UTR or the coding regions has also been reported [54]. When the targeted mRNA is bound to the RISC, it can be moved from the cytosol to cytoplasmic complexes called Processing bodies (P-bodies) [55-57]. Here, de-adenylation and de-capping of the mRNAs followed by 5'→3' degradation occurs [56, 58]. In addition, the protein translation of the mRNAs is prevented as they become sequestered from the ribosomes residing in the cytosol. Nevertheless, degradation of mRNA accounts for the vast majority of miRNA induced gene silencing [59].

If there is perfect complementarity between the bound guide strand and its target, the target is not transported to P-bodies. Instead, Ago2 cuts the target RNA between the 10th and 11th nucleotide as measured from the 5' end of the guide strand [46, 47, 60-62].

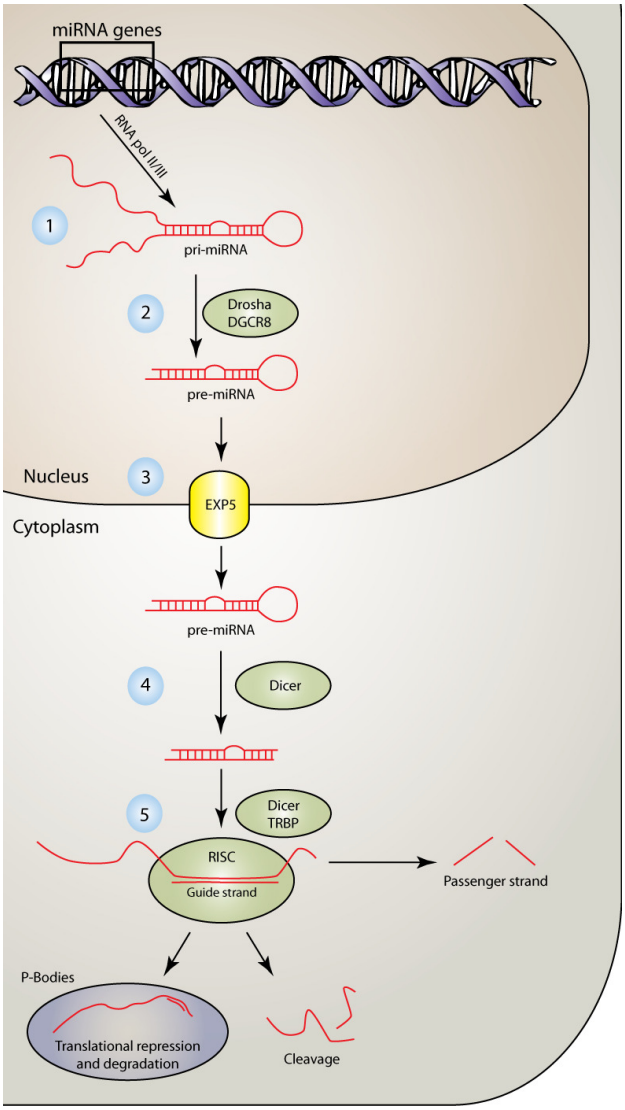

Figure 1: The miRNA pathway. MiRNA genes are transcribed to pri-miRNA often several kilobases long (1). Pri-miRNA is then processed by Drosha to form hairpin structures known as pre-miRNA (2). Exportin 5 recognizes the hairpin structure by its 3' dinucleotide overhang, and exports it from the nucleus to the cytoplasm (3). In the cytoplasm, pre-miRNA is recognized by Dicer, which cuts the pre-miRNA into a mature miRNA ~22 nt long (4). The dsRNA is then transferred into the RISC, where the passenger strand is cleaved and removed. The guide strand is used as a template for binding target mRNA according to base-pairing. If there is full complementarity, the mRNA is cleaved. If there is partial complementarity, the mRNA is transferred to P-bodies where translation is repressed and the mRNA is eventually degraded (5), see text for details. Modified by permission from Macmillan Publishers Ltd: Gonzalez-Alegre, P. and H.L. Paulson July, 2007. "Technology insight: therapeutic RNA interference--how far from the neurology clinic?" Nat. Clin. Pract. Neurol. 3(7):394-404.

3.1.3. The natural functions of RNAi in animals

Since Argonaute-like and Dicer-like proteins are present in all eukaryotic supergroups, it is evident that dsRNA-mediated silencing was already established in the last common ancestor of eukaryotes, but that it was also not required for life since it has been lost several times in various single-cellular organisms [reviewed in 10]. DsRNA-based silencing has probably evolved as a defence mechanism against genomic parasites such as tranposons and viruses [63-68]. Until recently, it has been assumed that defence is the main task of RNAi systems in mammals. Still, the discovery of endogenous siRNA (endo-siRNA) transcribed from L1 transposons in human cultured cells has opened the possibility of additional tasks for siRNA [69]. It has been shown in mouse oocytes that transcribed pseudogenes interact with homologous protein coding mRNAs to form dsRNA being processed to 21 nt siRNAs by Dicer [70, 71].

3.1.4. The natural functions of miRNA in animals

Thus far, miRNAs have only been described in multi-cellular organisms, in which they have evolved to regulators essential for the development of both animals and plants [23, 72-74]. Exactly when miRNAs evolved in evolution is debated, although it seems that the regulation of genes by miRNAs could be a requirement for the emergence of multi-cellular organisms since both plants and animals have evolved miRNA systems out of a separate evolutionary origin [10, 75]. From its discovery, it has taken miRNA merely a decade to achieve status as a regulator of most biological processes in animals and plants, including cell cycle, differentiation, development and metabolism [13, 76-78]. The number of mature miRNA products in the human genome has exceeded 1000 (mirBase version 16.0), while it is estimated that more than 60% of human mRNAs contain conserved miRNA target sites in their 3' UTR [79]. This means that on average each miRNA can target a large amount of mRNAs, e.g. the *miR-15a/16-1* cluster, which is predicted to potentially control 14% of all genes in the human genome [80]. To further add to this complexity, in most cases mRNAs harbour target sites for several different miRNAs [81-83]. Given the immense complexity and biological importance of miRNAs, it is of no surprise that their dysregulation is implicated in a vast number of human diseases, e.g. cancer, diabetes, muscular disorders and even psychiatric diseases [84-87]. MiRNAs were shown to potentially act as both oncogenes and

tumour suppressors in 2005 [88-91], and the dysregulation of miRNAs is now regarded as a vital contributor to the pathogenesis of many tumours [92, 93].

3.1.5. Targeted gene regulation using exogenous RNA

Previously, antisense technology was the most feasible approach for reducing the expression of specific genes, and both antisense DNA and RNA have been used for the modulation of biological processes [reviewed in 94]. However, since the discovery of RNAi, these approaches have been superseded, given the higher efficiency of RNAi compared to antisense technologies [95-97]. Scientists can now exploit RNAi to suppress virtually any gene simply by introducing siRNAs that are perfectly complementary to the target of interest. The miRNA biogenesis pathway contains three distinct RNA intermediates: the pri-miRNA transcript, the pre-miRNA hairpin and the miRNA duplex. All of these intermediates can be exploited as entry points for RNAi (Figure 2).

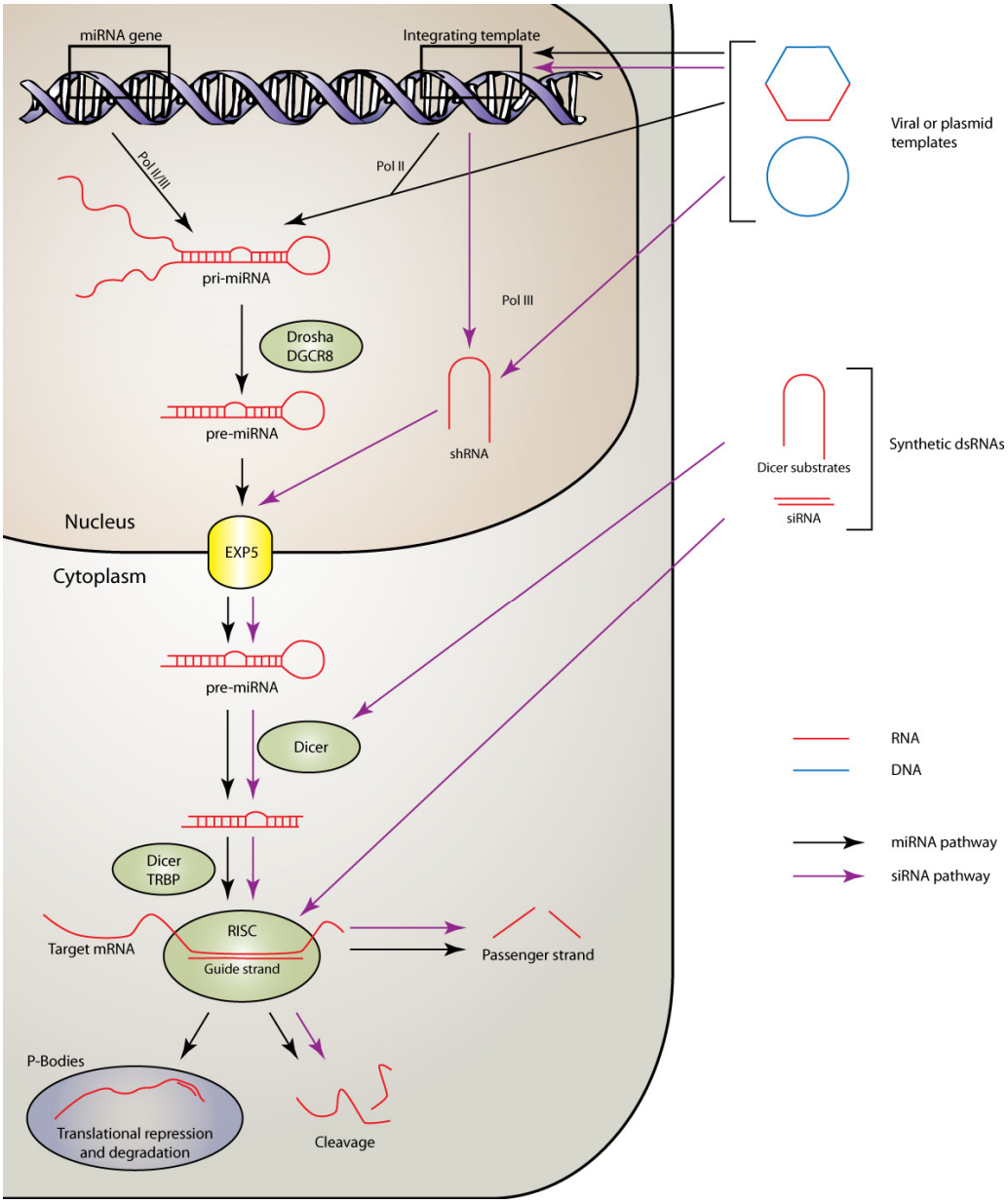

Figure 2: The process of RNAi and its manipulation. For a description of the miRNA pathway, confer with Figure 1. RNAi can be initiated by introducing siRNA or shRNA stems at all steps in the miRNA pathway, see text for details (Chapter 3.1.5). Modified by permission from Macmillan Publishers Ltd: Gonzalez-Alegre, P. and H.L.Paulson July 2007. "Technology insight: therapeutic RNA interference--how far from the neurology clinic?" Nat. Clin. Pract. Neurol. 3(7):394-404.

Imitating the miRNA duplex: siRNA

Synthetic siRNAs are small RNA duplexes designed to imitate the mature miRNA duplex in order to obtain RNAi-mediated gene suppression. In the first study, in which RNAi were shown to mediate effective silencing, dsRNA fragments several hundred nucleotides long were used [8]. Even so, the presence of long dsRNA in the cytoplasm often triggers the non-

specific interferon response pathway in mammalian cells, thereby leading to a broad inhibition of protein synthesis, transcriptional activation of cytokines and ultimately cell death [reviewed in 98]. It is generally believed that dsRNA molecules less than 30 bp long are not able to induce the interferon response [99]. Nonetheless, this is debated, and it has been demonstrated that the triggering of the interferon response pathway by dsRNAs >23 nt long is cell-type dependent [100]. To prevent activation of the interferon pathway, researchers have generally used shorter siRNAs (19-23 bp) that imitate the products of Dicer [46]. To further mimic natural Dicer products, siRNAs are also designed with a dinucleotide 3' overhang in both ends for more efficient loading [47]. It is the strand with the least thermodynamically stable 5' end which is preferred as the guide strand [48]. To ensure that the desired strand is loaded onto RISC, siRNAs are constructed with accordingly GC bp asymmetry.

Imitating the pre-miRNA: Synthetic Dicer products and shRNA

Synthetic Dicer products are 25-30 bp RNA duplexes designed to interact directly with Dicer [101]. They contain only one 3' dinucleotide overhang to ensure that Dicer cuts the RNA at the intended end, thereby producing identical mature siRNAs with the predicted sequence [102]. As a result, synthetic Dicer products mimic cytoplasmic pre-miRNA.

While siRNAs and Dicer products are introduced as RNA directly to the cytoplasm, short hairpin RNAs (shRNAs) are transcribed from DNA in the nucleus of the cell before they are exported by exp5 to the cytoplasm for further processing by Dicer and loading into the RISC [103]. ShRNAs are generally transcribed from RNA polIII into hairpins, thus mimicking nuclear pre-miRNA. In the appendix, we show that cloning of vectors expressing shRNAs are an easy and inexpensive technique for achieving efficient knockdown of a desired target gene.

The RNA polIII promoter is located directly upstream of the gene it is transcribing. It has a well defined starting point, and terminates when transcribing 4-5 consecutive thymidines [reviewed in 104]. When transcribed in the nucleus, the shRNAs folds into hairpins with a 3' dinucleotide overhang in one end and a loop in the other. The stem of the hairpin usually ranges from 23 to 29 bp. This configuration is similar to pre-miRNA constructs, and is therefore recognised as substrates by exp5 and Dicer [105-110]. Regardless of the initial length of the hairpin, Dicer cuts the shRNA into ~22 nt effector dsRNAs before incorporation to the RISC [39].

Imitating the pri-miRNA: shRNA-mir

RNA transcribed from PolII promoters includes elements such as 5' end caps and 3' polyA tails. These elements must be removed by Drosha before the transcript can interact with exp5 and the remaining miRNA pathway [22]. For this reason, polII promoters were initially avoided for transcription of shRNAs. However, shRNAs can also be expressed from RNA PolII promoters by inserting the hairpin within the backbone of a miRNA (usually that of *miR-30*), resulting in a primary transcript with extensive length and folding compared to standard shRNAs [111, 112]. Consequently, this shRNA-mir transcript is a target for processing by Drosha, and utilises the full miRNA pathway instead of accessing it in downstream entry points.

3.1.6. Efficiency of RNAi

All of the above described forms of RNAi exploit the miRNA pathway to exert their effect, and they can all be transiently transfected for short-term suppression of a desired gene. To evaluate the efficiency of the various constructs, one important aspect to consider is how much mRNA the construct is able to suppress on a numerical basis.

SiRNAs enter the miRNA pathway directly into the RISC, which means that they are not bound or processed by Dicer. The main function of Dicer is to cleave long dsRNAs into shorter products, but it is also a vital part of the RISC loading complex, which strongly facilitates the transfer of the guide strand into the RISC. Since siRNAs <23 bp are loaded directly onto the RISC, they are not able to take advantage of this feature [101, 113]. Dicer products are designed to interact with Dicer, and have been shown to be more efficient than siRNAs targeting the same target sequence [39, 101, 114].

There are three promoters used to express shRNAs: the H1, U6 and tRNA promoter [115]. Of these, the U6 and H1 promoters are generally being favoured, and it has been debated as to which of these promoters is the most efficient. Some groups find that U6 is the most effective in terms of expressed shRNA and the duration of gene suppression [115, 116], while others groups find no significant difference [117]. Our results reveal that the efficiency may vary between cell-lines but that the U6 promoter usually demonstrated a marginally higher efficiency (Paper I, [118]). This suggests discrepancies depending on different variables such as type of target cells, delivery method and shRNA sequence and that the most efficient

promoter should be decided on a case-by-case basis. Since shRNAs are processed by Dicer, they are also inserted into the RISC with higher efficiency than siRNAs. It has been shown that shRNAs expressed from a U6 promoter are more than 100 fold more effective on a numerical basis than siRNAs containing the same target sequence [115]. Nonetheless, a vector containing the shRNA is often 100 fold larger than naked siRNA. In addition, the vector needs to enter the nucleus in order to be transcribed, which is shown to be one of the biggest challenges when transfecting [119]. For that reason, the number of shRNA transcripts actually being produced is much lower than the number of siRNAs being introduced to the cytoplasm when the same amount of nucleic acid by weight is transfected. As a result of this, the practical gene suppression efficiency ranges from similar to slightly better for siRNAs compared to shRNAs [105, 115, 120].

By expressing the shRNA placed within the backbone of a miRNA, the resulting shRNA-mir is processed by Drosha in the same manner as the miRNA itself. MiRNAs are almost exclusively expressed from RNA polII promoters, as opposed to traditional shRNAs which are generally expressed from polIII promoters. The suppression efficiency of identical shRNAs expressed from either PolII or PolIII promoters has been compared with conflicting results. It has been shown that shRNA-mir expressed from a CMV PolII promoter slightly outperformed the shRNA transcribed from a U6 RNA polIII promoter [121]. Boden *et al.* reported that the transient expression of shRNAs from PolII promoters with miRNA backbones significantly outperformed conventional shRNAs [122], while it has also been reported that conventional shRNAs are more efficient than shRNA-mir [123]. Boudreau *et al.* however have stated that the above reports could be flawed as a result of missing 3' dinucleotide overhangs in addition to the failure to consider the effect of GC asymmetry in the stem when the conventional shRNAs were designed. When these important features are under control, it has been shown that conventional shRNAs are more potent than shRNA-mirs for three different target sequences, both *in vitro* and *in vivo* [124]. It is not clear whether this is a result of increased expression or higher stability of the transcribed shRNA in comparison to shRNA-mir.

3.1.7. Duration of RNAi-based gene suppression

It is only possible to introduce synthetic siRNAs and Dicer products to cells in a transient manner, which means that all gene suppression resulting from these synthetic RNAs is only

temporary. Bartlett and Davis found that it seems as if the duration of siRNA-mediated knockdown is dependent on how fast the harbouring cells are dividing [125]. Here, it was demonstrated that the levels of the targeted genes returned from optimal knockdown at 24-48 hours to background levels within six days in the dividing cells, and similar dynamics have been reported by other groups [114, 126]. However, it has also been reported that the maximum amount of introduced siRNA molecules peaks at approximately 24 hrs and diminishes within 48 hrs, which indicates a high degradation and turnover [127]. It has been shown that transiently transfected vector-based shRNAs give more durable gene suppression than the transfection of siRNA since shRNAs can be continuously transcribed by the host cell as long as the vector remains in the nucleus [115]. There are two main concerns when considering gene suppression using RNAi with transiently transfected effectors. First, all transient expressions by definition are temporal, and suffer from dilution effects as a result of cell division and RISC turnover. Because of this, it is not possible to maintain gene suppression for more than a week (our unpublished results). Second, transfection efficiency is rarely 100% and might vary considerably between cell lines. As a result, there will always be a background of cells without gene suppression, and this untransfected fraction could vary considerably between different cell lines (our results). Vector-based RNAi has the advantage of being able to produce stable gene suppression through the insertion of the expression cassette into the genome of cells, which is an approach that solves both concerns mentioned above.

3.1.8. Strategies for achieving stable shRNA expression

When an expression cassette is inserted into the genome of a cell, it will not be lost and will be inherited to all offspring. Therefore, the expression of shRNA will remain in the entire cell population. Generally speaking, an expression cassette being genomically inserted is coded on the same plasmid as a construct expressing an enzyme, making the stably transfected cell resistant towards a selection marker. When this selection marker is later added to cell media, untransfected cells will die, leaving behind a population in which all cells express the desired shRNA. Thus, stable transfection will generate populations in which all cells are transfected, and gene suppression does not diminish over time.

There are several strategies for the stable delivery of exogenous DNA to cells [reviewed in 128]. The ones most used in RNAi strategies are random plasmid integration [105, 106] and

viral delivery [129-131]. In random plasmid integration, cells are transfected by any conventional method [reviewed in 128]. On rare occasions, transfected DNA is integrated into the genome of the cell in a random manner. These relatively rare cells will then be able to produce resistance towards a selective drug on a permanent basis, and therefore can be sorted out from the majority of cells not being stably transfected. As a consequence, the expression of the inserted transgene may vary between clones. Transgenes inserted in high density chromatin areas generally show a low expression, whereas insertion in low density areas suggests a higher expression. The plasmid might have been linearised in a manner that resulted in expression of only the resistance gene and no functional version of the transgene. Additionally, the number of copies being inserted may vary [reviewed in 128], which means that every clone should be controlled for plasmid integrity and expression.

Retroviral vectors have become an important tool for stable gene transfer both *in vitro* and *in vivo*. Retroviruses are constituted of RNA packed into a capsid and a membranous envelope. When the virus infects a cell, it transfers the RNA into the target cell, where it is reverse transcribed in the cytoplasm and integrated randomly into the genome [reviewed in 132]. The frequently used Moloney murine leukemia virus (MLV) retroviruses are not able to cross the nuclear membrane, and are thereby only able to integrate into the genome when the nucleus is disassembled during mitosis [133]. For this reason, MLV retroviruses are only able to infect dividing cells. Lentiviruses are a complex class of retroviruses which are able to also transduce non-dividing cells [reviewed in 134]. Both classes of retroviruses are mainly adapted in the same manner for transductions in laboratories. Genes encoding proteins that are necessary for the assembly of the envelope are transcribed from a packaging cell line, which is transiently transfected with the remainder of the viral genome containing an inserted transgene and a resistance gene. This leads to the release of functional viruses which codes for the insert, but not for the envelop proteins into the media. The media containing viral particles can then be used to transduce other cells. The lack of genes encoding the envelope proteins, as well as additional modifications in the viral genome, abolishes the possibility of transduced cells being able to produce viable viruses [reviewed in 132].

All of the strategies mentioned above have both positive and negative properties. Random plasmid integration is cheap and does not require any safety precautions, but is very ineffective. MLV retroviruses have a vastly increased efficiency and are easy to produce, although they are not able to transduce non-dividing cells, while lentiviral vectors can also

infect non-dividing cells [reviewed in 132]. Since viruses released from the packaging cells are theoretically capable of infecting all human cells, including those of the person performing the transduction, there are safety issues involved when transducing cells.

3.1.9. Conditional shRNA expression

The constitutive and ubiquitous expression of shRNAs suffers from limitations when it comes to the study of gene functions involving cell survival, growth and development. The reason for this is that the selection of transduced cells into a pure cell population typically takes several days from the time of the transduction. Within this time frame, the effects of the shRNA will have begun. This has prompted the construction of inducible gene silencing systems based on conditional RNAi expression. In such systems, the expression of shRNA will remain shut off until some sort of signal turns the expression on. In some systems, this expression is reversible.

There are several approaches for achieving conditional expression of shRNA.

Recombination

In the Cre/lox (Cyclization recombination/locus of X over P1) system, the shRNA is generally expressed from a polIII promoter. The complete shRNA, however, is separated from the promoter by a gene sequence flanked by two lox recombination sites. This site is recognised by the recombinase enzyme Cre, which will excise the DNA between the two lox sites. This recombination will result in transcription of the intact shRNA [135-138]. The advantage of this system is that there is no background expression of shRNA until Cre is present and that Cre only needs to be present for a short period to achieve permanent shRNA transcription. The Cre/lox system can also be used to shut down the expression of shRNA. Here, the promoter is placed between two lox sites, which will then be removed by recombination by the addition of Cre [138]. A similar system uses the yeast-derived recombinase FLP and its recognition site FRT [139]. The main disadvantage of both systems is that once the recombination has taken place, it is impossible to reverse it.

The Tet-inducible system

The most commonly used system for achieving conditional regulation of shRNA expression is based on Tetracycline (Tet) -inducible systems. There are three components necessary for the

functioning of this system: The constitutive expression of a Tet-repressor (TetR), a plasmid allowing the inducible expression of RNA through a promoter containing a TetR-binding sequence named Tet-operator (TetO) and the inducer Tet or one of its derivates, usually Doxycycline (Dox). TetR has a high affinity to the TetO, and thus binds tightly to DNA strands containing its sequence. The Tet-inducible system was originally developed in polII promoters and later adapted to polIII promoters in order to control the expression of shRNA [140]. An inducible polII promoter is minimal, meaning that sequences binding enhancers/activators necessary for transcription initiation are replaced. Instead, a Tet-Responsive element (TRE), which contains seven TetO sequences linked to a short stretch of sequences containing the PolII transcriptional start site of the CMV promoter, is added [141]. TetR is then fused to an activator, which recruits RNA polII to a minimal polII promoter and initiates transcription. In the Tet-Off system, the addition of Dox releases TetR and its activator from the TRE, turning the transcription off [141]. In Tet-On systems, the activator has four amino acids in the TetR moiety that are reversed, giving it the reverse phenotype. Here, Dox is required for the binding of TetR and the addition of Dox recruits the activator complex, thus turning gene expression on [142]. Of the two, Tet-Off is regarded as the most effective system [143].

Since PolIII promoters produce RNAs without 3' polyA tails and 5' end caps that are able to interact directly with exp5 and Dicer, they were the first promoters used for the stable expression of shRNAs. It is the U6 and H1 promoters which have been utilised for inducible expression via an adapted Tet-off system. Both the U6 and H1 promoters are extremely compact, and have three essential domains: the distal sequence element (DSE), the proximal sequence element (PSE) and the TATA box. The PSE and the TATA box are binding sites for the RNA polymerase itself, while the DSE binds the transactivators necessary for activation of the polymerase [144]. The activity of the promoters relies on a correct spacing between these elements and the transcription start, while the sequence between them is of lesser importance [145]. These intermediate sequences can be adapted to possess a TetO, one upstream and one downstream of the TATA box. TetO sequences placed upstream of the PSE and in the proximity of the DSE, severely impair transcription from the promoter [146]. When the inducer is absent, the TetR will bind to the TetO, thereby sterically preventing binding of the polIII. The addition of the inducer leads to a conformational change of TetR into a configuration not able to bind to the TetO. This allows polIII to bind and transcription to take place (Figure 3). There are two TetOs that have been used extensively in PolIII-inducible

promoters, the TetO1 and TetO2 [147]. Several combinations of the two TetOs in US, DS or both positions have been described for both the H1 and U6 promoters [140, 148-151]. The general conclusion is that one operator alone is not sufficient for achieving tight regulation of the promoter in an uninduced state. In addition, it seems as though the TetO2 operator is the most effective in terms of suppression [149]. In Paper I, we compared the tightness and efficiency in a number of previously described inducible U6 and H1 promoters in several different human cell lines, in addition to describing an H1 promoter containing two TetO2s for the first time [118]. It was concluded that overall the newly designed promoter performed better than the remaining promoters, including the similar U6 promoter containing two type 2 TetOs. The H12O2 promoter presented a very low background in an uninduced state and up to 90% gene suppression after the addition of the inducer Dox.

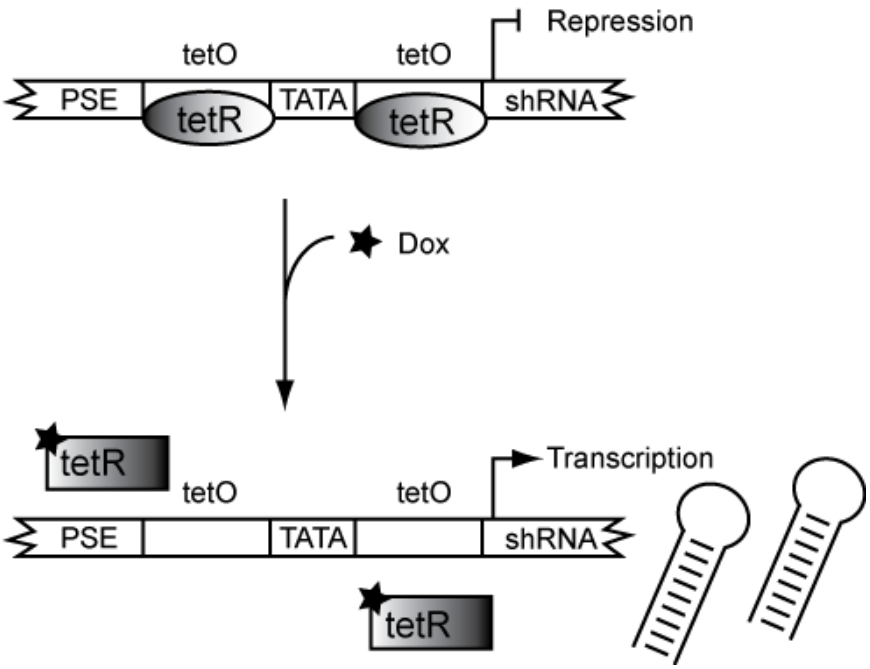

Figure 3: Conditional expression of shRNA from a PolIII promoter. When the inducer Dox is absent, TetR is bound to the TetO, thereby sterically obstructing the binding of polIII to the promoter. Dox induces a conformational change of the TetR into a form with a low affinity to the TetO. This leads to the dissociation of TetR from the promoter, allowing PolIII to transcribe the shRNA.

The U6 RNA polIII promoter has also been modified to an inducible version following the same principles as polII promoters. Here, the DSE was replaced by a TRE, and TetR fused to the activator normally binding to the DSE [152, 153].

Following the discovery of shRNA-mir, which are transcribed by polII, the original Tet-inducible polII promoters returned to the field of RNAi [112, 154]. Here, it was shown that these vectors presented tight regulation, high penetrance and high efficiency, even in single copy levels of the inserted cassette. Although the Tet-Off system has been previously regarded as superior to the Tet-On system, the transcriptional activator originating from the Tet-On system has been improved using viral evolution as a tool to better adapt it from its original host, *E. coli*, to mammalian systems [155]. The resulting activator has been utilised in inducible shRNA systems to yield improved gene suppression [156]. Two shRNAs targeting different mRNAs from the same promoter were also expressed, thereby acquiring the ability to knockdown two genes simultaneously.

Ecdysone

The ecdysone system is similar to the Tet system in its principle of function. The ecdysone receptor is fused to an activator, and binds to the Gal4-binding sequences. It uses ecdysone-analogs as inducers, and the addition of the inducer releases the receptor along with its activator from the minimal promoter, thereby turning transcription off. The system is functional in both polII and polIII promoters [157, 158].The vector integration site strongly influences expression, which requires careful selection of effective clones. Additionally, ecdysone is a steroid prohormone, and activation of its receptor could trigger endogenous gene expression in target cells [reviewed in 159].

3.1.10. Off-target effects

Off-target effects of RNAi are defined as consequences that arise from any effect other than the intended gene suppression. The off-target effects are divided into two main categories: specific and non-specific.

Specific off-target effects

Specific off-target effects arise as a result of a full or partial complementarity between the passenger or guide strand towards any unintended target. In order to achieve target cleavage through the action of Ago, it is necessary to have perfect complementarity extending through at least 13 nt of the strand mounted in the RISC [160]. A BLAST search of the transcriptome of the species investigated will quickly expose siRNAs harbouring unspecific complementarity of this degree, allowing for those siRNAs to be discarded. As a consequence

of this, there is more concern regarding partial mismatches, particularly when including nt 2 – 8 counted from the 5' end of the guide strand. These nucleotides form the seed sequence that allows the guide strand of the siRNA to function as a miRNA [61]. It is has been shown that the off-target effects of siRNAs are strongly biased to occur from ~7 nt complementarity between the "seed sequence" of the guide strand and the 3' UTR of the unintended targets and that the unintended target sequences are often conserved in several mRNAs [161]. The magnitude of the regulation of transcripts targeted as siRNA off-targets is generally less than twofold, which is similar to that of miRNAs [161, 162]. This suggests that siRNAs are prone to target unintended miRNA seed sequences of ~7 nt. Because of this, there could be a discussion as to whether the less than twofold regulation realised by off-target siRNAs has any biological relevance. Adverse unintended phenotypes arising from such off-target effects have been described [161, 163]. There is no algorithm that can significantly eliminate 7-8 nt matches in the transcriptome of a species; therefore, some off-target effects are likely to occur when using any form of RNAi-mediated gene silencing, and there are developed algorithms that try to minimize off-target effects [164-166].

Non-specific target effects

Non-specific target effects are effects that do not result from direct interaction between an RNAi construct and an mRNA target. This includes immune-responses as a result of defence mechanisms triggered against exogenous RNA, any effect related to the delivery vehicle in addition to any effects arising from saturation of the miRNA pathway.

Initially, it was thought that RNA duplexes shorter than 30 nt were small enough to evade stimulation of the interferon response [9]. However, this assumption has been questioned, as activation of immune responses resulting from the introduction of small siRNAs has been described [167, 168]. The 13 Toll-like receptors (TLRs) are a class of proteins that recognises signs of infection and activates the innate immune system. Of these, the ones most relevant for activation as a result of RNAi are TLR3, which recognises the duplex form of siRNA, and TLRs 7 and 8, both of which are activated either by the duplex or its corresponding single strand [169-171]. TLR receptors are often concentrated in endosomes, thus transfection methods utilising cationic lipids enhance the immune response [171]. In contrast, ShRNAs are less likely to induce an immune response since they are presented from a DNA plasmid, thereby avoiding the dsRNA activation of TLR3. In addition, the 5' ends of shRNA, which

are produced endogenously, seem to be less immunogenic than corresponding 5' ends of exogenous siRNAs [101, 172]. Chemical modifications of siRNAs can reduce their immunogenicity [reviewed in 173].

RNAi uses the miRNA pathway in order to exert its effect. As a result, any exogenous RNAi effector competes with endogenous miRNAs for access to the miRNA machinery. ShRNAs are entering the miRNA pathway at a higher level than siRNAs (Figure 2), and are therefore competing with miRNAs in more steps than siRNAs. The most rate-limiting step in the miRNA pathway seems to be the export of pre-miRNA from the nucleus to the cytoplasm by exp5, and shRNA expression is shown to interfere with endogenous miRNAs as a result of saturation from this step [174]. Also, the sustained expression of shRNAs stably delivered to liver cells in adult mice has been revealed to severely downregulate the expression of endogenous miRNA [175]. This was demonstrated to be a result of saturation due to Exportin5 activity as well as the activity of Ago2 in RISC [176]. By expressing the shRNAs from a miR backbone, the toxicity of shRNAs has been shown to be diminished [177]. One group has proposed that siRNAs are unable to saturate the miRNA pathway by showing that the expression of three different miRNAs in liver cells did not change when siRNA-mediated gene suppression was utilised [178]. Nonetheless, it has also been shown that both shRNAs and siRNAs compete not only with each other, but with endogenous miRNAs for incorporation to RISC [179]. In addition, it has been proposed that transfected small RNAs have a global effect on genes under the control of endogenous miRNAs [180]. Here, the results from 151 published experiments based on the transfection of either siRNA or miRNA into cells in culture were analysed. A statistical analysis of the published mRNA profiling or protein mass spectrometry revealed that in the majority of the experiments, endogenous mRNAs containing targets of miRNAs with high endogenous expression were upregulated as a result of competition from exogenous mi/siRNAs.

3.2. Neuroblastoma

3.2.1. Embryonal development and neoplasms

The development of an embryo begins with a single fertilised egg. Countless cell divisions of this perfect stem cell eventually lead to the generation of organs and every other component of the organism. After the first few cell divisions of the zygote, it is already apparent that cell-cell interactions start to decide the fate of the daughter cells [181]. From this point on, the development of the embryo is a process comprised of strictly controlled proliferation and differentiation signals. In the early embryo, there is a majority of strong mitogenic signals that limit the ability of cells to exit the cell cycle. During embryonal development, changes in the concentration of key regulatory signals promote the exit of the cell cycle and the onset of differentiation for the targeted cells. In normal development, the signals indicating proliferation or differentiation are under tight control, though in tumour growth this control is lost. If a strong mitogenic signal expressed transiently during development achieves constitutive expression, it acts as an oncogene. Alternatively, if a protein involved in signalling pathways leading to cell cycle exit and differentiation loses its function, it may no longer act as a tumour suppressor. Tumours originating from tissues that normally proliferate only in a developing embryo are known as embryonal tumours. If the tumour arises from primitive precursor cells, it is given the suffix blastoma. These tumours can arise in various parts of the body and include medulloblastoma in the brain, neuroblastoma in the sympathetic nervous system, retinoblastoma in the eye, Wilms' tumour (nephroblastoma) in the kidney, hepatoblastoma in the liver and embryonal rhabdomyosarcoma in soft tissue. These tumours are very rare after childhood, and most commonly occur during the first years of life.

3.2.2. Development of the sympathetic nervous system

On day 19 of the embryo, the neural plate starts to form on the ectoderm of the embryo. The edge of the neural plate is defined by neural crest precursors, and as the neural plate folds in on itself, the neural crest precursors from each outer edge join and form the dorsal part of the newly developed neural tube. The neural tube is developing to form the central nervous system, while the now mature neural crest cells start to migrate from the dorsal part of the neural tube into several areas of the embryo [reviewed in 182]. Neural crest cells are the origin of several cell lineages: cranial (e.g. forming facial bones), vagal and sacral (e.g. parasympathetic neurons), cardiac (contributing to the development of the heart) and trunk

neural crest-derived cells (e.g. melanocytes and the sympathetic nervous system, including the adrenal medulla) [183].

Trunk neural cells destined to form the sympathetic neural system are of the sympathoadrenal lineage. These migrating sympathetic neuroblasts arrange themselves alongside both sides of the neural tube before they start forming chains of sympathetic ganglia. As internal organs are being developed, sympathetic fibres formed by axonal outgrowth from the ganglia reach out to and connect them to the sympathetic nervous system in a process known as innervation [183].

The differentiation from neural crest precursors at the neural plate to non-dividing neural cells in the sympathetic nervous system requires involvement of a large amount of signalling pathways. The formation of both the neural plate and neural crest precursors are dependent on expression levels of the bone morphogenetic protein (BMP) pathway, the fibroblast growth factor (FGF) pathway and the Wnt signalling pathway [reviewed in 184]. As the neural tube is formed, the neural crest precursors mature to neural crest cells before going through an epithelial to mesenchymal transition, in which they shed from the neural tube and start migrating. This process is largely governed by Wnt signalling, and leads to expression of a set of genes known as neural crest specifiers. As the migrating neural crest cells reach their final target, they start differentiating, while many of the neural crest specifiers are downregulated [reviewed in 185]. Neural crest cells destined for the sympathoadrenal lineage demonstrate increased BMP signalling [186, 187]. As they further mature, they start expressing enzymes required for the synthesis of noradrenalin, e.g. tyrosine hydroxylase [188, 189], and as they acquire a neuronal fate they start expressing neurofilaments, neuron-specific tubulin and other neuronal markers [187, 190, 191]. After the acquisition of neuronal traits, the sympathoadrenal cells undergo a second migration step away from the dorsal aorta to form the secondary sympathetic ganglia, the prevertebral ganglia and the adrenal medulla in a process that probably involves FGF and NGF signalling [192]. This differentiation process also involves a myriad of transcription factors required to be expressed at the correct time and in the correct amount [reviewed in 192]. Among these are *MYCN*, which is expressed in migrating neural crest cells [193]. It seems as if *MYCN* is necessary for keeping the cell in a migrating state, in addition to being an important signal for committing the neural crest cells where it is expressed towards the sympathoadrenal lineage [193]. Like many of the neural

crest specifiers, *MYCN* expression is turned off as the neural crest cells reach their final destination and differentiate towards their ultimate phenotype [194].

As the neural crest cells differentiate and spread throughout the embryo in order to form the sympathetic nervous system, the number of cells in each differential stage must be under strict control. Developmental apoptosis is crucially important in this matter, and progenitor cells of all stages are prone to enter apoptosis if given the appropriate signals [reviewed in 195]. For instance, it has been proposed that during normal development neuronal progenitor cells compete with each other for access to NGF, and as NGF becomes limited, the losers will enter apoptosis via a pathway that includes the tumour suppressor KIF1Bβ [196].

3.2.3. From neuroblasts to neuroblastic tumours

Being an embryonal tumour, neuroblastoma is regarded as a consequence of the disordered normal development of cells from the sympathoadrenal lineage of neural crest cells [197]. As described above, the cells of the sympathetic nervous system originate from neural crest cells, going through an epithelial to mesenchymal transition, before migrating as single cells until they reach their destination. A second migration step is then initiated in order to complete the sympathetic nervous system. Migrating mesenchymal cell types are often related to cancer [reviewed in 198], and it is not difficult to imagine that the failure of neuroblasts to exit the mesenchymal mode and alternatively returning to it, could result in the development of malignant neoplasms.

Neuroblastic tumours (i.e. neoplasms of the sympathoadrenal lineage) can arise anywhere in the sympathetic nervous system, although the majority of primary tumours appear in the abdomen, with a major site being the adrenal medulla. Other common sites include the neck, chest and pelvis [199]. Neuroblastic tumours can be divided into three categories based on their morphologic features: Ganglioneuroma, ganglioneuroblastoma and neuroblastoma [200]. Ganglioneuromas appear as clusters of mature neurons surrounded by a stroma of Schwann cells, while neuroblastoma cells appear as undifferentiated tumours consisting of small, round neuroblasts. Ganglioneuroblastomas are the intermediate of the two [200]. Ganglioneuromas are well encapsulated benign tumours not capable of invading or metastasizing. Ganglioneuroblastomas are generally benign, while neuroblastoma often appear as a very aggressive cancer which commonly metastasizes [200].

3.2.4. Neuroblastoma – the disease

Neuroblastoma is not a common disease. In Sweden, the incidence over a period of 27 years was 1 case/100,000 children below the age of 15 years [201]. Despite being rare, neuroblastoma accounts for 7-10% of all diagnosed childhood cancers and 15% of all childhood cancer deaths [199, 202]. Neuroblastoma is divided into risk groups based on criteria such as age of the patient at diagnosis, International Neuroblastoma Risk Group (INRG) tumour stage and MYCN copy number (Table 1) [203, 204]. Patients in the low and intermediate risk group show fairly good prognosis, while the event-free survival (EFS) rate for patients diagnosed with high risk neuroblastoma is less than 50% [203].

Table 1: International Neuroblastoma Risk Group (INRG) Consensus Pretreatment Classification schema. Pretreatment risk group H has two entries. Blank field = "any"; DI, diploid (DNA index ≤ 1.0); HDI, hyperdiploid (DNA index > 1.0 and includes near-triploid and near-tetraploid tumours); very low risk (A-C, 5-year EFS > 85%); low risk (D-F, 5-year EFS > 75% to ≤ 85%); intermediate (intermed) risk (G-J, 5-year EFS ≥ 50% to ≤ 75%); high risk (K-R, 5-year EFS < 50%). GN, ganglioneuroma; GNB, ganglioneuroblastoma; Amp, amplified; NA, not amplified; L1, localised tumour confined to one body compartment and with absence of image-defined risk factors (IDRFs); L2, locoregional tumour with presence of one or more IDRFs; M, distant metastatic disease (except stage MS); MS, metastatic disease confined to skin, liver and/or bone marrow in children < 18 months of age; EFS, event-free survival [adapted from 203].

INRG	*Age (Months)*	*Histologic Category*	*Grade of Tumour Differentiation*	*MYCN*	*11q Aberration*	*Ploidy*	*Pretreatment Risk Group*
L1/L2		GN maturing; GNB intermixed					A Very low
L1		Any, except GN maturing or GNB intermixed		NA			B Very Low
				Amp			K High
L2	< 18	Any, except GN maturing or GNB intermixed		NA	No		D Low
					Yes		G Intermed
	≥ 18	GNB nodular; neuroblastoma	Differentiating	NA	No		E Low
					Yes		H Intermed
			Poorly differentiated or undifferentiated	NA			
				Amp			N High
M	< 18			NA		HDI	F Low
	< 12			NA		DI	I Intermed
	12 to < 18			NA		DI	J Intermed
	< 18			Amp			O High
	≥ 18						P High
MS	< 18			NA	No		C Very low
					Yes		Q High
				Amp			R High

Neuroblastoma has a high rate of spontaneous regression. The total amount of neuroblastomas that are detected clinically and regress without any treatment is approximately 5-10% [202]. This clinical phenotype (INRG MS stage, risk group C) is mainly seen in infants below the age of 18 months, and is presented with small localised primary tumours with metastases in the liver, skin or bone marrow. It is assumed that the cause of these naturally regressing tumours is the delayed activation of differentiation or apoptosis pathways [202]. In fact, it is shown that microscopic neuroblastic nodules occur uniformly in all fetuses, peaking between 17 and 20 weeks of gestation, and then gradually regressing by the time of birth [205, 206]. Additionally, neuroblastomas within INRG C rarely, if ever, evolve into any of its malignant forms, which indicates that the malignant forms of neuroblastoma affecting children older than 18 months are of a distinct type [202]. Neuroblastoma often contains a range of genomic

aberrations. Neuroblastomas that are prone to spontaneous regression are often characterised by a mitotic dysfunction, resulting in a hyperploid or near triploid phenotype with few structural abnormalities [207, 208]. On the other hand, neuroblastomas in patients one year or older are often characterised by a near-diploid or near-tetraploid karyotype in addition to numeral structural abnormalities [207, 208].

The most frequent aberration in neuroblastoma is gain of chromosome 17q, which is found to be present in a majority of tumours [209, 210]. In neuroblastoma, it seems as if chromosome 17q gain is a result of translocation from several other chromosomes [211]. A frequent aberration is an 11q loss of heterozygosity (LOH), which is a prognostic marker for poor outcome in neuroblastoma without *MYCN* amplification [212, 213]. Another frequent allelic loss occurs on chromosome 1p [214]. Deletions in chromosome 1 are also found more frequently in patients with advanced disease, but LOH on 11q and 1p rarely occurs in the same tumours [202, 215]. Many tumours with 1p LOH also contain an amplification of the 2p24 locus, which is the site of the proto-oncogene *MYCN* [216, 217]. *MYCN* amplification rarely exists without 1p LOH, whereas not all cases of 1p LOH contain MYCN amplification, an observation that suggests that 1p LOH is a prerequisite for *MYCN* amplification [202]. Patients with 1p LOH and eventual *MYCN* amplification are typically 1-5 years old with advanced stage, rapidly progressive and often fatal neuroblastoma, while patients with 11q LOH neuroblastoma are often older, with an advanced stage of disease that slowly progresses and is often fatal [202].

3.2.5. Expression of MYCN in neuroblastoma

MYCN is a member of the MYC gene family of transcription factors, all of which initiate transcription in similar ways. The MYCN transcription factors form an active complex when heterodimerised with its partner MAX [218, 219]. Both MYCN and MAX contain DNA binding motifs, and the active protein complex can initiate transcription when bound to its DNA binding sites. The most frequently targeted DNA sequence is the E-box motif (5'-CAC(A/G)TG) [220-222]. In addition, H4-K3 methylation of a promoter region has been shown to be an indicator for MYCN/MAX binding [223]. MAX can also dimerise with MAD, and the resulting complex also has an affinity towards E-boxes, but functions as a transcriptional repressor instead of an activator [224-226]. MYCN is also shown to be involved in transcriptional repression in neuroblastoma [227]. Here, MYCN has been

demonstrated to act as a bridge between the DNA binding protein Sp1 and the repressor histone deacetylase (HDAC), resulting in transcriptional repression of tissue transglutaminase (TG2).

The amplification of a gene is a result of chromosomal rearrangements leading to an increased copy number of the amplified gene. Amplification of *MYCN* was first observed in 1983, when it was shown that *MYCN* could be amplified up to 140 fold [228]. It seems as if all copies of the amplified gene contribute to the expression of *MYCN* and that the increased gene number is the reason for the high *MYCN* mRNA expression in *MYCN* amplified (MNA) neuroblastoma cells [217, 229]. Generally speaking, it seems that levels of mRNA resulting from *MYCN* amplifications reach a 40-60 fold increase in comparison to single copy cell lines with a low expression of *MYCN*, and that the increase in mRNA level is not always proportional to the number of gene copies [230].

As described above, *MYCN* is naturally expressed in neural crest cells of the sympathoadrenal lineage, which is assumed to be important for maintaining the cells in a migrating state [193]. In cancer terminology, mesenchymal cells that are able to migrate are closely related to a malignant phenotype, so it is therefore not surprising that a protein devoted to maintaining this phenotype is a potent oncogene. Indeed, *MYCN* amplification is one of the most prominent prognostic indicators for a bad outcome in neuroblastoma [203]. *MYCN* has been shown to be causally involved in tumourigenesis and tumour progression, as transgene mice expressing *MYCN* in the neuroectoderm develop neuroblastoma several months after birth [231].

3.2.6. MYCN targets

The exact mechanism *MYCN* uses to mediate its oncogenic effect is still largely unknown, but some pathways are emerging as likely candidates for executing the malignant potential of *MYCN*. Here follows a brief description of a few direct targets of MYCN:

MYCN expression has been shown to increase proliferation by shortening the time used to progress through the cell cycle [232]. E2F1-3 are transcription factors which mainly regulate the expression of numerous genes necessary for the S-phase of the cell cycle such as *thymidine kinase*, *dihydrofolate reductase* (*DHFR*), *DNA Pol*α and *cell division cycle 6* (*cdc6*). Thus, active E2F1-3 pushes the cell into the S-phase [reviewed in 233].When E2F1-3

are bound by hypophosphorylated retinoblastoma protein (RB), it is inactive, and the cell remains in the G1 phase. Phosphorylation of RB through the cyclin D/CDK4/6 complex removes RB from the RB/E2F complex, thereby releasing active E2F. Several possible MYCN targets engaged in the cell cycle progression are probably functioning through regulation of the E2F1-3 transcription factors [reviewed in 234]. *E2F1* has been demonstrated to be a transcriptional target of MYCC, and there are indications that MYCN also regulates *E2F1* expression, while at the same time E2F1-3 activates the expression of *MYCN* itself [reviewed in 234].

MYCN is known to increase the susceptibility of cells entering apoptosis following cellular stress such as DNA damage, survival factor withdrawal, substrate detachment and hypoxia [reviewed in 235]. p53 is known as the guardian of the genome, and is involved in DNA repair and/or initiation of apoptosis as a result of extensive DNA damage. It has recently been reported that p53 is a direct transcriptional target of MYCN [236], and this finding suggests a mechanism for the *MYCN*-driven p53-dependent apoptosis necessary for achieving control of rapidly dividing neuroblasts in normal development. However, MYCN is also a transcriptional activator of *MDM2*, which is a negative regulator of p53 [237].

Bmi1 is a transcriptional repressor required for the self-renewal of stem cells of the central- and peripheral nervous system [238], and are highly expressed in a vast majority of primary neuroblastoma tumours regardless of *MYCN* status [239]. Ochiai *et al.* have shown that its promoter contains E-box sequences and that as a result, *Bmi1* is a direct transcriptional target of MYCN [240]. In addition, they have shown that Bmi1 directly downregulates several tumour suppressors in neuroblastoma, among them *KIF1Bβ* and *TSLC1*, both of which have been correlated to a bad prognosis when downregulated [241, 242]. KIF1Bβ is an important signal for apoptosis of neural progenitor cells when NGF access is reduced [196]. The exact function of TSCL1 in neuroblastoma is not known, but it is suspected that it demonstrates an antiproliferative and/or proapoptotic activity [241].

3.2.7. Targeted MYCN downregulation

Given that *MYCN* is a strong oncogene being expressed naturally primarily in embryonal life only, it has long been regarded as an ideal candidate for targeted therapy [243]. The first approaches for a targeted reduction of *MYCN* expression were conducted by using standard antisense technology [244]. Here, it was found that repression of *MYCN* expression leads to

reduced proliferation and differentiation towards a more neuronal phenotype in a MNA neuroblastoma cell line. Peptide nucleic acids (PNA) are nucleic acid analogues in which the sugar backbone is replaced by a synthetic peptide backbone. The resulting mimic is uncharged, and thus binds with greater affinity to complementary nucleic acids (both DNA and RNA) than nucleic acids. Because there are no naturally occurring PNAs, they are not targets of enzymatic degradation [reviewed in 245]. PNAs have successfully been used for targeted downregulation of both *MYCN* mRNA [246, 247] and the *MYCN* gene at the DNA level [248]. Although fairly effective and selective, PNAs are expensive to design and synthesise. As RNAi has evolved as a superior tool for targeted gene suppression, transient siRNA-based *MYCN*-knockdown has also been used to show reduced cell growth, induced differentiation and induced apoptosis in MNA neuroblastoma cells [249, 250].

The SHEP Tet21N system has been evolved for mainly studying *MYCN*-related cell cycle effects [232]. Neuroblastoma cell lines established in culture appear to be heterogenous, and can be divided into three different subgroups: neuroblastic (N), substrate adherent (S) and intermediate (I) cell types. N-type cells appear as being small, rounded and loosely attached, with numerous neurite-like processes. The S-type is larger, flatter and more strongly substrate adherent, and appears to be fibroblastic/epithelial and do not express any neuronal markers. The I-type appears as a morphological intermediate between the N- and S- types, and can be induced to differentiate towards both subgroups [251, 252]. In the SHEP Tet21N system, a *MYCN* gene is stably transfected into an S-type clone derived from the I-type SKNSH neuroblastoma cell line [232]. In this Tet-Off system, the expression of *MYCN* can be turned off by adding the inducer tet (confer with Chapter 3.1.9 above).

3.2.8. MiRNA in neuroblastoma

MiRNAs are regarded as vital contributors to the pathogenesis of a wide array of tumours [92, 93]. The first expression profiling study indicated that miRNAs were differentially expressed in various genomic subtypes of neuroblastoma [253]. It has now been established that MNA and other chromosomal imbalances lead to vast dysregulation of the miRNA expression in primary neuroblastoma tumours [reviewed in 254]. As mentioned above, MYCN is a transcription factor that mainly induces the transcription of genes with E-boxes in the proximity of their promoter. MiRNAs are also expressed from RNA polII promoters, and MYCN has been shown to regulate the expression of miRNAs [255]. MiRNAs also have the

potential to act as both tumour suppressors and oncogenes in neuroblastoma [reviewed in 254].

An example of a miRNA acting as a tumour suppressor is *miR-34a*, which is frequently downregulated in primary neuroblastomas [256]. *MiR-34a* is located in a region of chromosome 1p36 that is often deleted in neuroblastoma, and is shown to have an anti-proliferative effect when overexpressed in neuroblastoma cell lines [256]. Oncogenes found to be targets of *miR-34a* are the transcription factor *E2F3* and *MYCN* [256, 257].

The *miR-17* family of miRNAs are expressed from three different miRNA clusters located on three different chromosomes: The *17-5p-92* (*miR 17, -18a, -19a, -20a, -19b1 and -92a1*), the *miR 106a-363* (*miR 106a, -18b, -20b, -19b2, -92a2, -363*) and the *miR 106b-25* (*miR 106b*, *-93, -25*) [258]. The *miR-17* family is shown to be vital for development of the embryo and initiating of the differentiation of pluripotent stem cells [259]. All three clusters harbour E-box motifs in its proximity [260], and all clusters are shown to be directly regulated by MYCN [261, 262]. Several members of the *miR-17* family, especially those of the *17-5p-92* cluster, are shown to act as potent oncogenes in neuroblastoma cells [261, 262]. This is a clear indication that at least parts of the oncogenic effect of *MYCN* are mediated directly through the transcriptional activation of miRNAs. MYCN is primarily a transcriptional activator, and as described above, only rarely acts as a transcriptional repressor. So far, no miRNA has been shown to be directly downregulated by MYCN. However, miRNAs can be inversely correlated to *MYCN* expression as a result of indirect mechanisms [253].

In paper III, we document for the first time that *miR-92b* might be activated by MYCN. We also suggest that most miRNAs inversely correlated to MYCN are probably involved in differentiation.

3.2.9. *DKK3* and neuroblastoma

In neural crest development, the BMP-, FGF- and Wnt pathways are the main regulators of neurulation and the subsequent formation of neural crest cells [184]. The disturbance of these early developmental pathways has been shown to be involved in several other forms of cancers [263-265], and these pathways are therefore interesting to study in neuroblastoma as well. In the canonical Wnt pathway, a Wnt protein binds to its trans-membranous receptor frizzled and the co-receptor low-density lipoprotein receptor-related protein 5 (LRP5)/LRP6.

This leads to activation of an intracellular pathway that ultimately leads to the accumulation of the protein β-catenin in the nucleus where it activates the T-cell factor/lymphocyte enhancer factor (TCF/Lef) family of transcription factors. Activation of the canonical Wnt pathway regulates a wide array of biological effects, including activation of cell cycle progression and proliferation, inhibition of apoptosis, regulation of embryonic development, cell differentiation, cell growth and cell migration [reviewed in 266]. Wnt signalling can also activate independent non-canonical pathways, the two most described being: 1. The Wnt/Ca^{2+} pathway, which activates the protein kinase C and the Ca^{2+}- calmodulin dependent protein kinase II, 2. the cytoskeleton pathway, which regulates the organisation and formation of the cytoskeleton and planar cell polarity [reviewed in 267]. There are also several other less described and characterised non-canonical Wnt pathways [268].

The family of dickkopf proteins (DKK1-4 and Soggy) is a group of secreted glycoproteins primarily regarded as inhibitors of the Wnt pathway [269]. While DKK1 and DKK2 inactivate Wnt signalling by obstructing the binding between LRP5/6 and Wnt ligands, DKK3 is not able to interact with LRPR6 [270]. DKK3 has been revealed to have distinct roles in the modulation of the Wnt pathway, depending on the cell types being studied. DKK3 increases Wnt signalling in mouse glia cells and HEK293 [271], but inhibits Wnt signalling in pheochromocytoma cells from rat (PC12) [272] and osteocarcinoma (Saos-2) cells [273]. Since DKK3 does not bind to the LRPR5/6 receptors, little is known about the molecular basis for DKK3-dependent Wnt inhibition. DKK3 does however bind to the membrane bound Wnt inhibitor Kremen, and Nakamura and Hackam have proposed that DKK3 potentiates Wnt signalling by facilitating a relocation of Kremen from the cell membrane by endocytosis [270].

DKK3 is an established tumour suppressor shown to be downregulated in a range of tumour-derived cells, e.g. Saos-2, hepatoblastoma, acute lymphoblastic leukaemia and non-small-cell lung cancer [reviewed in 269]. The downregulation of *DKK3* is often a result of hypermethylation of the *DKK3* promoter [274, 275], whereas the overexpression of *DKK3* has been demonstrated to suppress tumour growth of, e.g. Saos-2 [273], prostate cancer [274, 276] and neuroblastoma [277].

It has been shown that there is an inverse correlation between the expression of *MYCN* and the Wnt antagonists *DKK1* and *DKK3* in neuroblastoma [278, 279]. In particular, the

correlation between *DKK3* and *MYCN* has been proven to be a strong one by Koppen *et al.* [277]. Here, it was documented that *DKK3* is a marker for neuroblastic tumour maturation and that it is indirectly downregulated by MYCN. In paper IV, we show that *DKK3* is repressed by *miR-92a*, *miR-92b* and *let-7e*, all of which are MYCN–regulated miRNAs [261, Paper III].

4. Aims

Neuroblastoma with *MYCN* amplification represents the most aggressive form of this disease. Although *MYCN* has been regarded as the most prominent prognostic indicator for bad outcomes, the role of *MYCN* in neuroblastoma tumourigenesis remains largely unknown. The silencing of *MYCN* and its downstream targets are attractive goals for targeted therapy, but very little is known about the long-term effects of *MYCN* silencing of MNA neuroblastomas. The main aim of this study was to establish an efficient knockdown of *MYCN* in MNA neuroblastoma cell lines in a stable and inducible manner and to use these cell lines to obtain further knowledge of *MYCN* and its downstream targets, including miRNAs.

Paper I

Evaluate available options for inducible expression of shRNA. Design and establish an inducible promoter system that is tight when uninduced, and which has a high expression of shRNA when induced. In addition, the vector system should allow easy incorporation of any desired shRNA.

Paper II

Establish MNA cell lines with stably integrated shRNA expression targeting *MYCN* under inducible control using the promoter system designed and developed in Paper I.

Paper III

Use shRNA to silence *MYCN* and study the differential expression of miRNA expression both before and after knockdown. Investigate the biological effect of the miRNA with the most pronounced change in expression.

Paper IV

Previous data published by others has suggested that the possible tumour suppressor *DKK3* was regulated by MYCN in an indirect manner. We aimed to use the miRNA profiling data obtained in Paper III to search for MYCN-regulated miRNAs with predicted targets in the *DKK3* 3' UTR, as well as investigating whether MYCN regulates *DKK3* through miRNAs.

5. Discussion

5.1. Papers I and II

5.1.1. Brief description of the studies

In Paper I, we compared the properties of six polIII promoters with tet-inducible expression. Four of the promoters were previously described by others [140, 148, 149, 280], while two versions of the H1 promoter were novel designs. The tightness and expression efficiency of the promoters in an induced and uninduced state were compared using a luciferase reporter system. Here, cells containing a stable expression of TetR were transiently cotransfected with three plasmids: a plasmid with a constitutive expression of the firefly luciferase reporter, a plasmid with a constitutive expression of β-galactosidase for normalisation and a plasmid expressing an anti-luciferase shRNA expressed from the promoter being evaluated. Luciferase activities were measured and normalised against β-galactosidase expression. The experiments were performed with the absence of the inducer Dox for an evaluation of tightness, as well as in the presence of Dox for an evaluation of transcription efficiency.

For both U6 and H1 promoters, constructs containing only one tet operator in the promoter were unacceptably leaky. Overall, we found the novel H12O2 promoter to perform slightly better than the similar U62O2 promoter when directly compared.

In Paper II, we introduced a shRNA (aMN-1658) that specifically downregulated the MYCN protein expression ~90% without any observations of off-target effects. This shRNA was inserted into the H12O2 US/DS inducible promoter cassette designed in Paper I before being stably transduced to the MNA neuroblastoma cell lines Kelly and SK-N-BE(2) using an MLV retroviral delivery system. The resulting RV-1658 cell lines appeared with a similar morphology to control cells in an uninduced state. When induced with 1 µg/ml dox, MYCN expression was efficiently downregulated, the cells differentiated towards neuron-like cells, entered G1 arrest and showed a significantly reduced clonogenic growth.

5.1.2. Discussion

The novel H12O2 promoter designed by us was developed by introducing a second TetO2 downstream of the TATA-box in a commercially available pENTRH1-O2 plasmid

(Invitrogen). The sequence between the TATA-box and the transcription start (25 bp) can be altered without affecting the transcription efficiency of the H1 promoter as long as the spacing between the two remains the same [281]. The TetO2 sequence of 19 bp ends with the nucleotides AGA, which is a part of the BglII restriction site (AGATCT). The design of the H12O2 promoter allows the positioning of a stuffer sequence directly downstream of the transcription start site. This stuffer can be removed by BglII restriction enzymes and replaced by a properly designed shRNA sequence targeting a desired gene.

The conditional expression of shRNAs is feasible from both polIII promoters and polII promoters. As described above, it seems that conditional expression from polII promoters may provide some advantages over polIII promoters such as less off-target effects [177], tighter regulation [112, 154] and the possibility of expressing several shRNAs in a polycistronic manner [156]. Even so, shRNAs expressed from polIII promoters seem more potent than similar shRNAs expressed from polII promoters, thus allowing a higher efficiency when the silencing of highly expressed targets is desired [124]. In MNA neuroblastoma cell lines, the expression of *MYCN* mRNAs is generally 40-60 fold higher than in single copy cells [230]. As a result of this, the potency of the shRNAs is of great importance when *MYCN* silencing in MNA cell lines is considered.

In Paper II, we have described a system for the conditional and stable expression of shRNAs targeting *MYCN* in MNA neuroblastoma cell lines. One of the main reasons for developing this cell line was the desire to specifically study the long-term effect of *MYCN* knockdown in MNA cell lines. The SHEP Tet21N system is perhaps the most widely used cell system for studying the effect of *MYCN* silencing in neuroblastoma [232]. Here, *MYCN* is introduced to an S-type neuroblastoma cell line normally not expressing *MYCN*. When S-type neuroblastoma cell lines are exposed to the vitamin A metabolite retinoic acid (RA), they enter apoptosis, while N-type cells generally differentiate towards a more neuronal phenotype [282]. As a consequence, this system is not suitable for studying the effect of *MYCN* on differentiation in neuroblastoma cell lines. The SHEP Tet21N system however has proven especially valuable for determining the effect of *MYCN* on proliferation and apoptosis.

Traditional antisense technology has previously been used for the stable silencing of *MYCN* in non-MNA neuroblastoma cell lines with a high MYCN expression [283]. Still, antisense technology is not efficient enough to successfully silence *MYCN* in MNA cell lines, as it has

been shown that the antisense:sense RNA ratio must be on the order of 1000:1 for obtaining antisense-sense duplexes of 50% of the target mRNA [284]. Successful antisense-based silencing of *MYCN* in the IMR-32 cell line has been reported, but here the authors used an Epstein-Barr viral approach in which the antisense *MYCN* expression was magnified by episomal replication [285]. Here, the *MYCN* suppression was significant, though no differentiation was observed. Later experiments using siRNAs targeting *MYCN* have demonstrated that IMR-32 differentiates extensively upon *MYCN* silencing [250]. This discrepancy might be a result of off-target effects since it has been shown that *MYCN* antisense RNAs are targets for the interferon pathway in a MNA cell line [286].

The superior efficiency of shRNA compared to antisense approaches is apparent when considering the RV-1658 constructs presented in Paper II. Here, we achieved a specific, efficient and conditional downregulation of *MYCN* in two MNA cell lines as a result of shRNA being expressed from a single genomic insert. In addition to this, no off-target effects resulting from interferon response were detected. When using any type of small RNA, the off-target effects most widespread seem to be those resulting from saturation of the miRNA pathway [180]. We did not observe any signs of such off-target effects in our study, although they cannot be ruled out since these symptoms could be very difficult to detect.

We chose to use a MLV retroviral system for stably delivering the inducible expression cassettes to neuroblastoma cell lines. The inducible promoter described in Paper I can easily be gated into a retroviral expression vector, which was then used to transfect the Hek-293 Phoenix packaging cell line for the synthesis of retroviral particles. The entire process utilises vectors and cell lines easily propagated in any lab with suitable facilities, and thus it is relatively easy and cost efficient to produce any new shRNAs towards any target in any dividing human cell. After induction of the RV-1658 cell lines, it typically took 3-5 days before full silencing of *MYCN* was achieved. As a result of this, the inducible system is not optimal for investigating direct targets of MYCN.

As described in Paper II, we observed minimal amounts of leakage of anti-*MYCN* shRNA in an uninduced state within the time frame the cells were grown in. Nevertheless, some leakage is inevitable when Tet-inducible polIII promoters are being used. In our experience, there was no significant leakage within the first month after transduction. When we tried to isolate single clones of transduced cells, leakage in uninduced cells was evident. After proliferating

for approximately 10 weeks, the cells appeared to be morphologically undifferentiated, but expressed up to 30% less MYCN than the control cells. Yet, induction led the MYCN levels to drop further, which was then followed by differentiation of the cells (data not included in the manuscripts). This suggests that a relatively fast drop of MYCN concentration initiates differentiation and growth arrest, rather than an absolute concentration threshold. This however is an issue that must be further investigated before any conclusions can be drawn.

5.2. Paper III

5.2.1. Brief description of the study

MYCN was downregulated using transient shRNA in the MNA cell lines SKNBE(2) and Kelly. MiRNA expression profiling was performed on two independent experiments, and miRNAs differentially expressed as a result of *MYCN* silencing were identified. We found most members of the three clusters of the miR 17 family to correlate with *MYCN* expression, an observation supported by previous findings. Moreover, we observed a clear correlation between *MYCN* and *miR-92b* and *miR-103*. Several non-clustered miRNAs were found to be negatively correlated by *MYCN*.

The miRNA that was most upregulated following *MYCN* suppression was *miR-21*, a miRNA that has been shown to act as an oncomir in a range of other tumours. The potential function of *miR-21* in neuroblastoma was investigated further, but no effect on proliferation or differentiation was observed. Hence, we were not able to establish any role for *miR-21* expression in differentiating neuroblastoma cells.

5.2.2. Discussion

Apart from the members of the miR 17 family, we observed two miRNAs potentially being upregulated by MYCN: *miR-92b* and *miR-103*, neither of which have been experimentally validated as direct MYCN targets.

MiR-103 expression is linked to mesenchymal stem cells [reviewed in 287], which have been recently argued to be a sub-population of neural crest cells [288]. *MiR-103* is expressed in the majority of human cells, but is generally more expressed in the brain. It is expected to be involved in metabolism. So far, oesophageal carcinoma is the only cancer in which it has a prognostic value [reviewed in 289].

MiR-92b appears to be a miRNA that is primarily expressed in neuronal-specific stem cells, the developing brain or brain tumours [290]. Deep sequencing has shown that *miR-92b* is highly expressed in human embryonic stem cells, but diminishes during differentiation [291]. In stem cells, *miR-92b* has been reported to push cells to a proliferative state by downregulating p57 [292]. Despite the indications of *miR-92b* being an oncomir in neural neoplasms, very little has been done to elucidate its potential role in various cancers.

We also found 11 miRNAs inversely correlated to *MYCN* expression, with many of these being shown to be involved in neuronal differentiation in other cell systems. Theoretically, some of these miRNAs could be tumour suppressors inhibited by MYCN, though MYCN is predominately a transcriptional activator, and has not yet been shown to directly repress any miRNA. Thus, miRNAs being inhibited by MYCN are expected to be regulated in an indirect manner. The miRNA most elevated after *MYCN* silencing was *miR-21*. This miRNA has been shown to be highly expressed in a variety of tumours and acts as an oncomir [293]. In addition, increased *miR-21* expression has been documented in differentiating SH-SY5Y non-MNA neuroblastoma cells [294]. We did not find any effects on neither proliferation nor differentiation when *miR-21* mimics or *miR-21* antagomirs were introduced to the SK-N-BE(2) cell line. Furthermore, *miR-21* antagomir did not inhibit differentiation when MYCN was downregulated. This indicates that *miR-21* does not have a proliferative effect in MNA neuroblastoma and that its increase is a consequence of differentiation. Even so, we were not able to reveal a functional role for *miR-21* during the differentiation of neuroblasotoma cells.

The lack of phenotypic changes observed by *miR-21* mimics and antagomirs are in accordance with data recently published by Mestdagh *et al.* [295]. Here, miRNAs correlating with *MYCN* (i.e. possibly transactivation targets of MYCN) were shown to have strongly predicted target enrichment on mRNAs negatively correlated to these miRNAs (i.e. possible targets for MYCN-activated miRNAs). This was not the case for miRNAs negatively correlated with *MYCN* and their putative targets. These observations suggest that it is primarily MYCN-activated miRNAs that account for the miRNA-mediated regulation of mRNAs.

5.3. Paper IV

5.3.1. Brief description of the study

Bell *et al.* have shown that the transcription of the Wnt antagonist DKK3 is downregulated by MYCN. Koppen *et al.* later revealed that this regulation was in an indirect manner. By conducting an *in silico* analysis we found that both *miR-92a* and *miR-92b*, two of the miRNAs upregulated by MYCN in Paper III, shared a predicted miRNA target site on the DKK3 3' UTR sequence. Additionally, members of the *let-7* family were predicted to bind to another target site. We hypothesised that MYCN regulates *DKK3* expression through miRNAs.

By the use of ELISA, we first demonstrated that DKK3 secretion in the culture medium was increased when *MYCN* was downregulated using the inducible Kelly and SK-N-BE(2) RV-1658 cell lines described in Paper II and the SHEP Tet21N cell line. The *DKK3* 3' UTR sequence was cloned downstream of the luciferase gene, and repression of the luciferase expression was observed when cotransfecting these constructs with mimics of *miR-92a*, *miR-92b* and *let-7e*. Mutation of the target sites led to a complete rescue of luciferase expression for *miR-92a* and *miR-92b*, but not for *let-7e*. The reduction of *miR-92a* and *miR-92b* using antagomirs led to an increased secretion of DKK3 in the MNA cell lines SK-N-BE(2) and Kelly, while transfection of *miR-92a* and *miR-92b* mimics into non-amplified cell lines SK-N-AS and SH-SY-5Y led to downregulation of *DKK3* expression. *Let-7e* mimics only led to a moderate reduction of DKK3 levels compared to those obtained by the *miR-92a* and *miR-92b* mimics. DKK3 measurements were performed by ELISA and qRT-PCR. We also performed methylation-specific PCR on genomic DNA from 10 primary neuroblastoma samples (five MNA, five non-MNA) and five neuroblastoma cell lines (three MNA, two non-MNA), and found no hypermethylation of the *DKK3* promoter.

The immunohistochemistry of 25 primary neuroblastoma tissue samples from various biological subsets showed an inverse correlation between the expression of *MYCN* and *DKK3*. DKK3 was mainly detected in the vasculature of the tumours, illustrated by its co-localisation with the vascular endothelial marker CD31.

5.3.2. Discussion

DKK3 is a secreted antagonist of the Wnt pathway. To establish whether MYCN downregulates DKK3 secretion, we utilised the RV-1658 cell lines described in Paper II as a model system. This system was well suited for these experiments since we could suppress *MYCN* for a longer period, thereby allowing the cells to differentiate for five days before measuring DKK3 levels. Fresh media were then added to the cells 24 hrs prior to the measurement of accumulated DKK3 by enzyme-linked immunosorbent assay (ELISA). To the best of our knowledge, this is the first time changes in the secretion of endogenous DKK3 protein have been measured directly in neuroblastoma. Previous studies have either measured mRNA levels or the expression of ectopic Flag-tagged DKK3 [270, 277, 278]. Nonetheless, we cannot be certain that the observed upregulation of DKK3 following *MYCN* silencing is solely the effect of changes in *miR-92a/b* and *let-7* alone, or whether additional unknown factors are involved.

We have established that *DKK3* expression is regulated by *miR-92a*, *miR-92b* and *let-7*. In Paper III, we showed that *miR-92a* and *92b* are downregulated when *MYCN* expression is repressed. Two separate *miR-92a* genes are found in the human genome, one in the *miR-17-92* cluster and one in the paralogue *miR-106a* cluster, and both clusters are direct transcriptional targets of MYCN [261, 262]. *MiR-92b* is expressed as a single intergenic miRNA on chromosome 1q, and little is known about the promoter of *miR-92b*. An E-box is located upstream of the *miR-92b* gene, but no ChIP analysis has been performed to investigate whether this is a direct binding site for MYCN. The mature sequence of *miR-92b* is identical to that of *miR-92a* apart from three nucleotides, which does not theoretically impair with seed sequence binding. Thus, *miR-92a* and *miR-92b* share the same targets. *MiR-92b* is mainly expressed in neuronal-specific stem cells, the developing brain or brain tumours [290]. The expression of *miR-92b* instead of *miR-92a* in these tissues could be an approach for targeting *miR-92a/b* binding sites, while avoiding expression of the remaining miRNAs of the *miR-17-92* cluster. Since the *miR-17-92* cluster is a direct target of MYCN, the distinct expression of *miR-92b* is probably governed by other mechanisms.

The biological function of *DKK3* is debated. *DKK3* knock-out mice are viable, fertile and show no obvious abnormalities [296]. The lack of a distinct *DKK3* knockout phenotype might be a result of Soggy replacing DKK3 in important pathways. Although DKK3 does not

interact with LRP5/6 [270], DKK3-mediated repression of the canonical Wnt pathway has been reported in some cellular settings [272, 273]. Others have reported Wnt activation as a result of *DKK3* expression [271]. A proposed mechanism for DKK3-mediated activation of the Wnt pathway has been described by Nakamura *et al.* [270], whereas the mechanism of DKK3-mediated inhibition of the canonical Wnt pathway remains unknown. Upon discovery of the inverse correlation between *MYCN* and *DKK3*, Bell *et al.* proposed that MYCN could exert its proliferative effect by allowing high canonical Wnt signalling through downregulation of the Wnt inhibitor *DKK3* [278]. However, Koppen *et al.* later documented that DKK3 reduces proliferation in neuroblastoma cells, but not through the canonical Wnt pathway [277]. Here, it was suggested that DKK3 may exert its effect through the non-canonical Wnt pathways. It was also debated whether the Wnt pathway was a significant contributor to malignancy in MNA neuroblastoma. It has been demonstrated that the canonical Wnt pathway is deregulated in high-risk non-MNA neuroblastoma, but not in MNA neuroblastoma. In high-risk non-MNA neuroblastoma, this was proposed to cause increased proliferation as a result of a higher expression of *MYCC* and *cyclinD* [297].

DKK3 is shown to be necessary for Activin/nodal (members of the transforming growth factor beta (TGF-β) superfamily) signalling in *Xenopus* embryos [298]. Here, DKK3 was shown to exert its function by maintaining normal levels of Smad4, a key downstream mediator of all TGF-β pathways. TGF-β signalling induces inhibition of proliferation and increased differentiation of many neuroblastoma cells, and it has been proposed that the effect of retinoic acid is dependent on establishing and maintaining a negative autocrine growth loop involving TGF-β1 [299]. It was also proposed that failure to establish such a loop might be a reason for the resistance to retinoic acid shown by many neuroblastoma cell lines. These results implicate that the loss of DKK3 could theoretically be a reason for a loss of responsiveness to TGF-β signalling. Another member of the TGF-β family shown to be of relevance in neuroblastoma is *Activin A*. Schramm *et al.* revealed that enhanced expression of Activin A suppresses proliferation and colony formation in MNA neuroblastoma cells. It also inhibits neuroblastoma growth and angiogenesis *in vivo*, and is highly expressed in differentiated, but not undifferentiated neuroblastomas [300, 301]. *Activin A* also seems to be downregulated by MYCN [302]. This potential role of DKK3 in TGF-β signalling is highly speculative, and further investigations are needed in order to elucidate whether DKK3 does interact with TGF-β signalling in neuroblastoma.

We analysed a selection of primary tumours by immunohistochemistry, and found that DKK3 was expressed in the tumour endothelium. The amount of DKK3 in the endothelium was inversely correlated to *MYCN* amplification. Expression of DKK3 in the tumour endothelium rather than the tumour parenchyma has been described in many other types of cancer [303-308]. Untergasser *et al.* used murine melanoma cells with ectopical overexpression of DKK3 to establish xenografts in mice. They observed that DKK3 overexpression resulted in slightly larger tumours with a significantly increased microvessel density (MVD) [304]. MVD is a measure of angiogenesis which is considered a prognostic indicator that correlates with an increased risk of metastasis in various epithelial cancers. These results, and the observation of a high expression of DKK3 in the developing heart and blood vessel system in both mice and chicken embryos, suggests that DKK3 has a conserved role in vascularisation [309]. The observations of DKK3 functioning as an inducer of angiogenesis is contradictory to its established role as a tumour suppressor. Compared to low-risk ganglioneuromas, we observed lower expression of DKK3 in the vasculature of high-risk MNA neuroblastomas, an observation which is supported by others [277].

In summary it seems as if DKK3 has distinct roles in cancer cells and epithelial cells involved in angiogenesis. In pancreatic cells, the pro-angiogenetic effect of DKK3 did not contribute to a poor prognosis [303]. Very little is known of the exact function of DKK3 as a tumour suppressor in neuroblastoma. It does not seem to influence the canonical Wnt pathway, but could be involved in regulation of some of the non-canonical pathways. However, none of the Wnt pathways has so far been shown to play a significant role in contributing to the proliferation in MNA neuroblastoma. There is a theoretical possibility that DKK3 are involved in TGF-β signalling in neuroblastoma, but no research has thus far confirmed this.

6. Conclusions

In this thesis we have focused on the oncogene *MYCN* that is often amplified in neuroblastoma. We have designed and developed a system that allows conditional expression of any shRNA from a Tet-inducible RNA polIII H1 promoter (Paper I). In Paper II we used this Tet-inducible promoter to express an anti-*MYCN* shRNA in two MNA neuroblastoma cell lines. The shRNA was introduced to the genome of the cells by the use of an MLV based retroviral vector system. Efficient suppression of MYCN was observed within 3 days after addition of the inducer Dox to the media.

In Paper III the effect of *MYCN* suppression on miRNA expression was investigated. We found that *MYCN* downregulation resulted in a decrease of several miRNAs, many of which are members of the miR 17 family. In addition we found several miRNAs being upregulated as *MYCN* was suppressed. One of these was *miR-21*, which was investigated further. We could not reveal any function for *miR-21* in differentiation or proliferation in MNA neuroblastoma.

Other miRNAs demonstrated to be affected by *MYCN* expression were *miR-92a*, *miR-92b* and *let-7e*. In Paper IV we showed that these three miRNAs suppresses the expression of *DKK3*, a tumour suppressor frequently downregulated in MNA neuroblastoma.

7. References

1. CRICK FH. On protein synthesis. Symp Soc Exp Biol 1958:12:138-163.

2. Britten RJ, Davidson EH. Gene regulation for higher cells: a theory. Science 1969:165:349-357.

3. Vaquerizas JM, Kummerfeld SK, Teichmann SA, Luscombe NM. A census of human transcription factors: function, expression and evolution. Nat Rev Genet 2009:10:252-263.

4. Napoli C, Lemieux C, Jorgensen R. Introduction of a Chimeric Chalcone Synthase Gene into Petunia Results in Reversible Co-Suppression of Homologous Genes in trans. Plant Cell 1990:2:279-289.

5. van der Krol AR, Mur LA, Beld M, et al. Flavonoid genes in petunia: addition of a limited number of gene copies may lead to a suppression of gene expression. Plant Cell 1990:2:291-299.

6. Izant JG, Weintraub H. Inhibition of thymidine kinase gene expression by anti-sense RNA: a molecular approach to genetic analysis. Cell 1984:36:1007-1015.

7. Guo S, Kemphues KJ. par-1, a gene required for establishing polarity in C. elegans embryos, encodes a putative Ser/Thr kinase that is asymmetrically distributed. Cell 1995:81:611-620.

8. Fire A, Xu S, Montgomery MK, et al. Potent and specific genetic interference by double-stranded RNA in Caenorhabditis elegans. Nature 1998:391:806-811.

9. Elbashir SM, Harborth J, Lendeckel W, et al. Duplexes of 21-nucleotide RNAs mediate RNA interference in cultured mammalian cells. Nature 2001:411:494-498.

10. Cerutti H, Casas-Mollano JA. On the origin and functions of RNA-mediated silencing: from protists to man. Curr Genet 2006:50:81-99.

11. Lee RC, Feinbaum RL, Ambros V. The C. elegans heterochronic gene lin-4 encodes small RNAs with antisense complementarity to lin-14. Cell 1993:75:843-854.

12. Lagos-Quintana M, Rauhut R, Lendeckel W, Tuschl T. Identification of novel genes coding for small expressed RNAs. Science 2001:294:853-858.

13. Lau NC, Lim LP, Weinstein EG, Bartel DP. An abundant class of tiny RNAs with probable regulatory roles in Caenorhabditis elegans. Science 2001:294:858-862.

14. Lee RC, Ambros V. An extensive class of small RNAs in Caenorhabditis elegans. Science 2001:294:862-864.

15. Bernstein E, Caudy AA, Hammond SM, Hannon GJ. Role for a bidentate ribonuclease in the initiation step of RNA interference. Nature 2001:409:363-366.

16. Knight SW, Bass BL. A role for the RNase III enzyme DCR-1 in RNA interference and germ line development in Caenorhabditis elegans. Science 2001:293:2269-2271.

17. Grishok A, Pasquinelli AE, Conte D, et al. Genes and mechanisms related to RNA interference regulate expression of the small temporal RNAs that control C. elegans developmental timing. Cell 2001:106:23-34.

18. Hutvagner G, McLachlan J, Pasquinelli AE, et al. A cellular function for the RNA-interference enzyme Dicer in the maturation of the let-7 small temporal RNA. Science 2001:293:834-838.

19. Ketting RF, Fischer SE, Bernstein E, et al. Dicer functions in RNA interference and in synthesis of small RNA involved in developmental timing in C. elegans. Genes Dev 2001:15:2654-2659.

20. Ambros V, Bartel B, Bartel DP, et al. A uniform system for microRNA annotation. RNA 2003:9:277-279.

21. Cai X, Hagedorn CH, Cullen BR. Human microRNAs are processed from capped, polyadenylated transcripts that can also function as mRNAs. RNA 2004:10:1957-1966.

22. Lee Y, Kim M, Han J, et al. MicroRNA genes are transcribed by RNA polymerase II. EMBO J 2004:23:4051-4060.

23. Bartel DP. MicroRNAs: genomics, biogenesis, mechanism, and function. Cell 2004:116:281-297.

24. Lee Y, Jeon K, Lee JT, et al. MicroRNA maturation: stepwise processing and subcellular localization. EMBO J 2002:21:4663-4670.

25. Lee Y, Ahn C, Han J, et al. The nuclear RNase III Drosha initiates microRNA processing. Nature 2003:425:415-419.

26. Han J, Lee Y, Yeom KH, et al. The Drosha-DGCR8 complex in primary microRNA processing. Genes Dev 2004:18:3016-3027.

27. Denli AM, Tops BB, Plasterk RH, et al. Processing of primary microRNAs by the Microprocessor complex. Nature 2004:432:231-235.

28. Gregory RI, Yan KP, Amuthan G, et al. The Microprocessor complex mediates the genesis of microRNAs. Nature 2004:432:235-240.

29. Landthaler M, Yalcin A, Tuschl T. The human DiGeorge syndrome critical region gene 8 and Its D. melanogaster homolog are required for miRNA biogenesis. Curr Biol 2004:14:2162-2167.

30. Zeng Y, Cullen BR. Efficient processing of primary microRNA hairpins by Drosha requires flanking nonstructured RNA sequences. J Biol Chem 2005:280:27595-27603.

31. Basyuk E, Suavet F, Doglio A, et al. Human let-7 stem-loop precursors harbor features of RNase III cleavage products. Nucleic Acids Res 2003:31:6593-6597.

32. MacRae IJ, Doudna JA. Ribonuclease revisited: structural insights into ribonuclease III family enzymes. Curr Opin Struct Biol 2007:17:138-145.

33. Lund E, Guttinger S, Calado A, et al. Nuclear export of microRNA precursors. Science 2004:303:95-98.

34. Yi R, Qin Y, Macara IG, Cullen BR. Exportin-5 mediates the nuclear export of pre-microRNAs and short hairpin RNAs. Genes Dev 2003:17:3011-3016.

35. Bohnsack MT, Czaplinski K, Gorlich D. Exportin 5 is a RanGTP-dependent dsRNA-binding protein that mediates nuclear export of pre-miRNAs. RNA 2004:10:185-191.

36. Zeng Y, Cullen BR. Structural requirements for pre-microRNA binding and nuclear export by Exportin 5. Nucleic Acids Res 2004:32:4776-4785.

37. Song JJ, Liu J, Tolia NH, et al. The crystal structure of the Argonaute2 PAZ domain reveals an RNA binding motif in RNAi effector complexes. Nat Struct Biol 2003:10:1026-1032.

38. Carmell MA, Hannon GJ. RNase III enzymes and the initiation of gene silencing. Nat Struct Mol Biol 2004:11:214-218.

39. Siolas D, Lerner C, Burchard J, et al. Synthetic shRNAs as potent RNAi triggers. Nat Biotechnol 2005:23:227-231.

40. MacRae IJ, Zhou K, Li F, et al. Structural basis for double-stranded RNA processing by Dicer. Science 2006:311:195-198.

41. Chendrimada TP, Gregory RI, Kumaraswamy E, et al. TRBP recruits the Dicer complex to Ago2 for microRNA processing and gene silencing. Nature 2005:436:740-744.

42. Haase AD, Jaskiewicz L, Zhang H, et al. TRBP, a regulator of cellular PKR and HIV-1 virus expression, interacts with Dicer and functions in RNA silencing. EMBO Rep 2005:6:961-967.

43. Liu J, Carmell MA, Rivas FV, et al. Argonaute2 is the catalytic engine of mammalian RNAi. Science 2004:305:1437-1441.

44. Rivas FV, Tolia NH, Song JJ, et al. Purified Argonaute2 and an siRNA form recombinant human RISC. Nat Struct Mol Biol 2005:12:340-349.

45. Nykanen A, Haley B, Zamore PD. ATP requirements and small interfering RNA structure in the RNA interference pathway. Cell 2001:107:309-321.

46. Elbashir SM, Lendeckel W, Tuschl T. RNA interference is mediated by 21- and 22-nucleotide RNAs. Genes Dev 2001:15:188-200.

47. Elbashir SM, Martinez J, Patkaniowska A, et al. Functional anatomy of siRNAs for mediating efficient RNAi in Drosophila melanogaster embryo lysate. EMBO J 2001:20:6877-6888.

48. Schwarz DS, Hutvagner G, Du T, et al. Asymmetry in the assembly of the RNAi enzyme complex. Cell 2003:115:199-208.

49. Rand TA, Petersen S, Du F, Wang X. Argonaute2 cleaves the anti-guide strand of siRNA during RISC activation. Cell 2005:123:621-629.

50. Parker JS, Roe SM, Barford D. Structural insights into mRNA recognition from a PIWI domain-siRNA guide complex. Nature 2005:434:663-666.

51. Stark A, Brennecke J, Russell RB, Cohen SM. Identification of Drosophila MicroRNA targets. PLoS Biol 2003:1:E60.

52. Lewis BP, Shih IH, Jones-Rhoades MW, et al. Prediction of mammalian microRNA targets. Cell 2003:115:787-798.

53. Doench JG, Sharp PA. Specificity of microRNA target selection in translational repression. Genes Dev 2004:18:504-511.

54. Vatolin S, Navaratne K, Weil RJ. A novel method to detect functional microRNA targets. J Mol Biol 2006:358:983-996.

55. Liu J, Valencia-Sanchez MA, Hannon GJ, Parker R. MicroRNA-dependent localization of targeted mRNAs to mammalian P-bodies. Nat Cell Biol 2005:7:719-723.

56. Ding L, Spencer A, Morita K, Han M. The developmental timing regulator AIN-1 interacts with miRISCs and may target the argonaute protein ALG-1 to cytoplasmic P bodies in C. elegans. Mol Cell 2005:19:437-447.

57. Sen GL, Blau HM. Argonaute 2/RISC resides in sites of mammalian mRNA decay known as cytoplasmic bodies. Nat Cell Biol 2005:7:633-636.

58. Zamore PD, Haley B. Ribo-gnome: the big world of small RNAs. Science 2005:309:1519-1524.

59. Guo H, Ingolia NT, Weissman JS, Bartel DP. Mammalian microRNAs predominantly act to decrease target mRNA levels. Nature 2010:466:835-840.

60. Chiu YL, Rana TM. RNAi in human cells: basic structural and functional features of small interfering RNA. Mol Cell 2002:10:549-561.

61. Doench JG, Petersen CP, Sharp PA. siRNAs can function as miRNAs. Genes Dev 2003:17:438-442.

62. Hutvagner G, Zamore PD. A microRNA in a multiple-turnover RNAi enzyme complex. Science 2002:297:2056-2060.

63. Baulcombe D. RNA silencing in plants. Nature 2004:431:356-363.

64. Buchon N, Vaury C. RNAi: a defensive RNA-silencing against viruses and transposable elements. Heredity 2006:96:195-202.

65. Li HW, Ding SW. Antiviral silencing in animals. FEBS Lett 2005:579:5965-5973.

66. Matzke MA, Birchler JA. RNAi-mediated pathways in the nucleus. Nat Rev Genet 2005:6:24-35.

67. Plasterk RH. RNA silencing: the genome's immune system. Science 2002:296:1263-1265.

68. Waterhouse PM, Wang MB, Lough T. Gene silencing as an adaptive defence against viruses. Nature 2001:411:834-842.

69. Yang N, Kazazian HH, Jr. L1 retrotransposition is suppressed by endogenously encoded small interfering RNAs in human cultured cells. Nat Struct Mol Biol 2006:13:763-771.

70. Tam OH, Aravin AA, Stein P, et al. Pseudogene-derived small interfering RNAs regulate gene expression in mouse oocytes. Nature 2008:453:534-538.

71. Watanabe T, Totoki Y, Toyoda A, et al. Endogenous siRNAs from naturally formed dsRNAs regulate transcripts in mouse oocytes. Nature 2008:453:539-543.

72. Chen X. MicroRNA biogenesis and function in plants. FEBS Lett 2005:579:5923-5931.

73. Kidner CA, Martienssen RA. The developmental role of microRNA in plants. Curr Opin Plant Biol 2005:8:38-44.

74. Wienholds E, Plasterk RH. MicroRNA function in animal development. FEBS Lett 2005:579:5911-5922.

75. Shabalina SA, Koonin EV. Origins and evolution of eukaryotic RNA interference. Trends Ecol Evol 2008:23:578-587.

76. Carleton M, Cleary MA, Linsley PS. MicroRNAs and cell cycle regulation. Cell Cycle 2007:6:2127-2132.

77. Harfe BD. MicroRNAs in vertebrate development. Curr Opin Genet Dev 2005:15:410-415.

78. Boehm M, Slack FJ. MicroRNA control of lifespan and metabolism. Cell Cycle 2006:5:837-840.

79. Friedman RC, Farh KK, Burge CB, Bartel DP. Most mammalian mRNAs are conserved targets of microRNAs. Genome Res 2009:19:92-105.

80. Calin GA, Cimmino A, Fabbri M, et al. MiR-15a and miR-16-1 cluster functions in human leukemia. Proc Natl Acad Sci U S A 2008:105:5166-5171.

81. Krek A, Grun D, Poy MN, et al. Combinatorial microRNA target predictions. Nat Genet 2005:37:495-500.

82. Lewis BP, Burge CB, Bartel DP. Conserved seed pairing, often flanked by adenosines, indicates that thousands of human genes are microRNA targets. Cell 2005:120:15-20.

83. Wu S, Huang S, Ding J, et al. Multiple microRNAs modulate p21Cip1/Waf1 expression by directly targeting its 3' untranslated region. Oncogene 2010:29:2302-2308.

84. Eisenberg I, Eran A, Nishino I, et al. Distinctive patterns of microRNA expression in primary muscular disorders. Proc Natl Acad Sci U S A 2007:104:17016-17021.

85. Garzon R, Calin GA, Croce CM. MicroRNAs in Cancer. Annu Rev Med 2009:60:167-179.

86. Tang X, Tang G, Ozcan S. Role of microRNAs in diabetes. Biochim Biophys Acta 2008:1779:697-701.

87. Miller BH, Wahlestedt C. MicroRNA dysregulation in psychiatric disease. Brain Res 2010:1338:89-99.

88. He L, Thomson JM, Hemann MT, et al. A microRNA polycistron as a potential human oncogene. Nature 2005:435:828-833.

89. Lu J, Getz G, Miska EA, et al. MicroRNA expression profiles classify human cancers. Nature 2005:435:834-838.

90. O'Donnell KA, Wentzel EA, Zeller KI, et al. c-Myc-regulated microRNAs modulate E2F1 expression. Nature 2005:435:839-843.

91. Johnson SM, Grosshans H, Shingara J, et al. RAS is regulated by the let-7 microRNA family. Cell 2005:120:635-647.

92. Blenkiron C, Miska EA. miRNAs in cancer: approaches, aetiology, diagnostics and therapy. Hum Mol Genet 2007:16 Spec No 1:R106-R113.

93. Wiemer EA. The role of microRNAs in cancer: no small matter. Eur J Cancer 2007:43:1529-1544.

94. Weiss B, Davidkova G, Zhou LW. Antisense RNA gene therapy for studying and modulating biological processes. Cell Mol Life Sci 1999:55:334-358.

95. Aoki Y, Cioca DP, Oidaira H, et al. RNA interference may be more potent than antisense RNA in human cancer cell lines. Clin Exp Pharmacol Physiol 2003:30:96-102.

96. Coma S, Noe V, Lavarino C, et al. Use of siRNAs and antisense oligonucleotides against survivin RNA to inhibit steps leading to tumor angiogenesis. Oligonucleotides 2004:14:100-113.

97. Miyagishi M, Hayashi M, Taira K. Comparison of the suppressive effects of antisense oligonucleotides and siRNAs directed against the same targets in mammalian cells. Antisense Nucleic Acid Drug Dev 2003:13:1-7.

98. Gantier MP, Williams BR. The response of mammalian cells to double-stranded RNA. Cytokine Growth Factor Rev 2007:18:363-371.

99. Manche L, Green SR, Schmedt C, Mathews MB. Interactions between double-stranded RNA regulators and the protein kinase DAI. Mol Cell Biol 1992:12:5238-5248.

100. Reynolds A, Anderson EM, Vermeulen A, et al. Induction of the interferon response by siRNA is cell type- and duplex length-dependent. RNA 2006:12:988-993.

101. Kim DH, Behlke MA, Rose SD, et al. Synthetic dsRNA Dicer substrates enhance RNAi potency and efficacy. Nat Biotechnol 2005:23:222-226.

102. Rose SD, Kim DH, Amarzguioui M, et al. Functional polarity is introduced by Dicer processing of short substrate RNAs. Nucleic Acids Res 2005:33:4140-4156.

103. Cullen BR. RNAi the natural way. Nat Genet 2005:37:1163-1165.

104. Schramm L, Hernandez N. Recruitment of RNA polymerase III to its target promoters. Genes Dev 2002:16:2593-2620.

105. Paddison PJ, Caudy AA, Bernstein E, et al. Short hairpin RNAs (shRNAs) induce sequence-specific silencing in mammalian cells. Genes Dev 2002:16:948-958.

106. Brummelkamp TR, Bernards R, Agami R. A system for stable expression of short interfering RNAs in mammalian cells. Science 2002:296:550-553.

107. McManus MT, Petersen CP, Haines BB, et al. Gene silencing using micro-RNA designed hairpins. RNA 2002:8:842-850.

108. Paul CP, Good PD, Winer I, Engelke DR. Effective expression of small interfering RNA in human cells. Nat Biotechnol 2002:20:505-508.

109. Sui G, Soohoo C, Affar eB, et al. A DNA vector-based RNAi technology to suppress gene expression in mammalian cells. Proc Natl Acad Sci U S A 2002:99:5515-5520.

110. Yu JY, DeRuiter SL, Turner DL. RNA interference by expression of short-interfering RNAs and hairpin RNAs in mammalian cells. Proc Natl Acad Sci U S A 2002:99:6047-6052.

111. Zeng Y, Cai X, Cullen BR. Use of RNA polymerase II to transcribe artificial microRNAs. Methods Enzymol 2005:392:371-380.

112. Dickins RA, Hemann MT, Zilfou JT, et al. Probing tumor phenotypes using stable and regulated synthetic microRNA precursors. Nat Genet 2005:37:1289-1295.

113. Murchison EP, Partridge JF, Tam OH, et al. Characterization of Dicer-deficient murine embryonic stem cells. Proc Natl Acad Sci U S A 2005:102:12135-12140.

114. Takahashi Y, Yamaoka K, Nishikawa M, Takakura Y. Moment analysis for kinetics of gene silencing by RNA interference. Biotechnol Bioeng 2006:93:816-819.

115. Takahashi Y, Yamaoka K, Nishikawa M, Takakura Y. Quantitative and temporal analysis of gene silencing in tumor cells induced by small interfering RNA or short hairpin RNA expressed from plasmid vectors. J Pharm Sci 2009:98:74-80.

116. Makinen PI, Koponen JK, Karkkainen AM, et al. Stable RNA interference: comparison of U6 and H1 promoters in endothelial cells and in mouse brain. J Gene Med 2006:8:433-441.

117. Wu MT, Wu RH, Hung CF, et al. Simple and efficient DNA vector-based RNAi systems in mammalian cells. Biochem Biophys Res Commun 2005:330:53-59.

118. Henriksen JR, Lokke C, Hammero M, et al. Comparison of RNAi efficiency mediated by tetracycline-responsive H1 and U6 promoter variants in mammalian cell lines. Nucleic Acids Res 2007:35:e67.

119. Wagstaff KM, Jans DA. Nucleocytoplasmic transport of DNA: enhancing non-viral gene transfer. Biochem J 2007:406:185-202.

120. Baroy T, Sorensen K, Lindeberg MM, Frengen E. shRNA expression constructs designed directly from siRNA oligonucleotide sequences. Mol Biotechnol 2010:45:116-120.

121. Silva JM, Li MZ, Chang K, et al. Second-generation shRNA libraries covering the mouse and human genomes. Nat Genet 2005:37:1281-1288.

122. Boden D, Pusch O, Silbermann R, et al. Enhanced gene silencing of HIV-1 specific siRNA using microRNA designed hairpins. Nucleic Acids Res 2004:32:1154-1158.

123. Li L, Lin X, Khvorova A, et al. Defining the optimal parameters for hairpin-based knockdown constructs. RNA 2007:13:1765-1774.

124. Boudreau RL, Monteys AM, Davidson BL. Minimizing variables among hairpin-based RNAi vectors reveals the potency of shRNAs. RNA 2008:14:1834-1844.

125. Bartlett DW, Davis ME. Insights into the kinetics of siRNA-mediated gene silencing from live-cell and live-animal bioluminescent imaging. Nucleic Acids Res 2006:34:322-333.

126. Raab RM, Stephanopoulos G. Dynamics of gene silencing by RNA interference. Biotechnol Bioeng 2004:88:121-132.

127. Rao DD, Vorhies JS, Senzer N, Nemunaitis J. siRNA vs. shRNA: similarities and differences. Adv Drug Deliv Rev 2009:61:746-759.

128. Recillas-Targa F. Multiple strategies for gene transfer, expression, knockdown, and chromatin influence in mammalian cell lines and transgenic animals. Mol Biotechnol 2006:34:337-354.

129. Brummelkamp TR, Bernards R, Agami R. Stable suppression of tumorigenicity by virus-mediated RNA interference. Cancer Cell 2002:2:243-247.

130. Devroe E, Silver PA. Retrovirus-delivered siRNA. BMC Biotechnol 2002:2:15.

131. Barton GM, Medzhitov R. Retroviral delivery of small interfering RNA into primary cells. Proc Natl Acad Sci U S A 2002:99:14943-14945.

132. Blesch A. Lentiviral and MLV based retroviral vectors for ex vivo and in vivo gene transfer. Methods 2004:33:164-172.

133. Roe T, Reynolds TC, Yu G, Brown PO. Integration of murine leukemia virus DNA depends on mitosis. EMBO J 1993:12:2099-2108.

134. Logan AC, Lutzko C, Kohn DB. Advances in lentiviral vector design for gene-modification of hematopoietic stem cells. Curr Opin Biotechnol 2002:13:429-436.

135. Fritsch L, Martinez LA, Sekhri R, et al. Conditional gene knock-down by CRE-dependent short interfering RNAs. EMBO Rep 2004:5:178-182.

136. Kasim V, Miyagishi M, Taira K. Control of siRNA expression using the Cre-loxP recombination system. Nucleic Acids Res 2004:32:e66.

137. Tiscornia G, Tergaonkar V, Galimi F, Verma IM. CRE recombinase-inducible RNA interference mediated by lentiviral vectors. Proc Natl Acad Sci U S A 2004:101:7347-7351.

138. Ventura A, Meissner A, Dillon CP, et al. Cre-lox-regulated conditional RNA interference from transgenes. Proc Natl Acad Sci U S A 2004:101:10380-10385.

139. Voutev R, Hubbard EJ. A "FLP-Out" system for controlled gene expression in Caenorhabditis elegans. Genetics 2008:180:103-119.

140. Ohkawa J, Taira K. Control of the functional activity of an antisense RNA by a tetracycline-responsive derivative of the human U6 snRNA promoter. Hum Gene Ther 2000:11:577-585.

141. Gossen M, Bujard H. Tight control of gene expression in mammalian cells by tetracycline-responsive promoters. Proc Natl Acad Sci U S A 1992:89:5547-5551.

142. Gossen M, Freundlieb S, Bender G, et al. Transcriptional activation by tetracyclines in mammalian cells. Science 1995:268:1766-1769.

143. Mizuguchi H, Hayakawa T. The tet-off system is more effective than the tet-on system for regulating transgene expression in a single adenovirus vector. J Gene Med 2002:4:240-247.

144. Myslinski E, Krol A, Carbon P. Optimal tRNA((Ser)Sec) gene activity requires an upstream SPH motif. Nucleic Acids Res 1992:20:203-209.

145. Kunkel GR, Pederson T. Transcription of a human U6 small nuclear RNA gene in vivo withstands deletion of intragenic sequences but not of an upstream TATATA box. Nucleic Acids Res 1989:17:7371-7379.

146. Zhang J, Wang C, Ke N, et al. A more efficient RNAi inducible system for tight regulation of gene expression in mammalian cells and xenograft animals. RNA 2007:13:1375-1383.

147. Hillen W, Schollmeier K, Gatz C. Control of expression of the Tn10-encoded tetracycline resistance operon. II. Interaction of RNA polymerase and TET repressor with the tet operon regulatory region. J Mol Biol 1984:172:185-201.

148. Czauderna F, Santel A, Hinz M, et al. Inducible shRNA expression for application in a prostate cancer mouse model. Nucleic Acids Res 2003:31:e127.

149. Lin X, Yang J, Chen J, et al. Development of a tightly regulated U6 promoter for shRNA expression. FEBS Lett 2004:577:376-380.

150. Matthess Y, Kappel S, Spankuch B, et al. Conditional inhibition of cancer cell proliferation by tetracycline-responsive, H1 promoter-driven silencing of PLK1. Oncogene 2005:24:2973-2980.

151. Chen Y, Stamatoyannopoulos G, Song CZ. Down-regulation of CXCR4 by inducible small interfering RNA inhibits breast cancer cell invasion in vitro. Cancer Res 2003:63:4801-4804.

152. Amar L, Desclaux M, Faucon-Biguet N, et al. Control of small inhibitory RNA levels and RNA interference by doxycycline induced activation of a minimal RNA polymerase III promoter. Nucleic Acids Res 2006:34:e37.

153. Pluta K, Diehl W, Zhang XY, et al. Lentiviral vectors encoding tetracycline-dependent repressors and transactivators for reversible knockdown of gene expression: a comparative study. BMC Biotechnol 2007:7:41.

154. Stegmeier F, Hu G, Rickles RJ, et al. A lentiviral microRNA-based system for single-copy polymerase II-regulated RNA interference in mammalian cells. Proc Natl Acad Sci U S A 2005:102:13212-13217.

155. Das AT, Zhou X, Vink M, et al. Viral evolution as a tool to improve the tetracycline-regulated gene expression system. J Biol Chem 2004:279:18776-18782.

156. Shin KJ, Wall EA, Zavzavadjian JR, et al. A single lentiviral vector platform for microRNA-based conditional RNA interference and coordinated transgene expression. Proc Natl Acad Sci U S A 2006:103:13759-13764.

157. Gupta S, Schoer RA, Egan JE, et al. Inducible, reversible, and stable RNA interference in mammalian cells. Proc Natl Acad Sci U S A 2004:101:1927-1932.

158. Rangasamy D, Tremethick DJ, Greaves IK. Gene knockdown by ecdysone-based inducible RNAi in stable mammalian cell lines. Nat Protoc 2008:3:79-88.

159. Lee SK, Kumar P. Conditional RNAi: towards a silent gene therapy. Adv Drug Deliv Rev 2009:61:650-664.

160. Haley B, Zamore PD. Kinetic analysis of the RNAi enzyme complex. Nat Struct Mol Biol 2004:11:599-606.

161. Jackson AL, Burchard J, Schelter J, et al. Widespread siRNA "off-target" transcript silencing mediated by seed region sequence complementarity. RNA 2006:12:1179-1187.

162. Jackson AL, Bartz SR, Schelter J, et al. Expression profiling reveals off-target gene regulation by RNAi. Nat Biotechnol 2003:21:635-637.

163. Lin X, Ruan X, Anderson MG, et al. siRNA-mediated off-target gene silencing triggered by a 7 nt complementation. Nucleic Acids Res 2005:33:4527-4535.

164. Qiu S, Adema CM, Lane T. A computational study of off-target effects of RNA interference. Nucleic Acids Res 2005:33:1834-1847.

165. Yamada T, Morishita S. Accelerated off-target search algorithm for siRNA. Bioinformatics 2005:21:1316-1324.

166. Naito Y, Yamada T, Matsumiya T, et al. dsCheck: highly sensitive off-target search software for double-stranded RNA-mediated RNA interference. Nucleic Acids Res 2005:33:W589-W591.

167. Kariko K, Bhuyan P, Capodici J, Weissman D. Small interfering RNAs mediate sequence-independent gene suppression and induce immune activation by signaling through toll-like receptor 3. J Immunol 2004:172:6545-6549.

168. Sioud M, Sorensen DR. Cationic liposome-mediated delivery of siRNAs in adult mice. Biochem Biophys Res Commun 2003:312:1220-1225.

169. Hornung V, Guenthner-Biller M, Bourquin C, et al. Sequence-specific potent induction of IFN-alpha by short interfering RNA in plasmacytoid dendritic cells through TLR7. Nat Med 2005:11:263-270.

170. Judge AD, Sood V, Shaw JR, et al. Sequence-dependent stimulation of the mammalian innate immune response by synthetic siRNA. Nat Biotechnol 2005:23:457-462.

171. Sioud M. Induction of inflammatory cytokines and interferon responses by double-stranded and single-stranded siRNAs is sequence-dependent and requires endosomal localization. J Mol Biol 2005:348:1079-1090.

172. Marques JT, Devosse T, Wang D, et al. A structural basis for discriminating between self and nonself double-stranded RNAs in mammalian cells. Nat Biotechnol 2006:24:559-565.

173. Jackson AL, Linsley PS. Recognizing and avoiding siRNA off-target effects for target identification and therapeutic application. Nat Rev Drug Discov 2010:9:57-67.

174. Yi R, Doehle BP, Qin Y, et al. Overexpression of exportin 5 enhances RNA interference mediated by short hairpin RNAs and microRNAs. RNA 2005:11:220-226.

175. Grimm D, Streetz KL, Jopling CL, et al. Fatality in mice due to oversaturation of cellular microRNA/short hairpin RNA pathways. Nature 2006:441:537-541.

176. Grimm D, Kay MA. Therapeutic application of RNAi: is mRNA targeting finally ready for prime time? J Clin Invest 2007:117:3633-3641.

177. McBride JL, Boudreau RL, Harper SQ, et al. Artificial miRNAs mitigate shRNA-mediated toxicity in the brain: implications for the therapeutic development of RNAi. Proc Natl Acad Sci U S A 2008:105:5868-5873.

178. John M, Constien R, Akinc A, et al. Effective RNAi-mediated gene silencing without interruption of the endogenous microRNA pathway. Nature 2007:449:745-747.

179. Castanotto D, Sakurai K, Lingeman R, et al. Combinatorial delivery of small interfering RNAs reduces RNAi efficacy by selective incorporation into RISC. Nucleic Acids Res 2007:35:5154-5164.

180. Khan AA, Betel D, Miller ML, et al. Transfection of small RNAs globally perturbs gene regulation by endogenous microRNAs. Nat Biotechnol 2009:27:549-555.

181. Graham CF, Deussen ZA. Features of cell lineage in preimplantation mouse development. J Embryol Exp Morphol 1978:48:53-72.

182. Gammill LS, Bronner-Fraser M. Neural crest specification: migrating into genomics. Nat Rev Neurosci 2003:4:795-805.

183. Carlson BM. Human Embryology and Developmental Biology. Philadelphia: Elsevier Mosby; 2004.

184. Knecht AK, Bronner-Fraser M. Induction of the neural crest: a multigene process. Nat Rev Genet 2002:3:453-461.

185. Meulemans D, Bronner-Fraser M. Gene-regulatory interactions in neural crest evolution and development. Dev Cell 2004:7:291-299.

186. Reissmann E, Ernsberger U, Francis-West PH, et al. Involvement of bone morphogenetic protein-4 and bone morphogenetic protein-7 in the differentiation of the adrenergic phenotype in developing sympathetic neurons. Development 1996:122:2079-2088.

187. Schneider C, Wicht H, Enderich J, et al. Bone morphogenetic proteins are required in vivo for the generation of sympathetic neurons. Neuron 1999:24:861-870.

188. Ernsberger U, Patzke H, Tissier-Seta JP, et al. The expression of tyrosine hydroxylase and the transcription factors cPhox-2 and Cash-1: evidence for distinct inductive steps in the differentiation of chick sympathetic precursor cells. Mech Dev 1995:52:125-136.

189. Cochard P, Goldstein M, Black IB. Ontogenetic appearance and disappearance of tyrosine hydroxylase and catecholamines in the rat embryo. Proc Natl Acad Sci U S A 1978:75:2986-2990.

190. Cochard P, Paulin D. Initial expression of neurofilaments and vimentin in the central and peripheral nervous system of the mouse embryo in vivo. J Neurosci 1984:4:2080-2094.

191. Sommer L, Shah N, Rao M, Anderson DJ. The cellular function of MASH1 in autonomic neurogenesis. Neuron 1995:15:1245-1258.

192. Huber K. The sympathoadrenal cell lineage: specification, diversification, and new perspectives. Dev Biol 2006:298:335-343.

193. Wakamatsu Y, Watanabe Y, Nakamura H, Kondoh H. Regulation of the neural crest cell fate by N-myc: promotion of ventral migration and neuronal differentiation. Development 1997:124:1953-1962.

194. Thiele CJ, Israel MA. Regulation of N-myc expression is a critical event controlling the ability of human neuroblasts to differentiate. Exp Cell Biol 1988:56:321-333.

195. Sommer L, Rao M. Neural stem cells and regulation of cell number. Prog Neurobiol 2002:66:1-18.

196. Schlisio S, Kenchappa RS, Vredeveld LC, et al. The kinesin KIF1Bbeta acts downstream from EglN3 to induce apoptosis and is a potential 1p36 tumor suppressor. Genes Dev 2008:22:884-893.

197. Grimmer MR, Weiss WA. Childhood tumors of the nervous system as disorders of normal development. Curr Opin Pediatr 2006:18:634-638.

198. Larue L, Bellacosa A. Epithelial-mesenchymal transition in development and cancer: role of phosphatidylinositol 3' kinase/AKT pathways. Oncogene 2005:24:7443-7454.

199. Maris JM, Hogarty MD, Bagatell R, Cohn SL. Neuroblastoma. Lancet 2007:369:2106-2120.

200. Shimada H, Ambros IM, Dehner LP, et al. The International Neuroblastoma Pathology Classification (the Shimada system). Cancer 1999:86:364-372.

201. Träger C. Neuroblastoma Incidence, Biology and Outcome. In: Karolinska Institutet, Stockholm, Sweden; 2009.

202. Brodeur GM. Neuroblastoma: biological insights into a clinical enigma. Nat Rev Cancer 2003:3:203-216.

203. Cohn SL, Pearson AD, London WB, et al. The International Neuroblastoma Risk Group (INRG) classification system: an INRG Task Force report. J Clin Oncol 2009:27:289-297.

204. Monclair T, Brodeur GM, Ambros PF, et al. The International Neuroblastoma Risk Group (INRG) staging system: an INRG Task Force report. J Clin Oncol 2009:27:298-303.

205. Turkel SB, Itabashi HH. The natural history of neuroblastic cells in the fetal adrenal gland. Am J Pathol 1974:76:225-244.

206. Ikeda Y, Lister J, Bouton JM, Buyukpamukcu M. Congenital neuroblastoma, neuroblastoma in situ, and the normal fetal development of the adrenal. J Pediatr Surg 1981:16:636-644.

207. Kaneko Y, Kanda N, Maseki N, et al. Different karyotypic patterns in early and advanced stage neuroblastomas. Cancer Res 1987:47:311-318.

208. Janoueix-Lerosey I, Schleiermacher G, Michels E, et al. Overall genomic pattern is a predictor of outcome in neuroblastoma. J Clin Oncol 2009:27:1026-1033.

209. Bown N, Cotterill S, Lastowska M, et al. Gain of chromosome arm 17q and adverse outcome in patients with neuroblastoma. N Engl J Med 1999:340:1954-1961.

210. Spitz R, Hero B, Ernestus K, Berthold F. Gain of distal chromosome arm 17q is not associated with poor prognosis in neuroblastoma. Clin Cancer Res 2003:9:4835-4840.

211. Lastowska M, Roberts P, Pearson AD, et al. Promiscuous translocations of chromosome arm 17q in human neuroblastomas. Genes Chromosomes Cancer 1997:19:143-149.

212. Schleiermacher G, Michon J, Huon I, et al. Chromosomal CGH identifies patients with a higher risk of relapse in neuroblastoma without MYCN amplification. Br J Cancer 2007:97:238-246.

213. Srivatsan ES, Ying KL, Seeger RC. Deletion of chromosome 11 and of 14q sequences in neuroblastoma. Genes Chromosomes Cancer 1993:7:32-37.

214. Brodeur GM, Green AA, Hayes FA, et al. Cytogenetic features of human neuroblastomas and cell lines. Cancer Res 1981:41:4678-4686.

215. Guo C, White PS, Weiss MJ, et al. Allelic deletion at 11q23 is common in MYCN single copy neuroblastomas. Oncogene 1999:18:4948-4957.

216. Fong CT, Dracopoli NC, White PS, et al. Loss of heterozygosity for the short arm of chromosome 1 in human neuroblastomas: correlation with N-myc amplification. Proc Natl Acad Sci U S A 1989:86:3753-3757.

217. Schwab M, Varmus HE, Bishop JM, et al. Chromosome localization in normal human cells and neuroblastomas of a gene related to c-myc. Nature 1984:308:288-291.

218. Wenzel A, Cziepluch C, Hamann U, et al. The N-Myc oncoprotein is associated in vivo with the phosphoprotein Max(p20/22) in human neuroblastoma cells. EMBO J 1991:10:3703-3712.

219. Wenzel A, Schwab M. The mycN/max protein complex in neuroblastoma. Short review. Eur J Cancer 1995:31A:516-519.

220. Blackwell TK, Kretzner L, Blackwood EM, et al. Sequence-specific DNA binding by the c-Myc protein. Science 1990:250:1149-1151.

221. Blackwood EM, Eisenman RN. Max: a helix-loop-helix zipper protein that forms a sequence-specific DNA-binding complex with Myc. Science 1991:251:1211-1217.

222. Prendergast GC, Lawe D, Ziff EB. Association of Myn, the murine homolog of max, with c-Myc stimulates methylation-sensitive DNA binding and ras cotransformation. Cell 1991:65:395-407.

223. Guccione E, Martinato F, Finocchiaro G, et al. Myc-binding-site recognition in the human genome is determined by chromatin context. Nat Cell Biol 2006:8:764-770.

224. Nikiforov MA, Popov N, Kotenko I, et al. The Mad and Myc basic domains are functionally equivalent. J Biol Chem 2003:278:11094-11099.

225. Ayer DE, Kretzner L, Eisenman RN. Mad: a heterodimeric partner for Max that antagonizes Myc transcriptional activity. Cell 1993:72:211-222.

226. Xu D, Popov N, Hou M, et al. Switch from Myc/Max to Mad1/Max binding and decrease in histone acetylation at the telomerase reverse transcriptase promoter during differentiation of HL60 cells. Proc Natl Acad Sci U S A 2001:98:3826-3831.

227. Liu T, Tee AE, Porro A, et al. Activation of tissue transglutaminase transcription by histone deacetylase inhibition as a therapeutic approach for Myc oncogenesis. Proc Natl Acad Sci U S A 2007:104:18682-18687.

228. Schwab M, Alitalo K, Klempnauer KH, et al. Amplified DNA with limited homology to myc cellular oncogene is shared by human neuroblastoma cell lines and a neuroblastoma tumour. Nature 1983:305:245-248.

229. Lutz W, Schwab M. In vivo regulation of single copy and amplified N-myc in human neuroblastoma cells. Oncogene 1997:15:303-315.

230. Schwab M. MYCN in neuronal tumours. Cancer Lett 2004:204:179-187.

231. Weiss WA, Aldape K, Mohapatra G, et al. Targeted expression of MYCN causes neuroblastoma in transgenic mice. EMBO J 1997:16:2985-2995.

232. Lutz W, Stohr M, Schurmann J, et al. Conditional expression of N-myc in human neuroblastoma cells increases expression of alpha-prothymosin and ornithine decarboxylase and accelerates progression into S-phase early after mitogenic stimulation of quiescent cells. Oncogene 1996:13:803-812.

233. Yee AS, Shih HH, Tevosian SG. New perspectives on retinoblastoma family functions in differentiation. Front Biosci 1998:3:D532-D547.

234. Bell E, Chen L, Liu T, et al. MYCN oncoprotein targets and their therapeutic potential. Cancer Lett 2010:293:144-157.

235. Hogarty MD. The requirement for evasion of programmed cell death in neuroblastomas with MYCN amplification. Cancer Lett 2003:197:173-179.

236. Chen L, Iraci N, Gherardi S, et al. p53 is a direct transcriptional target of MYCN in neuroblastoma. Cancer Res 2010:70:1377-1388.

237. Slack AD, Chen Z, Ludwig AD, et al. MYCN-directed centrosome amplification requires MDM2-mediated suppression of p53 activity in neuroblastoma cells. Cancer Res 2007:67:2448-2455.

238. Molofsky AV, Pardal R, Iwashita T, et al. Bmi-1 dependence distinguishes neural stem cell self-renewal from progenitor proliferation. Nature 2003:425:962-967.

239. Nowak K, Kerl K, Fehr D, et al. BMI1 is a target gene of E2F-1 and is strongly expressed in primary neuroblastomas. Nucleic Acids Res 2006:34:1745-1754.

240. Ochiai H, Takenobu H, Nakagawa A, et al. Bmi1 is a MYCN target gene that regulates tumorigenesis through repression of KIF1Bbeta and TSLC1 in neuroblastoma. Oncogene 2010:29:2681-2690.

241. Ando K, Ohira M, Ozaki T, et al. Expression of TSLC1, a candidate tumor suppressor gene mapped to chromosome 11q23, is downregulated in unfavorable neuroblastoma without promoter hypermethylation. Int J Cancer 2008:123:2087-2094.

242. Caren H, Ejeskar K, Fransson S, et al. A cluster of genes located in 1p36 are down-regulated in neuroblastomas with poor prognosis, but not due to CpG island methylation. Mol Cancer 2005:4:10.

243. Lu X, Pearson A, Lunec J. The MYCN oncoprotein as a drug development target. Cancer Lett 2003:197:125-130.

244. Negroni A, Scarpa S, Romeo A, et al. Decrease of proliferation rate and induction of differentiation by a MYCN antisense DNA oligomer in a human neuroblastoma cell line. Cell Growth Differ 1991:2:511-518.

245. Ray A, Norden B. Peptide nucleic acid (PNA): its medical and biotechnical applications and promise for the future. FASEB J 2000:14:1041-1060.

246. Sun L, Fuselier JA, Murphy WA, Coy DH. Antisense peptide nucleic acids conjugated to somatostatin analogs and targeted at the n-myc oncogene display enhanced cytotoxity to human neuroblastoma IMR32 cells expressing somatostatin receptors. Peptides 2002:23:1557-1565.

247. Pession A, Tonelli R, Fronza R, et al. Targeted inhibition of NMYC by peptide nucleic acid in N-myc amplified human neuroblastoma cells: cell-cycle inhibition with induction of neuronal cell differentiation and apoptosis. Int J Oncol 2004:24:265-272.

248. Tonelli R, Purgato S, Camerin C, et al. Anti-gene peptide nucleic acid specifically inhibits MYCN expression in human neuroblastoma cells leading to cell growth inhibition and apoptosis. Mol Cancer Ther 2005:4:779-786.

249. Nara K, Kusafuka T, Yoneda A, et al. Silencing of MYCN by RNA interference induces growth inhibition, apoptotic activity and cell differentiation in a neuroblastoma cell line with MYCN amplification. Int J Oncol 2007:30:1189-1196.

250. Kang JH, Rychahou PG, Ishola TA, et al. MYCN silencing induces differentiation and apoptosis in human neuroblastoma cells. Biochem Biophys Res Commun 2006:351:192-197.

251. Ciccarone V, Spengler BA, Meyers MB, et al. Phenotypic diversification in human neuroblastoma cells: expression of distinct neural crest lineages. Cancer Res 1989:49:219-225.

252. Ross RA, Biedler JL, Spengler BA. A role for distinct cell types in determining malignancy in human neuroblastoma cell lines and tumors. Cancer Lett 2003:197:35-39.

253. Chen Y, Stallings RL. Differential patterns of microRNA expression in neuroblastoma are correlated with prognosis, differentiation, and apoptosis. Cancer Res 2007:67:976-983.

254. Stallings RL, Foley NH, Bryan K, et al. Therapeutic targeting of miRNAs in neuroblastoma. Expert Opin Ther Targets 2010:14:951-962.

255. Schulte JH, Horn S, Otto T, et al. MYCN regulates oncogenic MicroRNAs in neuroblastoma. Int J Cancer 2008:122:699-704.

256. Welch C, Chen Y, Stallings RL. MicroRNA-34a functions as a potential tumor suppressor by inducing apoptosis in neuroblastoma cells. Oncogene 2007:26:5017-5022.

257. Wei JS, Song YK, Durinck S, et al. The MYCN oncogene is a direct target of miR-34a. Oncogene 2008:27:5204-5213.

258. Tanzer A, Stadler PF. Molecular evolution of a microRNA cluster. J Mol Biol 2004:339:327-335.

259. Foshay KM, Gallicano GI. miR-17 family miRNAs are expressed during early mammalian development and regulate stem cell differentiation. Dev Biol 2009:326:431-443.

260. O'Donnell KA, Wentzel EA, Zeller KI, et al. c-Myc-regulated microRNAs modulate E2F1 expression. Nature 2005:435:839-843.

261. Fontana L, Fiori ME, Albini S, et al. Antagomir-17-5p abolishes the growth of therapy-resistant neuroblastoma through p21 and BIM. PLoS One 2008:3:e2236.

262. Loven J, Zinin N, Wahlstrom T, et al. MYCN-regulated microRNAs repress estrogen receptor-alpha (ESR1) expression and neuronal differentiation in human neuroblastoma. Proc Natl Acad Sci U S A 2010:107:1553-1558.

263. Thawani JP, Wang AC, Than KD, et al. Bone morphogenetic proteins and cancer: review of the literature. Neurosurgery 2010:66:233-246.

264. Klaus A, Birchmeier W. Wnt signalling and its impact on development and cancer. Nat Rev Cancer 2008:8:387-398.

265. Turner N, Grose R. Fibroblast growth factor signalling: from development to cancer. Nat Rev Cancer 2010:10:116-129.

266. Vlad A, Rohrs S, Klein-Hitpass L, Muller O. The first five years of the Wnt targetome. Cell Signal 2008:20:795-802.

267. Inestrosa NC, Arenas E. Emerging roles of Wnts in the adult nervous system. Nat Rev Neurosci 2010:11:77-86.

268. Semenov MV, Habas R, Macdonald BT, He X. SnapShot: Noncanonical Wnt Signaling Pathways. Cell 2007:131:1378.

269. Niehrs C. Function and biological roles of the Dickkopf family of Wnt modulators. Oncogene 2006:25:7469-7481.

270. Nakamura RE, Hackam AS. Analysis of Dickkopf3 interactions with Wnt signaling receptors. Growth Factors 2010.

271. Nakamura RE, Hunter DD, Yi H, et al. Identification of two novel activities of the Wnt signaling regulator Dickkopf 3 and characterization of its expression in the mouse retina. BMC Cell Biol 2007:8:52.

272. Caricasole A, Ferraro T, Iacovelli L, et al. Functional characterization of WNT7A signaling in PC12 cells: interaction with A FZD5 x LRP6 receptor complex and modulation by Dickkopf proteins. J Biol Chem 2003:278:37024-37031.

273. Hoang BH, Kubo T, Healey JH, et al. Dickkopf 3 inhibits invasion and motility of Saos-2 osteosarcoma cells by modulating the Wnt-beta-catenin pathway. Cancer Res 2004:64:2734-2739.

274. Lodygin D, Epanchintsev A, Menssen A, et al. Functional epigenomics identifies genes frequently silenced in prostate cancer. Cancer Res 2005:65:4218-4227.

275. Kobayashi K, Ouchida M, Tsuji T, et al. Reduced expression of the REIC/Dkk-3 gene by promoter-hypermethylation in human tumor cells. Gene 2002:282:151-158.

276. Abarzua F, Sakaguchi M, Takaishi M, et al. Adenovirus-mediated overexpression of REIC/Dkk-3 selectively induces apoptosis in human prostate cancer cells through activation of c-Jun-NH2-kinase. Cancer Res 2005:65:9617-9622.

277. Koppen A, Ait-Aissa R, Koster J, et al. Dickkopf-3 expression is a marker for neuroblastic tumor maturation and is down-regulated by MYCN. Int J Cancer 2008:122:1455-1464.

278. Bell E, Lunec J, Tweddle DA. Cell cycle regulation targets of MYCN identified by gene expression microarrays. Cell Cycle 2007:6:1249-1256.

279. Koppen A, Ait-Aissa R, Hopman S, et al. Dickkopf-1 is down-regulated by MYCN and inhibits neuroblastoma cell proliferation. Cancer Lett 2007:256:218-228.

280. van de Wetering M, Oving I, Muncan V, et al. Specific inhibition of gene expression using a stably integrated, inducible small-interfering-RNA vector. EMBO Rep 2003:4:609-615.

281. Myslinski E, Ame JC, Krol A, Carbon P. An unusually compact external promoter for RNA polymerase III transcription of the human H1RNA gene. Nucleic Acids Res 2001:29:2502-2509.

282. Piacentini M, Annicchiarico-Petruzzelli M, Oliverio S, et al. Phenotype-specific "tissue" transglutaminase regulation in human neuroblastoma cells in response to retinoic acid: correlation with cell death by apoptosis. Int J Cancer 1992:52:271-278.

283. Schmidt ML, Salwen HR, Manohar CF, et al. The biological effects of antisense N-myc expression in human neuroblastoma. Cell Growth Differ 1994:5:171-178.

284. Wang S, Dolnick BJ. Quantitative evaluation of intracellular sense: antisense RNA hybrid duplexes. Nucleic Acids Res 1993:21:4383-4391.

285. Whitesell L, Rosolen A, Neckers LM. Episome-generated N-myc antisense RNA restricts the differentiation potential of primitive neuroectodermal cell lines. Mol Cell Biol 1991:11:1360-1371.

286. Schilbach K, Pollwein P, Schwab M, et al. Reduction of N-myc expression by antisense RNA is amplified by interferon: possible involvement of the 2-5A system. Biochem Biophys Res Commun 1990:170:1242-1248.

287. Liu SP, Fu RH, Yu HH, et al. MicroRNAs regulation modulated self-renewal and lineage differentiation of stem cells. Cell Transplant 2009:18:1039-1045.

288. Morikawa S, Mabuchi Y, Niibe K, et al. Development of mesenchymal stem cells partially originate from the neural crest. Biochem Biophys Res Commun 2009:379:1114-1119.

289. Finnerty JR, Wang WX, Hebert SS, et al. The miR-15/107 Group of MicroRNA Genes: Evolutionary Biology, Cellular Functions, and Roles in Human Diseases. J Mol Biol 2010:402:491-509.

290. Nass D, Rosenwald S, Meiri E, et al. MiR-92b and miR-9/9* are specifically expressed in brain primary tumors and can be used to differentiate primary from metastatic brain tumors. Brain Pathol 2009:19:375-383.

291. Bar M, Wyman SK, Fritz BR, et al. MicroRNA discovery and profiling in human embryonic stem cells by deep sequencing of small RNA libraries. Stem Cells 2008:26:2496-2505.

292. Sengupta S, Nie J, Wagner RJ, et al. MicroRNA 92b controls the G1/S checkpoint gene p57 in human embryonic stem cells. Stem Cells 2009:27:1524-1528.

293. Krichevsky AM, Gabriely G. miR-21: a small multi-faceted RNA. J Cell Mol Med 2009:13:39-53.

294. Fukuda Y, Kawasaki H, Taira K. Exploration of human miRNA target genes in neuronal differentiation. Nucleic Acids Symp Ser (Oxf) 2005:341-342.

295. Mestdagh P, Fredlund E, Pattyn F, et al. MYCN/c-MYC-induced microRNAs repress coding gene networks associated with poor outcome in MYCN/c-MYC-activated tumors. Oncogene 2010:29:1394-1404.

296. Barrantes IB, Montero-Pedrazuela A, Guadano-Ferraz A, et al. Generation and characterization of dickkopf3 mutant mice. Mol Cell Biol 2006:26:2317-2326.

297. Liu X, Mazanek P, Dam V, et al. Deregulated Wnt/beta-catenin program in high-risk neuroblastomas without MYCN amplification. Oncogene 2008:27:1478-1488.

298. Pinho S, Niehrs C. Dkk3 is required for TGF-beta signaling during Xenopus mesoderm induction. Differentiation 2007:75:957-967.

299. Cohen PS, Letterio JJ, Gaetano C, et al. Induction of transforming growth factor beta 1 and its receptors during all-trans-retinoic acid (RA) treatment of RA-responsive human neuroblastoma cell lines. Cancer Res 1995:55:2380-2386.

300. Schramm A, von S, V, Christiansen H, et al. High activin A-expression in human neuroblastoma: suppression of malignant potential and correlation with favourable clinical outcome. Oncogene 2005:24:680-687.

301. Breit S, Ashman K, Wilting J, et al. The N-myc oncogene in human neuroblastoma cells: down-regulation of an angiogenesis inhibitor identified as activin A. Cancer Res 2000:60:4596-4601.

302. Breit S, Rossler J, Fotsis T, Schweigerer L. N-myc down-regulates activin A. Biochem Biophys Res Commun 2000:274:405-409.

303. Fong D, Hermann M, Untergasser G, et al. Dkk-3 expression in the tumor endothelium: a novel prognostic marker of pancreatic adenocarcinomas. Cancer Sci 2009:100:1414-1420.

304. Untergasser G, Steurer M, Zimmermann M, et al. The Dickkopf-homolog 3 is expressed in tumor endothelial cells and supports capillary formation. Int J Cancer 2008:122:1539-1547.

305. Zenzmaier C, Untergasser G, Hermann M, et al. Dysregulation of Dkk-3 expression in benign and malignant prostatic tissue. Prostate 2008:68:540-547.

306. Pei Y, Kano J, Iijima T, et al. Overexpression of Dickkopf 3 in hepatoblastomas and hepatocellular carcinomas. Virchows Arch 2009:454:639-646.

307. Muhlmann G, Untergasser G, Zitt M, et al. Immunohistochemically detectable dickkopf-3 expression in tumor vessels predicts survival in gastric cancer. Virchows Arch 2010:456:635-646.

308. You A, Fokas E, Wang LF, et al. Expression of the Wnt antagonist DKK3 is frequently suppressed in sporadic epithelial ovarian cancer. J Cancer Res Clin Oncol 2010.

309. Monaghan AP, Kioschis P, Wu W, et al. Dickkopf genes are co-ordinately expressed in mesodermal lineages. Mech Dev 1999:87:45-56.

PAPER I

Published online 10 April 2007

Nucleic Acids Research, 2007, Vol. 35, No. 9 ***e67***
doi:10.1093/nar/gkm193

Comparison of RNAi efficiency mediated by tetracycline-responsive H1 and U6 promoter variants in mammalian cell lines

Jørn R. Henriksen[1,2], Cecilie Løkke[2], Martin Hammerø[1,2], Dirk Geerts[3], Rogier Versteeg[3], Trond Flægstad[1,2] and Christer Einvik[1,2,*]

[1]Department of Pediatrics, University Hospital of North-Norway, [2]Department of Pediatrics, Institute of Clinical Biology, University of Tromsø, 9037 Tromsø, Norway and [3]Department of Human Genetics, Academic Medical Center, University of Amsterdam, Meibergdreef 9, 1105 AZ Amsterdam, The Netherlands

Received January 5, 2007; Revised and Accepted March 20, 2007

ABSTRACT

Conditional expression of short hairpin RNAs (shRNAs) to knock down target genes is a powerful tool to study gene function. The most common inducible expression systems are based on tetracycline-regulated RNA polymerase III promoters. During the last years, several tetracycline-inducible U6 and H1 promoter variants have been reported in different experimental settings showing variable efficiencies. In this study, we compare the most common variants of these promoters in several mammalian cell lines. For all cell lines tested, we find that several inducible U6 and H1 promoters containing single tetracycline operator (tetO) sequences show high-transcriptional background in the non-induced state. Promoter variants containing two tetO sequences show tight suppression of transcription in the non-induced state, and high tet responsiveness and high gene knockdown efficiency upon induction in all cell lines tested. We report a variant of the H1 promoter containing two O2-type tetO sequences flanking the TATA box that shows little transcriptional background in the non-induced state and up to 90% target knockdown when the inducer molecule (dox–doxycycline) is added. This inducible system for RNAi-based gene silencing is a good candidate for use both in basic research on gene function and for potential therapeutic applications.

INTRODUCTION

The technology of small interfering RNA (siRNA)-based gene knockdown has become a common method to study gene function in mammalian cells (1,2). The introduction of short double-stranded RNA's into cells leads to sequence-specific down regulation of endogenous mRNAs that match the siRNA. This post-transcriptional gene suppression process is referred to as RNA interference or simply RNAi.

RNAi can be induced in mammalian cells either by introduction of synthetic 21–23 nt siRNA's or by plasmids and viral vectors that express the siRNA molecules (3). In the latter case, siRNA molecules can be produced intracellularly as two single-stranded complementary RNA molecules from separate promoters or, more commonly, from a single promoter as a short hairpin RNA (shRNA). The shRNA molecule is then further processed to siRNA by cellular ribonuclease complexes (4,5). RNA suppression by hairpin siRNA (shRNA) has been shown to be more efficient than other siRNA methods tested (6).

Plasmid vector based siRNA expression strategies have several advantages over other methods. First, the costs of DNA oligomers for construction are much lower than of synthetic siRNA molecules. Plasmid vectors encoding a selectable marker are expected to be more efficiently transfected into cells than naked RNA molecules. And last, vector-based siRNA expression strategies offer the advantage of inducible expression in the cases where gene knockdown is expected to have a deleterious effect on the targeted cell. Stable expression of the siRNA can easily be obtained when selectable plasmids or viral vectors are used to deliver the expression module into cells. Stable gene-knockdown studies involving genes essential for cell growth or survival require a conditional system where siRNA expression is tightly regulated.

siRNA and shRNA synthesis systems in cells are most often driven by RNA polymerase III (pol III) promoters. There are several advantages to using RNA pol III systems. siRNA transcription is high, and the fact that it is driven by *cis*-acting elements found exclusively in

*To whom correspondence should be addressed. Tel: +47 77 644735; Fax: +47 77 645350; Email: christer@fagmed.uit.no

the 5′-flanking region, results in uniform RNA molecules containing defined 5′ and 3′ ends (7–9). During the last years, several inducible promoter systems have been developed to control expression of small RNAs. Most of these are based on variants of the U6 and H1 RNA pol III promoters. Several different strategies exist to make these promoters respond to external signals: the Cre-loxP system (10), the ecdysone-inducible system (11), the lac-repressor system (12) and the tet-repressor system (13).

Tetracycline-responsive variants of both the U6 and H1 RNA pol III promoters have been used in several studies to drive conditional shRNA production (14–18). In these systems, a tetracycline operator (tetO) sequence is inserted near the TATA box of the promoters. TetO sequences are high-affinity binding sites for the specific binding of the tetracycline repressor (tetR). Once bound, tetR will prevent RNA pol III from binding to the promoter and transcription is prevented. Addition of the inducer tetracycline or various analogs (e.g. dox), which have high affinity for tetR, causes the tetR to dissociate from tetO and transcription to proceed (19).

Previous studies using tetracycline-inducible small RNA expression systems have reported variable results regarding background transcription and induction potential of the systems. We and others have noted that RNA pol III promoters containing a single tetO sequence show significant leakiness, resulting in high background transcription, in the non-induced state (15,17). On the other hand, similar promoter variants have been used with considerable success in other studies (14,16,20). Therefore, we have now performed a comparison of several tetracycline-inducible U6 and H1 promoter variants for conditional shRNA expression in a number of mammalian cell lines. The results show that U6 and H1 promoters containing a single tetO sequence show variable background transcription levels and response to the inducing agent depending on the cell line used. Both U6 and H1 promoter variants containing two tetO sequences show tight regulation of shRNA expression in all cell lines used in this study. We also describe a variant of the H1 promoter containing 2 tetO sequences (H1-2O2) that is almost completely inactive in the non-induced state and gives high shRNA expression level upon induction by dox. This inducible system for RNAi-based gene silencing is a good candidate for use both in basic research on gene function and for potential therapeutic applications.

RESULTS AND DISCUSSION

Generation of tet-inducible derivatives of the U6 and H1 promoters

To compare the effectiveness of conditional shRNA expression from RNA pol III promoters, three tetracycline-responsive forms of the U6 and H1 promoters were constructed in addition to the wild-type (wt) promoters. TetO sequences were inserted to replace wt promoter sequences adjacent to the TATA box as indicated in Figure 1. Both promoters were generated with the tetO sequence in an upstream (US), downstream (DS) or upstream plus downstream (US/DS) position relative to the TATA box. Both the U6 and H1 promoters are extremely compact and correct spacings between the transcriptional start and the essential 5′ flanking sequences (TATA box and PSE- proximal sequence element) are important for proper RNA expression. Therefore, to preserve the correct spacing in these promoters, only one complete tetO sequence can be inserted in each of the abovementioned positions of these promoters (see Figure 1).

Figure 1. Nucleotide sequence presentation of the tetracycline-inducible U6 and H1 promoter variants and anti-luc shRNA used in this study. PSE (proximal sequence element) is shown in italic letters. The TATA box is shaded in gray. O1 and O2 indicate O1-type and O2-type tetracycline operator (tetO) sequences, respectively. TetO sequences are shown in bold letters. The anti-luciferase shRNA sequence is underlined.

For the tet-inducible U6 promoter, we used three previously reported variants: U6-O1-US, contains a O1-type tetO located upstream of the TATA box in the U6 promoter (13). U6-O2-DS and U6-2O2-US/DS, contain O2-type tetO in the downstream position (14) and two O2-type tetO flanking the TATA box (15,20), respectively.

For the tet-inducible H1 promoter variants we only included the O2-type operator sequences,

since Lin *et al.* (15) had already shown that single O2-type tetO sequences are tighter regulators than O1-type tetO. Also, a US/DS inducible H1 promoter/operator variant containing two O1-type tetO sequences reported earlier (17), showed moderate transcriptional background and required high concentrations of the inducer molecule for high levels of transcription in transient transfection studies. We therefore set out to test H1-O2 variants. H1-O2-US was generated with an O2-type tetO upstream of the TATA box in the H1 promoter. Like for the U6 promoter, we also constructed an H1 promoter containing an O2-type tetO in the DS position relative to the TATA box (H1-O2-DS) (18). Finally, we constructed H1-2O2-US/DS, which contains two O2-type tetO sequences flanking the TATA box of the H1 promoter.

In order to monitor the expression level of the promoter/operator systems in non-induced and induced states, we cloned an efficient anti-luciferase (anti-luc) shRNA construct immediately downstream of the U6 and H1 transcription start sites (Figure 1). A termination sequence consisting of six uridine nucleotides was included to define the 3′ end of the shRNA transcript.

We were also interested in examining the characteristics of the various inducible promoter variants in different mammalian cell lines. Therefore, we constructed several cell lines stably expressing tetR. These include several human neuroblastoma cell lines (SK-N-BE2, SJNB8, IMR32, Kelly and SK-N-AS), a human cervical carcinoma cell line (HeLa) and a human osteosarcoma cell line (Saos-2). In addition, we analyzed inducible shRNA expression in a human embryonic kidney cell line (HEK293T-REx) available from Invitrogen, Carlsbad, CA, USA.

Analysis of the tet-inducible U6 and H1 promoters

The tetR-expressing cell lines were transiently co-transfected with three plasmids; a plasmid constitutively expressing the firefly luciferase reporter (pGL3-control), a plasmid constitutively expressing β-galactosidase in order to correct for variations in transfection efficiencies (pCMV-β-gal) and a test plasmid expressing the anti-luc shRNA from various U6 and H1 promoter variants.

Both the wt-U6 and wt-H1 promoters showed very efficient expression of anti-luc shRNA as seen by a dramatic reduction of luciferase activity (88–99%, see Figures 2 and 3). Expression of several different scrambled shRNA constructs showed no change in reporter activity as expected (data not shown).

The addition of 1 μg/ml dox (a tetracycline derivative) to tetR-expressing cells transfected with pGL3-control and pCMV-β-gal had only minor effects on reporter expression (PC; positive control in Figures 2 and 3). This indicates that the measured differences in luciferase activity between the induced and non-induced states were due to the effect of the anti-luc shRNA. Addition of 5 or 10 μg/ml dox resulted in changes in cell morphology and growth inhibition, so in all other experiments 1 μg/ml dox was used (data not shown).

U6 promoter variants. As can be seen in Figure 2, the non-induced U6-O1-US promoter gives high background transcription of the anti-luc shRNA in all cell lines tested. This is observed as a dramatic drop in luciferase activity in the absence of dox compared to the positive controls (PC). Addition of 1 μg/ml dox had only minor effects on shRNA expression. Similar results published by other research groups support our observation that an O1-type tetO located between the PSE and TATA box of the U6 promoter is not efficiently regulated by the tetR protein in transient transfection experiments (15,16,20). Matsukura *et al.* (16) were able to show efficient regulation of the U6-O1-US promoter when stably transfected HCT116 cells were used. Here, induction of shRNA synthesis required high levels of dox (10 μg/ml), which might be due to high tetR levels in these cells. A difference in regulation between transient and stable transfection experiments similar to this was not observed by another research group (15).

When an O2-type tetO is placed between the TATA box and the transcriptional start of the U6 promoter (U6-O2-DS), a more variable result is observed. In the SJNB8 TR (Figure 2B), IMR32 TR (Figure 2C), SK-N-AS TR (Figure 2D), HeLa TR (Figure 2E) and Kelly TR (data not shown) cell lines, the U6-O2-DS promoter is poorly repressed by tetR, while the HEK293T-REx (Figure 2F), SK-N BE2 TR (Figure 2A) and Saos2 TR (data not shown) cell lines show a tighter regulation of the promoter. The observed difference cannot be explained by different tetR expression levels, since all these cell lines express similar levels of the tetR protein (data not shown). Previous reports also indicate a cell type difference in regulation of a similar U6-O2-DS inducible promoter. Lin *et al.* (15) reported low transcription repression from this promoter in the HeLa-TREx cell line (Invitrogen), while others have reported tight control of this promoter in PC-3 and 293T cells (14,20). These observations are consistent with our results.

Addition of an O2-type tetO in the US position of U6-O2-DS creates the U6-2O2-US/DS tet-inducible U6 promoter. When an anti-luc shRNA expressing plasmid under the control of this promoter is cotransfected with the reporter plasmid into tetR-expressing cell lines, high levels of luciferase were measured in the absence of dox. Addition of dox gave a dramatic reduction of luciferase activity in all cell lines tested (Figure 2). Compared to U6-wt promoter activity, the induced U6-2O2 promoter shows 69, 84, 89, 82, 77 and 78% reporter knockdown in SK-N-AS TR, SJNB-8 TR, IMR32 TR, SK-N-AS TR, HeLa TR and HEK293-T REx cell lines, respectively.

Together, these results show that the U6-2O2-US/DS promoter exhibit the best dox response in all tested cell lines compared to other tetO containing U6 promoter variants. These results are in agreement with previous published data (15), and we here show that this is valid in a wide variety of different cell lines.

H1 promoter variants. All H1 promoter variants used in this study contained the O2-type tetO sequence. When this operator was inserted in the US position (H1-O2-US),

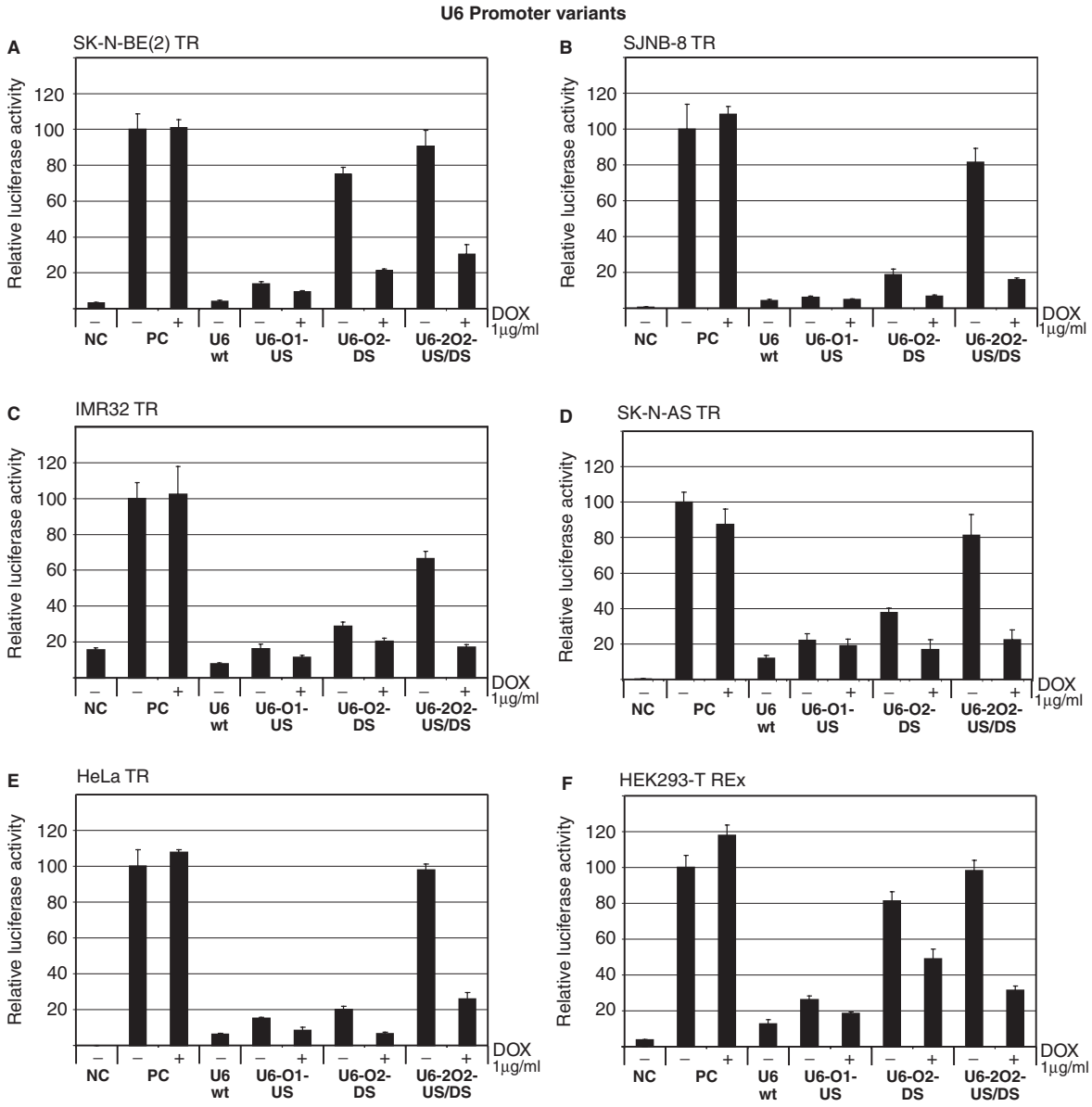

Figure 2. Conditional shRNA expression from U6 promoter variants. TetR-expressing cells were transfected with 100 ng pCMV-β-gal, 800 ng pGL3-control (Promega) and 100 ng anti-luc shRNA expressing test plasmids under control of various U6 promoter variants. Several different tetR-expressing cell lines were used. (**A**) SK-N-BE (2) TR, (**B**) SJNB-8 TR, (**C**) IMR32 TR, (**D**) SK-N-AS TR, (**E**) HeLa TR, (**F**) HEK293-T REx (Invitrogen). NC: negative control; 100 ng pCMV-β-gal and 800 ng pGL3-basic (no luciferase expression), PC: positive control; 100 ng pCMV-β-gal and 800 ng pGL3-control (constitutive luciferase expression), + indicates addition of 1 μg/ml dox 1-day post-transfection. Cells were incubated for a total of 3 days. Error bars indicate SDs.

moderate to high shRNA repression (Figure 3) was seen in the absence of dox in all cell lines tested. This indicates low to moderate background transcription in the non-induced state. In contrast to the U6 promoter containing tetO in a similar position, H1-O2-US is responsive to tetR repression. The observed difference could be explained by the fact that the O2-type tetO is a tighter regulator than O1-type tetO (15). Addition of 1 μg/ml dox increased shRNA expression significantly in all cell lines.

shRNA expression from H1 promoter containing an O2-type tetO sequence in the DS position (H1-O2-DS) has previously been reported to give efficient knockdown of β-catenin in stably transfected CRC cell lines (18). Significant promoter leakage was observed in non-induced cell lines that exhibited efficient knockdown upon induction. Our results show that this promoter variant gives moderate to high transcriptional background in all tested cell lines (Figure 3). Induction of anti-luc shRNA expression by addition of dox efficiently down-regulates the luciferase reporter to levels below that observed for the similar U6 promoter variant, indicating that transcriptional activity of the H1 promoter variant is higher.

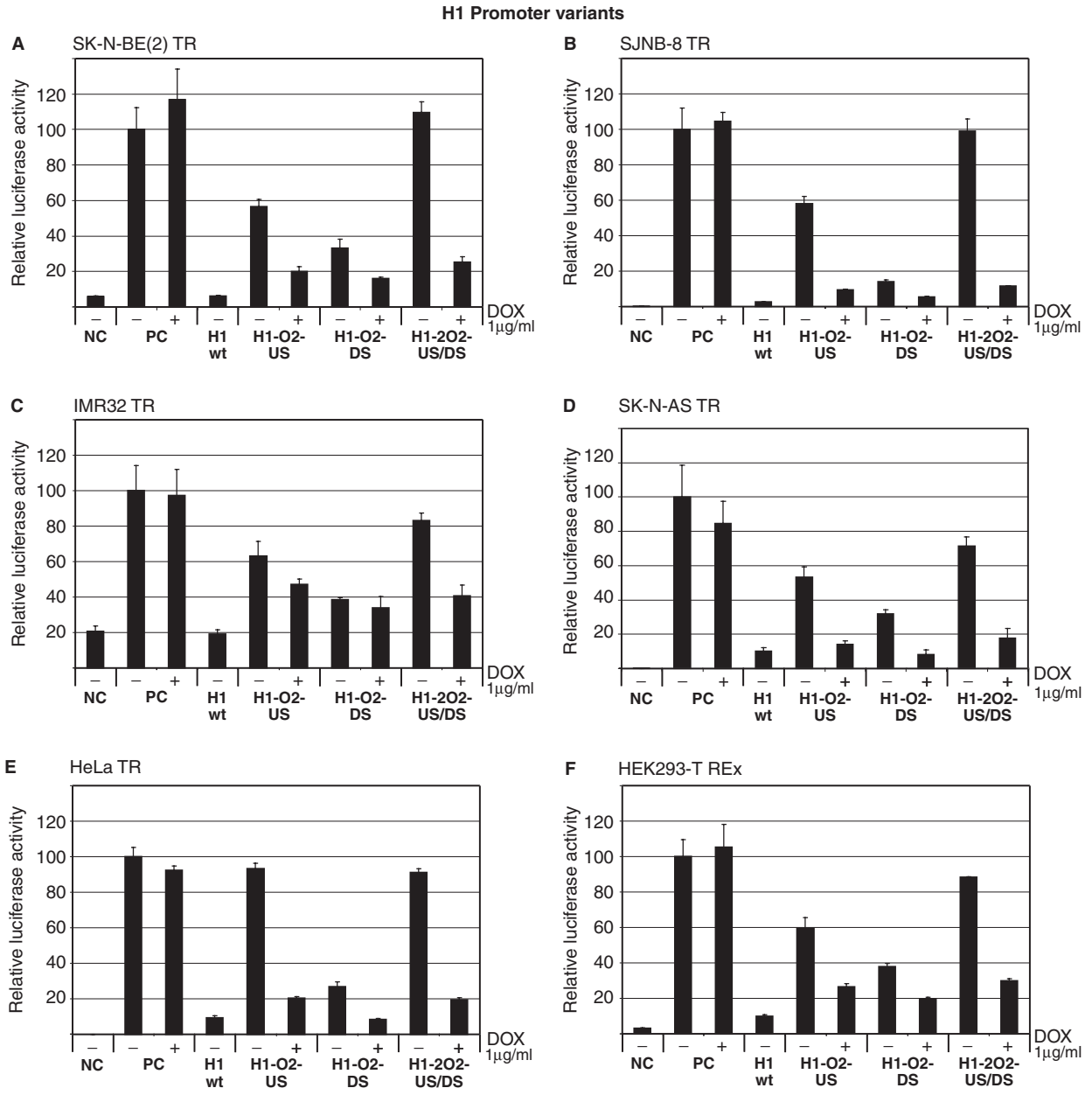

Figure 3. Conditional shRNA expression from H1 promoter variants. TetR-expressing cells were transfected with 100 ng pCMV-β-gal, 800 ng pGL3-control (Promega) and 100 ng anti-luc shRNA expressing test plasmids under control of various H1 promoter variants. Several different tetR-expressing cell lines were used. (**A**) SK-N-BE (2) TR, (**B**) SJNB-8 TR, (**C**) IMR32 TR, (**D**) SK-N-AS TR, (**E**) HeLa TR, (**F**) HEK293-T REx (Invitrogen). NC: negative control; 100 ng pCMV-β-gal and 800 ng pGL3-basic (no luciferase expression), PC: positive control; 100 ng pCMV-β-gal and 800 ng pGL3-control (constitutive luciferase expression), + indicates addition of 1 μg/ml dox 1-day post-transfection. Cells were incubated for a total of 3 days. Error bars indicate SDs.

Finally, we created an H1 promoter containing two O2-type operators in the US and DS positions (H1-2O2-US/DS). This inducible promoter shows tight shRNA repression in absence of dox in all tested cell lines (Figure 3). Addition of 1 μg/ml dox induces shRNA expression resulting in low levels of luciferase after 2 days of incubation. This means that the tetR protein efficiently blocks transcription from the H1-2O2-US/DS promoter. Compared to H1-wt promoter activity, the induced H1-2O2 promoter shows 81, 91, 67, 84, 87 and 74% reporter knockdown in SK-N-AS TR, SJNB-8 TR, IMR32 TR, SK-N-AS TR, HeLa TR and HEK293-T REx cell lines, respectively. Matthess *et al.* (17) have reported moderate tightness and only a small difference between the induced and non-induced state of an H1 promoter containing two O1-type tetO sequences (2O1). This is in agreement with earlier observations showing that O2-type tetO are tighter regulators of RNA pol III

promoters than O1-type tetO sequences (15). Very recently, Kappel *et al.* (21) showed that the background transcription of the 2O1-US/DS H1 promoter variant is less pronounced in stably transfected HeLa cells.

As can be seen from Figure 3, down-regulation of the luciferase reporter is most efficient in the neuroblastoma SJNB8 cell line (Figure 3B), where 91% reduction (compared to H1-wt) in luciferase activity was observed after addition of dox. Importantly, no background transcription from the promoter was observed in the non-induced state, indicating that this inducible promoter system is extremely tight.

In summary, most U6 and H1 promoter variants containing single tetO sequences are poorly regulated by tetR. In contrast, both U6-2O2-US/DS and H1-2O2-US/DS containing two O2-type tetO sequences are tight regulators of shRNA expression in all cell lines tested. For the cell lines used in this study, the H1-2O2-US/DS promoter is slightly more efficient for shRNA expression upon addition of the inducer dox than the U6-2O2-US/DS promoter The new tetO-containing RNA pol III promoters described in this study will be useful in basic research on gene function and possibly also for potential therapeutic applications.

Both single and double tetO inducible shRNA expression systems exist on the market today. In this work, we have constructed two new variants of an inducible H1 promoter (H1-O2-US and H1-2O2-US/DS) that show tight suppression of shRNA expression in the non-induced state, and high tet responsiveness and high reporter gene knock-down efficiency upon induction by dox. In addition, we have performed, for the first time, a detailed comparison of inducible shRNA expression systems in several different cell lines. Our results show that U6 and H1 promoter variants containing double tetO2 sequences are efficiently regulated by tetR in all cell lines tested, and we expect these promoter variants to be useful in other tetR-expressing cell lines as well.

MATERIALS AND METHODS

Molecular cloning

pSHAG-1 and pSHAG-Ff1 (5) contain a wt U6 promoter-driven expression cassette. pSHAG-Ff1 (U6 wt anti-luc shRNA in this study) encodes an anti-luc shRNA homologous to nucleotides 1340–1368 of the coding sequence of the firefly luciferase gene (NCBI accession number U47296) while pSHAG-1 is the negative control (NC) without shRNA sequence.

Table 1 shows the sequence of the oligonucleotides used for molecular cloning in this study.

Plasmids containing variants of the U6 promoter were constructed by PCR. An U6 promoter containing a tetO sequence upstream of the TATA box (U6-O1-US) was made by PCR amplification of the U6 promoter from pSHAG-1 using ON22 and ON31 (encodes the operator sequence) as primers. The resulting PCR product was used as template in a second PCR with ON22 and ON34 as primers to add the anti-luc shRNA sequence downstream of the U6-O1 promoter. This PCR product was digested with NotI/BamHI and ligated into a NotI/BamH1 cut pSHAG-1 vector to produce pU6-O1-US anti-luc.

Construction of U6 promoters containing one O2-type tetO sequence downstream of the TATA box and two O2-type tetO sequences flanking the TATA box, were performed with PCR in a similar procedure using ON22/ON37 and ON22/ON84, respectively. These PCR products were further amplified using ON22/ON38 and ON22/ON83 as primers, digested and ligated into

Table 1. Oligonucleotids used in this study

Name	Sequence (5′–3′)
ON22	ATAAGAATGCGGCCGCAAGGTCGGGCAGGAAGAGGGCC
ON31	GATCGGATCCGGTGTTTCGTCCTTTCCACAAGATATATAACTCTATCAATGATAGAGTACTTTCAAGTTA CGGTAAGCA
ON34	AGTCGGATCCAAAAAATGGATTCCAACTCAGCGAGAGCCACCCGATCAAGCTTCATCAGGTGGCTCCCG CTGAATTGGAATCCGGTGTTTCGTCCTTTCCAC
ON37	ACGATCTCTATCACTGATAGGGAGATATATAAAGCCAAGAAATCG
ON38	CGGGATCCAAAAAATGGATTCCAACTCAGCGAGAGCCACCCGATCAAGCTTCATCAGGTGGCTCCCGCT GAATTGGAATCCACGATCTCTATCACTGATAGGGAG
ON46	GATCGAATTCGAACGCTGACGTCATCAAC
ON47	GATCAGATCTGAGTGGTCTCATACAGAACTTATAAGATTCCCAAA
ON75	GATCAGATCTGAGTGGTCTCATACAGAACTTATAAGTCTCTATCACTGATAGGGATTTCACGTTTATGGT GATTTCCCA
ON76	GATCAGATCTCTATCACTGATAGGGAACTTATAAGTCTCTATCACTGATAGGGATTTCACGTTTATGGTGA TTTCCCA
ON77	GATCCCGGATTCCAATTCAGCGGGAGCCACCTGATGAAGCTTGACGGGTGGCTCTCGCTGAGTTGGAATC CATTTTTTGGAAA
ON78	AGCTTTTCCAAAAAATGGATTCCAACTCAGCGAGAGCCACCCGTCAAGCTTCATCAGGTGGCTCCCGCTGA ATTGGAATCCGG
ON83	GATCGGATCCAAAAAATGGATTCCAACTCAGCGAGAGCCACCCGATCAAGCTTCATCAGGTGGCTCCCGCT GAATTGGAATCCGGTCTCTATCACTGATAGGGAGATATATAA
ON84	GATCGGATCCGGTCTCTATCACTGATAGGGAGATATATAATCTCTATCACTGATAGGGAGTTTCAAGTTACG GTAAGCAT

pSHAG-1 to produce pU6-O2-DS anti-luc and pU6-2O2-US/DS anti-luc.

H1 variant promoters expressing the anti-luc shRNA were made as follows: pENTRH1-O2 is a pENTR3c (Invitrogen)-based plasmid that contains an H1 promoter with an O2-type tet operator in the DS position, followed by a BglII/HindIII-removable 750 bp 'stuffer' fragment. The H1 promoter sequence can be removed from this plasmid by EcoRI/BglII digestion. pENTRH1-wt (containing a wt H1 promoter) was made by amplifying the H1 promoter from pENTRH1-O2-DS with ON46 (EcoRI)/ON47 (BglII) as primers, digesting the resulting PCR product with EcoRI/BglII and ligation into a EcoRI/BglII digested pENTRH1-O2-DS vector. pENTRH1-O2-US and pENTRH1-2O2-US/DS were made in a similar way using ON46/ON75 and ON46/ON76 as PCR primers, respectively. The BglII/HindIII-removable 750 bp 'stuffer' fragment was then replaced with an anti-luc shRNA sequence by ligation of annealed primers ON77/ON78 into these vectors to produce: pH1-wt anti-luc, pH1-O2-US anti-luc, pH1-O2-DS anti-luc and pH1-2O2-US/DS anti-luc. All plasmid constructs were verified by DNA sequencing.

Cell culture and transfection

SK-N-BE (2), Kelly, SK-N-AS, Saos-2 and HeLa cells were grown in RPMI1640 supplemented with 10% FBS. SJNB8 and IMR32 cells were grown in Dulbecco's modified Eagle's medium supplemented with 10% FBS. HEK293-TREx cells (Invitrogen) were grown in Dulbecco's modified Eagle's medium supplemented with 10% FBS and 15 μg/ml blasticidin. All cells were maintained in a humidified 37°C incubator with 5% CO_2, supplied with fresh complete medium every 3 days, and subcultured before confluence was reached.

Also, $4–5 \times 10^5$ cells were seeded into each well of a 12-well tissue culture plate and transfection was performed the following day with Lipofectamin2000 (Invitrogen) according to the manufacturer's protocol.

Generation of stable cell lines producing tetracyclin repressor (tetR)

Cell lines were maintained and transfected as described above with the plasmid pcDNA6TR (Invitrogen) carrying a gene encoding the selectable marker, blasticidin, and a gene coding for the tetracycline operon repressor protein (tetR). Stably transfected cell lines resistant to blasticidin were selected and cultured in blasticidin-containing media.

Luciferase/β-galactosidase assay

TetR-expressing cells were transfected with the luciferase reporter plasmid pGL3-control (Promega, Madison, WI, USA), the β-galactosidase expressing pCMV-β-gal (Stratagene, La Jolla, CA, USA) and a test-plasmid expressing the anti-luc shRNA from various U6 and H1 promoters. HEK293T-REx cells were not transfected with pCMV-β-gal, since these cells already express β-galactosidase from the Flp-In cassette. The NC was transfected with pGL3-Basic (Promega), which lacks a promoter for expressing the reporter gene.

An aliquot of 1 μg/ml dox was added 24 h after transfection and cells were harvested after an additional 48 h of incubation. Luciferase and β-galactosidase activities were measured in triplicate immediately using the Dual-Light® System (Applied Biosystems, Foster City, CA, USA) according to the manufacturer's instructions. Normalization of luciferase measurements from HEK293T-REx was done using total protein. All experiments were performed at least in triplicate.

ACKNOWLEDGEMENTS

This work was supported by grants from the Northern-Norwegian Health Authorities (gene therapy program to T.F.), the Erna and Olav Aakre Foundation for Cancer research (to T.F. and C.E.), the Dutch Cancer Society 'KWF Kankerbestrijding' (Grants UVA 2003-2849 to D.G. and R.V., and UVA 2005-3665 to D.G.) and the SKK ('Stichting Kindergeneeskundig Kankeronderzoek') (to R.V.). pENTRH1-O2 was a kind gift from Sylvia Sagen at University of Tromsø. Funding to pay the Open Access publication charges for this article was provided by the Northern-Norwegian Health Authorities (gene therapy program).

Conflict of interest statement. None declared.

REFERENCES

1. Hannon,G.J. (2002) RNA interference. *Nature*, **418**, 244–251.
2. Zhou,D., He,Q.S., Wang,C., Zhang,J. and Wong-Staal,F. (2006) RNA interference and potential applications. *Curr. Top. Med. Chem.*, **6**, 901–911.
3. Amarzguioui,M., Rossi,J.J. and Kim,D. (2005) Approaches for chemically synthesized siRNA and vector-mediated RNAi. *FEBS Lett.*, **579**, 5974–5981.
4. Bernstein,E., Caudy,A.A., Hammond,S.M. and Hannon,G.J. (2001) Role for a bidentate ribonuclease in the initiation step of RNA interference. *Nature*, **409**, 363–366.
5. Paddison,P.J., Caudy,A.A., Bernstein,E., Hannon,G.J. and Conklin,D.S. (2002) Short hairpin RNAs (shRNAs) induce sequence-specific silencing in mammalian cells. *Genes Dev.*, **16**, 948–958.
6. Yu,J.Y., DeRuiter,S.L. and Turner,D.L. (2002) RNA interference by expression of short-interfering RNAs and hairpin RNAs in mammalian cells. *Proc. Natl Acad. Sci. USA*, **99**, 6047–6052.
7. Campbell,F.E.Jr. and Setzer,D.R. (1992) Transcription termination by RNA polymerase III: uncoupling of polymerase release from termination signal recognition. *Mol. Cell. Biol.*, **12**, 2260–2272.
8. Myslinski,E., Ame,J.C., Krol,A. and Carbon,P. (2001) An unusually compact external promoter for RNA polymerase III transcription of the human H1RNA gene. *Nucleic Acids Res.*, **29**, 2502–2509.
9. Park,J.S. and Kunkel,G.R. (1995) Both RNA polymerase III and RNA polymerase II accurately initiate transcription from a human U6 promoter in vitro. *Biochem. Biophys. Res. Commun.*, **214**, 934–940.
10. Yu,J. and McMahon,A.P. (2006) Reproducible and inducible knockdown of gene expression in mice. *Genesis*, **44**, 252–261.
11. Gupta,S., Schoer,R.A., Egan,J.E., Hannon,G.J. and Mittal,V. (2004) Inducible, reversible, and stable RNA interference in mammalian cells. *Proc. Natl Acad. Sci. USA*, **101**, 1927–1932.
12. Higuchi,M., Tsutsumi,R., Higashi,H. and Hatakeyama,M. (2004) Conditional gene silencing utilizing the lac repressor reveals a role of SHP-2 in cagA-positive Helicobacter pylori pathogenicity. *Cancer Sci.*, **95**, 442–447.

13. Ohkawa,J. and Taira,K. (2000) Control of the functional activity of an antisense RNA by a tetracycline-responsive derivative of the human U6 snRNA promoter. *Hum. Gene Ther.*, **11**, 577–585.
14. Czauderna,F., Santel,A., Hinz,M., Fechtner,M., Durieux,B., Fisch,G., Leenders,F., Arnold,W., Giese,K. *et al.* (2003) Inducible shRNA expression for application in a prostate cancer mouse model. *Nucleic Acids Res.*, **31**, e127.
15. Lin,X., Yang,J., Chen,J., Gunasekera,A., Fesik,S.W. and Shen,Y. (2004) Development of a tightly regulated U6 promoter for shRNA expression. *FEBS Lett.*, **577**, 376–380.
16. Matsukura,S., Jones,P.A. and Takai,D. (2003) Establishment of conditional vectors for hairpin siRNA knockdowns. *Nucleic Acids Res.*, **31**, e77.
17. Matthess,Y., Kappel,S., Spankuch,B., Zimmer,B., Kaufmann,M. and Strebhardt,K. (2005) Conditional inhibition of cancer cell proliferation by tetracycline-responsive, H1 promoter-driven silencing of PLK1. *Oncogene*, **24**, 2973–2980.
18. van de Wetering,M., Oving,I., Muncan,V., Pon Fong,M.T., Brantjes,H., van Leenen,D., Holstege,F.C., Brummelkamp,T.R., Agami,R. *et al.* (2003) Specific inhibition of gene expression using a stably integrated, inducible small-interfering-RNA vector. *EMBO Rep.*, **4**, 609–615.
19. Berens,C. and Hillen,W. (2004) Gene regulation by tetracyclines. *Genet. Eng. (NY)*, **26**, 255–277.
20. Chen,Y., Stamatoyannopoulos,G. and Song,C.Z. (2003) Down-regulation of CXCR4 by inducible small interfering RNA inhibits breast cancer cell invasion in vitro. *Cancer Res.*, **63**, 4801–4804.
21. Kappel,S., Matthess,Y., Zimmer,B., Kaufmann,M. and Strebhardt,K. (2006) Tumor inhibition by genomically integrated inducible RNAi-cassettes. *Nucleic Acids Res.*, **34**, 4527–4536.

PAPER II

Conditional expression of retrovirally delivered anti-MYCN shRNA as an in vitro model system to study neuronal differentiation in MYCN-amplified neuroblastoma

Jørn R. Henriksen[1,2], Bjørn Helge Haug[1], Jochen Buechner[1,2], Cecilie Løkke[1], Trond Flaegstad[1,2], Christer Einvik[1§]

[1] Department of Pediatrics, University Hospital of North-Norway, 9038 Tromsø, Norway

[2] Department of Pediatric Research, Institute of Clinical Medicine, University of Tromsø, 9037 Tromsø, Norway

[§]Corresponding author:

Email addresses:

JRH: joern.remi.henriksen@uit.no

BHH: bjorn.haug@uit.no

JB: jochen.buchner@unn.no

CL: cecilie.lokke@uit.no

TF: trond.flaegstad@unn.no

CE[§]: christer.einvik@uit.no

Abstract

Background: Neuroblastoma is a childhood cancer derived from immature cells of the sympathetic nervous system. The disease is clinically heterogeneous, ranging from neuronal differentiated benign ganglioneuromas to aggressive metastatic tumours with poor prognosis. Amplification of the MYCN oncogene is a well established poor prognostic factor found in up to 40 % of high risk neuroblastomas.

Using neuroblastoma cell lines to study neuronal differentiation *in vitro* is now well established. Several protocols, including exposure to various agents and growth factors, will differentiate neuroblastoma cell lines into neuron-like cells. These cells are characterized by a neuronal morphology with long extensively branched neurites and expression of several neurospecific markers.

Results: In this study we use retrovirally delivered inducible short-hairpin RNA (shRNA) modules to knock down *MYCN* expression in *MYCN*-amplified (MNA) neuroblastoma cell lines. By addition of the inducer doxycycline, we show that the Kelly and SK-N-BE(2) neuroblastoma cell lines efficiently differentiate into neuron-like cells with an extensive network of neurites. These cells are further characterized by increased expression of the neuronal differentiation markers *NFL* and *GAP43*. In addition, we show that induced expression of retrovirally delivered anti-*MYCN* shRNA inhibits cell proliferation by increasing the fraction of MNA neuroblastoma cells in the G1 phase of the cell cycle and that the clonogenic growth potential of these cells was also dramatically reduced.

Conclusion: We have developed an efficient *MYCN*-knockdown *in vitro* model system to study neuronal differentiation in MNA neuroblastomas.

Background

Neuroblastoma is a childhood cancer arising from the sympaticoadrenal lineage of the neural crest. It is characterized by diverse clinical behaviours ranging from spontaneous regression, maturation to more benign forms (ganglioneuroblastoma or ganglioneuroma), to rapid tumour progression and death [1]. Amplification of the *MYCN* oncogene has been considered the most important prognostic factor for progressive disease and poor outcome. Despite intense efforts to elucidate a mechanism by which *MYCN* overexpression acts to promote the aggressive phenotype, the functional roles of the MYCN protein in neuroblastoma are poorly understood [2].

Several alternative mechanisms for neuroblastoma regression have been proposed over the past 20 years, although the principal mechanism underlying this peculiar phenomenon remains to be fully elucidated [3-5]. Tumour maturation via neuronal differentiation has recently been proposed as a plausible candidate mechanism to explain neuroblastoma regression [6]. Therefore, the study of neuroblastoma as a model system for the general process of tumour cell differentiation, as well as neuronal development, is important to reveal the secrets of both tumour maturation and spontaneous regression.

Using neuroblastoma cell lines to study neuronal differentiation *in vitro* is now well established. Induced neuron-like morphological and biochemical changes to the SH-SY-5Y neuroblastoma cell line was demonstrated almost 30 years ago using a bioactive phorbolester as the inducing agent [7]. Since then, a variety of various agents and growth factors have been shown to induce neuronal differentiation in many neuroblastoma cell lines (reviewed in [8]). Furthermore, specific suppression of *MYCN* expression using traditional antisense techniques or small interfering RNA molecules (siRNA) have also been shown to promote neuronal differentiation in several *MYCN*-amplified (MNA) neuroblastoma cell lines [9-12].

Plasmid and viral vector-based systems containing RNA polymerase III promoters for the expression of short hairpin RNAs (shRNAs) have become useful tools for modulating gene expression in mammalian cells [13]. Compared to siRNAs, the use of shRNAs to suppress gene function has been demonstrated to be more effective [14]. In addition, shRNA-based strategies offer the advantage of inducible expression in situations in which gene knockdown is expected to have a deleterious effect on the targeted cell.

Retroviral expression systems have proven to be useful tools for sustained long-term expression of transgenes in mammalian cells [15]. With the development of protocols to produce high-titer infectious, replication-incompetent retroviral particles, these expression systems are now commonly used for shRNA delivery.

In this study, we have developed a retroviral tetracycline-inducible anti-*MYCN* shRNA expression system to study MYCN knockdown-mediated neuronal differentiation in MNA neuroblastoma cell lines. We reveal that MNA neuroblastoma cell lines induced to express the anti-*MYCN* shRNAs efficiently undergo morphological and biochemical changes consistent with neuronal differentiation.

Results and Discussion

Retrovirally delivered inducible shRNA expression in HEK293T-Rex cells

We have previously developed and characterized an efficient doxycyclin (dox)-inducible variant of the H1 promoter (H1-2O2-US/DS) for shRNA expression in human cells. The H1-2O2-US/DS promoter was shown to be almost completely inactive in the non-induced state,

while induction by dox yielded a high shRNA expression in transient transfection studies using an anti-luciferase (anti-luc) shRNA reporter system [16].

As a first step towards developing a long-term inducible shRNA expression system, we subcloned the previously described anti-luc shRNA constructs and the corresponding scrambled control shRNA into a retroviral expression vector. shRNA-expressing retroviruses were transduced into HEK293T-Rex cells followed by transient transfection of the luciferase reporter vector. Two days after transfection, cells were monitored for dox-regulated shRNA expression. Addition of dox to the transduced cells had only minor effects on luciferase expression as can be seen from both the inducible scrambled negative control (H1-2O2 Scr) and the H1-wt expressed anti-luc shRNA (H1-wt a-Luc) (**Figure 1**). Induction of anti-luc shRNA expression from the H1-2O2 promoter by the addition of dox downregulated the luciferase reporter to levels similar to that observed for the H1-wt promoter. At the same time, no transcriptional activity was observed in the non-induced state (H1-2O2 aLuc, –dox) when compared to the scrambled shRNA control.

These data clearly show that retroviral delivery of the H1-2O2 US/DS-inducible shRNA expression system to HEK293T-Rex cells allows an efficient inducible expression of mature shRNA molecules.

Efficient downregulation of *MYCN* expression in MNA neuroblastoma cell lines

We have previously designed an anti-*MYCN* shRNA construct (aMN-887) for downregulation of *MYCN* oncogene expression in *MYCN*-amplified (MNA) neuroblastoma cells [17]. This design procedure was based on the original Hannon protocol for shRNA construction, recommending 29 bp stem structures [18]. We have now constructed a new anti-*MYCN* shRNA construct (aMN-1658) targeting the 3'UTR of the *MYCN* mRNA.

The MNA Kelly and SK-N-BE(2) neuroblastoma cell lines were transiently transfected with plasmids expressing the aMN-887 or aMN-1658 shRNAs. A scrambled shRNA (Scr) construct was used as the control. Three days after transfection, cells receiving the aMN (anti-*MYCN*) shRNAs appeared to have a more neuron-like phenotype characterized by neurite outgrowth, while cells transfected with the control shRNA did not reveal any morphological alterations as compared to non-transfected cells **(Figure 2)**. Western immunoblot and quantitative real-time RT-PCR analysis confirmed specific suppression of the MYCN protein and *MYCN* mRNA in both cell lines, respectively **(Figure 3a and Figure 3b)**.

Consistent with previous data, an inverse correlation between *MYCN* and *c-MYC* mRNA expression was also confirmed (**Figure 3c**) [19,20]. The observed morphological changes were documented biochemically by increased expression of the early neuronal differentiation marker *NFL* (**Figure 3d**). Furthermore, expression of aMN-1658, but not of aMN-887, resulted in a marked increase in the late neuronal differentiation marker *GAP43*, which is known to be involved in axonal outgrowth and synapse formation (**Figure 3e**) [21]. This observation is consistent with the more extensive neuronal differentiation observed for both Kelly and SK-N-BE(2) cells transfected with aMN-1658 compared to cells transfected with aMN-887 (**Figure 2**).

These data show that aMN-1658 is an efficient anti-*MYCN* shRNA construct which suppresses *MYCN* expression and induces prominent neuronal differentiation in MNA neuroblastoma cell lines. For that reason, the aMN-1658 shRNA was used in the following research to knock down MYCN expression.

Previous reports document conflicting results on cell cycle distribution data of SK-N-BE(2) cells treated with anti-*MYCN* siRNAs. While Yu et al. reported no apparent difference in the

fraction of G1 cells after siRNA treatment, Bell et al. showed that *MYCN* siRNA treatment increased the G1 population by 8.1 % compared to a negative scrambled control siRNA [9,22]. In order to investigate the effect of shRNA-mediated *MYCN* knockdown on the cell cycle distribution pattern, we transiently transfected SK-N-BE(2) cells with plasmids expressing the aMN-887, aMN-1658 or a scrambled shRNA from a wt H1 promoter. Three days posttransfection the cell cycle distribution pattern was monitored using flow cytometry. The fraction of cells in the G1 phase of the cell cycle increased from 57% (Scr) to 74% for SK-N-BE(2) cells transfected with the aMN-1658 shRNA (**Figure 3f**). Similar results were obtained with aMN1658-transfected Kelly cells (**Figure 3g**).

A discrepancy between the knockdown levels for the MYCN protein (85-94 %) and mRNA (45-70 %) was observed in our *MYCN* shRNA knockdown experiments, with similar results being previously reported for *MYCN* siRNA knockdown by others [23]. In order to further document that only the expression of the *MYCN* shRNAs results in reduced MYCN expression, we set up additional experiments. The complete *MYCN* 3'UTR sequence, including the aMN-1658 target sequence, was cloned behind a luciferase reporter gene in the pMIR-REPORT vector (Ambion). Co-transfecting this reporter vector and the aMN-shRNA expressing plasmids into HEK-293 cells demonstrated the specific knockdown, monitored as an 80% reduction in luciferase activity, by the aMN-1658 shRNA (**Additional file 2a**). When aMN-1658 was co-transfected with a control reporter vector containing a 3'UTR lacking the aMN-1658 target sequence (Luc NT-3'UTR), no change in luciferase expression was observed, and similar results were obtained in the non-MNA neuroblastoma cell line SH-SY-5Y (data not shown).

In addition, we co-expressed the aMN-shRNA constructs and the *MYCN* cDNA lacking the 3'UTR sequence in a MNA neuroblastoma cell line. Downregulation of both the endo- and

exogenously expressed MYCN protein was only observed for the aMN-887 shRNA targeting the coding region of *MYCN*. The aMN-1658 shRNA was not able to suppress the exogenously expressed *MYCN* cDNA lacking the 3'UTR structure (**Additional file 2b**).

These experiments show that the aMN-1658 shRNA specifically reduces expression of mRNAs containing the *MYCN* 3'UTR target. However, we have not been able to confirm or rule out the possibility that a part of the MYCN protein reduction by aMN-1658 shRNA knockdown is mediated by a miRNA-like mechanism not involving mRNA degradation. Nonspecific cellular effects induced by shRNA expression were excluded by showing that the expression level of several genes involved in the interferon response (*OAS2*, *MX1*, *IFITM1* and *ISGF3γ*) remained unaltered during transfection of various shRNA constructs (data not shown).

Retrovirally delivered inducible anti-*MYCN* shRNA expression in MNA neuroblastoma cell lines

In order to generate a long-term inducible anti-*MYCN* shRNA expression system, we first cloned the aMN-1658 shRNA module behind the inducible H1-2O2-US/DS promoter and then gated the resulting construct into a retroviral expression vector to generate pRV-1658. A similar vector expressing a scrambled shRNA was constructed as a negative control (pRV-Scr).

Kelly and SK-N-BE(2) neuroblastoma cell lines stably expressing the TetR (tetracycline repressor) were transduced with the retroviruses RV-1658 and RV-Scr and then incubated for 6 days in a growth medium both with and without dox. As can be seen from **Figure 4a and Figure 4b**, only the cells induced to express the aMN-1658 shRNA demonstrated prominent neuronal differentiation. The lack of morphological changes in non-induced RV-1658

transduced cells indicates that the H1-2O2 promoter shows minimal transcriptional leakage in the absence of dox. The addition of dox to RV-Scr transduced cells had no significant effect on the cell morphology. Western blot analysis of the retrovirally transduced Kelly and SK-N-BE(2) cells revealed efficient repression of MYCN expression in cells induced to express the aMN-1658 shRNA (**Figure 4c**). Similar to the observations made in transient expression analyses, the *MYCN* mRNA levels were reduced to a lesser extent when compared to the western blot data (data not shown and Figure 5b).

In order to investigate the reversibility of the inducible retroviral shRNA expression system, we performed a time-course experiment in which the aMN-1658 expression was turned on for 3 days before removing dox from the media for another 3 days to eliminate shRNA expression.

Compared to the differentiated cells continuously exposed to aMN-1658 shRNA for 6 days, no significant change in cell morphology was observed when shRNA expression was turned off (data not shown). When the MYCN protein and mRNA levels were measured during the 6 days of shRNA induction, a steady decrease in MYCN expression was observed. Removal of dox from the media after 3 days of exposure did not efficiently recover MYCN expression. Consistent with the observed neuron-like phenotype, GAP43 protein levels remained high after dox removal (**Figure 5a and Figure 5b**).

By the use of a quantitative RT-PCR protocol designed to measure the mature antisense shRNA strand, we observed a maximum 90-fold increase in aMN-1658 RNA after 3 days of dox induction in the Kelly cells (**Figure 5c**). After additional 3 days of induction, a slight decrease in shRNA expression was observed. For the SK-N-BE(2) cell line, a maximum 50-fold increase in shRNA expression was observed after 6 days of continuous induction. Removing the inducing agent from the media did not efficiently cease shRNA expression. We

suggest that this lack of reversibility is most likely due to high intracellular shRNA stability and/or insufficient removal of dox from the media.

We also analysed the expression of the neuronal differentiation markers *NFL* and *GAP43* in Kelly and SK-N-BE(2) cells transduced with shRNA-expressing retroviruses. Consistent with the observed morphological changes towards a neuronal phenotype, both differentiation markers increased upon aMN-1658 induction (**Figure 5a, Additional file 3a and Additional file 3b**). Quantitative real-time PCR revealed a 5-8 fold increase in *NFL* mRNA and a 3-fold increase in *GAP43* mRNA in both cell lines induced to express the aMN-1658 shRNA.

In summary, these data show that retroviral delivery of inducible anti-*MYCN* shRNAs to MNA neuroblastoma cells efficiently reduces MYCN protein expression and induces neuronal differentiation.

Induced anti-*MYCN* shRNA expression inhibits cell proliferation and clonogenic growth of MNA neuroblastoma cells

The Alamar Blue Assay was used to measure cell proliferation in MNA neuroblastoma cells induced to express the anti-*MYCN* shRNA from retroviral vectors. **Figure 6** shows that the rate of cell proliferation was selectively decreased from day 2 in SK-N-BE(2) and day 3 in Kelly cells induced to express the aMN-1658 shRNA. Cells expressing the scrambled shRNA showed no differences in cell proliferation due to the presence or absence of dox. The slight reduction in cell proliferation observed in the non-induced aMN-1658 transduced cells is most likely due to a small leakage from the shRNA-expressing promoter. The delayed decrease in cell proliferation observed in Kelly cells is consistent with the ~5-fold higher *MYCN* mRNA levels in comparison to MNA SK-N-BE(2) [24,25].

The observed reduction in the proliferation of cells induced to express the anti-*MYCN* shRNA was further investigated by flow cytometry in order to elucidate the cell cycle distribution pattern. Induced *MYCN* knockdown in the MNA Kelly cells increased the fraction of G1 cells from 63% to 72%. For the MNA SK-N-BE(2) cells the fraction of G1 cells increased from 46% to 57% upon induction of aMN-1658 expression. Additon of dox alone had no effect on the cell cycle distribution pattern in cells transduced with retroviruses expressing a scrambled shRNA control (**Additional file 4**).

Finally, *in vitro* clonogenic assays were used to measure the reproductive cell survival in MNA neuroblastoma cells induced to differentiate by *MYCN* knockdown. **Figure 7** shows that *MYCN* knockdown leads to dramatic growth inhibition only in MNA neuroblastoma cells induced to express the anti-*MYCN* shRNA.

Together, these data indicate that the induced expression of retrovirally delivered anti-*MYCN* shRNA inhibits cell proliferation by increasing the fraction of MNA neuroblastoma cells in the G1 phase of the cell cycle. The clonogenic growth potential of these cells was also dramatically reduced.

Conclusion

We have developed an efficient *MYCN*-knockdown *in vitro* model system to study neuronal differentiation in MNA neuroblastomas.

Methods

Cell cultures and transfection

The human *MYCN*-amplified neuroblastoma cell lines Kelly and SK-N-BE(2), and their derivatives SKNBE(2)-TetR and Kelly-TetR (constitutively expressing the Tetracycline Repressor), were cultivated as previously described [16]. HEK293 and Hek293 Phoenix-amphopack (a kind gift from Dr. James Lorens) cells were grown in a Dulbecco's modified Eagle's medium (DMEM) [26]. HEK293-TREx cells (Invitrogen, Carlsbad, CA, USA) were grown in DMEM with 15 µg/ml blasticidin. All media were supplemented with 10% FBS. Cells were maintained in a humidified 37°C incubator with 5% CO_2, supplied with a fresh complete medium every 3 days and subcultured before confluence was reached.
Cell lines were transfected using Lipofectamine 2000 (Invitrogene) according to the manufacturer's instructions.

Molecular cloning

The number denotation of anti-*MYCN* (aMN) shRNAs describes the first position of the shRNA target recognition site in the *MYCN* cDNA sequence (NM_005378).
Construction of the following shRNAs was performed by annealing a sense and an antisense oligonucleotide: aMN-887 (ON106/ON107) and aMN-1658 (ON413/ON414).
Oligonucleotide (ON) sequences are listed in **Additional file 1**. Annealed oligonucleotides were ligated into BglII/HindIII digested pENTR-H1-wt or pENTR-H1-2O2-US/DS vectors as previously described [16] to generate paMN-887/H1wt, paMN-887/H1-2O2, paMN-1658/H1wt and paMN-1658/H1-2O2. Scrambled (Scr) shRNA expressing vectors pScr/H1wt and pScr/H1-2O2 were made in a similar way using ON110/ON111. The vectors paMN-887/H1wt and paMN-1658/H1wt were used in transient transfection studies.

To generate the inducible retroviral expression vectors pRV-1658 and pRV-Scr, the shRNA expression modules from paMN-1658/H1-2O2 and pScr/H1-2O2 respectively, were gated into the retroviral destination vector L193 RRI-GreenattR1ccdBCmRattR2 (a kind gift from Dr. David Micklem) using the Gateway LR Clonase Enzyme Mix (Invitrogen). L193 RRI-GreenattR1ccdBCmRattR2 is based on the L071 RRI-Green vector [27]. The U6promoter/shRNA cloning cassette of L071 (flanked by HindIII and SalI sites) was replaced with an attR1-ccdB-CmR-attR2 Gateway cloning cassette derived from pDONR221 (Invitrogen). This cassette allows L193 to be used as a Gateway Destination Vector and requires that the vector is propagated in a ccdB-resistant strain. All plasmid constructs were verified by DNA sequencing.

Production of retroviruses, transduction and induction of shRNA expression

Retroviral destination vectors pRV-1658 and pRV-Scr were transfected into the Hek293-Phoenix packaging cell line seeded in 6-well plates. 24h after transfection, the culture media were replaced by fresh media corresponding to the cell line being transduced. After another 24h of incubation, the media were passed through a Millex HV 0.45 µm PVDF filter (Millipore, Bedford, MA, USA) to isolate retroviral particles. Polybrene (Sigma, St. Louis, MO, USA) was added to a final concentration of 4 µg/ml.

Cells were transduced by replacing the growth media with the solution of isolated retroviruses containing polybrene. The following day the virus-containing media were replaced with normal growth media containing puromycin (HEK293T-Rex and Kelly: 200 ng/ml, SK-N-BE(2): 2500 ng/ml).

Induction of shRNA expression was performed by the addition of 1µg/ml doxycyclin (dox) to the media.

Quantitative real-time RT-PCR

Total RNA was extracted using the Qiagen miRNeasy Mini Kit (Qiagen, Hilden, Germany). 1 µg total RNA was reverse transcribed in 20 µl using a Qiagen miScript Reverse Transcription Kit according to the manufacturer's instructions. Real-time PCR analysis was performed in 25 µl reactions using *Power* SYBR Green PCR Master Mix (Applied Biosystems, Warrington, UK) as recommended by the manufacturer (2.5 µl of a 20x-diluted RT-reaction as template, 0.2 µM of each primer). *UBC* (ON56/ON57) and *PPIA* (ON174/ON175) were used as reference genes for normalizing expression levels of *MYCN* (ON440/ON441 and ON145/146 were used for comparing the effect of aMN-887 and aMN-1658), *NFL* (ON58/ON59), *GAP43* (ON298/ON299) and *c-myc* (ON100/ON101). Primer sequences are listed in **Additional file 1**.

Quantification of the aMN-1658 shRNA was performed using miScript SYBR green PCR Kit (Qiagen) in 50 µl reactions with 1 µl of the 20x-diluted RT-reaction as template. Specific primers for quantifying aMN-1658 shRNA were ordered as a custom miScript Primer Assay from Qiagen using 5'CACACAAGGUGACUUCAACAGUU3' as the mature miRNA sequence, and were used at concentrations specified by the manufacturer. *UBC* and *PPIA* were used for normalizing. All quantitative PCR reactions were performed using the Applied Biosystems 7300 Real-Time PCR System (Applied Biosystems) with thermal profiles as recommended by the manufacturer. The fold change in mRNA and miRNA levels were calculated using the ΔΔCT method with the qBASE software [28].

Western blotting

Cells were trypsinized and lysed in a Tropix Lysis Solution (Bedford, MA, USA). Lysate cleared by centrifugation was measured for total protein using Bio-Rad *DC* protein assay (Bio-Rad, Hercules, CA, USA), and 35 µg protein were loaded in each well on pre-casted NuPAGE 4-12% Bis-Tris Gels (Invitrogen). The separated proteins were transferred to an

Immobilon-FL PVDF transfer membrane (Millipore) and blocked for 1 hour at room temperature in Odyssey Blocking Buffer (LI-COR, Lincoln, NE, USA) before incubation at 4°C overnight with the following primary antibodies: mouse anti-NMYC (Calbiochem/Merck, Darmstadt, Germany), mouse anti-GAP43 (Abcam, Cambridge, UK), goat anti-NFL (Santa Cruz Biotech., Santa Cruz, CA, USA) and rabbit anti-βActin (Sigma) diluted in the blocking buffer. Secondary antibodies were goat anti-rabbit IRDye800CW (Rockland, Gilbertsville, PA, USA) and goat anti-mouse Alexa Fluor 680 (Invitrogen). Antibody binding was detected using the Odyssey Infrared Imaging System (LI-COR). NFL was detected by HRP conjugated rabbit anti-goat secondary antibody (DAKO, Glostrup, Denmark) and SuperSignal West Pico Chemiluminescent Substrate (Pierce, Rockford, IL, USA).

Luciferase assay

Retrovirus-transduced HEK293T-Rex cells were seeded in 12-well plates. 48 hrs following induction with 1µg/ml dox, each well was transfected with 0.02 µg pGL4.75[hRluc/CMV] Vector (Promega, Madison, WI, USA) and 0.1 µg pGL3 Control Vector (Promega). Firefly and renilla luciferace activity were measured after 48 hrs using the Dual-Luciferase Reporter Assay System (Promega) according to the manufacturer's instructions. Luminescence was measured on a Luminoskan Ascent luminometer (Thermo Sci., Waltham, MA, USA). Renilla luciferase was used to normalize the data, and all experiments were performed in triplicate.

Clonogenic assay

The cells were grown for 7-11 days with replacement of the media every third day. On the last day of the experiment, the cells were washed once in 1 x PBS and stained with the clonogenic reagent (50% EtOH, 0.25% 1,9-dimethyl-methylene blue) for 45 min. Cells were washed twice in PBS before visible colonies were counted.

Cell viability assay

The cytotoxic effect of induced *MYCN* knockdown on MNA neuroblastoma cells was analysed using the Alamar Blue Assay according to the manufacturer's instructions. In brief, the cells were seeded at a density of 40000 (Kelly) and 15000 (SK-N-BE(2)) cells per well in 12-well plates. Media were replaced every second day. On the indicated days, 100 µl of Alamar Blue solution were added to each well and incubated for 4 hrs at 37^{o}C. Absorbance at 570 and 600 nm was measured on a plate reader and the relative reduction of Alamar Blue was calculated as described by the manufacturer. The calculated average relative reduction from three independent experiments was calculated.

Flow cytometric analysis of cell cycle distribution

Cells were harvested using Trypsin-EDTA (Sigma-Aldrich) and washed once in 1 x PBS. The cells were then fixed for 2 hrs in ice-cold 70% EtOH. After fixation, the EtOH was removed by centrifugation and the cells were washed once in 1 x PBS before being stained for 30 min at room temperature in a propidium iodide (PI)-staining solution (PBS with 20 µg/ml PI (Sigma), 60 µg/ml RNase A (Sigma) and 0.1% v/v Triton X-100 (Sigma)). Fluorescence emitted from the PI-DNA complex was analysed by flow cytometry, using a FACS Aria Flow Cytometer (BD Biosciences, San Jose, CA, USA).

Competing interests

The authors have declared that no conflicts of interests exist.

Author's contributions

JRH designed and constructed the vectors, performed most of the experiments, drafted the manuscript, and critically planned and discussed all aspects of this work. BHH performed the clonogenic assays, participated in transduction studies. BHH, JB and TF helped to plan and critically discuss the study and participated in drafting the manuscript. CL cultivated the cell cultures and participated in the experimental work involving cell cultures and luciferase measurements. CE designed and supervised the experimental work and wrote the final manuscript.

Acknowledgements

This work was supported by grants from the Northern-Norwegian Health Authorities (gene therapy program) and Norwegian Cancer Society (Ragnvarda F. Sørvik and Håkon Starheims Foundation).

References

1. Maris JM, Hogarty MD, Bagatell R, Cohn SL: **Neuroblastoma.** *Lancet* 2007, **369:** 2106-2120.
2. Bell E, Chen L, Liu T, Marshall GM, Lunec J, Tweddle DA: **MYCN oncoprotein targets and their therapeutic potential.** *Cancer Lett* 2010, **293:** 144-157.
3. Kitanaka C, Kato K, Ijiri R, Sakurada K, Tomiyama A, Noguchi K *et al*.: **Increased Ras expression and caspase-independent neuroblastoma cell death: possible mechanism of spontaneous neuroblastoma regression.** *J Natl Cancer Inst* 2002, **94:** 358-368.
4. Pritchard J, Hickman JA: **Why does stage 4s neuroblastoma regress spontaneously?** *Lancet* 1994, **344:** 869-870.
5. Bolande RP: **The spontaneous regression of neuroblastoma. Experimental evidence for a natural host immunity.** *Pathol Annu* 1991, **26 Pt 2:** 187-199.

6. Koizumi H, Hamano S, Doi M, Tatsunami S, Nakada K, Shinagawa T *et al*.: **Increased occurrence of caspase-dependent apoptosis in unfavorable neuroblastomas.** *Am J Surg Pathol* 2006, **30:** 249-257.

7. Pahlman S, Odelstad L, Larsson E, Grotte G, Nilsson K: **Phenotypic changes of human neuroblastoma cells in culture induced by 12-O-tetradecanoyl-phorbol-13-acetate.** *Int J Cancer* 1981, **28:** 583-589.

8. Edsjo A, Holmquist L, Pahlman S: **Neuroblastoma as an experimental model for neuronal differentiation and hypoxia-induced tumor cell dedifferentiation.** *Semin Cancer Biol* 2007, **17:** 248-256.

9. Bell E, Premkumar R, Carr J, Lu X, Lovat PE, Kees UR *et al*.: **The role of MYCN in the failure of MYCN amplified neuroblastoma cell lines to G1 arrest after DNA damage.** *Cell Cycle* 2006, **5:** 2639-2647.

10. Haber M, Bordow SB, Gilbert J, Madafiglio J, Kavallaris M, Marshall GM *et al*.: **Altered expression of the MYCN oncogene modulates MRP gene expression and response to cytotoxic drugs in neuroblastoma cells.** *Oncogene* 1999, **18:** 2777-2782.

11. Negroni A, Scarpa S, Romeo A, Ferrari S, Modesti A, Raschella G: **Decrease of proliferation rate and induction of differentiation by a MYCN antisense DNA oligomer in a human neuroblastoma cell line.** *Cell Growth Differ* 1991, **2:** 511-518.

12. Tonelli R, Purgato S, Camerin C, Fronza R, Bologna F, Alboresi S *et al*.: **Anti-gene peptide nucleic acid specifically inhibits MYCN expression in human neuroblastoma cells leading to cell growth inhibition and apoptosis.** *Mol Cancer Ther* 2005, **4:** 779-786.

13. Wang SL, Yao HH, Qin ZH: **Strategies for short hairpin RNA delivery in cancer gene therapy.** *Expert Opin Biol Ther* 2009, **9:** 1357-1368.

14. Yu JY, DeRuiter SL, Turner DL: **RNA interference by expression of short-interfering RNAs and hairpin RNAs in mammalian cells.** *Proc Natl Acad Sci U S A* 2002, **99:** 6047-6052.

15. Lorens JB, Sousa C, Bennett MK, Molineaux SM, Payan DG: **The use of retroviruses as pharmaceutical tools for target discovery and validation in the field of functional genomics.** *Curr Opin Biotechnol* 2001, **12:** 613-621.

16. Henriksen JR, Lokke C, Hammero M, Geerts D, Versteeg R, Flaegstad T *et al*.: **Comparison of RNAi efficiency mediated by tetracycline-responsive H1 and U6 promoter variants in mammalian cell lines.** *Nucleic Acids Res* 2007, **35:** e67.

17. Henriksen JR, Buechner J, økke C, Flægstad T, Einvik C: **Inhibition of gene function in mammalian cells using short-hairpin RNA (shRNA).** *In: Methods in Molecular Biology*, in press.

18. Paddison PJ, Caudy AA, Bernstein E, Hannon GJ, Conklin DS: **Short hairpin RNAs (shRNAs) induce sequence-specific silencing in mammalian cells.** *Genes Dev* 2002, **16:** 948-958.

19. Breit S, Schwab M: **Suppression of MYC by high expression of NMYC in human neuroblastoma cells.** *J Neurosci Res* 1989, **24:** 21-28.

20. Westermann F, Muth D, Benner A, Bauer T, Henrich KO, Oberthuer A *et al*.: **Distinct transcriptional MYCN/c-MYC activities are associated with spontaneous regression or malignant progression in neuroblastomas.** *Genome Biol* 2008, **9:** R150.

21. Schrama LH, Lepperdinger G, Moritz A, van den Engel NK, Marquart A, Oestreicher AB *et al*.: **B-50/growth-associated protein-43, a marker of neural development in Xenopus laevis.** *Neuroscience* 1997, **76:** 635-652.

22. Yu UY, Cha JE, Ju SY, Cho KA, Yoo ES, Ryu KH *et al*.: **Effect on Cell Cycle Progression by N-Myc Knockdown in SK-N-BE(2) Neuroblastoma Cell Line and Cytotoxicity with STI-571 Compound.** *Cancer Res Treat* 2008, **40:** 27-32.

23. Bell E, Lunec J, Tweddle DA: **Cell cycle regulation targets of MYCN identified by gene expression microarrays.** *Cell Cycle* 2007, **6:** 1249-1256.

24. Edsjo A, Nilsson H, Vandesompele J, Karlsson J, Pattyn F, Culp LA *et al*.: **Neuroblastoma cells with overexpressed MYCN retain their capacity to undergo neuronal differentiation.** *Lab Invest* 2004, **84:** 406-417.

25. De PK, Pattyn F, Berx G, Strumane K, Menten B, Van RF *et al*.: **Combined subtractive cDNA cloning and array CGH: an efficient approach for identification of overexpressed genes in DNA amplicons.** *BMC Genomics* 2004, **5:** 11.

26. Swift S, Lorens J, Achacoso P, Nolan GP: **Rapid production of retroviruses for efficient gene delivery to mammalian cells using 293T cell-based systems.** *Curr Protoc Immunol* 2001, **Chapter 10:** Unit 10.17C.

27. Evensen L, Micklem DR, Blois A, Berge SV, Aarsaether N, Littlewood-Evans A *et al*.: **Mural cell associated VEGF is required for organotypic vessel formation.** *PLoS One* 2009, **4:** e5798.

28. Hellemans J, Mortier G, De PA, Speleman F, Vandesompele J: **qBase relative quantification framework and software for management and automated analysis of real-time quantitative PCR data.** *Genome Biol* 2007, **8:** R19.

Figures

Figure 1 - Retrovirally delivered inducible shRNA expression in HEK293 cells

TetR-expressing HEK293 cells (HEK293T-Rex) were transduced with retroviruses expressing anti-Luciferase (a-Luc) or scrambled (Scr) shRNAs. The a-Luc shRNA was expressed from a wt-H1 or the inducible H1-2O2 promoter in the absence (-) or presence (+) of 1 μg/ml doxycyclin (dox) for 48 hrs. Error bars indicate SDs.

Figure 2 – MYCN knockdown induces neurite outgrowth in MNA neuroblastoma cell lines

MNA Kelly **(A)** and SK-N-BE(2) **(B)** cells transiently transfected for 3 days with anti-*MYCN* (aMN-887 and aMN-1658) and scrambled (Scr control) shRNA expressing plasmids. Cells

expressing the aMN shRNAs show neurite outgrowth characteristic of neuronal differentiated cells. White arrows indicate neurite outgrowth.

Figure 3 – Transient *MYCN* knockdown in MNA Kelly and SK-N-BE(2) cells using shRNA technology

(**A):** A representative western blot analysis of MYCN protein expression in Kelly and SK-N-BE(2) cells transiently transfected for 3 days with plasmids expressing the aMN-887 and aMN1658 shRNAs. β–actin expression was used for normalization. Quantitative real-time RT-PCR was used to investigate the expression of *MYCN* **(B)**, *c-MYC* **(C)**, neurofilament light-chain – *NFL* **(D)** and growth-associated protein 43 - *GAP43* **(E)** mRNAs. Error bars indicate SDs. (**F)** and (**G)**: Flow cytometric analyses showing the cell cycle distribution of SK-N-BE(2) and Kelly cells transiently transfected with the aMN-887 and aMN-1658 shRNA expressing plasmids. Scr indicates the scrambled shRNA controls.

Figure 4 – Inducible *MYCN* knockdown in retrovirally transduced MNA neuroblastoma cell lines

Representative micrographs showing the morphology of Kelly **(A)** and SK-N-BE(2) **(B)** cells transduced with retroviruses delivering the dox-inducible aMN-1658 shRNA module (RV-1658). RV-Scr indicates the cells receiving retroviruses delivering an inducible scrambled shRNA module. **(C):** A representative western blot showing MYCN and NFL expression in Kelly and SK-N-BE(2) cells transduced with retrovirus RV-1658 and induced to express the shRNA by addition of 1μg/ml doxycyclin (dox).

Figure 5 - Induced anti-MYCN shRNA expression decreases MYCN and increases GAP43 expression in MNA neuroblastoma cells

(A) A representative western blot analysis of MYCN, GAP43 and β-actin protein expression in Kelly and SK-N-BE(2) cells induced to express the aMN-1658 shRNA. Real-time RT-PCR

analysis of *MYCN* mRNA **(B)** and aMN-1658 shRNA **(C)** expression was performed on total RNA isolated from Kelly and SK-N-BE(2) cells treated as described. Cells were transduced with retrovirus RV-1658 and incubated for the indicated numbers of days in the presence (+) or absence (-) of 1 μg/ml doxycyclin (dox). 3/3 and +/- indicate that the cells were incubated for 3 days in the presence of dox, followed by 3 days in the absence of dox. Error bars indicate SDs.

Figure 6 - The proliferative inhibition effect of induced *MYCN* knockdown in MNA neuroblastoma cells

The Alamar Blue Assay was used to measure cell viability in Kelly **(A)** and SK-N-BE(2) **(B)** cells transduced with retrovirus RV-Scr (scrambled control) and RV-1658 (anti-*MYCN*). The addition of doxycyclin (+ dox) induces expression of the shRNAs. AB reduction = Alamar Blue reduction.

Figure 7 - Reproductive cell survival in MNA neuroblastoma cells after *MYCN* knockdown

(A): Graphic presentation of colony forming units (CFU) after induced expression (+ dox) of scrambled (Scr) and anti-*MYCN* (aMN1658) shRNA in Kelly and SK-N-BE(2) cells. **(B)**: Representative pictures of CFU from retrovirally transduced Kelly cells as presented in A.

Additional files

Additional file 1 – Oligonucleotides

Oligonucleotides used in this study.

Additional file 2 - Specific *MYCN* 3'UTR knockdown mediated by the aMN-1658 shRNA

(A): The 3'UTR of *MYCN* was PCR-amplified from human genomic DNA with primers ON178 (5'AAAGCTGCGCACTAGTATCTGGACCAGGCTGTGGGTAGA3' –SpeI site) and ON181 (5' GATCAAGCTTAATTTTAAGCTATTTATTTT 3' –HindIII site). PCR products were digested with SpeI/HindIII and ligated into SpeI/HindIII-digested pMIR-REPORT vector (Invitrogen) to produce Luc-*MYCN*-3'UTR. A control Luc no-target (NT)-3'UTR plasmid was made by amplification of the 3'UTR region from REIC using ON361 (5'GATCAAGCTTAATTTTAAGCTATTTATTTT3'-SpeI site) and ON327 (5'GATCAAGCTTCTATGGAAGATTTTTAATACAGG3' -HindIII) as primers and ligated into SpeI/HindIII digested pMIR-REPORT vector using the In-Fusion Dry-Down PCR Cloning Kit (Clontech). HEK-293 cells were seeded in 12-well plates, incubated for 48 hrs and transfected with a cocktail containing: 0.02 μg pGL4.75[hRluc/CMV] Vector (Promega), 0.1 μg pMIR-Report containing either the *MYCN* 3'UTR (Luc *MYCN*-3'UTR) or control (Luc-NT-3'UTR), and 1 μg shRNA expressing plasmid (pScr/H1wt, paMN-887/H1wt or paMN-1658/H1wt). Transfected cells were then incubated for 48 hrs before luciferase activities were measured as described.

(B): Western blot analysis of MYCN and β-actin expression in SK-N-BE(2) transfected cells. CMV-MYCN (kind gift from Dr. Jason Shohet) expresses the MYCN cDNA lacking a 3'UTR. SK-N-BE(2) cells were transiently co-transfected with the shRNA-expressing plasmids (pScr/H1wt, paMN-887/H1wt or paMN-1658/H1wt) and pCMV-MYCN (+) or the shRNA-expressing plasmids and pCMV-GFP (-). The aMN-1658 shRNA is not able to suppress expression of MYCN from the 3'UTR-lacking pCMV-MYCN plasmid. M=Magic Mark XP (Invitrogen)

Additional file 3 – mRNA expression of neuronal markers in neuroblastoma cell lines after transduction with inducible anti-*MYCN* shRNA expressing retroviruses

Real-time RT-PCR analysis of *NFL* **(A)** and *GAP43* **(B)** mRNA expression in Kelly and SK-N-BE(2) cells transduced with the retrovirus RV-1658. Cells were incubated for the indicated numbers of days in the presence (+) or absence (-) of 1 μg/ml doxycyclin (dox). 3/3 and +/- indicate that the cells were incubated for 3 days in the presence of dox, followed by 3 days in the absence of dox.

Additional file 4 – Cell cycle distribution of neuroblastoma cell lines after transduction with inducible anti-*MYCN* shRNA expressing retroviruses

Flow cytometric analysis showing the cell cycle distribution of Kelly **(A)** and SK-N-BE(2) **(B)** cells transduced with the RV-1658 and RV-Scr retroviruses in the presence (+) or absence (-) of 1 μg/ml doxycyclin (dox).

Figure 1

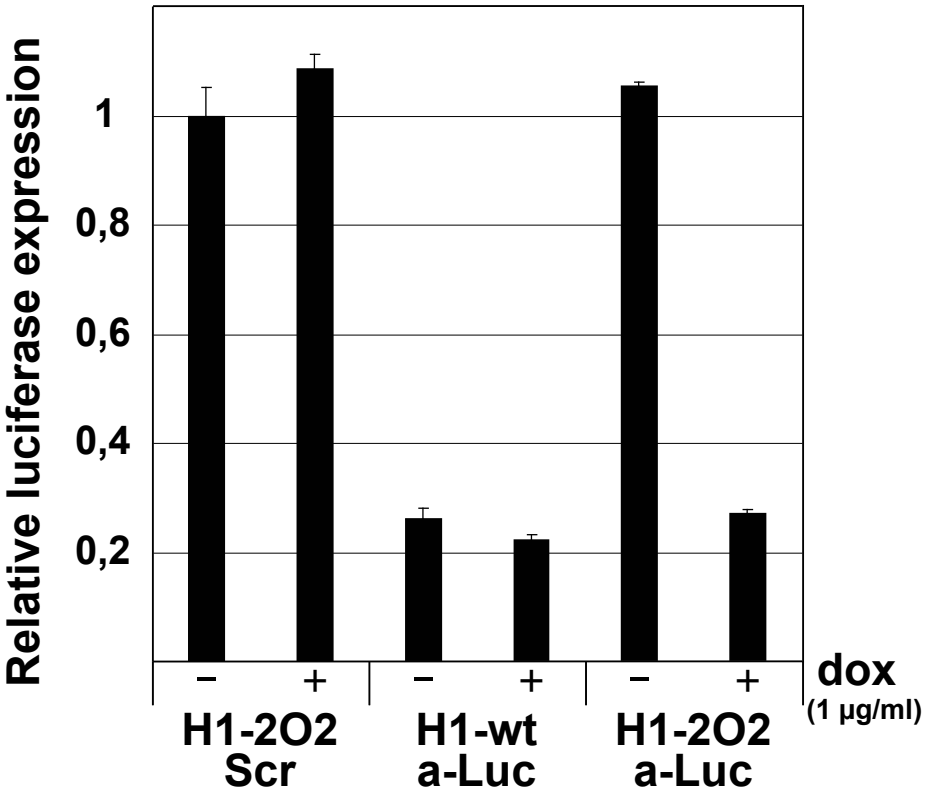
Relative luciferase expression
1
0,8
0,6
0,4
0,2
–
+
–
+
–
+
dox
(1 µg/ml)
H1-2O2
Scr
H1-wt
a-Luc
H1-2O2
a-Luc

Figure 2

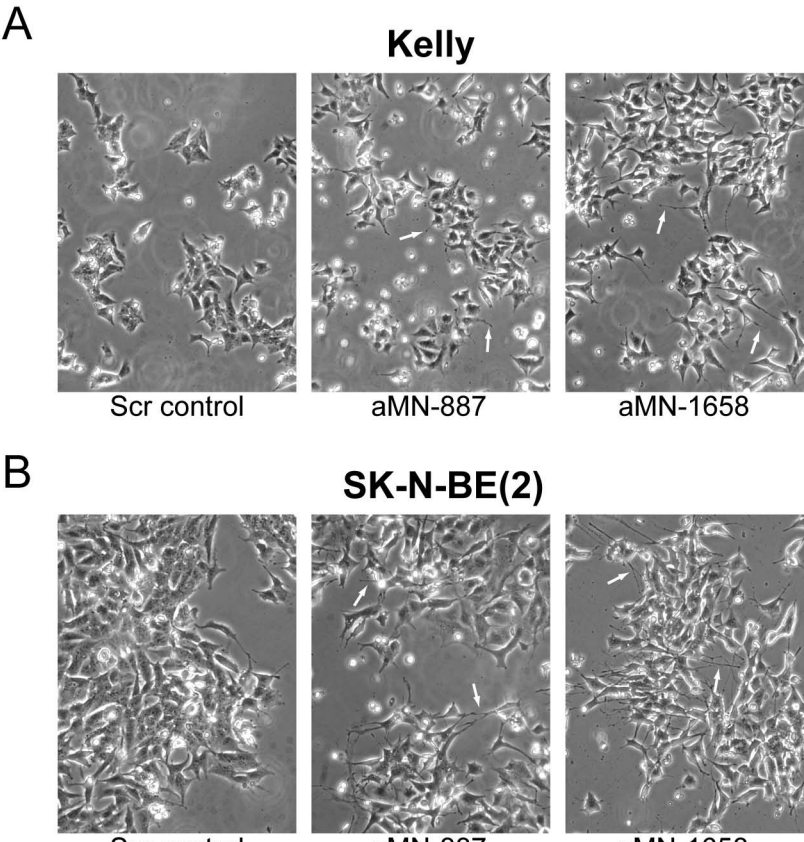
A
Kelly
Scr control
aMN-887
aMN-1658
B
SK-N-BE(2)
Scr control
aMN-887
aMN-1658

Figure 3

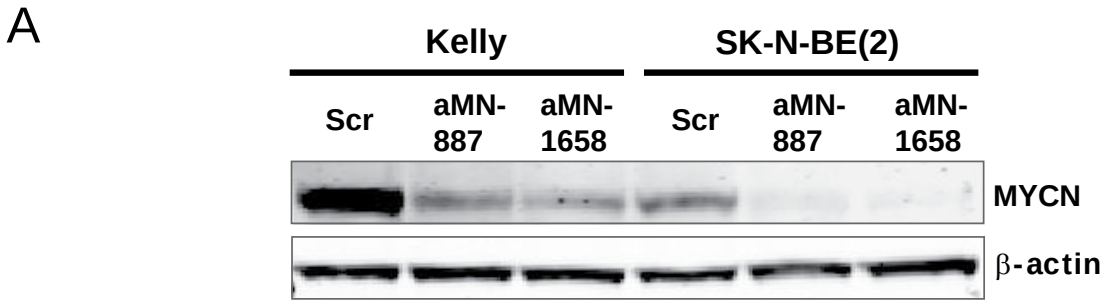
A
Kelly
SK-N-BE(2)
Scr
aMN-887
aMN-1658
Scr
aMN-887
aMN-1658
MYCN
β-actin

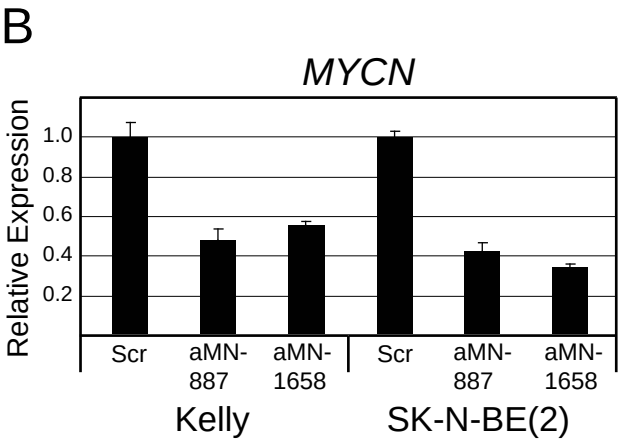
B
MYCN
Relative Expression
1.0
0.8
0.6
0.4
0.2
Scr
aMN-887
aMN-1658
Scr
aMN-887
aMN-1658
Kelly
SK-N-BE(2)

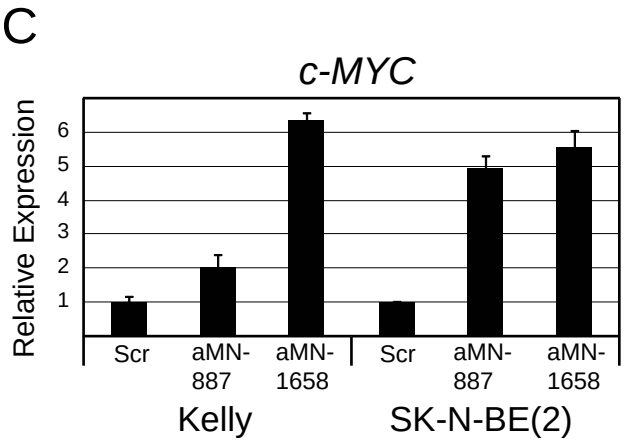
C
c-MYC
Relative Expression
6
5
4
3
2
1
Scr
aMN-887
aMN-1658
Scr
aMN-887
aMN-1658
Kelly
SK-N-BE(2)

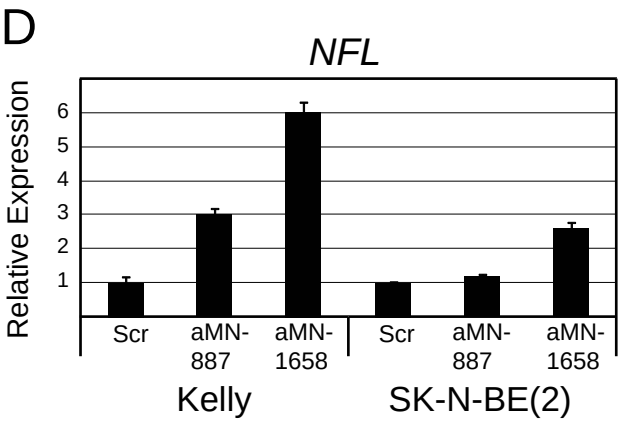
D
NFL
Relative Expression
6
5
4
3
2
1
Scr
aMN-887
aMN-1658
Scr
aMN-887
aMN-1658
Kelly
SK-N-BE(2)

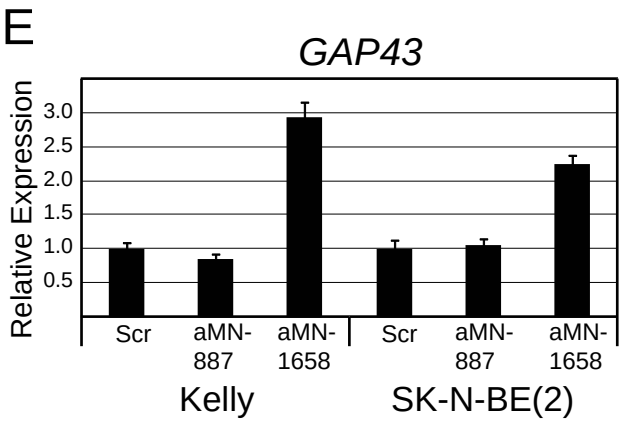
E
GAP43
Relative Expression
3.0
2.5
2.0
1.5
1.0
0.5
Scr
aMN-887
aMN-1658
Scr
aMN-887
aMN-1658
Kelly
SK-N-BE(2)

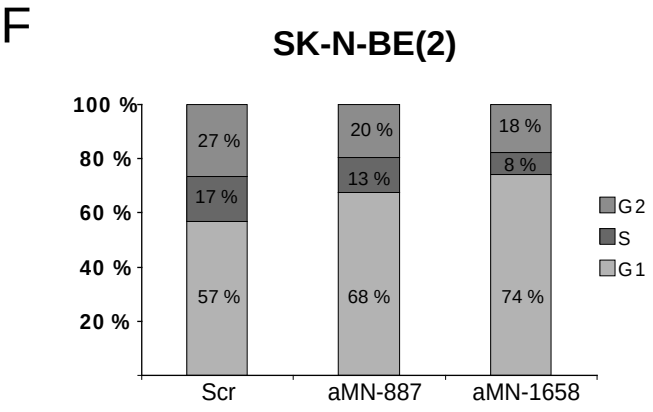
F
SK-N-BE(2)
100 %
80 %
60 %
40 %
20 %
27 %
17 %
57 %
20 %
13 %
68 %
18 %
8 %
74 %
G2
S
G1
Scr
aMN-887
aMN-1658

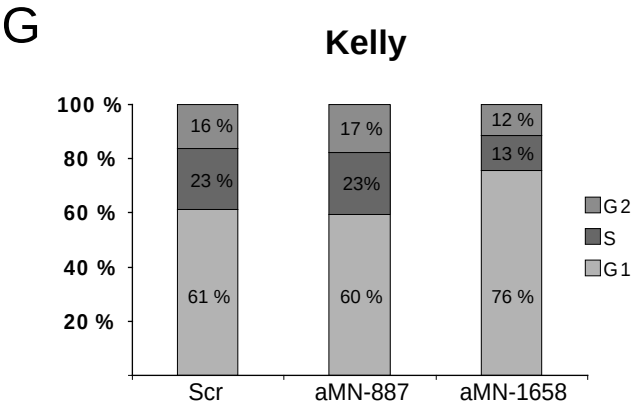
G
Kelly
100 %
80 %
60 %
40 %
20 %
16 %
23 %
61 %
17 %
23%
60 %
12 %
13 %
76 %
G2
S
G1
Scr
aMN-887
aMN-1658

Figure 4

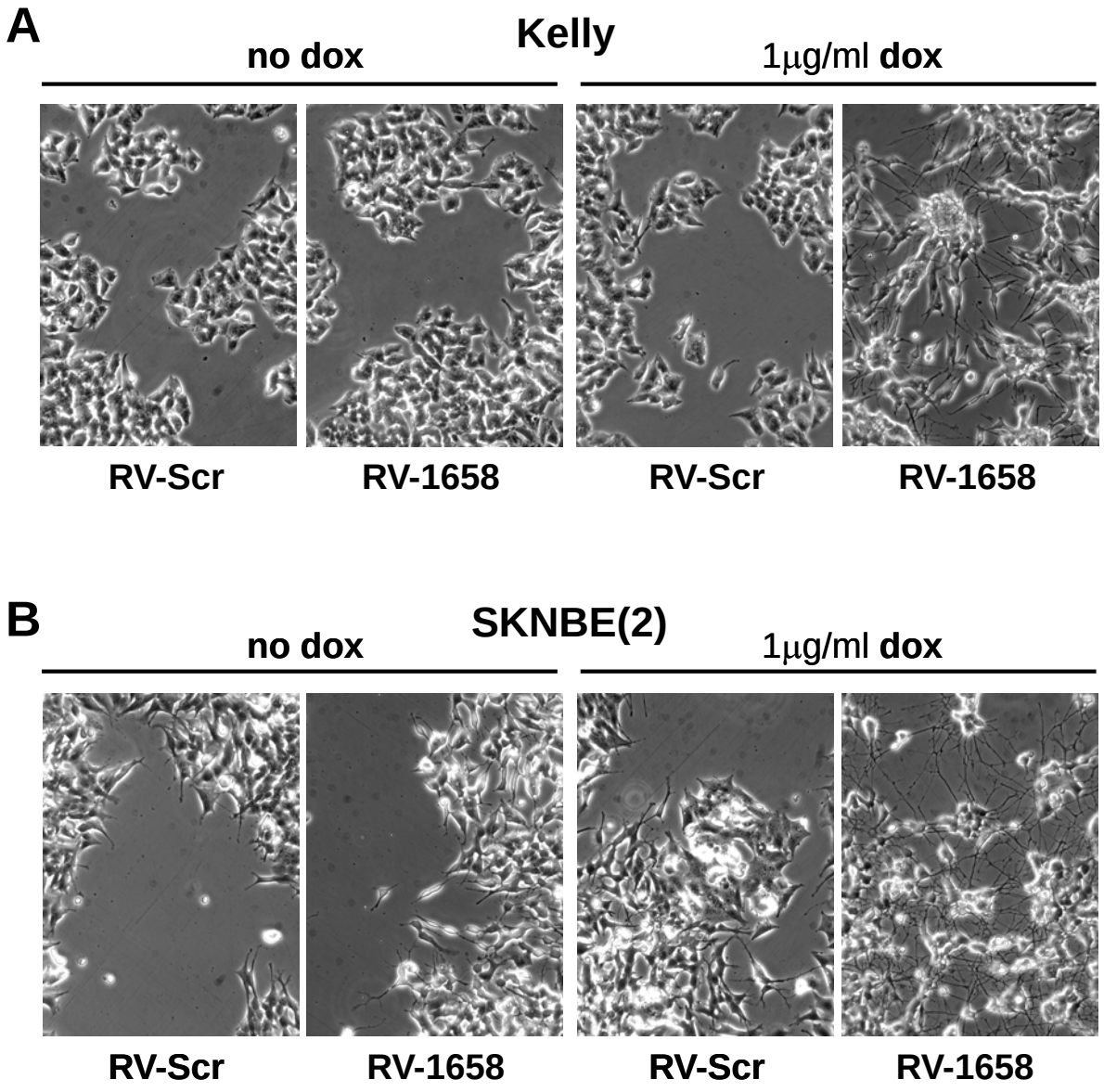
A
Kelly
no dox
1μg/ml dox
RV-Scr
RV-1658
RV-Scr
RV-1658
B
SKNBE(2)
no dox
1μg/ml dox
RV-Scr
RV-1658
RV-Scr
RV-1658
C
RV-Scr
RV-1658
RV-Scr
RV-1658
+
+
+
+
1μg/ml dox
MYCN
NFL
β-actin
Kelly
SKNBE(2)

Figure 5

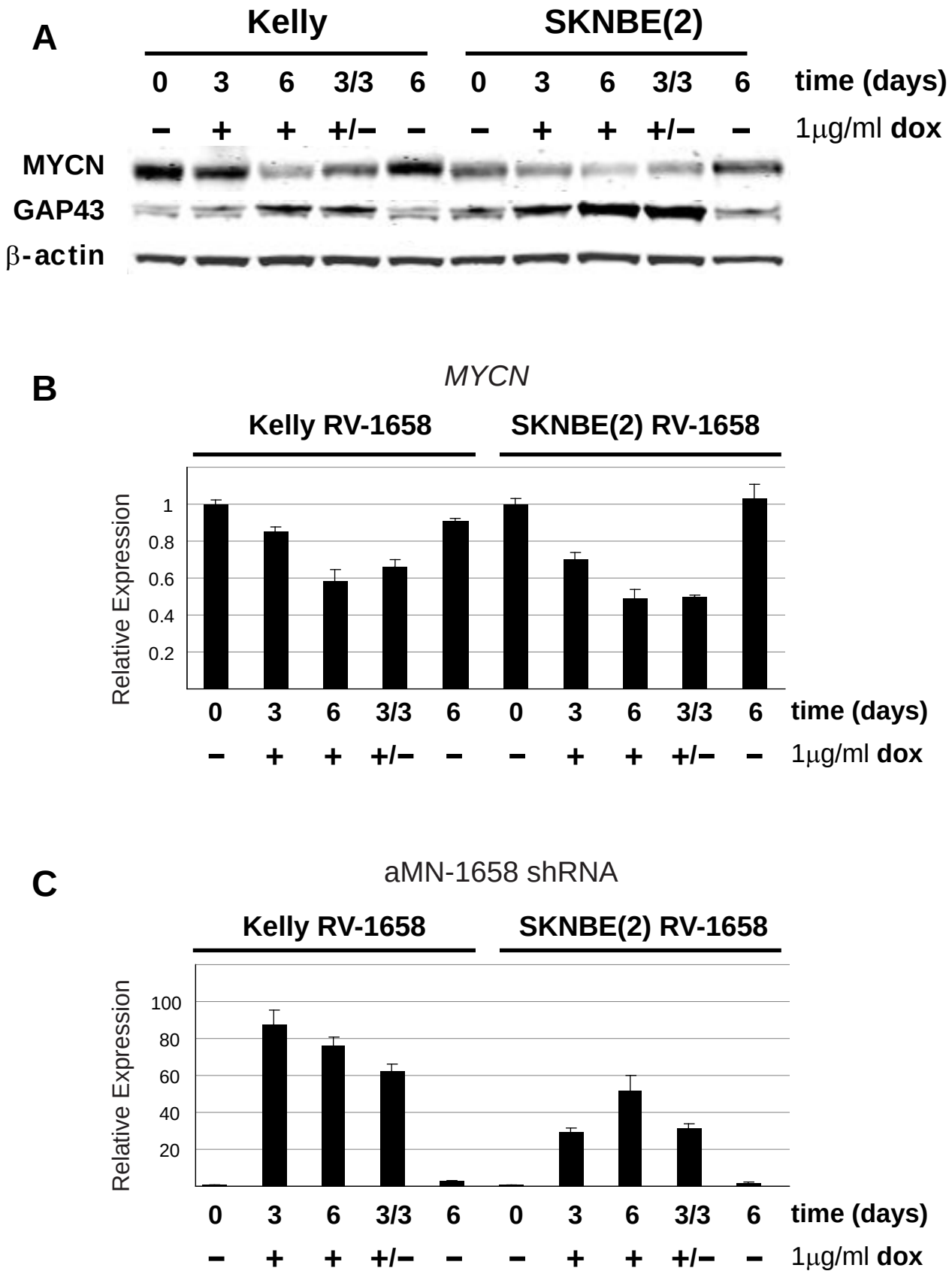
A
Kelly
SKNBE(2)
0 3 6 3/3 6 0 3 6 3/3 6
time (days)
– + + +/– – – + + +/– –
1μg/ml dox
MYCN
GAP43
β-actin
B
MYCN
Kelly RV-1658
SKNBE(2) RV-1658
Relative Expression
1
0.8
0.6
0.4
0.2
0 3 6 3/3 6 0 3 6 3/3 6
time (days)
– + + +/– – – + + +/– –
1μg/ml dox
C
aMN-1658 shRNA
Kelly RV-1658
SKNBE(2) RV-1658
Relative Expression
100
80
60
40
20
0 3 6 3/3 6 0 3 6 3/3 6
time (days)
– + + +/– – – + + +/– –
1μg/ml dox

Figure 6

A

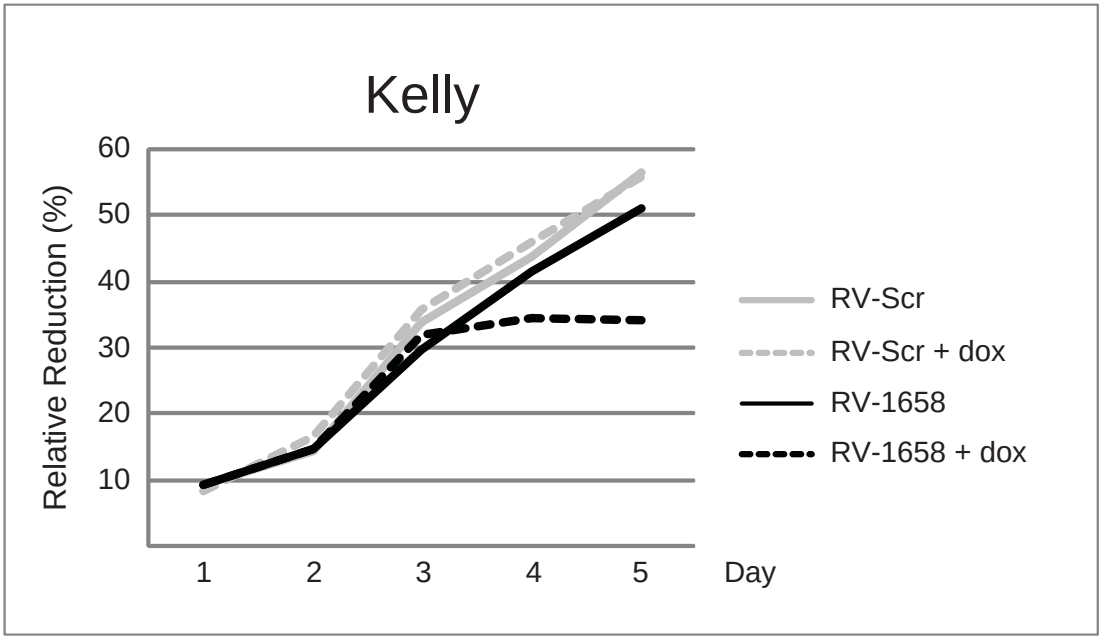
Kelly
Relative Reduction (%)
60
50
40
30
20
10
1
2
3
4
5
Day
RV-Scr
RV-Scr + dox
RV-1658
RV-1658 + dox

B

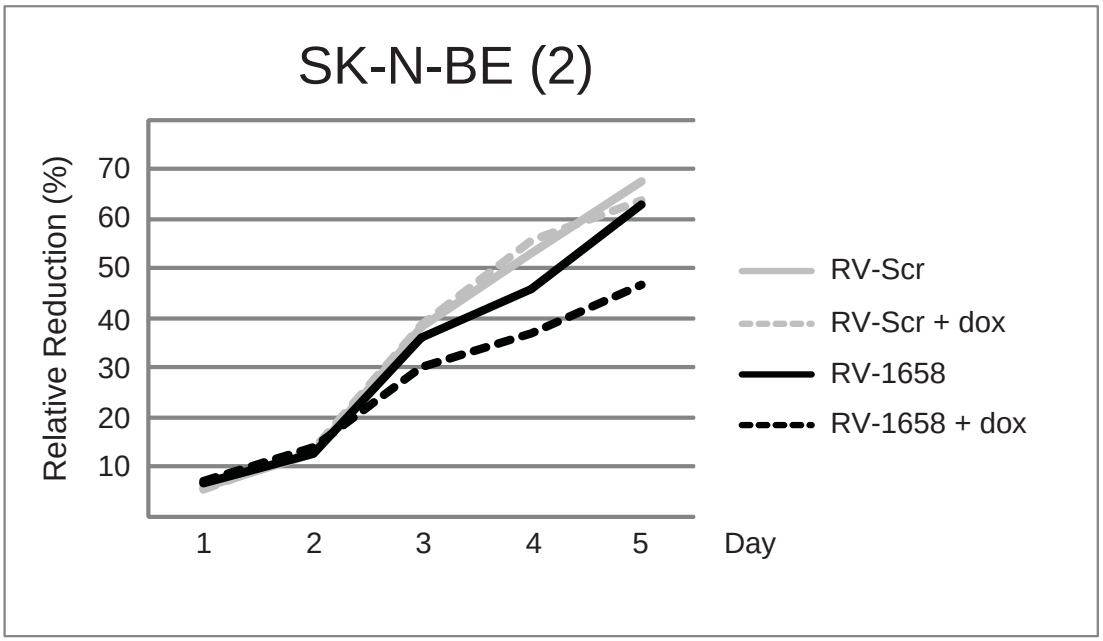
SK-N-BE (2)
Relative Reduction (%)
70
60
50
40
30
20
10
1
2
3
4
5
Day
RV-Scr
RV-Scr + dox
RV-1658
RV-1658 + dox

Figure 7

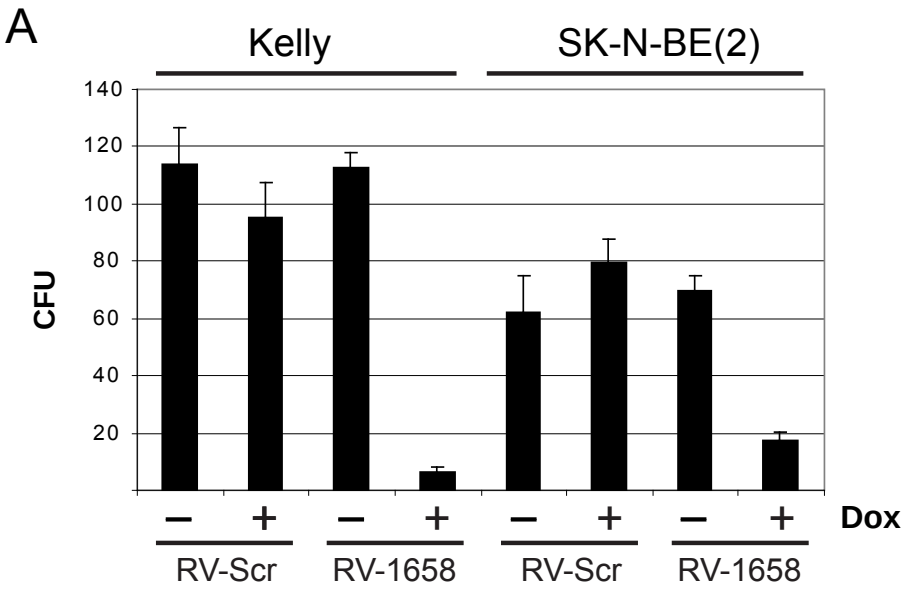
A
Kelly
SK-N-BE(2)
140
120
100
80
60
40
20
CFU
– + – + – + – +
Dox
RV-Scr
RV-1658
RV-Scr
RV-1658

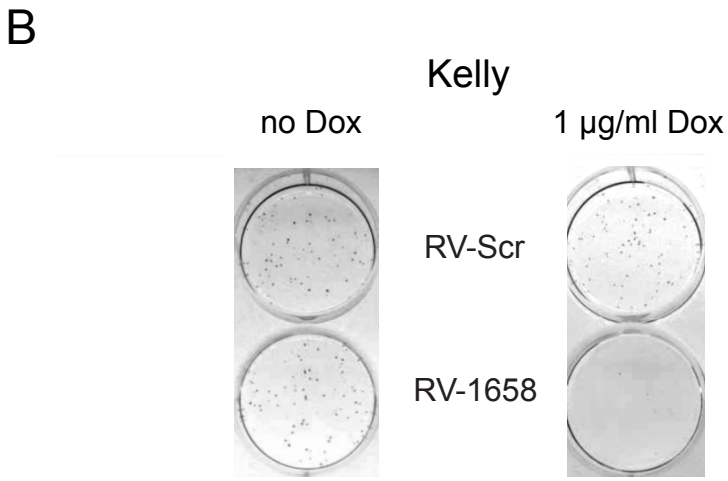
B
Kelly
no Dox
1 µg/ml Dox
RV-Scr
RV-1658

Additional file 2

A

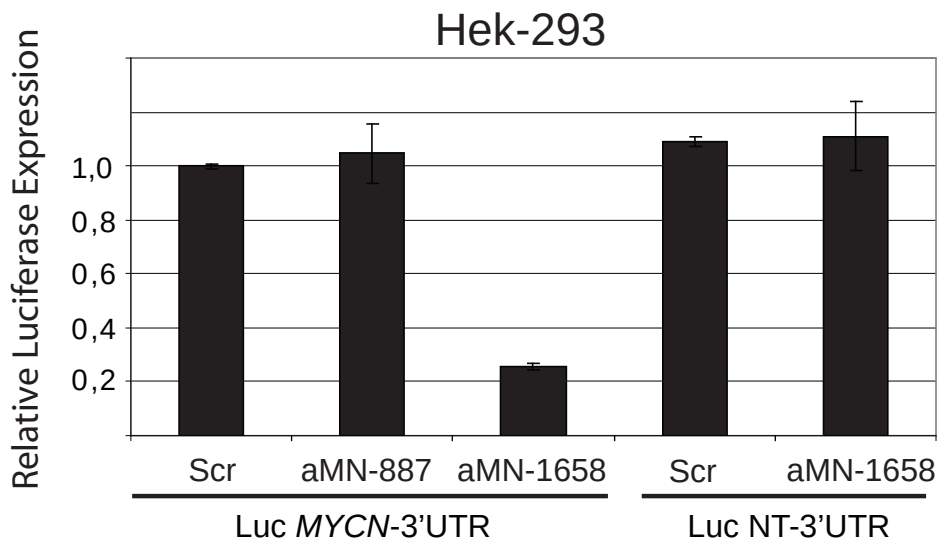

B

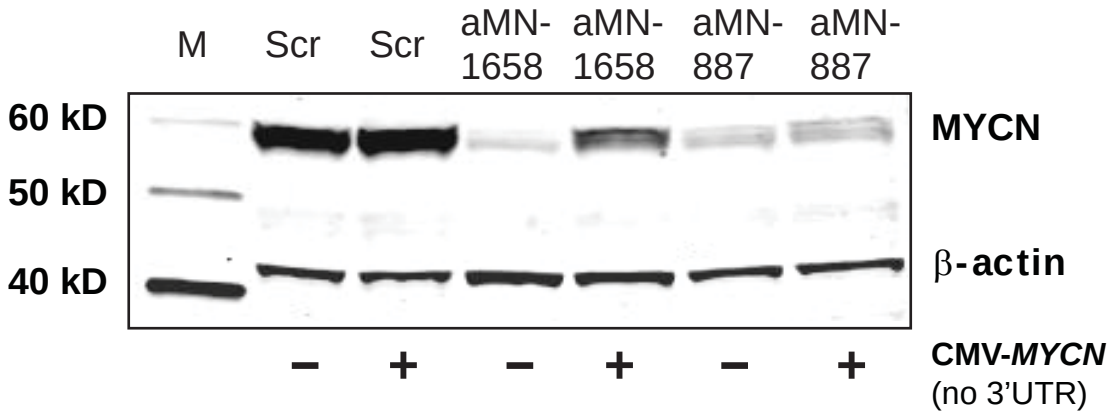

Additional file 3

A

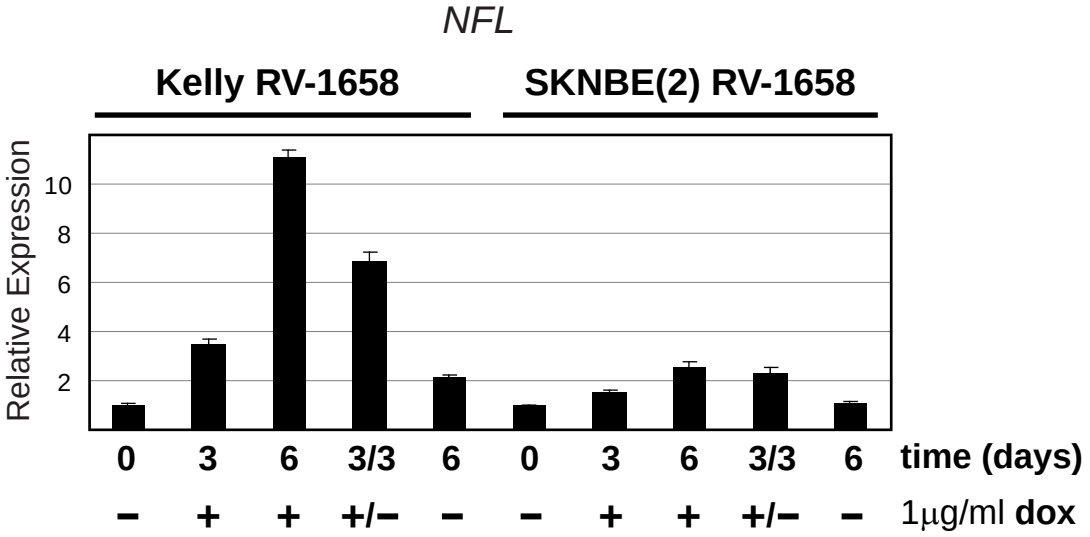

B

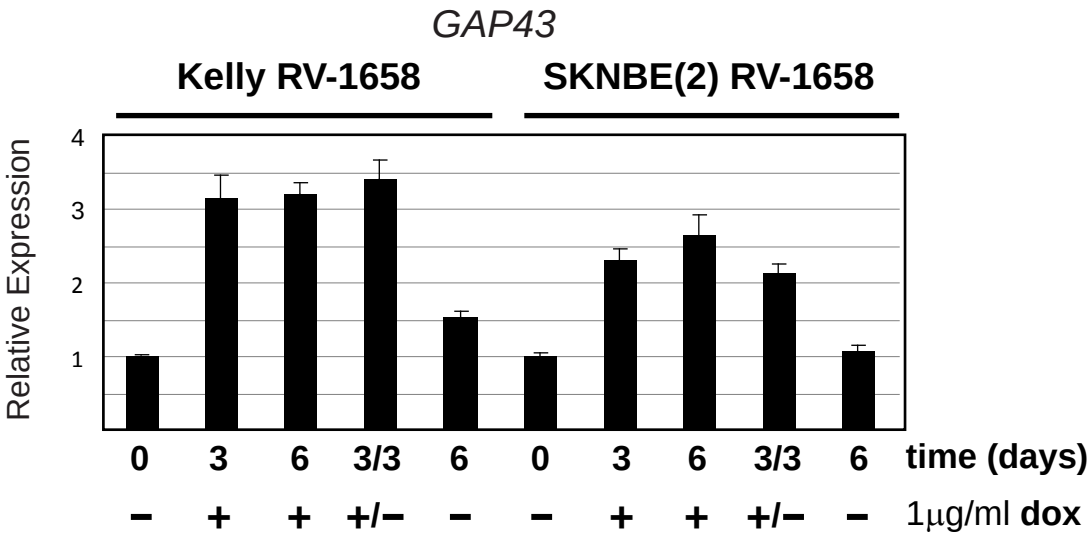

Additional file 4

A

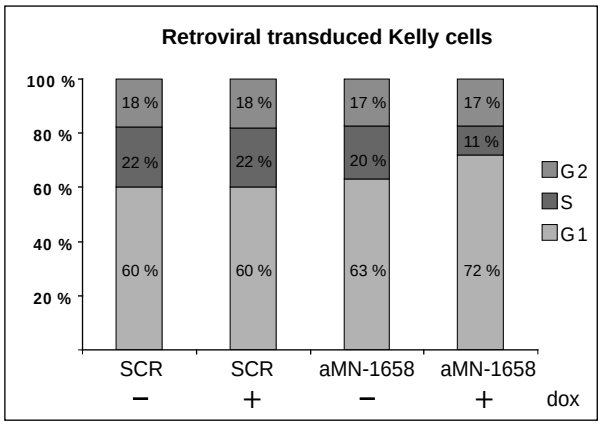

B

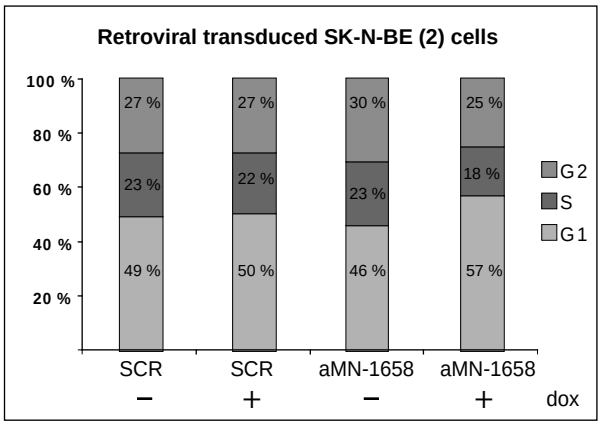

Additional file 1

Oligonucleotides used in this study

Name	*Sequence (5'-3')*
ON056	ATTTGGGTCGCGGTTCTTG
ON057	TGCCTTGACATTCTCGATGGT
ON058	GCAGCTACTCCTCCAGCTCT
ON059	ACTTGAGGTCGTTGCTGATG
ON100	AGATCCCGGAGTTGGAAAAC
ON101	AGCTTTTGCTCCTCTGCTTG
ON106	GATCCCGTTCTTGGGACGCACAGTGATGGTGAATGCAAGCTTCCATTTA CCATCGCTGTGTGTCTCAAGAACTTTTTTGGAAA
ON107	AGCTTTTCCAAAAAAGTTCTTGAGACACACAGCGATGGTAAATGGAAG CTTGCATTCACCATCACTGTGCGTCCCAAGAACGG
ON110	GATCCCGAGCGTTCGGAGTTGGTGGTCATAAGTACCAAGCTTCGTATTT ATGGCCATCAGCTCCGAACGCTCTTTTTTGGAAA
ON111	AGCTTTTCCAAAAAAGAGCGTTCGGAGCTGATGGCCATAAATACGAAG CTTGGTACTTATGACCACCAACTCCGAACGCTCGG
ON145	GGTCACGGAGATGCTGCTTGAGAAC
ON146	AGAAGCCGCTCCACATGCAGTCC
ON174	GTCAACCCCACCGTGTTCTT
ON175	CTGCTGTCTTTGGGACCTTGT
ON298	ACGACCAAAAGATTGAACAAGATG
ON299	TCCACGGAAGCTAGCCTGAA
ON413	GATCCCGCTGTTGAAGTCACCTTGTGTGTTTCAAGAGAACACACAAGGT GACTTCAACAGTTTTTTGGAAA
ON414	AGCTTTTCCAAAAAACTGTTGAAGTCACCTTGTGTGTTCTCTTGAAACA CACAAGGTGACTTCAACAGCGG
ON440	CTAAACGTTGGTGACGGTTG
ON441	GTATCAAATGGCAAACCCCT

PAPER III

Inhibition of *mir-21*, which is up-regulated during *MYCN* knockdown-mediated differentiation, does not prevent differentiation of neuroblastoma cells

Jochen Buechner[1,2], Joern R. Henriksen[1,2], Bjørn Helge Haug[2], Ellen Tømte[2], Trond Flaegstad[1,2], Christer Einvik[1§]

[1] Department of Paediatrics, University Hospital of North-Norway, 9038 Tromsø, Norway
[2] Department of Paediatric Research, Institute of Clinical Medicine, University of Tromsø, 9037 Tromsø, Norway

[§]Corresponding author.
Fax +47-77626369
Phone: +47-47416023

Email addresses:

JB - jochen.buchner@unn.no
JRH - Joern.Remi.Henriksen@fagmed.uit.no
BHH – bjorn.haug@gmail.com
ET – ellen.tomte@uit.no
TF - trond.flaegstad@unn.no
CE - christer@fagmed.uit.no

Key words:

Neuroblastoma; MYCN; microRNA; neuronal differentiation; mir-21

Abbreviations:

MNA - MYCN-amplified
TPA - 12-O-tetradecanoyl phorbol 13-acetate
RA - Retinoic acid
BDNF - Brain-derived neurotrophic factor
bFGF - Basic fibroblast growth factor
IGF - Insulin-like growth factor
NGF - Nerve growth factor
IFN-γ - Interferon-gamma

Abstract

Background: Neuroblastoma is a malignant childhood tumour arising from precursor cells of the sympathetic nervous system. Genomic amplification of the *MYCN* oncogene is associated with dismal prognosis. For this group of high-risk tumours, the induction of tumour cell differentiation is part of current treatment protocols. MicroRNAs (miRNAs) are small non-coding RNA molecules that effectively reduce the translation of target mRNAs. MiRNAs play an important role in cell proliferation, apoptosis, differentiation and cancer. In this study, we investigated the role of N-myc on miRNA expression in *MYCN*-amplified neuroblastoma. We performed a miRNA profiling study on SK-N-BE (2) cells, and determined differentially expressed miRNAs during differentiation initiated by *MYCN* knockdown, using anti-*MYCN* short-hairpin RNA (shRNA) technology.

Results: Microarray analyses revealed 23 miRNAs differentially expressed during the *MYCN* knockdown-mediated neuronal differentiation of MNA neuroblastoma cells. The expression changes were bidirectional, with 11 and 12 miRNAs being up- and down-regulated, respectively. Among the down-regulated miRNAs, we found several members of the mir-17 family of miRNAs. *Mir-21*, an established oncomir in a variety of cancer types, became strongly up-regulated upon *MYCN* knockdown and the subsequent differentiation. Neither overexpression of *mir-21* in the high-*MYCN* neuroblastoma cells, nor repression of increased *mir-21* levels during *MYCN* knockdown-mediated differentiation had any significant effects on cell differentiation or proliferation.

Conclusions: We describe a subset of miRNAs that were altered during the N-myc deprived differentiation of *MYCN*-amplified neuroblastoma cells. In this context, N-myc acts as both an activator and suppressor of miRNA expression. *Mir-21* was up-regulated during cell differentiation, but inhibition of *mir-21* did not prevent this process. We were unable to establish a role for this miRNA during differentiation and proliferation of the two

1 neuroblastoma cell lines used in this study.

Introduction

Neuroblastoma is a highly malignant embryonic childhood tumour arising from primitive cells of the neural crest [1]. As shown in mass screening studies, localised tumours can frequently be detected in the paediatric population. However, many of these tumours differentiate into more benign histological subtypes or regress spontaneously [2]. By contrast, disseminated disease and certain genetic alterations define high-risk groups of neuroblastoma patients in which long-term survival is still below 40%, despite multi-modality treatment efforts [3].

One of the strongest biological predictors of poor outcome is genomic amplification of the oncogene *MYCN* [4]. The gene product, N-myc protein, is a basic helix-loop-helix (bHLH) transcription factor expressed during neural crest development. It belongs to the Myc/Max/Mad network and plays a key role in the regulation of cell growth, differentiation and apoptosis [5]. Like other members of the myc-family, N-myc can both activate and repress transcription. The direct binding of N-myc/Max heterodimers to specific genomic DNA binding sites (E-box motifs) induces the transcription of target genes. By contrast, the transcriptional repression by N-myc [6-8] is presumably mediated through interaction with other DNA-binding proteins [9].

MicroRNAs (miRNAs) are a class of small (19-22 nt), non-coding RNAs capable of repressing protein expression by binding to sequences in the 3'untranslated region (3'UTR) of respective target mRNAs. Most miRNAs are transcribed as long monocistronic, bicistronic or polycistronic primary transcription units (pri-miRNAs) by RNA polymerase II, and cleaved by a series of cellular processing events to produce mature miRNAs. The degree of complementarity between mature miRNA and its target mRNAs determines the mechanism responsible for blocking protein synthesis. In mammals, miRNAs-mRNA interactions are most often through imperfect base pairing, resulting in translational repression [10].

To understand the mechanisms that control the neuronal differentiation of neuroblastoma cells is crucial since induction of differentiation is one of the treatment strategies for this type of cancer. Most model systems used to study neuroblastoma differentiation *in vitro* are based on the addition of various agents and growth factors to neuroblastoma cell lines without *MYCN*-amplification (reviewed in [11]). Typically, SH-SY-5Y cells are exposed to retinoids, phorbolesters or combinations of growth factors to induce a neuronal-like phenotype characterised by neurite outgrowth. The addition of RA to MYCN-amplified (MNA) neuroblastoma cells has also been shown to induce neuronal differentiation with the subsequent down-regulation of *MYCN* expression [12]. The function of N-myc during RA-induced differentiation of MNA neuroblastomas, however, is contradictory and unclear [13-15].

Another method to induce neuronal differentiation in MNA neuroblastomas is the specific reduction of *MYCN* expression by traditional antisense techniques or short-interfering RNA molecules (siRNA) [16-19]. In addition, we have previously reported an efficient method to down-regulate *MYCN* in MNA neuroblastoma cell lines by the use of vector-based anti-*MYCN* short-hairpin RNA (shRNA) technology [20]. In SK-N-BE (2) cells, the knockdown of *MYCN* resulted in prominent morphological and biochemical neuronal differentiation. During the last few years, several studies have been reported which address miRNA expression during induced neuroblastoma differentiation [21-26]. With the exception of one study using anti-*MYCN* siRNA [22], all reports have focused on non-MNA neuroblastoma cell lines induced to differentiate by TPA or RA alone, or in combination with growth factors. To investigate how the miRNA transcriptome is affected during the *MYCN* knockdown-mediated neuronal differentiation of MNA neuroblastoma cells, we performed a miRNA profiling study on SK-N-BE (2) cells, and determined differentially expressed miRNAs during cell differentiation using anti-*MYCN* shRNA technology.

Materials and Methods

Neuroblastoma cell lines

SK-N-BE (2) cells have a complex karyotype which includes a del(1p), monosomy 17 and unbalanced der(3)t(3;17). Homogeneously stained regions (HSRs) in 6p and 4q are reported sites of *MYCN* amplification [27, 28]. Kelly cells are *MYCN*-amplified at der(17), and the complex near-diploid karyotype includes a del(1)(p34). SK-N-BE (2), Kelly, SMS-KCN, SMS-KCNR, SKNAS and SKNSH cells were grown in RPMI-1640, LAN-5 cells in DMEM medium with 1% NEAA and 2 mM glutamine, all supplemented with 10% heat-inactivated FBS, at 37 °C under 5% CO2.

Short-hairpin RNA vectors and transfection

The design and validation of shRNA molecules targeting human *MYCN* mRNA (sh*MYCN*) were previously reported by us in detail [20]. For the present study we used sh*MYCN* sequence aMN-887, in which the number indicates the first position of the shRNA target recognition site in the *MYCN* cDNA (GeneBank accession NM_005378) sequence. The aMN-887 sequence and an upstream human U6 promoter from plasmid panti*MYCN*-887 [20] were gated into vector pDS_hpCG (ATCC-Nr. 10326383) using Gateway technology (Invitrogen) to generate the aMN-887 shRNA expressing plasmid pDS-anti*MYCN*-887. As a negative control, we designed vector pDS-shSCR, expressing a scrambled shRNA sequence with no complementarity to any known mRNA in the human genome (shSCR sequence available on request). At a 70% confluence, cells were transfected with Lipofectamine2000 (Invitrogen) according to the manufacturer`s standard recommendations, and the transfection efficiency reached 70-80%.

Immunofluorescence confocal laser microscopy

Morphological changes and *in situ* N-myc expression were evaluated by immunostaining and confocal laser microscopy. Cells were cultured on round poly-L-lysine coated glass slides (Hecht Assistant, Germany, No.1014), transfected in six well dishes, and fixated three days after transfection with 4% paraformaldehyde. After permeabilisation with ice-cold MeOH and blocking with BSA, cells were incubated with primary antibodies either against N-Myc (mouse polyclonal antibody, Calbiochem) or Neuronal Class III β-Tubulin (rabbit polyclonal antibody, Covance), and covalent bindings visualised by fluorescent secondary antibodies (Alexa Fluor -546 goat anti-mouse and -633 donkey anti-rabbit conjugated IgG, respectively; both from Molecular Probes/Invitrogen). Cell nuclei were stained with Draq5 (BioStatus, UK). We used a Zeiss LSM500 confocal microscope, the software LSM Image Browser (Zeiss), ImageJ (NIH, USA), and an Adobe Illustrator for image processing and preparation.

MiRNA microarray profiling

MiRNA microarrays: MicroRNA expression in SK-N-BE (2) cells transfected with pDS-shSCR or pDS-anti*MYCN*-887 was measured in two independent miRNA microarray experiments (SK07 and SK08), and the cells were harvested three days after transfection. Total RNA was isolated with the miRVana miRNA isolation kit (Ambion) according to the manufacturer`s instructions. The miRNA microarray assay started with 10 µg total RNA and was performed on µParaflo® Microfluidic Biochips using a service provider (LCSciences). The technical details of the assay, including miRNA enrichment, fluorescent dye labelling and hybridisation conditions, are described elsewhere [29]. Microarrays SK07 and SK08 included all miRNAs listed in the Sanger miRBase Release 9.2 (471 human miRNAs) and Release 10.1 (723 human miRNAs), respectively. The exogenously expressed shRNA (shSCR and aMN-887) molecules and 18 endogenous small housekeeping RNAs were added as custom probes on the SK08 array (Supplementary 1). SK07 and SK08 included seven and four redundant probes for each miRNA, respectively.

Data analysis: The data analysis included subtraction of the background and the normalisation step. The background was determined using a regression-based background mapping method. The regression was performed on 5–25% of the lowest intensity data points excluding blank spots. Raw data matrix was then subtracted by the background matrix.
To be regarded as detectable, a transcript must meet at least two conditions: signal intensity higher than 3 × (background standard deviation) and spot CV < 0.5. CV was calculated by (standard deviation)/(signal intensity). In addition, signals from at least 50% of the repeating probes must be above the detection level.
Normalisation was carried out using a LOWESS (Locally Weighted Regression) method on the background-subtracted data. After normalisation, the p-values of the difference between the two fluorescent signals were calculated. Differentially expressed miRNAs were those with a p-value < 0.01 in at least 50% of the array replicates. Due to a systematic dye bias, mir-377 and mir-542-5p were excluded. In addition, 10 miRNAs from Sanger miRBase Release 9.2 were no longer included in Release 10.1. By making these adjustments, the expression data on 459 identical human miRNAs were comparable on both arrays.

Microarray validation by Taqman miRNA RT-PCR

The microarray data was validated by Taqman quantitative stem-loop real-time RT-PCR (provided by LCSciences) with the same RNA preparations used in the microarray analyses. Sequences of the miRNA specific stem-loop-primers are available at www.lcsciences.com. RNU38B was unaffected by *MYCN* knockdown on the miRNA microarray (Supplementary 1) and was used for qRT-PCR normalisation. All PCR reactions were done in triplets. A two-sided student's t-test was used to calculate the p-values for differential expression.

Overexpression and inhibition of *mir-21*

Premir-21 miRNA Precursor Molecules ("mimics") and anti-mir-21 miRNA Inhibitors (both from Ambion) were used to overexpress and inhibit *mir-21* expression, respectively. Pre-miR Precursor Negative Control and Anti-miR Inhibitors Negative Control (Ambion) were used as negative controls. The cells were transfected with Lipofectamin 2000 according to the manufacturer's instructions. The transfection efficiency of a FAM-labeled miRNA negative control mimic reached 85-90 % as measured by flow cytometry.

pmir-21-luc assay

SK-N-BE(2) and Kelly cells were seeded in 12-well culture plates and co-transfected with 30 pmol anti-mir-21 or anti-NC (negative control antagomir), 1,2 μg,(SK-N-BE(2)) or 0,8 μg (Kelly) pmir-21-luc (kind gift from Anders H. Lund, University of Copenhagen, Denmark) and 20 ng pGL4.75[hRluc/CMV] (expressing Renilla luciferase for normalization) using Lipofectamin 2000. 48 hours after transfection, cells were harvested and luciferase activities were measured using the Dual Luciferase Assay (Promega).

Quantitative real-time RT-PCR

Three days following transfection, RNA was isolated using a Qiagen miRNeasy Mini Kit, and 1 μg total RNA was reverse transcribed using a Qiagen miScript Reverse Transcription Kit according to the manufacturer´s instructions. Power SYBR Green PCR Master Mix (Applied Biosystems) was used to determine the expression of MYCN (F: CACCCTGAGCGATTCAGATGA, R: CCGGGACCCAGGGCT), Neuropeptid Y (NPY) (F: TCCAGCCCAGAGACACTGATT, R: AGGGTCTTCAAGCCGAGTTCT), HPRT1 (F: TGACACTGGCAAAACAATGCA, R: GGTCCTTTTCACCAGCAAGCT) and UBC (F: ATTTGGGTCGCGGTTCTTG, R: TGCCTTGACATTCTCGATGGT). The expression of *miR-21* and SNORD38B were measured using a Qiagen miScript SYBRGreen PCR Kit and

the specific primer sets from Qiagen. HPRT1, UBC and SNORD38B were selected for cDNA normalisation, and the results were analysed using ΔΔCT method in qBase Software [30].

Western immunoblotting

Western immunoblotting was performed as previously described [20]. Primary antibodies were Anti-N-Myc Mouse (CALBIOCHEM), PDCD4 Rabbit (Cell Signaling), PTEN Rabbit (Cell Signaling) and Actin mouse (Santa Cruz).

Cell proliferation assay

SK-N-BE (2) cells were seeded in 24 well plates and transfected in three replicates with Lipofectamine 2000 the following day. Cell proliferation was determined in two replicates by AlamarBlue (Invitrogen) according to the manufacturer´s standard procedure.

Flow cytometric analysis

Cells were harvested using Trypsin-EDTA (Sigma-Aldrich) and washed once in 1 x PBS. The cells were then fixed for 2 hrs in ice-cold 70% EtOH. After fixation, the EtOH was removed by centrifugation and the cells were washed once in 1 x PBS before being stained for 30 min at room temperature in a propidium iodide (PI)-staining solution (PBS with 20 µg/ml PI (Sigma), 60 µg/ml RNase A (Sigma) and 0.1% v/v Triton X-100 (Sigma)). Fluorescence emitted from the PI-DNA complex was analysed by flow cytometry, using a FACS Aria Flow Cytometer (BD Biosciences, San Jose, CA, USA).

To determine the miRNA transfection efficiency, SK-N-BE (2) and Kelly cells were transfected with a FAM-labeled miRNA negative control mimic (GenePharma, Shanghai) and harvested after 24 hours. Cell fluorescence was measured using the FACS Aria Flow Cytometer.

Results

MYCN knockdown in the MNA neuroblastoma cell line SK-N-BE (2)

We have previously described the efficient knockdown of *MYCN* mRNA in a MNA neuroblastoma cell line using anti-*MYCN* shRNAs [20]. In brief, SK-N-BE (2) cells were transiently transfected with plasmid pDS-anti*MYCN*-887, expressing shRNA molecule aMN-887 specifically targeted against *MYCN* mRNA. A real-time RT-PCR analysis demonstrated that *MYCN* mRNA decreased by ~70% (Figure 1a), while Western immunoblotting revealed an almost complete depletion of N-myc protein (Figure 1b) when compared to transfections with a plasmid expressing scrambled control shRNA (shSCR). Morphologically, cells expressing aMN-887 shRNA exhibited multidirectional neurite-like projections, indicating neuronal cellular differentiation (Figure 1c).

Immunocytochemical stainings with antibodies against N-myc and neuronal class III β-tubulin confirmed that the neuronal phenotype was restricted to cells where N-myc was efficiently knocked down by aMN-887 shRNA. Moreover, the relative expression of several other neuronal differentiation markers such as Neuropeptide Y (NPY), Calreticulin (CRT) and Chromogranin B (CHGB) increased [20]. Neither differentiation markers nor several different housekeeping genes were affected by treatment with shSCR (data not shown). We also noticed the complete absence of non-specific stress responses after these treatments using the Interferon Response Detection kit (SBI) (data not shown).

These results clearly demonstrate that SK-N-BE (2) cells transfected with pDS-anti*MYCN*-887 undergo neuronal differentiation as a consequence of highly specific and potent shRNA-mediated inhibition of N-myc expression.

MicroRNA expression profile in MNA SK-N-BE (2) cells

The shSCR transfected control cells were used to generate a miRNA expression profile for the MNA SK-N-BE (2) cell line. Two individual shSCR transfections were analysed on two

separate miRNA microarrays, covering 471 (SK07) and 723 (SK08) known human microRNA genes. Of the 459 miRNAs common to both arrays, 259 miRNAs (56%) were not detectable. Of the remaining 200 detectable miRNAs, we found a high expression of 14 miRNAs located within the distinct miRNA gene clusters mir-17-92 (chromosome 13q31), mir-106a-363 (chromosome Xq26), mir-106b-25 (chromosome 7q22), mir-23b-24 (chromosome 9q22) and mir-15b-16 (chromosome 3q26) (Figure 2). None of the 252 miRNAs that distinguished Sanger miRBase Release 10.1 (SK08) from Release 9.2 (SK07) showed a high expression in SK-N-BE (2).

Differential miRNA expression upon *MYCN* knockdown-mediated differentiation

Two independent *MYCN* knockdown experiments were performed, and each was analysed on a separate miRNA microarray. To determine differentially expressed miRNAs, the expression profile of SK-N-BE (2) cells transfected with pDS-anti*MYCN*-887 (low N-myc and differentiated morphology) was compared to cells treated with pDS-shSCR (high N-myc and undifferentiated morphology). We identified 23 miRNAs with consistent differential expression on both arrays: 11 miRNAs were up-regulated and 12 miRNAs were down-regulated (Figure 3a and Supplementary 2). In the group of up-regulated miRNAs which includes *mir-21, -22, -126, -137, -181d, -218, -663, -671, let-7c, let-7d* and *let-7f*, we observed a 1.6 – 5.3 fold increase in expression. Among the down-regulated miRNAs, 7 of the 12 differentially expressed miRNAs are members of the mir-17 family encoded by three paralogous miRNA clusters: the mir-17-92 cluster, the mir-106a-363 cluster and the mir-106b-25 cluster (Figure 3b). The remaining five down-regulated miRNAs (*mir-24, -92b, -103, -494* and *mir-495)* are single intergenic or intron encoded. The differential expression pattern for 11 miRNAs was confirmed by real-time stem-loop quantitative RT-PCR (Supplementary 3).

Collectively, our data show that the expression level of several miRNAs is altered during the *MYCN* knockdown-mediated differentiation of SK-N-BE (2) cells. We observed both up- and down-regulation in miRNA expression, but were not able to differentiate between expressional changes due to *MYCN* knockdown or the following differentiation process. These data show the differential expression pattern of miRNAs during *MYCN* knockdown-mediated neuronal differentiation of an MNA neuroblastoma cell line.

Increased *mir-21* expression is not sufficient to induce neuronal differentiation in SK-N-BE (2) and Kelly cells

Mir-21, which is expressed from a single gene locus on chromosome 17q23, demonstrated the strongest inverse correlation with N-myc expression in SK-N-BE (2) cells (Figure 3a and Supplementary 2), with a similar observation being made in MNA Kelly cells (Supplementary figure 4). The *MYCN*-knockdown mediated increase in *mir-21* expression coincided early with *MYCN* downregulation (Supplementary Figure 5). By the use of the stem-loop RT-PCR assay for *mir-21* and real-time RT-PCR on *MYCN*, we measured the levels of *mir-21* and *MYCN* mRNA in 7 neuroblastoma cell lines. As shown in Figure 4a, we observed a reverse correlation between the expression of *mir-21* and *MYCN* mRNA. Cell lines with low to moderate *MYCN* mRNA levels expressed significantly higher levels of *mir-21*.

In order to elucidate a function for the substantial increase in *mir-21* expression during *MYCN* knockdown-mediated differentiation, SK-N-BE(2) and Kelly cells were transfected with premir-21 mimics or anti-mir-21 antagomirs. While *MYCN* knockdown increased *mir-21* expression ~2-fold, transfection of the *mir-21* mimic resulted in ~23-fold overexpression. Co-transfection of aMN-887 and anti-mir-21 abolished the aMN-887 induced increase in *mir-21* expression (Figure 4b). To functionally validate the efficiency of the antagomir treatment, SK-N-BE (2) and Kelly cells were co-transfected with anti-mir-21 and a luciferase reporter containing the *mir-21* target sequence in the 3'UTR (pmir-21-luc). The luciferase activity

increased ~ 2-fold compared to a negative control antagomir (anti-NC) demonstrating the specific repression of endogenous *mir-21* by the antimir-21 (Figure 4c). Treatment with premir-21 did not induce a noticeable neurite outgrowth, as was observed in differentiating SK-N-BE (2) and Kelly cells (data not shown). In consistence with a lack of morphological changes, the expression of the early neuronal differentiation marker NPY did not increase during the pre-mir-21 treatment (Figure 4d). Furthermore, decreasing *mir-21* expression with antagomir-21 in differentiating SK-N-BE (2) had no effect on NPY expression. Neither the overexpression of *mir-21* alone nor the repression of *mir-21* in combination with the anti-*MYCN* shRNA treatment had any significant effect on *MYCN* mRNA expression levels as expected (Figure 4e).

These data show that the increase in *mir-21* expression observed upon anti-*MYCN* shRNA treatment alone is not a sufficient stimulus to induce differentiation and might instead be a consequence of *MYCN* knockdown-mediated neuronal differentiation in MNA neuroblastoma. In addition, counterbalancing the increased *mir-21* expression with antagomir-21 during differentiation is not able to reverse the process.

Altered *mir-21* expression has no effect on proliferation during *MYCN* knockdown-induced differentiation

Mir-21 has tumour-promoting properties in a variety of cancers [31]. For that reason, we investigated the proliferative effects of *mir-21* in high-*MYCN* SK-N-BE (2) cells.

Premir-21 mimics were transfected into SK-N-BE (2) and Kelly and cell proliferation was monitored for three consecutive days. As shown in Figures 5a and 5b, premir-21 treatment had no significant effect on the cell proliferation of these cell lines, even when the premir concentration was increased to 80 nM. In contrast, control cells receiving culture media with low serum showed a marked decrease in cell proliferation.

Cell cycle analyses using flow cytometry after overexpression of *mir-21* in SK-N-BE (2) cells showed no significant differences in the fraction of proliferating cells (S-phase) when compared to cells transfected with the mir-NC control. The lack of a sub-G1 phase also indicated that few cells underwent apoptosis due to the treatments (Figure 5c).

Since *mir-21* was up-regulated during *MYCN*-knockdown mediated differentiation, we next investigated if proliferation was altered when the *mir-21* increase was abolished by antagomir treatment. As shown for the SK-N-BE (2) cells in Figure 5d and for the Kelly cells in Figure 5e, antimir-21 did not significantly affect the cell proliferation when co-transfected with MN-887 or sh-SCR at day 2 and 3 after transfection.

Finally, we performed Western blot analyses of SK-N-BE (2) and Kelly cells treated with premir-21 or antimir-21 to investigate if changes in *mir-21* levels affected the expression of the known *mir-21* target genes PDCD4 (Programmed Cell Death 4) or PTEN (Phosphatase and Tensin homolog). Neither overexpression of *mir-21*, nor repression of the observed *MYCN* knockdown-mediated *mir-21* increase by anti-mir-21 treatment resulted in significant changes to PDCD4 or PTEN expression (Supplementary Figure 6). This indicates that these tumour suppressor genes are not targeted by *mir-21* in SK-N-BE (2) and Kelly cells

Discussion

MYCN is amplified in a subgroup of neuroblastomas with highly aggressive behaviour. We have previously established an efficient model system to selectively down-regulate *MYCN* expression in MNA neuroblastoma by specific anti-*MYCN* shRNA molecules [20]. This approach allows us to investigate and compare cellular processes in both high- and low-*MYCN* neuroblastoma cells. In particular, our model system can be used to study neuronal differentiation in MNA neuroblastoma initiated by specific *MYCN* knockdown, as opposed to

induced neuronal differentiation using protocols with RA, TPA or various combinations of growth factors (BDNF, bFGF, IGF, NGF).

Over the past few years, several studies have addressed the role of N-myc on the expression of miRNAs in neuroblastoma [22, 32-39]. These studies were mainly performed by overexpressing *MYCN* in non-MNA neuroblastoma cell lines with or without the capacity to undergo neuronal differentiation (SH-SY-5Y or SHEP, respectively) or by comparing miRNA profiles in MNA vs. non-MNA neuroblastoma tumours. The contribution of miRNAs to the neuronal differentiation processes in neuroblastoma has mainly been investigated in SH-SY-5Y cells induced to differentiate by the addition of TPA or RA alone, or RA in combination with BDNF [21, 26].

In this study, we analysed the expression of 723 known human miRNAs during the differentiation of MNA SK-N-BE (2) cells upon *MYCN* knockdown. By comparing miRNA expression levels in high and low N-myc SK-N-BE (2) cells, we found 23 differentially expressed miRNAs. Twelve miRNAs (*mir-17, -18a, -20, -24, -25, -92a, -92b, -93, -103, -106a, -494 and mir-495)* were down-regulated, and 11 miRNAs (*mir-21, -22, -126, -137, -181d, -218, -663, -671, let-7c, let-7d* and *let-7f*) were up-regulated.

Among the down-regulated miRNAs, most are members of the oncogenic miRNA clusters which constitute the mir-17 family. It is now well established that N-myc is a transcriptional activator by direct binding to the promoter regions of several miRNAs, including the mir-17 family clusters [34, 36, 38]. In addition, miRNAs of the mir-17 family clusters have been shown to be down-regulated in non-MNA neuroblastoma cells in which differentiation was induced by various agents and growth factors [21]. In this study, we show for the first time that most miRNAs belonging to the mir-17 family are down-regulated upon the *MYCN* knockdown-mediated neuronal differentiation of MNA neuroblastoma cells. Interestingly, Lovén et al. recently reported that the stable knockdown of *mir-18a*, but not *mir-19a* (both from the mir-17-92 cluster), resulted in the differentiation of SK-N-BE (2) cells [36].

Similarly, we found *mir-18a*, but not *mir-19a,* down-regulation during the differentiation of SK-N-BE (2) upon N-myc knockdown.

We also observed several miRNAs being up-regulated upon *MYCN* knockdown in SK-N-BE (2) cells, and most have previously been linked to a neuronal phenotype or been shown to induce neuronal differentiation. The *let-7* family of miRNAs was found to be highly represented in miRNA populations in mouse, rat and primate brains [40, 41]. Moreover, the expression of *let-7*, *mir-218* and *mir-137* has been reported to increase during induced neuronal differentiation in mouse embryonic stem cells, mouse and human embryonic carcinoma cells and mouse neuronal stem cells (mNSC) [42-44]. Additionally, the exogenous expression of *mir-137* promoted neuronal-like differentiation in several mouse and human stem cells [43]. In a study using RA or *MYCN* siRNA to induce neuronal differentiation in MNA neuroblastoma cells, Chen and Stallings reported the vast majority of differentially expressed miRNAs to be up-regulated. In accordance with our data, *mir-137*, *mir-181* and *let-7* family members were among the up-regulated miRNAs reported.

In summary, these observations support the idea that miRNAs up-regulated during *MYCN* knockdown-mediated neuroblastoma differentiation are either directly involved in, or are a consequence of, the observed neuronal differentiation process.

The most prominent up-regulated miRNA in our study was *mir-21*. Neuroblastoma cell lines have been reported to express low or undetectable levels of *mir-21* [45]. However, Afanasyeva et al. reported *mir-21* to be among the most frequent miRNAs detected in primary neuroblastoma tumours [46]. We found *mir-21* expressed in all neuroblastoma cell lines investigated in this study. Interestingly, *mir-21* expression was inverse correlated to *MYCN* mRNA expression. However, we cannot exclude that the expression of *mir-21* is also influenced by variations in *mir-21* gene dosages, as *mir-21* is encoded on chromosome 17q which is frequently involved in unbalanced translocations in NB cell lines [28]. *Mir-21* is an miRNA with putative anti-apoptotic and tumour promoting activities, and has previously been

described to be highly expressed in a variety of solid tumours [31]. Experimentally validated *mir-21* targets include several proteins with a tumour suppressor function, eg. PDCD4 and PTEN [31, 47-51]. However, overexpression of *mir-21* in SK-N-BE (2) and Kelly cells did not alter proliferation of these cell lines. In addition, neither PCDC4, nor PTEN expression was changed upon *mir-21* overexpression. This indicates that *mir-21* is not involved in the regulation of these proteins in SK-N-BE (2) and Kelly cells. Similar to our studies, Folini et al. recently reported that changes in *mir-21* expression did not alter proliferation of prostate cancer cell lines [58].

Induced *mir-21* expression has previously been shown in neuronal differentiating neuroblastoma cells [24, 26, 45, 52-54]. In non-MNA SH-SY-5Y cells, RA, TPA and IFN-γ treatments increase *mir-21* expression. These treatments also induce neuronal differentiation in some MNA neuroblastoma cell lines and reduce N-myc expression through both transcriptional repression and the shortening of *MYCN* mRNA half-life [55, 56].

An increased expression of *mir-21* alone did not induce neuronal differentiation in SK-N-BE (2) or Kelly cells, and neither morphological nor biochemical alterations compatible with neuronal differentiation were observed. Using antagomir-21 to reduce the observed *mir-21* increase had no effect on differentiation. These observations indicate that the observed increase in *mir-21* expression does not directly influence the neuronal differentiation process in MNA neuroblastoma cells induced to differentiate by *MYCN* knockdown. We suggest that the increase of *mir-21* is a consequence rather than a cause for this differentiation process.

Recently, *mir-21* was reported to be the most significantly down-regulated miRNA when N-myc expression was induced in Tet21N neuroblastoma cells [36]. These cells (SHEP-based) are derived from the surface-adherent S-type fraction of SK-N-SH and lack the ability to differentiate into neuron-like cells. These results indicate an inverse connection between *MYCN* and *mir-21* that does not involve neuronal differentiation. We did not observe an

altered expression of *MYCN* in SK-N-BE (2) cells transfected with *mir-21* mimics or antagomirs.

From a wider perspective, the TPA-induced differentiation of human promyelocytic leukemia cells and the RA-induced differentiation of mouse embryonic stem cells have been shown to drastically increase *mir-21* expression [52, 53]. Kim et al. have recently demonstrated that the overexpression of *mir-21* enhanced adipogenic diffentiation by targeting *TGFBR2* [57]. Taken together, these reports could indicate that the up-regulation of *mir-21* expression has a more general role in cell differentiation.

In summary, we have found a subset of miRNAs that were altered during the *MYCN* knockdown-mediated differentiation of MNA neuroblastoma cells. We observed both up- and down-regulation of miRNA expression. The majority of down-regulated miRNAs are located in N-myc controlled miRNA gene clusters with established proliferative functions. By contrast, most up-regulated miRNAs have been previously linked to neuronal differentiation processes. *Mir-21* was found to be up-regulated during differentiation. Functional analyses indicate that the observed increase in *mir-21* expression is not a prerequisite to initiate the differentiation process since inhibition of *mir-21* did not prevent differentiation. In SK-N-BE (2) and Kelly cells, we were unable to establish a role for *mir-21* during differentiation and proliferation.

Conflict of Interest Statement

The authors have declared that no conflicts of interests exist.

Authors' contributions

JB and CE designed the research. JB and JRH performed the experimental work. CE supervised the experimental work. JB and CE wrote the manuscript. TF assisted the research design and critically commented on the manuscript. BHH and ET performed experiments for the revised version of the manuscript. The final manuscript was read and approved by all of the authors.

Acknowledgements

We wish to thank C. Løkke for the technical assistance. This work was supported by grants from the Norwegian Cancer Society and the Ragnvarda F. Sørvik and Håkon Starheims Foundation.

Reference List

[1] M.M. van Noesel and R. Versteeg, Pediatric neuroblastomas: genetic and epigenetic 'danse macabre'. Gene 325 (2004) 1-15.

[2] B. Hero, T. Simon, R. Spitz, K. Ernestus, A.K. Gnekow, H.G. Scheel-Walter, D. Schwabe, F.H. Schilling, G. Benz-Bohm, and F. Berthold, Localized infant neuroblastomas often show spontaneous regression: results of the prospective trials NB95-S and NB97. J. Clin. Oncol. 26 (2008) 1504-1510.

[3] J.M. Maris, M.D. Hogarty, R. Bagatell, and S.L. Cohn, Neuroblastoma. Lancet 369 (2007) 2106-2120.

[4] G.M. Brodeur and R.C. Seeger, Gene amplification in human neuroblastomas: basic mechanisms and clinical implications. Cancer Genet. Cytogenet. 19 (1986) 101-111.

[5] M. Henriksson and B. Luscher, Proteins of the Myc network: essential regulators of cell growth and differentiation. Adv. Cancer Res. 68 (1996) 109-182.

[6] S. Breit, K. Ashman, J. Wilting, J. Rossler, E. Hatzi, T. Fotsis, and L. Schweigerer, The N-myc oncogene in human neuroblastoma cells: down-regulation of an angiogenesis inhibitor identified as activin A. Cancer Res. 60 (2000) 4596-4601.

[7] J. Li and L. Kretzner, The growth-inhibitory Ndrg1 gene is a Myc negative target in human neuroblastomas and other cell types with overexpressed N- or c-myc. Mol. Cell Biochem. 250 (2003) 91-105.

[8] R. Judware and L.A. Culp, Concomitant down-regulation of expression of integrin subunits by N-myc in human neuroblastoma cells: differential regulation of alpha2, alpha3 and beta1. Oncogene 14 (1997) 1341-1350.

[9] K. Peukert, P. Staller, A. Schneider, G. Carmichael, F. Hanel, and M. Eilers, An alternative pathway for gene regulation by Myc. EMBO J. 16 (1997) 5672-5686.

[10] D.P. Bartel, MicroRNAs: target recognition and regulatory functions. Cell 136 (2009) 215-233.

[11] A. Edsjo, L. Holmquist, and S. Pahlman, Neuroblastoma as an experimental model for neuronal differentiation and hypoxia-induced tumor cell dedifferentiation. Semin. Cancer Biol. 17 (2007) 248-256.

[12] C.J. Thiele, C.P. Reynolds, and M.A. Israel, Decreased expression of N-myc precedes retinoic acid-induced morphological differentiation of human neuroblastoma. Nature 313 (1985) 404-406.

[13] A. Edsjo, H. Nilsson, J. Vandesompele, J. Karlsson, F. Pattyn, L.A. Culp, F. Speleman, and S. Pahlman, Neuroblastoma cells with overexpressed MYCN retain their capacity to undergo neuronal differentiation. Lab Invest 84 (2004) 406-417.

[14] F.A. Peverali, D. Orioli, L. Tonon, P. Ciana, G. Bunone, M. Negri, and G. Della-Valle, Retinoic acid-induced growth arrest and differentiation of neuroblastoma cells are counteracted by N-myc and enhanced by max overexpressions. Oncogene 12 (1996) 457-462.

[15] C.J. Thiele and M.A. Israel, Regulation of N-myc expression is a critical event controlling the ability of human neuroblasts to differentiate. Exp. Cell Biol. 56 (1988) 321-333.

[16] E. Bell, R. Premkumar, J. Carr, X. Lu, P.E. Lovat, U.R. Kees, J. Lunec, and D.A. Tweddle, The role of MYCN in the failure of MYCN amplified neuroblastoma cell lines to G1 arrest after DNA damage. Cell Cycle 5 (2006) 2639-2647.

[17] M. Haber, S.B. Bordow, J. Gilbert, J. Madafiglio, M. Kavallaris, G.M. Marshall, E.B. Mechetner, J.P. Fruehauf, L. Tee, S.L. Cohn, H. Salwen, M.L. Schmidt, and M.D. Norris, Altered expression of the MYCN oncogene modulates MRP gene expression and response to cytotoxic drugs in neuroblastoma cells. Oncogene 18 (1999) 2777-2782.

[18] A. Negroni, S. Scarpa, A. Romeo, S. Ferrari, A. Modesti, and G. Raschella, Decrease of proliferation rate and induction of differentiation by a MYCN antisense DNA oligomer in a human neuroblastoma cell line. Cell Growth Differ. 2 (1991) 511-518.

[19] R. Tonelli, S. Purgato, C. Camerin, R. Fronza, F. Bologna, S. Alboresi, M. Franzoni, R. Corradini, S. Sforza, A. Faccini, J.M. Shohet, R. Marchelli, and A. Pession, Anti-gene peptide nucleic acid specifically inhibits MYCN expression in human neuroblastoma cells leading to cell growth inhibition and apoptosis. Mol. Cancer Ther. 4 (2005) 779-786.

[20] J.R. Henriksen, J. Buechner, C. Løkke, T. Flægstad, and C. Einvik. Inhibition of gene function in mammalian cells using short-hairpin RNA (shRNA). In: Methods in Molecular Biology . 2010. In press.

[21] N.J. Beveridge, P.A. Tooney, A.P. Carroll, N. Tran, and M.J. Cairns, Down-regulation of miR-17 family expression in response to retinoic acid induced neuronal differentiation. Cell Signal. 21 (2009) 1837-1845.

[22] Y. Chen and R.L. Stallings, Differential patterns of microRNA expression in neuroblastoma are correlated with prognosis, differentiation, and apoptosis. Cancer Res. 67 (2007) 976-983.

[23] C. Evangelisti, M.C. Florian, I. Massimi, C. Dominici, G. Giannini, S. Galardi, M.C. Bue, S. Massalini, H.P. McDowell, E. Messi, A. Gulino, M.G. Farace, and S.A. Ciafre, MiR-128 up-regulation inhibits Reelin and DCX expression and reduces neuroblastoma cell motility and invasiveness. FASEB J. 23 (2009) 4276-4287.

[24] Y. Fukuda, H. Kawasaki, and K. Taira, Exploration of human miRNA target genes in neuronal differentiation. Nucleic Acids Symp. Ser. (Oxf)2005) 341-342.

[25] P. Laneve, L. Di Marcotullio, U. Gioia, M.E. Fiori, E. Ferretti, A. Gulino, I. Bozzoni, and E. Caffarelli, The interplay between microRNAs and the neurotrophin receptor tropomyosin-related kinase C controls proliferation of human neuroblastoma cells. Proc. Natl. Acad. Sci. U. S. A 104 (2007) 7957-7962.

[26] M.T. Le, H. Xie, B. Zhou, P.H. Chia, P. Rizk, M. Um, G. Udolph, H. Yang, B. Lim, and H.F. Lodish, MicroRNA-125b promotes neuronal differentiation in human cells by repressing multiple targets. Mol. Cell Biol. 29 (2009) 5290-5305.

[27] D.A. Tweddle, A.J. Malcolm, N. Bown, A.D. Pearson, and J. Lunec, Evidence for the development of p53 mutations after cytotoxic therapy in a neuroblastoma cell line. Cancer Res. 61 (2001) 8-13.

[28] G. Schleiermacher, V. Raynal, I. Janoueix-Lerosey, V. Combaret, A. Aurias, and O. Delattre, Variety and complexity of chromosome 17 translocations in neuroblastoma. Genes Chromosomes. Cancer 39 (2004) 143-150.

[29] X. Wang, S. Tang, S.Y. Le, R. Lu, J.S. Rader, C. Meyers, and Z.M. Zheng, Aberrant expression of oncogenic and tumor-suppressive microRNAs in cervical cancer is required for cancer cell growth. PLoS. ONE. 3 (2008) e2557.

[30] J. Hellemans, G. Mortier, A. De Paepe, F. Speleman, and J. Vandesompele, qBase relative quantification framework and software for management and automated analysis of real-time quantitative PCR data. Genome Biol. 8 (2007) R19.

[31] A.M. Krichevsky and G. Gabriely, miR-21: a small multi-faceted RNA. J. Cell Mol. Med. 13 (2009) 39-53.

[32] I. Bray, K. Bryan, S. Prenter, P.G. Buckley, N.H. Foley, D.M. Murphy, L. Alcock, P. Mestdagh, J. Vandesompele, F. Speleman, W.B. London, P.W. McGrady, D.G. Higgins, A. O'Meara, M. O'Sullivan, and R.L. Stallings, Widespread dysregulation of MiRNAs by MYCN amplification and chromosomal imbalances in neuroblastoma: association of miRNA expression with survival. PLoS. ONE. 4 (2009) e7850.

[33] O. Chayka, D. Corvetta, M. Dews, A.E. Caccamo, I. Piotrowska, G. Santilli, S. Gibson, N.J. Sebire, N. Himoudi, M.D. Hogarty, J. Anderson, S. Bettuzzi, A. Thomas-Tikhonenko, and A. Sala, Clusterin, a haploinsufficient tumor suppressor gene in neuroblastomas. J. Natl. Cancer Inst. 101 (2009) 663-677.

[34] L. Fontana, M.E. Fiori, S. Albini, L. Cifaldi, S. Giovinazzi, M. Forloni, R. Boldrini, A. Donfrancesco, V. Federici, P. Giacomini, C. Peschle, and D. Fruci, Antagomir-17-5p abolishes the growth of therapy-resistant neuroblastoma through p21 and BIM. PLoS. ONE. 3 (2008) e2236.

[35] H. Hu, L. Du, G. Nagabayashi, R.C. Seeger, and R.A. Gatti, ATM is down-regulated by N-Myc-regulated microRNA-421. Proc. Natl. Acad. Sci. U. S. A 107 (2010) 1506-1511.

[36] J. Loven, N. Zinin, T. Wahlstrom, I. Muller, P. Brodin, E. Fredlund, U. Ribacke, A. Pivarcsi, S. Pahlman, and M. Henriksson, MYCN-regulated microRNAs repress estrogen receptor-alpha (ESR1) expression and neuronal differentiation in human neuroblastoma. Proc. Natl. Acad. Sci. U. S. A 107 (2010) 1553-1558.

[37] P. Mestdagh, P. Van Vlierberghe, A. De Weer, D. Muth, F. Westermann, F. Speleman, and J. Vandesompele, A novel and universal method for microRNA RT-qPCR data normalization. Genome Biol. 10 (2009) R64.

[38] P. Mestdagh, E. Fredlund, F. Pattyn, J.H. Schulte, D. Muth, J. Vermeulen, C. Kumps, S. Schlierf, K. De Preter, N. Van Roy, R. Noguera, G. Laureys, A. Schramm, A. Eggert, F. Westermann, F. Speleman, and J. Vandesompele, MYCN/c-MYC-induced

microRNAs repress coding gene networks associated with poor outcome in MYCN/c-MYC-activated tumors. Oncogene 29 (2010) 1394-1404.

[39] J.H. Schulte, S. Horn, T. Otto, B. Samans, L.C. Heukamp, U.C. Eilers, M. Krause, K. Astrahantseff, L. Klein-Hitpass, R. Buettner, A. Schramm, H. Christiansen, M. Eilers, A. Eggert, and B. Berwanger, MYCN regulates oncogenic MicroRNAs in neuroblastoma. Int. J. Cancer 122 (2008) 699-704.

[40] M. Lagos-Quintana, R. Rauhut, W. Lendeckel, and T. Tuschl, Identification of novel genes coding for small expressed RNAs. Science 294 (2001) 853-858.

[41] E.A. Miska, E. Alvarez-Saavedra, M. Townsend, A. Yoshii, N. Sestan, P. Rakic, M. Constantine-Paton, and H.R. Horvitz, Microarray analysis of microRNA expression in the developing mammalian brain. Genome Biol. 5 (2004) R68.

[42] L.F. Sempere, S. Freemantle, I. Pitha-Rowe, E. Moss, E. Dmitrovsky, and V. Ambros, Expression profiling of mammalian microRNAs uncovers a subset of brain-expressed microRNAs with possible roles in murine and human neuronal differentiation. Genome Biol. 5 (2004) R13.

[43] J. Silber, D.A. Lim, C. Petritsch, A.I. Persson, A.K. Maunakea, M. Yu, S.R. Vandenberg, D.G. Ginzinger, C.D. James, J.F. Costello, G. Bergers, W.A. Weiss, A. Alvarez-Buylla, and J.G. Hodgson, miR-124 and miR-137 inhibit proliferation of glioblastoma multiforme cells and induce differentiation of brain tumor stem cells. BMC. Med. 6 (2008) 14.

[44] L. Smirnova, A. Grafe, A. Seiler, S. Schumacher, R. Nitsch, and F.G. Wulczyn, Regulation of miRNA expression during neural cell specification. Eur. J. Neurosci. 21 (2005) 1469-1477.

[45] P. Landgraf, M. Rusu, R. Sheridan, A. Sewer, N. Iovino, A. Aravin, S. Pfeffer, A. Rice, A.O. Kamphorst, M. Landthaler, C. Lin, N.D. Socci, L. Hermida, V. Fulci, S. Chiaretti, R. Foa, J. Schliwka, U. Fuchs, A. Novosel, R.U. Muller, B. Schermer, U. Bissels, J. Inman, Q. Phan, M. Chien, D.B. Weir, R. Choksi, G. De Vita, D. Frezzetti, H.I. Trompeter, V. Hornung, G. Teng, G. Hartmann, M. Palkovits, R. Di Lauro, P. Wernet, G. Macino, C.E. Rogler, J.W. Nagle, J. Ju, F.N. Papavasiliou, T. Benzing, P. Lichter, W. Tam, M.J. Brownstein, A. Bosio, A. Borkhardt, J.J. Russo, C. Sander, M. Zavolan, and T. Tuschl, A mammalian microRNA expression atlas based on small RNA library sequencing. Cell 129 (2007) 1401-1414.

[46] E.A. Afanasyeva, A. Hotz-Wagenblatt, K.H. Glatting, and F. Westermann, New miRNAs cloned from neuroblastoma. BMC. Genomics 9 (2008) 52.

[47] L.B. Frankel, N.R. Christoffersen, A. Jacobsen, M. Lindow, A. Krogh, and A.H. Lund, Programmed cell death 4 (PDCD4) is an important functional target of the microRNA miR-21 in breast cancer cells. J. Biol. Chem. 283 (2008) 1026-1033.

[48] G. Gabriely, T. Wurdinger, S. Kesari, C.C. Esau, J. Burchard, P.S. Linsley, and A.M. Krichevsky, MicroRNA 21 promotes glioma invasion by targeting matrix metalloproteinase regulators. Mol. Cell Biol. 28 (2008) 5369-5380.

[49] F. Meng, R. Henson, H. Wehbe-Janek, K. Ghoshal, S.T. Jacob, and T. Patel, MicroRNA-21 regulates expression of the PTEN tumor suppressor gene in human hepatocellular cancer. Gastroenterology 133 (2007) 647-658.

[50] S. Zhu, M.L. Si, H. Wu, and Y.Y. Mo, MicroRNA-21 targets the tumor suppressor gene tropomyosin 1 (TPM1). J. Biol. Chem. 282 (2007) 14328-14336.

[51] S. Zhu, H. Wu, F. Wu, D. Nie, S. Sheng, and Y.Y. Mo, MicroRNA-21 targets tumor suppressor genes in invasion and metastasis. Cell Res. 18 (2008) 350-359.

[52] H.B. Houbaviy, M.F. Murray, and P.A. Sharp, Embryonic stem cell-specific MicroRNAs. Dev. Cell 5 (2003) 351-358.

[53] K. Kasashima, Y. Nakamura, and T. Kozu, Altered expression profiles of microRNAs during TPA-induced differentiation of HL-60 cells. Biochem. Biophys. Res. Commun. 322 (2004) 403-410.

[54] S. Fujita, T. Ito, T. Mizutani, S. Minoguchi, N. Yamamichi, K. Sakurai, and H. Iba, miR-21 Gene expression triggered by AP-1 is sustained through a double-negative feedback mechanism. J. Mol. Biol. 378 (2008) 492-504.

[55] C. Cetinkaya, A. Hultquist, Y. Su, S. Wu, F. Bahram, S. Pahlman, I. Guzhova, and L.G. Larsson, Combined IFN-gamma and retinoic acid treatment targets the N-Myc/Max/Mad1 network resulting in repression of N-Myc target genes in MYCN-amplified neuroblastoma cells. Mol. Cancer Ther. 6 (2007) 2634-2641.

[56] A.G. Smith, N. Popov, M. Imreh, H. Axelson, and M. Henriksson, Expression and DNA-binding activity of MYCN/Max and Mnt/Max during induced differentiation of human neuroblastoma cells. J. Cell Biochem. 92 (2004) 1282-1295.

[57] Y.J. Kim, S.J. Hwang, Y.C. Bae, and J.S. Jung, miR-21 Regulates Adipogenic Differentiation Through the Modulation of TGF-beta Signaling in Mesenchymal Stem Cells Derived from Human Adipose Tissue. Stem Cells2009).

[58] M. Folini, P. Gandellini, N. Longoni, V. Profumo, M. Callari, M. Pennati, M. Colecchia, R. Supino, S. Veneroni, P. Salvioni, R. Valdagni, M.G. Daidone, and N. Zaffaroni, miR-21: an oncomir on strike in prostate cancer. Mol Cancer (2010) 9:12.

Figures

Figure 1: shRNA-mediated knockdown of *MYCN* in SK-N-BE (2) cells. (**A**) Bar graph showing the normalized expression of *MYCN* mRNA from qRT-PCR analyses. (**B**) Representative western blot analysis of N-myc and β–actin expression from shSCR and aMN-887 treated SK-N-BE (2) cells. (**C**) Confocal laser microscopy images. Transfected cells appear green due to GFP expression from the transfected plasmids. Nuclei are stained with Draq5 (blue). Merge is an overlay of all 3 pictures. Cells transfected with pDS-anti*MYCN*-887 display a neuronal phenotype with neurite outgrowth and expression of Neuronal Class III β-Tubulin (TUJ1, purple, white arrow). Nuclear N-myc disappears in anti-*MYCN* transfected cells (yellow arrow). In contrast, shSCR-transfected control cells remain undifferentiated and show abundant nuclear N-myc expression.

Figure 2: Highly expressed miRNAs in SK-N-BE (2) cells. MiRNAs with high expression in SK-N-BE (2) are transcribed either from miRNA gene clusters (grey boxes) or monocistronically (non-clustered miRNAs).

Figure 3: Differential miRNA expression in differentiating *MYCN* repressed SK-N-BE (2) cells.

(**A**) Summary of consistently differentially expressed miRNAs ($p<0.01$) represented in a horizontal bar graph as log2 values from microarray SK07. Down-regulated and up-regulated miRNAs are shown as blue and red bars, respectively. (**B**) MiRNAs from the paralogous miRNA clusters mir-17-92, mir-106a-363 and mir-106b-25 were down-regulated upon *MYCN* knockdown-induced differentiation, either on both arrays (indicated as blue boxes) or on one array (hatched boxes).

Figure 4: *Mir-21* is inverse correlated to *MYCN* mRNA expression: (**A**): *MYCN* mRNA (left) and *mir-21* (right) levels in SK-N-SH, SK-N-AS, KCN, KCNR, LAN5, Kelly and SK-N-BE (2) neuroblastoma cell lines. (**B**) Cells transfected with either aMN-887 or premir-21 displayed a ~2-fold and 20-fold increase in *mir-21* expression, respectively. Co-transfection of aMN-887 and anti-mir-21 prevented the *mir-21* increase. (**C**) Inhibition of endogenous *mir-21* by the anti-mir-21 antagomir. The luciferase-reporter plasmid (pmir-21-luc), containing a 3'UTR with the *mir-21* target sequence, was co-transfected into SK-N-BE (2) and Kelly cells along with anti-mir-21 or a negative control antagomir. (**D**) *MYCN*-knockdown with aMN-887 induced strong up-regulation of NPY, a neuronal differentiation marker. In contrast, overexpression of premir-21 alone did not alter NPY. Co-transfection of aMN-887 and anti-mir-21 did not prevent cells from differentiation. (**E**) *MYCN* mRNA levels were reduced in SK-N-BE (2) cells transfected with aMN-887. Overexpression or inhibition of *mir-21* did not alter *MYCN* mRNA levels compared to the respective negative controls.

Figure 5: Proliferation assays. SK-N-BE (2) cells (**A**) and Kelly cells (**B**) were transfected with premir-21 at different concentrations (40, 60 and 80 nM) and monitored for proliferation on 3 consecutive days after transfection. mir-NC= negative control miRNA mimic. (**C**) Flow cytometric data showing that the S-phase of the cell cycle was unaffected by premir-21 treatment of SK-N-BE (2) cells. SK-N-BE (2) cells (**D**) and Kelly cells (**E**) treated with antimir-21 in combination with aMN-887 showed no significant alterations in proliferation during the 2^{nd} and 3^{rd} day post-transfection compared to cells treated with a negative control antagomir (anti-NC).

Additional files

Supplementary 1:

Averaged signal intensity of small endogenous RNA molecules and short-hairpin RNA molecules after pDS-shSCR (high N-myc) and pDS-anti*MYCN*-887 transfection (N-myc knockdown).

Supplementary 2:

Overview of miRNAs with consistent differential expression on both microarrays SK07 and SK08.

Supplementary 3:

Validation of microarray data by quantitative RT-PCR. P-values refer to qRT-PCR data and are calculated by student´s t-test. Down-regulated and up-regulated miRNAs are shown as blue and red bars, respectively. A selection of 11 miRNAs which were consistently differentially expressed on both microarrays was confirmed by qRT-PCR with $p<0.05$. * indicates miRNAs shown to be significantly down-regulated on a miRNA microarray in a similar *MYCN*-knockdown study in Kelly cells ($p<0.01$) (data not shown)

Supplementary 4:

Differential expression of *mir-21* in Kelly cells. Cells were transfected with either sh-SCR or aMN-887. *Mir-21* levels were measured 3 days after transfection using a microRNA microarray and quantitative stem-loop RT-PCR.

Supplementary 5:

Mir-21 and *MYCN* mRNA expression at day 1 after transfection with sh-SCR and aMN-887. The MYCN-knockdown mediated increase in *mir-21* expression coincides early with *MYCN* downregulation.

Supplementary 6:

Western blot analyses of N-myc, PDCD4, PTEN and β-actin expression in SK-N-BE (2) and Kelly cells transfected with aMN-887, premir-21 and a combination of aMN-887 and antimir-21.

Figure 1

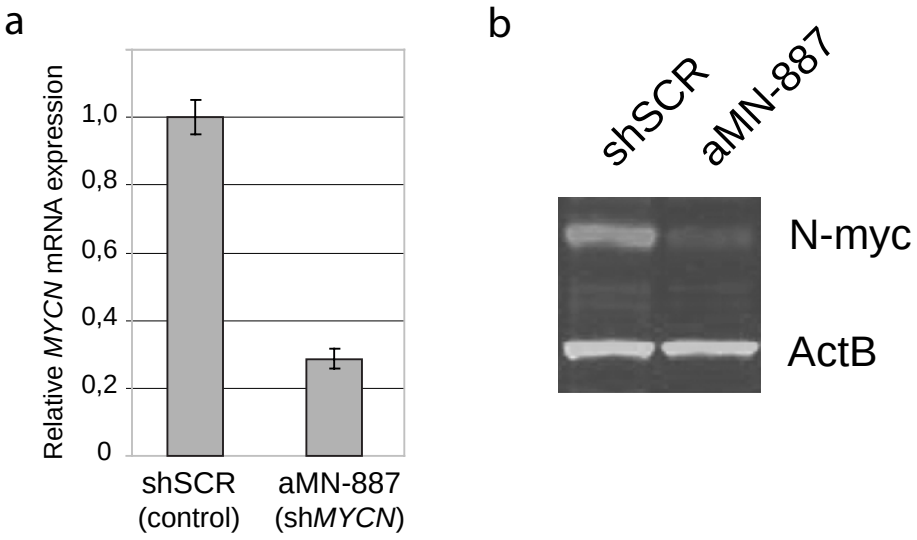
a
Relative MYCN mRNA expression
1,0
0,8
0,6
0,4
0,2
0
shSCR (control)
aMN-887 (shMYCN)
b
shSCR
aMN-887
N-myc
ActB
c
shSCR
aMN-887
Draq5 + TUJ1
GFP
N-myc
Merge
Draq5 + TUJ1
GFP
N-myc
Merge

Figure 2

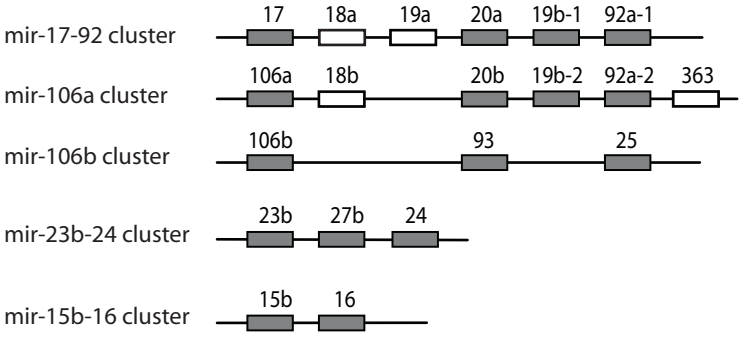

Non-clustered miR let-7a, mir-23a, mir-26a, mir-92b, mir-103, mir-107, mir-214, mir-218, mir-320, mir-638

Figure 3

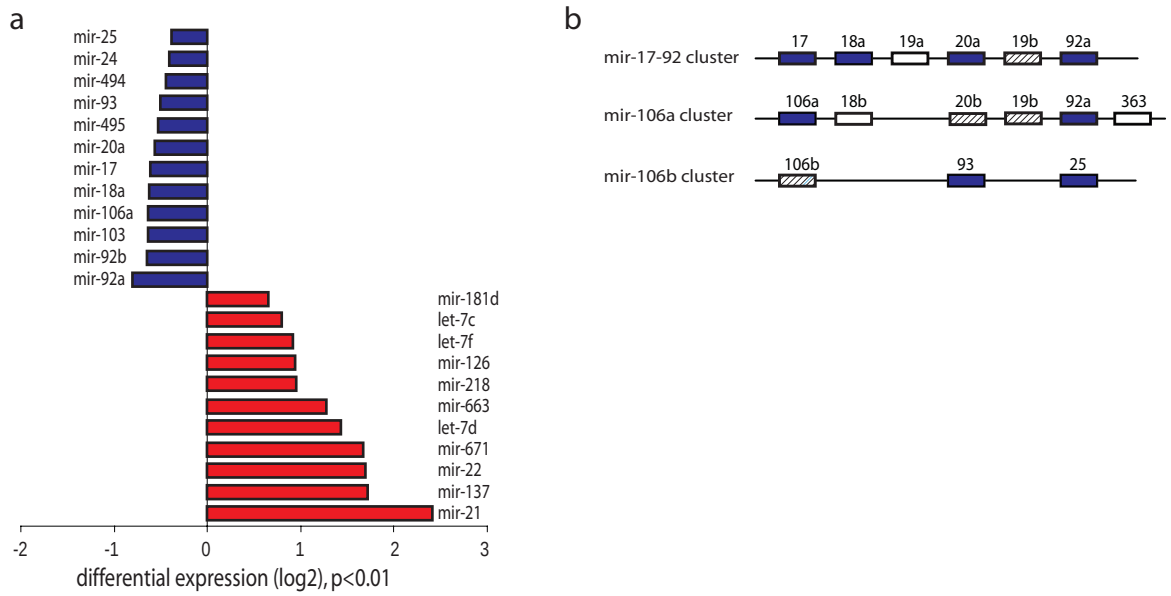
a
mir-25
mir-24
mir-494
mir-93
mir-495
mir-20a
mir-17
mir-18a
mir-106a
mir-103
mir-92b
mir-92a
mir-181d
let-7c
let-7f
mir-126
mir-218
mir-663
let-7d
mir-671
mir-22
mir-137
mir-21
-2
-1
0
1
2
3
differential expression (log2), p<0.01
b
mir-17-92 cluster
17
18a
19a
20a
19b
92a
mir-106a cluster
106a
18b
20b
19b
92a
363
mir-106b cluster
106b
93
25

Figure 4

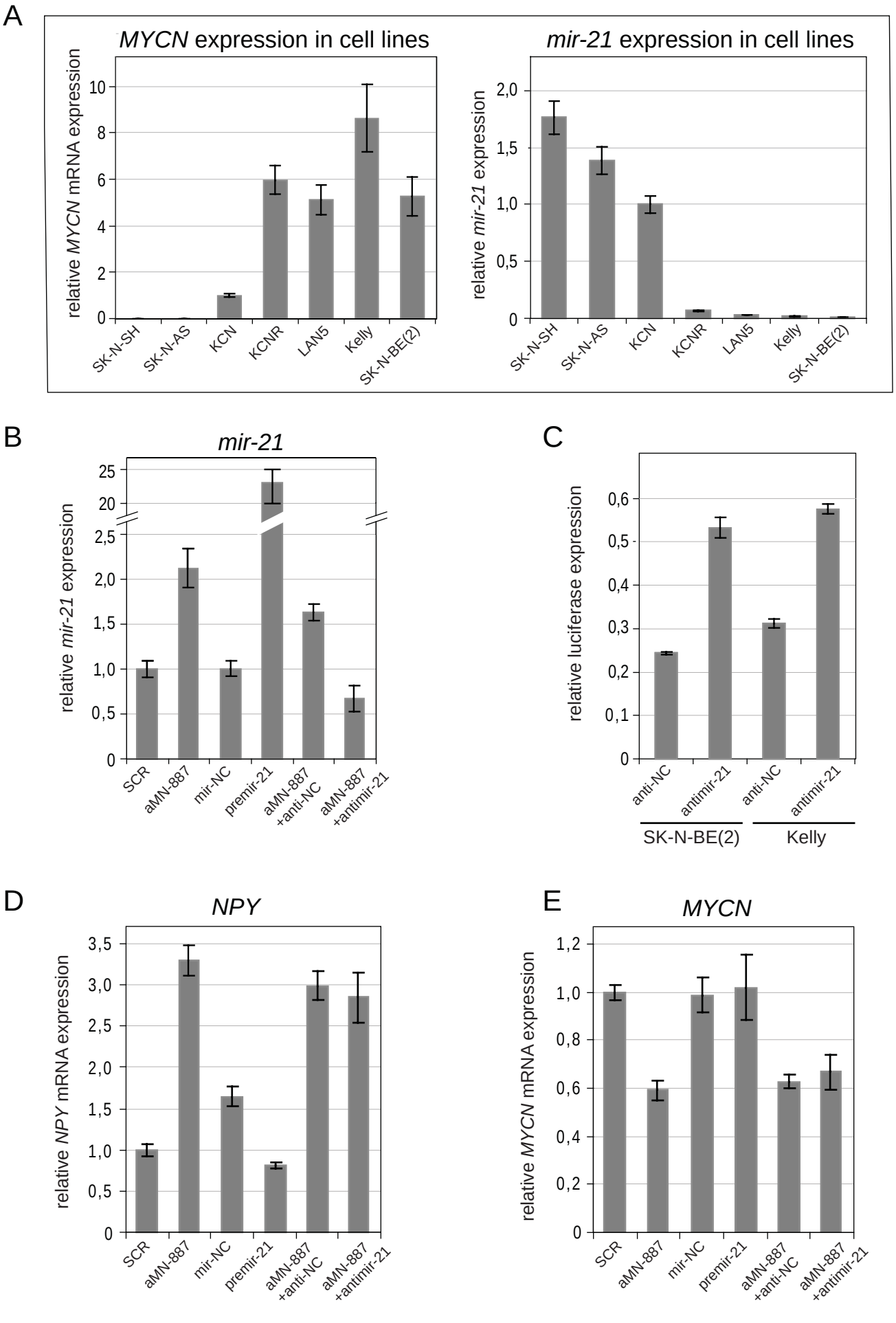
A
MYCN expression in cell lines
relative MYCN mRNA expression
0
2
4
6
8
10
SK-N-SH
SK-N-AS
KCN
KCNR
LAN5
Kelly
SK-N-BE(2)
mir-21 expression in cell lines
relative mir-21 expression
0
0,5
1,0
1,5
2,0
SK-N-SH
SK-N-AS
KCN
KCNR
LAN5
Kelly
SK-N-BE(2)
B
mir-21
relative mir-21 expression
0
0,5
1,0
1,5
2,0
2,5
20
25
SCR
aMN-887
mir-NC
premir-21
aMN-887 +anti-NC
aMN-887 +antimir-21
C
relative luciferase expression
0
0,1
0,2
0,3
0,4
0,5
0,6
anti-NC
antimir-21
anti-NC
antimir-21
SK-N-BE(2)
Kelly
D
NPY
relative NPY mRNA expression
0
0,5
1,0
1,5
2,0
2,5
3,0
3,5
SCR
aMN-887
mir-NC
premir-21
aMN-887 +anti-NC
aMN-887 +antimir-21
E
MYCN
relative MYCN mRNA expression
0
0,2
0,4
0,6
0,8
1,0
1,2
SCR
aMN-887
mir-NC
premir-21
aMN-887 +anti-NC
aMN-887 +antimir-21

Figure 5

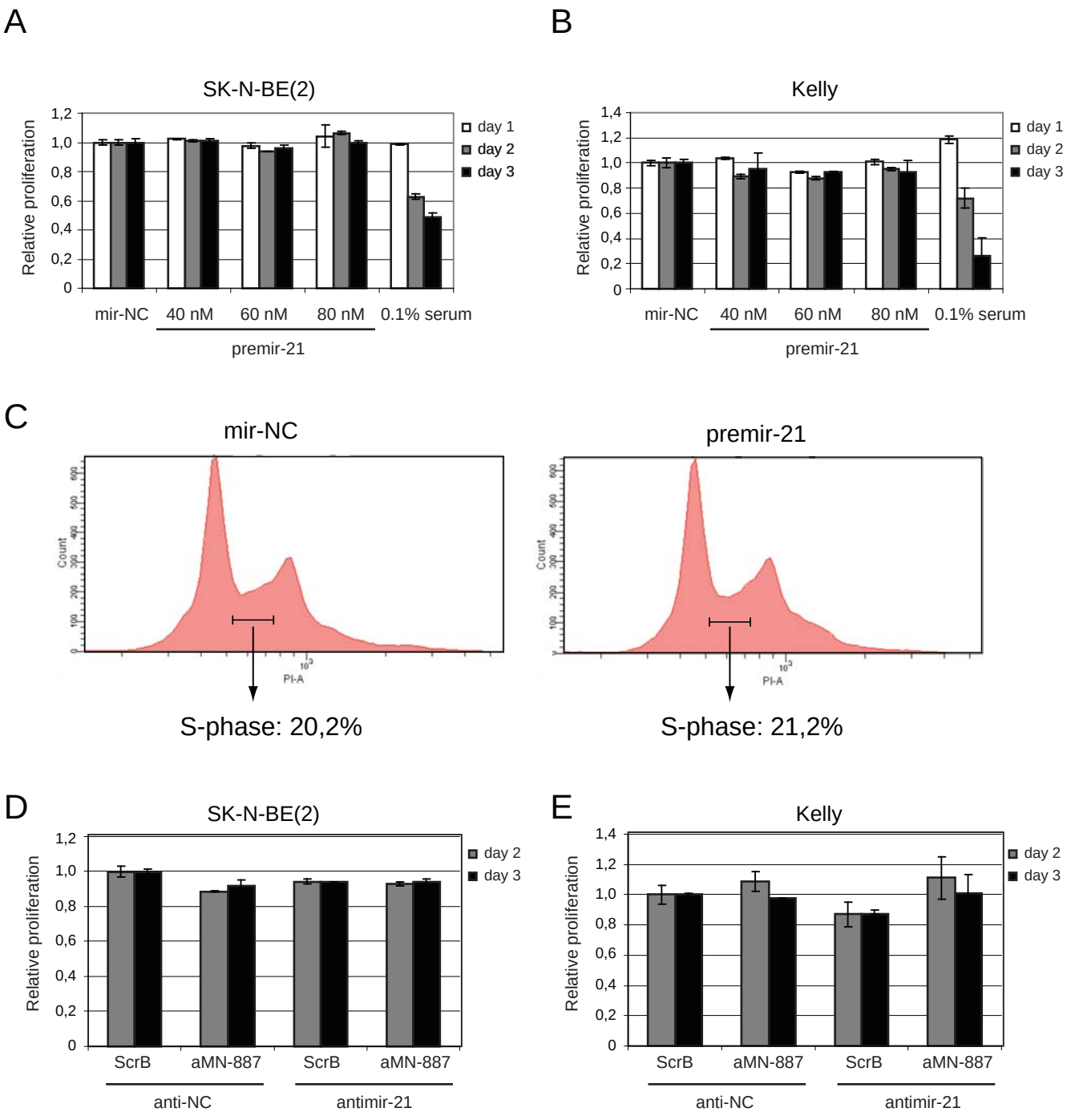
A
SK-N-BE(2)
Relative proliferation
1,2
1,0
0,8
0,6
0,4
0,2
0
day 1
day 2
day 3
mir-NC
40 nM
60 nM
80 nM
0.1% serum
premir-21
B
Kelly
Relative proliferation
1,4
1,2
1,0
0,8
0,6
0,4
0,2
0
day 1
day 2
day 3
mir-NC
40 nM
60 nM
80 nM
0.1% serum
premir-21
C
mir-NC
Count
PI-A
S-phase: 20,2%
premir-21
Count
PI-A
S-phase: 21,2%
D
SK-N-BE(2)
Relative proliferation
1,2
1,0
0,8
0,6
0,4
0,2
0
day 2
day 3
ScrB
aMN-887
ScrB
aMN-887
anti-NC
antimir-21
E
Kelly
Relative proliferation
1,4
1,2
1,0
0,8
0,6
0,4
0,2
0
day 2
day 3
ScrB
aMN-887
ScrB
aMN-887
anti-NC
antimir-21

Supplementary 1

small RNA	shSCR-transfected	aMN-887 transfected
RNU19	86,96	81,01
RNU43	80,05	77,51
RNU38B	**198,52**	**181,00**
RNU24	288,89	217,83
U18	39,80	43,72
RPL21	157,04	103,55
HY3	660,38	1 533,30
RNU44	3 439,07	1 701,35
RNU48	1 508,94	954,87
RNU49	1 030,45	585,84
RNU58B	313,48	202,84
RNU66	48,66	72,20
RNU6B	72,06	471,90
U47	536,65	301,00
RNU58A	Not detect.	Not detect.
U54	Not detect.	Not detect.
U75	Not detect.	Not detect.
Z30	Not detect.	Not detect.
shMYCN (aMN-887)	**146,91**	**68 710,01**
shSCR	**45 612,95**	**23,92**

Supplementary 2:

Down-regulated miRNAs

	SK07		SK08	
miRNA	**fold change**	**log2 change**	**fold change**	**log2 change**
mir-103	0,64	-0,64	0,86	-0,21
mir-93	0,70	-0,51	0,78	-0,35
mir-24	0,75	-0,41	0,84	-0,25
mir-25	0,76	-0,39	0,76	-0,39
mir-17	0,66	-0,61	0,73	-0,45
mir-106a	0,64	-0,64	0,68	-0,55
mir-494	0,73	-0,45	0,67	-0,58
mir-495	0,69	-0,53	0,66	-0,61
mir-18a	0,65	-0,62	0,65	-0,62
mir-92a	0,57	-0,80	0,63	-0,66
mir-20a	0,68	-0,56	0,63	-0,67
mir-92b	0,64	-0,65	0,62	-0,68

Up-regulated miRNAs

	SK07		SK08	
miRNA	**fold change**	**log2 change**	**fold change**	**log2 change**
mir-671	3,18	1,67	4,82	2,27
mir-663	2,43	1,28	2,66	1,41
mir-181d	1,58	0,66	1,69	0,76
mir-137	3,29	1,72	1,56	0,64
mir-22	3,25	1,70	1,54	0,62
mir-21	5,31	2,41	1,51	0,59
let-7d	2,69	1,43	1,38	0,46
let-7f	1,89	0,92	1,39	0,47
mir-126	1,92	0,94	1,30	0,38
let-7c	1,74	0,80	1,29	0,37
mir-218	1,93	0,95	1,21	0,28

Supplementary 3

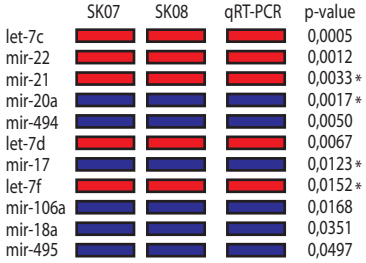

Supplementary Figure 4

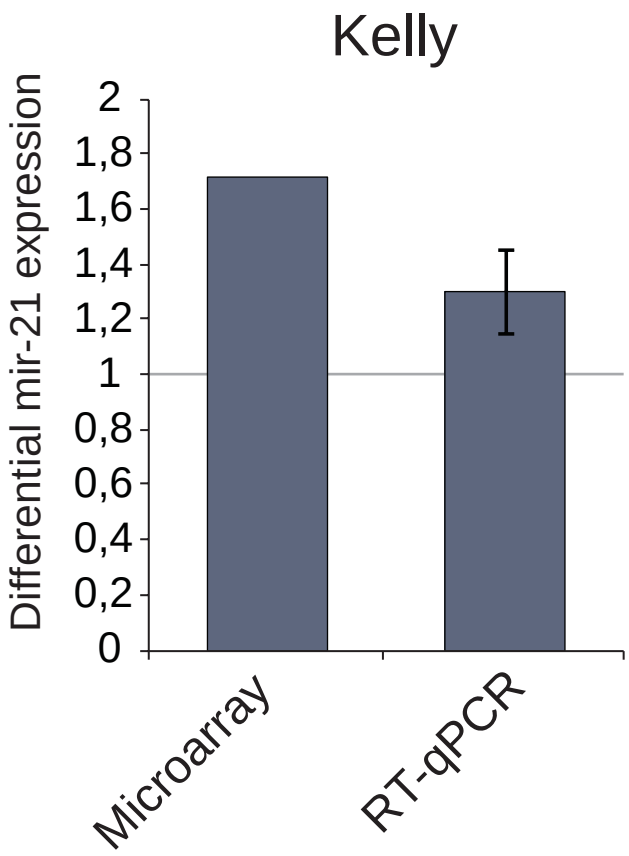

Supplementary Figure 5

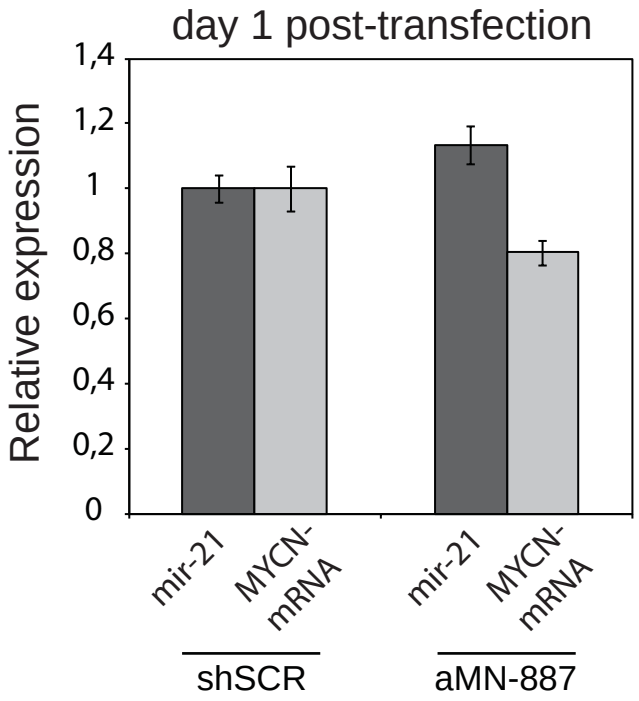

Supplementary Figure 6

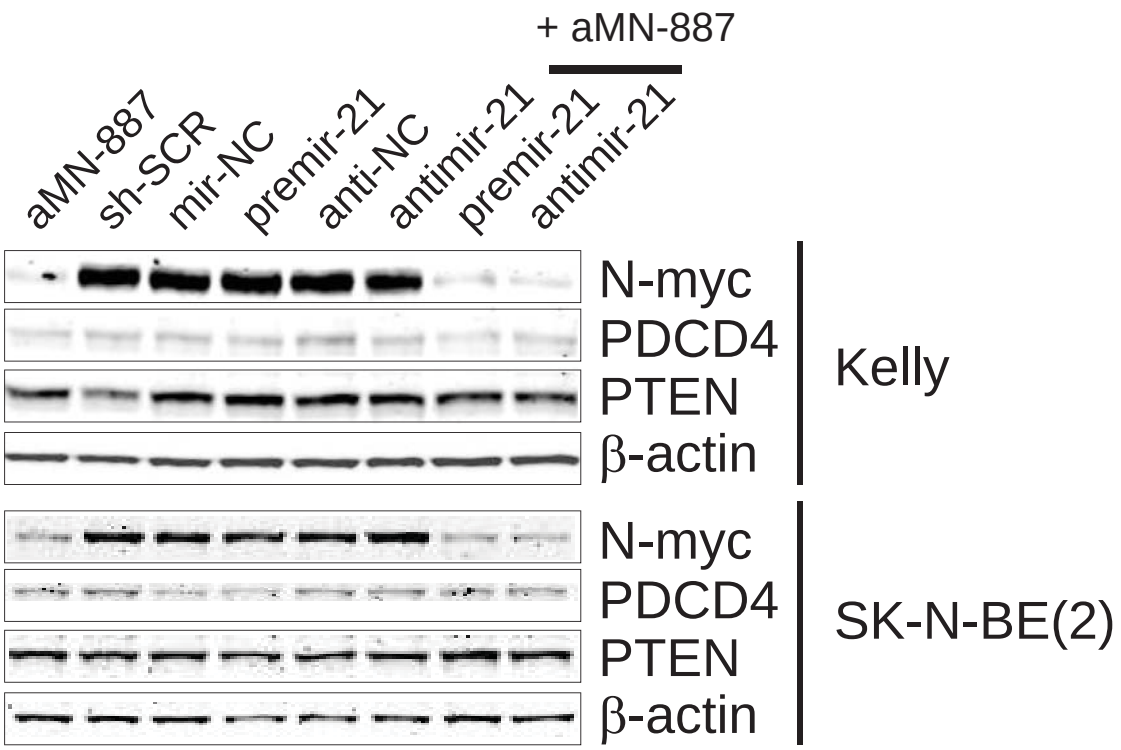

PAPER IV

Title Page

Title:

MYCN-regulated miRNAs Inhibit Secretion of the Tumor Suppressor *DICKKOPF-3* (*DKK3*) in Neuroblastoma

Running Title:

Dickkopf-3 Regulating miRNAs in Neuroblastoma

Authors with affiliations:

Bjørn Helge Haug[1,2], Jørn Remi Henriksen[1], Jochen Buechner[1], Per Kogner[3], Tommy Martinsson[4], Trond Flægstad[1,2], Baldur Sveinbjørnsson[3,5], Christer Einvik[1]

[1]Department of Pediatrics, University Hospital of North-Norway, 9038 Tromsø, Norway

[2]Pediatric Research Group, Department of Clinical Biology, Faculty of Health Science, University of Tromsø, 9037 Tromsø, Norway

[3]Childhood Cancer Research Unit, Department of Women's and Children's Health, Karolinska Institutet, Astrid Lindgren Children's Hospital, Stockholm, Sweden

[4]Department of Clinical Genetics, Institute of Biomedicine, University of Gothenburg, Sahlgrenska University Hospital, SE-413 45 Göteborg, Sweden

[5]Division of Immunology, Department of Medical Biology, Faculty of Health Science, University of Tromsø, 9037 Tromsø, Norway

Highest academic degrees obtained and e-mail addresses:

Bjørn Helge Haug	bhh022@uit.no
Jørn Remi Henriksen - MS	joern.remi.henriksen@uit.no
Jochen Buechner - MD	Jochen.Buchner@unn.no
Per Kogner - PhD, MD	Per.Kogner@ki.se

Tommy Martinsson - PhD, MD	tommy.martinsson@clingen.gu.se
Trond Flægstad - PhD, MD	trond.flaegstad@unn.no
Baldur Sveinbjørnsson - PhD	baldur.sveinbjornsson@uit.no
Christer Einvik – PhD	christer.einvik@uit.no

Corresponding author: Christer Einvik, postal address: Pediatric Research Group, Department of Clinical Biology, Faculty of Health Science, University of Tromsø, 9037 Tromsø, Norway - Telephone: +47 77 64 47 35, Fax: +47 77 64 53 50, E-mail: christer.einvik@uit.no.

Abstract

The *MYCN* oncogene is frequently amplified in neuroblastoma. It is one of the most consistent markers of a bad prognosis for this disease. Dickkopf-3 (DKK3) is a secreted protein of the Dickkopf family of Wnt regulators. It functions as a tumor suppressor in a range of cancers, including neuroblastoma. *MYCN* was recently found to downregulate *DKK3* mRNA. In this study, we show that *MYCN* knockdown in *MYCN*-amplified (MNA) neuroblastoma cell lines increases secretion of endogenous DKK3 to the culture media.

MiRNAs are ~20-nt-long RNAs encoded by the genome that downregulate mRNAs by targeting the 3`untranslated region (3'UTR). Many miRNAs regulate genes involved in the pathogenesis of cancer and are extensively deregulated in different tumors. Using miRNA target prediction software, we found several *MYCN*-regulated miRNAs that could target the 3'UTR sequence of *DKK3*, including *mir-92a*, *mir-92b* and *let-7e*. Luciferase expression from a reporter vector containing the *DKK3*-3`UTR was decreased when this construct was cotransfected with *mir-92a*, *mir-92b* and *let-7e* in HEK293 cells. Mutation of the *mir-92* seed sequence in the 3'UTR completely rescued the observed decrease in reporter expression when cotransfected with *mir-92a* and *mir-92b*. Antagomir and miRNA-mimic transfections in neuroblastoma cell lines confirmed that DKK3 secretion to the culture media is regulated by these miRNAs.

Consistent with reports from other cancers, we found DKK3 to be expressed in the endothelium of primary neuroblastoma samples and to be absent in tumors with *MYCN* amplification. These data demonstrate a previously unknown tumor promoting mechanism for *MYCN*-regulated miRNAs.

Keywords: *MYCN*, neuroblastoma, miRNA, *DKK3*

Introduction

Neuroblastoma accounts for 7% of childhood malignancies and 15% of pediatric cancer-related deaths. It is a heterogeneous disease, ranging from spontaneous regression to metastatic tumors resistant to multimodal treatment, as reviewed in (Maris *et al.*, 2007). The clinical outcome depends on several prognostic factors, with gene copy amplification of the *MYCN* oncogene being the most consistent marker of aggressive disease (Brodeur and Seeger, 1986). *MYCN* is a member of the MYC oncogene family, which also consists of *c-myc* and *MYCL* (Schwab, 2004; Schwab *et al.*, 1983), and functions by up and downregulating genes directly by transcriptional binding or through indirect pathways or mediators. It is known to regulate a wide range of microRNAs (Buechner *et al.*, 2010; Loven *et al.*, 2010; Mestdagh *et al.*, 2010; Schulte *et al.*, 2008) and is responsible for the methylation of target genes by activating methyltransferases, as well as affecting the chromatine structure (Liu *et al.*, 2007; Marshall *et al.*, 2010).

MicroRNAs (miRNAs) are small non-coding RNAs which participate in diverse biological processes including tumorigenesis by sequence-specific targeting of particular mRNAs, primarily in the 3' untranslated region (UTR) (Bartel, 2009; Kwak *et al.*, 2010). MiRNAs negatively regulate protein production by translational repression, mRNA destabilization or a combination of both (Filipowicz *et al.*, 2008). In mammals, miRNAs were recently shown to act predominantly through mRNA degradation (Guo *et al.*, 2010).

DKK3 is a member of the Dickkopf family of secreted Wnt antagonists, including DKK1-4 and Soggy, a member resembling DKK3. The functions of other members of this family have been well elucidated, although the role of DKK3 still remains unclear

(Barrantes Idel *et al.*, 2006; Niehrs, 2006). DKK3 is an N-glycosylated, secreted, tumor suppressor protein which inhibits proliferation, is of prognostic significance in neuroblastoma (Koppen *et al.*, 2008; Revet *et al.*, 2009) and functions as a tumor suppressor in a range of other tumors (Fong *et al.*, 2009; Hoang *et al.*, 2004; Hsieh *et al.*, 2004; Lee *et al.*, 2009; Maehata *et al.*, 2008; Mizobuchi *et al.*, 2008; Saeb-Parsy *et al.*, 2008; Veeck *et al.*, 2009; Yue *et al.*, 2008). The tumor suppressor mechanisms of DKK3 include inhibition of the canonical Wnt signaling by blocking β-catenin translocation to the nucleus (Caricasole *et al.*, 2003; Hoang *et al.*, 2004; Lee *et al.*, 2009; Yue *et al.*, 2008). However, DKK3 does not seem to affect Wnt/β-catenin signaling in neuroblastoma, thereby suggesting other mechanisms to suppress tumorigenicity in this tumor (Koppen *et al.*, 2008). This indicates that DKK3 has functions beyond mere canonical Wnt inhibition.

Previous reports have demonstrated that *MYCN* downregulates *DKK3* at the mRNA level in neuroblastoma by inducing *MYCN* expression in non-amplified cell lines (Bell *et al.*, 2007; Koppen *et al.*, 2008). The expression of *DKK3* mRNA in cell lines and tumor material was inversely correlated with *MYCN*, and variations in *DKK3* were solely attributed to changes in *MYCN* expression. No direct promoter binding was identified, which suggests an indirect regulatory mechanism (Koppen *et al.*, 2008). We therefore hypothesized that *MYCN* suppresses *DKK3* through miRNAs.

Results

MYCN Knockdown Increases Secretion of DKK3 Proteins in MYCN-amplified Neuroblastoma Cell Lines

The expression of *Dickkopf-3* (*DKK3*) mRNA has previously been shown to be inversely correlated with *MYCN* mRNA expression in neuroblastic tumors and neuroblastoma cell lines (Bell *et al.*, 2007; Koppen *et al.*, 2008).

Using a tetracycline-inducible retroviral *MYCN*-shRNA expression system, we observed that *MYCN* knockdown increased the expression of *DKK3* mRNA in the *MYCN*-amplified (MNA) neuroblastoma cell lines SK-N-BE(2) and Kelly (**Figure 1a**). Since DKK3 is a secreted glycoprotein, we further investigated DKK3 protein levels in culture supernatants from SK-N-BE(2) and Kelly cells upon induced *MYCN* knockdown. As shown in **Figures 1b and 1c,** increased levels of secreted DKK3 protein were detected. Similarly, SHEP Tet21N, a derivative of the *MYCN* single-copy SHEP neuroblastoma cell line containing a constitutively expressed doxycycline-repressible *MYCN* gene, revealed increased DKK3 secretion into the culture media when induced to suppress *MYCN* expression (**Figure 1d**).

These data clearly show an inverse correlation between *MYCN* expression and secretion of DKK3 proteins in neuroblastoma cell lines.

Methylation Status of the DKK3 Promoter in Neuroblastoma

Inactivation of *DKK3* expression by promoter methylation has been shown in several cancers (Ding *et al.*, 2009; Lee *et al.*, 2009; Veeck *et al.*, 2008). Because of this, we analyzed the methylation status of the *DKK3* promoter in ten primary neuroblastoma (five MNA, five non-MNA) samples and five neuroblastoma cell lines (three MNA, two non-MNA) using methylation-specific PCR (MSP). The breast cancer cell lines MDA-MB231 and HS578T were used as methylated and non-methylated *DKK3*

promoter controls, respectively (Veeck *et al.*, 2008). As shown in **Figure 2**, all neuroblastoma tumor samples and cell lines, irrespective of their *MYCN* status, showed specific amplification of the 150 bp band generated by the non-methylated primers.

These data demonstrate that the expression of *DKK3* is not regulated by promoter methylation in neuroblastoma.

MYCN-regulated miRNAs are Potential Regulators of DKK3 Expression

In order to investigate whether *MYCN* regulates *DKK3* expression indirectly through miRNAs, we used three independent miRNA target prediction programs (TargetScan v5.1, Diana-microT 3.0 and MicroCosm) to identify miRNAs that could target the 3'UTR of *DKK3* transcripts. The analyses revealed that *mir-92a*, *mir-92b* and *mir-32* were predicted to target the *DKK3*-3'UTR at position 25-31 (site-1) by all three programs used. In addition, *let-7* and *mir-98* were predicted to target a seed sequence at position 550-556 (site-2) by Targetscan 5.1 and Diana-microT 3.0, while *mir-363* was predicted to target site-1 by Targetscan 5.1 and MicroCosm (**Supplementary Figure 1a)**. We have recently shown that *mir-92a*, *mir-92b* and *let-7* expression levels in MNA neuroblastoma cell lines are regulated by *MYCN* (Buechner *et al.*, 2010).

Mir-92a, mir-92b and let-7e Target the 3'UTR Sequence of DKK3

Several reports have shown a correlation between *MYCN* and *mir-92a* expression in neuroblastoma. *Mir-92a* is a member of the oncogenic *mir*-17-92 cluster that has been

documented to be transcriptionally activated by *MYCN* (Fontana *et al.*, 2008; Loven *et al.*, 2010; Schulte *et al.*, 2008). We recently reported that both *mir-92a* and *mir-92b* are downregulated when *MYCN* expression is repressed by anti-*MYCN* shRNAs in MNA neuroblastoma cell lines (Buchner *et al.*, 2010). Since *mir-92a* and *mir-92b* are both inversely correlated with *MYCN* expression and predicted to target *DKK3*, we decided to investigate these miRNA:*DKK3*-3'UTR interactions experimentally. In addition, we also investigated the binding of *let-7e* to the target sequence at site-2 of the *DKK3*-3'UTR.

The full-length 3'UTR sequence of *DKK3* was cloned downstream of the *Firefly* luciferase gene in the pMIR-REPORT vector (pMIR-DKK3). HEK-293 cells were cotransfected with pMIR-DKK3 and microRNA mimics of *mir-92a, mir-92b, let-7e* or a negative control miRNA (mir-NC). Luciferase assays revealed that an overexpression of *mir-92a, mir-92b* and *let-7e* significantly reduced luciferase activity from the reporter vector when compared to the negative control miRNA (**Figure 3**). We observed a 38%, 45% and 30% decrease in luciferase activity with *mir-92a, mir-92b* and *let-7*e, respectively. These results indicate efficient repression of the luciferase *DKK3*-3'UTR reporter since large-scale proteomics studies have revealed that most miRNA:mRNA interactions result in the silencing of 30% or less (Baek *et al.*, 2008).

To test whether *mir-92a, mir-92b* and *let-7e* downregulated the luciferase activity of pMIR-DKK3 through binding to the predicted target sites, we mutated the putative seed sequences at site-1 and site-2. When the site-1 mutated version of pMIR-DKK3 (mut mir-92 seed) was coexpressed with *mir-92a* or *mir-92b*, the luciferase activity was rescued to levels similar to those observed for the negative control miRNA

(**Figures 3a and 3b**). Only a slight rescue of luciferase activity was observed when the site-2 mutated reporter vector (mut let-7 seed1) was cotransfected with *let-7e* (**Figure 3c**). In searching for alternative *let-7e* seed sequences in the *DKK3*-3'UTR sequence, the RNA22 miRNA software detected a new candidate seed sequence at position 180-185 (site-3) (Miranda *et al.*, 2006) (**Supplementary Figures 1b and 1c**). The mutated version of site-3 alone (mut let-7 seed2), or in combination with the mutated site-2 (mut let-7 seed1+2), did not result in the major rescue of luciferase activity (**Figure 3c**).

Since *mir-92a* is coexpressed with the other members of the mir-17-92 cluster, we also examined the effect of these miRNAs on the 3'UTR sequence of *DKK3*. Cotransfection of pMIR-DKK3 and the individual mir-17-92 miRNA mimics resulted in a slight decrease in luciferase activity by *mir-19a* and *-19b*, which was predicted to target *DKK3* by Targetscan. Cotransfections with *mir-17* or *mir-20a* had no effect when compared to the negative control. We unexpectedly observed an increase in luciferase activity when the reporter vector was cotransfected with *mir-18a* (**Supplementary Figure 2**).

DKK3 Secretion is Regulated by mir-92a, mir-92b and let-7e in Neuroblastoma Cell Lines

To investigate how changes in the expression of *MYCN*-regulated miRNAs influence secretion of DKK3 in neuroblastoma cell lines, we transfected the MNA neuroblastoma cell lines SK-N-BE(2) and Kelly with antimir-92a and -92b (antagomirs) to reduce the endogenous expression of these miRNAs. A stem-loop qRT-PCR assay revealed an approximate 50% decrease in *mir-92b* expression

compared to a negative control antagomir (antimir-NC) (**Supplementary Figure 3a**). After 72 h of antagomir treatment, secretion of DKK3 into the culture media was measured. As shown in **Figure 4a**, suppression of both *mir-92a* and *mir-92b* resulted in a 2-2.5 fold increase in DKK3 secretion.

Next, we transfected the non-MNA neuroblastoma cell lines SH-SY-5Y and SK-N-AS with the *mir-92a*, *mir-92b* and *let-7e* miRNA mimics. Transfection of SH-SY-5Y with the *mir-92b* mimic increased the cellular *mir-92b* levels approximately 100 fold (**Supplementary Figure 3b**). The overexpression of *mir-92a* and *mir-92b* resulted in a major reduction of secreted DKK3 proteins from SH-SY-5Y and SK-N-AS cells, while *let-7e* overexpression revealed a minor, but significant decrease (**Figure 4b**). Consistent with these results, *DKK3* mRNA levels were reduced when SH-SY-5Y cells were transfected with miRNA mimics of *mir-92a*, *mir-92b* and *let-7e* (**Supplementary Figure 4**).

In summary, these data show that the *MYCN*-regulated miRNAs *mir-92a*, *mir-92b* and *let-7e* reduce secretion of DKK3 proteins from human neuroblastoma cell lines.

DKK3 is Expressed in Neuroblastoma Vasculature

We investigated 25 primary neuroblastoma tissue samples from various biological subsets and clinical stages for the expression of DKK3 (**Supplementary Table 2)**. Twenty of 26 samples revealed specific DKK3 staining of the endothelial cells of the tumor, though no staining was seen in the tumor cells themselves (**Figure 5a**). Co-staining with CD31 (an endothelial marker) demonstrated a co-localization to the endothelium. The immunopositivity for DKK3 in the endotehelial cells was of a

different intensity between different tumors. The unfavorable MNA tumors demonstrated a very low or absent staining (**Supplementary Table 2**). Four ganglioneuromas were investigated and all were immunopositive for DKK3 in the tumor-derived ganglion cells, but not in the surrounding stroma (**Figure 5b, Supplementary Table 2**).

Discussion

MYCN-regulated miRNAs Decrease DKK3 Secretion from Neuroblastoma Cell Lines

DKK3 is an established tumor suppressor gene that inhibits the proliferation of several cancers, including neuroblastoma (Abarzua *et al.*, 2005; Chen *et al.*, 2009; Koppen *et al.*, 2008; Kurose *et al.*, 2004; Mizobuchi *et al.*, 2008; Sakaguchi *et al.*, 2009). It has previously been shown that *DKK3* mRNA levels are inversely correlated to *MYCN* mRNA expression in neuroblastic tumors and neuroblastoma cell lines (Bell *et al.*, 2007; Koppen *et al.*, 2008). In our study, we used an inducible retrovirally delivered anti-*MYCN* shRNA to downregulate *MYCN* expression in two MNA neuroblastoma cell lines, and observed increased secretion of the endogenous DKK3 protein into the cell culture media. We also documented that the *MYCN*-regulated microRNAs, *miR-92a*, *mir-92b* and *let-7e*, efficiently decreased expression of a luciferase reporter containing the 3'UTR sequence from *DKK3*. The predicted target seed sequence for *mir-92a* and *mir-92b* in the *DKK3*-3'UTR sequence was validated by mutagenesis. Two candidate seed sequences were found for *let-7e*. Mutation of the putative let-7e seed sequences, whether alone or in combination, could not rescue the *let-7e* repression of luciferase reporter expression similar to that observed for the *mir-92*

seed sequence. This indicates that other as yet unidentified *let-7e* seed sequences and/or *let-7e* targets are responsible for the majority of the observed *DKK3* repression by *let-7e*. By the use of miRNA mimics and antagomirs treatment, we further demonstrated that both *DKK3* mRNA expression and protein secretion into the media were inversely correlated to *mir-92a*, *mir-92b* and *let-7e* expression in neuroblastoma.

Mir-92a is a member of the oncogenic mir-17-92 cluster, which consists of six coexpressed miRNAs: *mir-17*, *mir-18a*, *mir-19a, mir-19b*, *mir-20 and mir92a* (Mendell, 2008). Members of this cluster have been shown to be aberrantly expressed and to promote tumorigenicity in neuroblastoma (Beveridge *et al.*, 2009; Fontana *et al.*, 2008), as well as in other types of cancer (Diosdado *et al.*, 2009; Hayashita *et al.*, 2005). Several reports have documented a correlation between the expression of *MYCN* and the mir-17-92 cluster (Fontana *et al.*, 2008; Loven *et al.*, 2010; Schulte *et al.*, 2008). With the exception of *mir-92a,* and to some extent *mir-19a* and *-19b*, none of the other mir-17-92 members reduced expression of the *DKK3* 3'UTR luciferase reporter. On the contrary, we observed an unexpected increase in luciferase activity when *mir-18a* was overexpressed. A similar observation has previously been reported and was proposed to be due to interference between *mir-18a* and regulation of the CMV promoter (Vreugdenhil *et al.*, 2009).

The DKK3 Promoter is Not Inactivated by Hypermethylation in Neuroblastoma

Hypermethylation of CpG islands in the promoter regions of genes is a powerful mechanism for transcriptional repression (reviewed in Illingworth and Bird, 2009). Nonetheless, the differential methylation of promoters is not a general mechanism for regulating gene expression since most inactive promoters remain unmethylated

(Weber *et al.*, 2007). *DKK3* is frequently inactivated by promoter methylation in cancers of the gastrointestinal tract, lung, cervix and breast (Ding *et al.*, 2009; Kobayashi *et al.*, 2002; Lee *et al.*, 2009; Maehata *et al.*, 2008; Sato *et al.*, 2007; Veeck *et al.*, 2009; Yue *et al.*, 2008). For the neuroblastic tumors arising from the sympathetic adrenal lineage of the neural crest, increased *DKK3* mRNA levels have been reported as a strong marker of differentiation. The well-differentiated ganglioneuromas showed a high *DKK3* mRNA expression, while the undifferentiated neuroblastomas showed a low *DKK3* expression, which also correlated with a bad prognosis (Koppen *et al.*, 2008)

The c-myc protein has previously been shown to repress gene expression through promoter hypermethylation by interaction with Miz-1 and Dnmt3a (Brenner *et al.*, 2005). Furthermore, global *MYCN* transcription factor binding analysis in neuroblastoma has revealed an association of the MYCN protein to regions of DNA hypermethylation (Murphy *et al.*, 2009).

We analyzed the methylation status of the *DKK3* promoter in 10 neuroblastoma primary tumors and five neuroblastoma cell lines using methylation-specific PCR (MSP). The results revealed that neither the primary tumors nor the cell lines were hypermethylated at the investigated CpG island of the *DKK3* promoter. In addition, a chromatin immunoprecipitation (ChIP) analysis performed by others failed to reveal a direct interaction between the MYCN protein and regulatory elements in the *DKK3* promoter (Koppen *et al.*, 2008). Low levels of DKK3 have also previously been reported in the absence of promoter methylation in malignant melanoma cell lines (Kuphal *et al.*, 2006).

These findings indicate that DKK3 levels in neuroblastoma are regulated by mechanisms other than promoter hypermethylation. Specifically, we have documented that *mir-92a*, *mir-92b* and *let-7e* target the 3'UTR sequence of *DKK3* to repress its expression.

DKK3 Expression in Tumor Endothelium is Inversely Correlated with *MYCN* Levels

Recently, several papers have shown *DKK3* to be involved in tumor vessel biology and to be highly expressed in tumor endothelium (Fong *et al.*, 2009; Muhlmann *et al.*, 2010; Pei *et al.*, 2009; Untergasser *et al.*, 2008; You *et al.*, 2010; Zenzmaier *et al.*, 2008). Consistent with these findings, we demonstrate an increased expression of DKK3 in neuroblastoma vasculature. It has been suggested that this vascular expression of DKK3 antagonizes the inactivation that frequently takes place in tumor cells during malignant transformation (Zenzmaier *et al.*, 2008). DKK3 has also been reported to stimulate vascular growth and increase vascular density in tumors (Untergasser *et al.*, 2008). The underlying mechanisms are not known, but bioinformatic analyses have indicated that DKK3 contains a cysteine-rich prokineticine domain also present in the potent angiogenic endocrine gland-derived vascular endothelial growth factor (EG-VEGF).

We observed that the expression of the DKK3 protein in neuroblastoma vasculature was significantly higher in non-MNA tumors and more benign ganglioneuroma in comparison to MNA tumors. This is in line with a previous report by Valentijn and co-workers, who demonstrated higher levels of *DKK3* mRNA expression in both non-MNA neuroblastoma tumors and ganglioneuromas (Koppen *et al.*, 2008).

The mir-17-92 cluster has been related to angiogenesis (Dews *et al.*, 2006; Doebele *et al.*). A recent work demonstrated that the *in vivo* inhibition of *mir-92a* enhanced blood vessel formation (Bonauer *et al.*, 2009). Here, we provide one possible explanation for this observation since DKK3 has been shown to stimulate angiogenesis (Untergasser *et al.*, 2008).

An increased serum level of *mir-92a* has also been reported to be of diagnostic value in colorectal cancer (Huang *et al.*, 2009), although *mir-92a* has been shown to be downregulated in the serum of patients with acute lymphatic leukemia (Tanaka *et al.*, 2009). The *mir-92a* homologue, *mir-92b*, is a marker for primary brain tumors and regulates cell cycle control (Nass *et al.*, 2009; Sengupta *et al.*, 2009). DKK3 is present in high levels in the adult brain and central nervous system (Krupnik *et al.*, 1999), thereby making it plausible that the link between *mir-92b* and *DKK3* may play a contributing role in these cancers and deserves further investigation. *Mir-92b* is also a negative regulator of PRMT5, which is an epigenetic regulator of several tumor suppressors in vivo (Pal *et al.*, 2007).

In some cellular settings, DKK3 has been shown to stimulate growth and inhibit apoptosis. Additionally, DKK3 could also stimulate or inhibit the canonical wnt pathway, depending on the cellular context (Nakamura and Hackam, 2010; Nakamura *et al.*, 2007). These contradictory findings illustrate the complex and cell specific nature of DKK3, so it therefore not surprising to find that *DKK3* is regulated by miRNAs with postulated oncogenic as well as tumor suppressor functions.

Material and Methods

Cell Cultures and miRNA Overexpression

The human SH-SY-5Y neuroblastoma cell line was cultivated in a DMEM/Ham'sF12 medium (1:1) supplemented with 10% fetal bovine serum (FBS), 2 mM L-glutamine and 1% NEAA (non-essential amino acid). The HEK-293 cell line was grown in DMEM supplemented with 10% FBS. The SK-N-AS, SK-N-BE(2), Kelly and SHEP Tet21N cell lines were grown in RPMI-1640 medium supplemented with 10% FBS. SHEP Tet21N cells express high *MYCN* in the absence of doxycycline (Lutz *et al.*, 1996). To switch off *MYCN* expression, 1 µg/ml doxycycline was added to the growth media at least 24 hours prior to the experiments. All cells were split before confluence and incubated at 37˚C in 5% humidity and 4.5% CO_2.

MicroRNA mimics (*let-7e*, *mir-92a*, *-92b*, *-17*, *-18a*, *-19a*, *-19b* and *-20*a) and antagomirs (antimir-92a and -92b), with corresponding negative controls, were from Shanghai GenePharma, (Shanghai, China). Transfections of miRNA mimics and antagomirs were carried out using Lipofectamine-2000 (Invitrogen, Carlsbad, CA) according to the manufacturer's instructions.

MYCN Knockdown

SK-N-BE(2) and Kelly cells stably transfected with pcDNA6/TR (constitutively expressing the Tetracycline Repressor) were transduced with a retrovirus (RV-aMN1658) containing a tetracycline-inducible anti-*MYCN* shRNA (aMN1658) expression module (Henriksen *et al.*, 2010). Retroviruses containing an inducible scrambled shRNA (SCR) were used as a negative control, and cells were cultivated as previously described (Henriksen *et al.*, 2007). Expression of the shRNAs was induced by adding 1 µg/ml doxocycline to the culture medium.

Human Tissue Samples

Tissue samples from tumors were obtained from neuroblastoma patients during surgery, snap-frozen in liquid nitrogen and transferred to storage at -80°C for future analysis. Twenty-six neuroblastoma samples derived from children of different ages and all clinical stages, including different biological subsets, were analyzed (**Supplementary Table 2**). Five childhood ganglioneuromas from children aged 12-25 months were also included. Genomic DNA was extracted from frozen (-70°C) tumor tissue according to standard procedures, and ethical approval was obtained by the Karolinska University Hospital Research Ethics Committee (approval 03-308).

Methylation-specific PCR (MSP)

DNA (100 ng) from neuroblastoma tumors or cell lines was bisulfite-treated using the EZ methylation gold kit (Zymo Research, CA, USA), and further purified using the DNA Clean and Concentrate Kit (Zymo). Previously published primers, specific to the methylated (ON-479/ON-480) and unmethylated sequence (ON-481/ON-482), were used to perform a methylation-specific PCR (MSP) on the promoter region of *DKK3* (Sato *et al.*, 2007). The primer sequences are listed in **Supplementary Table 1.** The Zymotaq premix polymerase (Zymo) was used in a 25 µl reaction, including 50 ng of treated template. Products were visualized on ethidium bromide-stained 3% agarose gels. We included DNA from the MDA-MB231 and HS578t as methylated and unmethylated controls, respectively (Veeck *et al.*, 2008).

In Silico Target Prediction

Diana microT v3.0 (www.microrna.gr/microT), EMBLs MicroCosm Targets v5 (www.ebi.ac.uk/enright-srv/microcosm/htdocs/targets/v5/) and TargetScan v5.1 (www.targetscan.org/) target prediction software were used to identify miRNAs that could potentially target the human *DKK3* 3'UTR.

Luciferase Reporter Assay

The *DKK3*-3`UTR region was amplified from human total DNA (neuroblastoma LAN5 cell line) using primers ON-361 and ON-327 that contain in-fusion recombinase overhangs. The insert was cloned into the pMIR-REPORT vector (Ambion, Austin, TX, USA) using the In-Fusion Cloning Kit (Clontech, CA, USA) to generate pMIR-DKK3(wt). Mutations were introduced in the miRNA seed sequences at positions 25-31 (site-1), 550-556 (site-2) and 180-185 (site-3) using the Site-Directed Mutagenesis Kit (Stratagene) with ON-447, ON-505 and ON-507 as primers to generate pMIR-DKK3(mut mir-92 seed), pMIR-DKK3(mut let-7 seed1) and pMIR-DKK3(mut let-7 seed2), respectively. A double mutant, pMIR-DKK3 (mut let-7 seed1 + seed2), was also generated using ON-505 and ON-507 as primers. All vectors were verified by DNA sequencing using ON-005 and ON-363. The primer sequences are listed in **Supplementary Table 1.**

Hek-293 cells grown in 12 well plates were Lipofectamin-2000-transfected with 25 pmoles synthetic miRNA or negative control, 0.05 µg pGL-renilla vector (Promega, WI, USA) and 0.1 µg luciferase-UTR reporter vector (pMIR-DKK3(wt) and mutated versions). Luciferase was measured two days after transfection using the dual

luciferase reporter kit according to the manufacturer's instructions (Promega). Firefly luciferase was normalized against renilla luciferase. All experiments were done in two parallels and at least three times.

Quantitative Polymerase Chain Reaction (qPCR)

SHSY5Y cells were seeded in 6-well plates and transfected with 100 pmoles of synthetic miRNAs. Cells were harvested 48 hours after transfection before total RNA was extracted and DNase-treated using the miRNeasy mini kit (Quiagen Inc., Valencia, CA, USA).

cDNA was created using the miScript reverse transcriptase kit (Qiagen) and 1 ug RNA. Quantitative PCR was performed using the *Power* SYBR Green PCR Master Mix (Applied Biosystems Inc., Carlsbad, CA, USA). *DKK3* mRNA levels were quantified using HPRT1 and UBC as housekeeping genes. 2.5 µl of a 20x diluted RT mix was loaded in a 25 µl reaction. The primer sequences are listed in **Supplementary Table 1.**

Quantification of *mir-92b* was performed on the same cDNA using a miScript SYBR GREEN detection kit with *mir-92b* primer assay (Quiagen). HPRT1 and UBC were used for normalization.

The ABI 7300 (Applied Biosystems) was used as a detection system.

DKK3 Enzyme Linked Immunosorbent Assay (ELISA)

SHSY5Y and SKNAS cells were seeded in 6-well plates, and transfected in three parallels with 100 pmol of synthetic miRNAs or a negative control miRNA. The cell

medium was changed 48 hours after transfection, and the cells were then incubated for another 24 hours before the conditioned medium was harvested for analysis using a DKK3 duoset Elisa assay (R&D Systems, Cambridge, UK). A high standard of 2000 pmoles/ml was chosen and diluted to a low standard of 15 pmoles/ml.

The transfection of antagomirs and the measuring of the DKK3 levels secreted by the SK-N-BE(2) and Kelly cell line were performed in the same manner as the overexpression of synthetic miRNAs (Shanghai GenePharma, China). The cell medium was changed 24 hours after transfection, while the harvesting of total cell protein and culture medium for ELISA was done after another 24 hours.

The human neuroblastoma cell lines Kelly and SK-N-BE(2), containing RV-aMN1658 and RV-SCR constructs, were incubated in the presence of 1 µg/ml doxycycline for six days before analyzing the DKK3 content in the medium (Henriksen *et al.*, 2007). The medium was changed 24 hours before analysis.

Levels of secreted DKK3 were normalized against total protein, measured at the time of harvesting, using the Biorad protein assay (Biorad Laboratories, Hercules, CA, USA).

Immunohistochemistry

Formalin-fixed and paraffin-embedded tissue sections were deparaffinized in xylene and graded alcohols, hydrated and washed in PBS. After antigen retrieval on sodium citrate buffer (pH 6) in a microwave oven, the endogenous peroxidase was blocked by 0.3% H2O2 for 15 min. Sections were incubated overnight at 4°C with a biotinylated goat anti-human DKK3 antibody (R&D Systems). Thereafter, sections were incubated with streptavidin-HRP (Invitrogen) for 30 min at room temperature. A matched

isotype control was used as a control for nonspecific background staining. For co-localization studies of DKK3 and CD31, tumor tissue sections were simultaneously stained with biotinylated anti-human DKK3 and mouse-anti-human CD31 (Dako, Glostrup, Denmark). For fluorescence visualization, streptavidin-Alexa Fluor 594 and anti-mouse Alexa Fluor 488 were used, respectively.

Statistical Analysis

All tests were performed two-sided. Differences between the two groups were studied using the two-sided Student`s *t* test. When more than two treatments were compared, we performed the one-way analysis of variance (ANOVA).

Conflict of Interest:

The authors declare no conflict of interests.

Acknowledgments:

The authors wish to thank Ellen Tømte for her technical contributions to this manuscript. This work was supported by grants from the Northern-Norwegian Health Authorities (gene therapy program) and the Norwegian Cancer Society (Ragnvarda F. Sørvik and Håkon Starheims Foundation and PR-2007-0052).

Supplementary information is available at the Oncogenes website.

References:

Abarzua F, Sakaguchi M, Takaishi M, Nasu Y, Kurose K, Ebara S *et al* (2005). Adenovirus-mediated overexpression of REIC/Dkk-3 selectively induces apoptosis in human prostate cancer cells through activation of c-Jun-NH2-kinase. *Cancer Res* **65:** 9617-22.

Baek D, Villen J, Shin C, Camargo FD, Gygi SP, Bartel DP (2008). The impact of microRNAs on protein output. *Nature* **455:** 64-71.

Barrantes Idel B, Montero-Pedrazuela A, Guadano-Ferraz A, Obregon MJ, Martinez de Mena R, Gailus-Durner V *et al* (2006). Generation and characterization of dickkopf3 mutant mice. *Mol Cell Biol* **26:** 2317-26.

Bartel DP (2009). MicroRNAs: target recognition and regulatory functions. *Cell* **136:** 215-33.

Bell E, Lunec J, Tweddle DA (2007). Cell cycle regulation targets of MYCN identified by gene expression microarrays. *Cell Cycle* **6:** 1249-56.

Beveridge NJ, Tooney PA, Carroll AP, Tran N, Cairns MJ (2009). Down-regulation of miR-17 family expression in response to retinoic acid induced neuronal differentiation. *Cell Signal*.

Bonauer A, Carmona G, Iwasaki M, Mione M, Koyanagi M, Fischer A *et al* (2009). MicroRNA-92a controls angiogenesis and functional recovery of ischemic tissues in mice. *Science* **324:** 1710-3.

Brenner C, Deplus R, Didelot C, Loriot A, Vire E, De Smet C *et al* (2005). Myc represses transcription through recruitment of DNA methyltransferase corepressor. *EMBO J* **24:** 336-46.

Brodeur GM, Seeger RC (1986). Gene amplification in human neuroblastomas: basic mechanisms and clinical implications. *Cancer Genet Cytogenet* **19:** 101-11.

Buchner J, Henriksen JR, Haug BH, Tømte E, Flægstad T, Einvik C (2010). Inhibition of mir-21, which is up-regulated during MYCN knockdown-mediated differentiation,
does not prevent differentiation of neuroblastoma cells. *Differentiation,* In press.

Caricasole A, Ferraro T, Iacovelli L, Barletta E, Caruso A, Melchiorri D *et al* (2003). Functional characterization of WNT7A signaling in PC12 cells: interaction with A FZD5 x LRP6 receptor complex and modulation by Dickkopf proteins. *J Biol Chem* **278:** 37024-31.

Chen J, Watanabe M, Huang P, Sakaguchi M, Ochiai K, Nasu Y *et al* (2009). REIC/Dkk-3 stable transfection reduces the malignant phenotype of mouse prostate cancer RM9 cells. *Int J Mol Med* **24:** 789-94.

Dews M, Homayouni A, Yu D, Murphy D, Sevignani C, Wentzel E *et al* (2006). Augmentation of tumor angiogenesis by a Myc-activated microRNA cluster. *Nat Genet* **38:** 1060-5.

Ding Z, Qian YB, Zhu LX, Xiong QR (2009). Promoter methylation and mRNA expression of DKK-3 and WIF-1 in hepatocellular carcinoma. *World J Gastroenterol* **15:** 2595-601.

Diosdado B, van de Wiel MA, Terhaar Sive Droste JS, Mongera S, Postma C, Meijerink WJ *et al* (2009). MiR-17-92 cluster is associated with 13q gain and c-myc expression during colorectal adenoma to adenocarcinoma progression. *Br J Cancer* **101:** 707-14.

Doebele C, Bonauer A, Fischer A, Scholz A, Reiss Y, Urbich C *et al* Members of the microRNA-17-92 cluster exhibit a cell intrinsic anti-angiogenic function in endothelial cells. *Blood*.

Filipowicz W, Bhattacharyya SN, Sonenberg N (2008). Mechanisms of post-transcriptional regulation by microRNAs: are the answers in sight? *Nat Rev Genet* **9:** 102-14.

Fong D, Hermann M, Untergasser G, Pirkebner D, Draxl A, Heitz M *et al* (2009). Dkk-3 expression in the tumor endothelium: a novel prognostic marker of pancreatic adenocarcinomas. *Cancer Sci* **100:** 1414-20.

Fontana L, Fiori ME, Albini S, Cifaldi L, Giovinazzi S, Forloni M *et al* (2008). Antagomir-17-5p abolishes the growth of therapy-resistant neuroblastoma through p21 and BIM. *PLoS One* **3:** e2236.

Guo H, Ingolia NT, Weissman JS, Bartel DP (2010). Mammalian microRNAs predominantly act to decrease target mRNA levels. *Nature* **466:** 835-40.

Hayashita Y, Osada H, Tatematsu Y, Yamada H, Yanagisawa K, Tomida S *et al* (2005). A polycistronic microRNA cluster, miR-17-92, is overexpressed in human lung cancers and enhances cell proliferation. *Cancer Res* **65:** 9628-32.

Henriksen JR, Haug BH, Buechner J, Løkke C, Flaegstad T, Einvik C (2010). Conditional expression of retrovirally delivered anti-MYCN shRNA as an in vitro model system to study neuronal differentiation in MYCN-amplified neuroblastoma. *BMC DEVELOPMENTAL BIOLOGY,* In press.

Henriksen JR, Lokke C, Hammero M, Geerts D, Versteeg R, Flaegstad T *et al* (2007). Comparison of RNAi efficiency mediated by tetracycline-responsive H1 and U6 promoter variants in mammalian cell lines. *Nucleic Acids Res* **35:** e67.

Hoang BH, Kubo T, Healey JH, Yang R, Nathan SS, Kolb EA *et al* (2004). Dickkopf 3 inhibits invasion and motility of Saos-2 osteosarcoma cells by modulating the Wnt-beta-catenin pathway. *Cancer Res* **64:** 2734-9.

Hsieh SY, Hsieh PS, Chiu CT, Chen WY (2004). Dickkopf-3/REIC functions as a suppressor gene of tumor growth. *Oncogene* **23:** 9183-9.

Huang Z, Huang D, Ni S, Peng Z, Sheng W, Du X (2009). Plasma microRNAs are promising novel biomarkers for early detection of colorectal cancer. *Int J Cancer*.

Illingworth RS, Bird AP (2009). CpG islands--'a rough guide'. *FEBS Lett* **583:** 1713-20.

Kobayashi K, Ouchida M, Tsuji T, Hanafusa H, Miyazaki M, Namba M *et al* (2002). Reduced expression of the REIC/Dkk-3 gene by promoter-hypermethylation in human tumor cells. *Gene* **282:** 151-8.

Koppen A, Ait-Aissa R, Koster J, Ora I, Bras J, van Sluis PG *et al* (2008). Dickkopf-3 expression is a marker for neuroblastic tumor maturation and is down-regulated by MYCN. *Int J Cancer* **122:** 1455-64.

Krupnik VE, Sharp JD, Jiang C, Robison K, Chickering TW, Amaravadi L *et al* (1999). Functional and structural diversity of the human Dickkopf gene family. *Gene* **238:** 301-13.

Kuphal S, Lodermeyer S, Bataille F, Schuierer M, Hoang BH, Bosserhoff AK (2006). Expression of Dickkopf genes is strongly reduced in malignant melanoma. *Oncogene* **25:** 5027-36.

Kurose K, Sakaguchi M, Nasu Y, Ebara S, Kaku H, Kariyama R *et al* (2004). Decreased expression of REIC/Dkk-3 in human renal clear cell carcinoma. *J Urol* **171:** 1314-8.

Kwak PB, Iwasaki S, Tomari Y (2010). Review Article: The microRNA pathway and cancer. *Cancer Sci*.

Lee EJ, Jo M, Rho SB, Park K, Yoo YN, Park J *et al* (2009). Dkk3, downregulated in cervical cancer, functions as a negative regulator of beta-catenin. *Int J Cancer* **124:** 287-97.

Liu T, Tee AE, Porro A, Smith SA, Dwarte T, Liu PY *et al* (2007). Activation of tissue transglutaminase transcription by histone deacetylase inhibition as a therapeutic approach for Myc oncogenesis. *Proc Natl Acad Sci U S A* **104:** 18682-7.

Loven J, Zinin N, Wahlstrom T, Muller I, Brodin P, Fredlund E *et al* (2010). MYCN-regulated microRNAs repress estrogen receptor-alpha (ESR1) expression and neuronal differentiation in human neuroblastoma. *Proc Natl Acad Sci U S A* **107:** 1553-8.

Lutz W, Stohr M, Schurmann J, Wenzel A, Lohr A, Schwab M (1996). Conditional expression of N-myc in human neuroblastoma cells increases expression of

alpha-prothymosin and ornithine decarboxylase and accelerates progression into S-phase early after mitogenic stimulation of quiescent cells. *Oncogene* **13:** 803-12.

Maehata T, Taniguchi H, Yamamoto H, Nosho K, Adachi Y, Miyamoto N *et al* (2008). Transcriptional silencing of Dickkopf gene family by CpG island hypermethylation in human gastrointestinal cancer. *World J Gastroenterol* **14:** 2702-14.

Maris JM, Hogarty MD, Bagatell R, Cohn SL (2007). Neuroblastoma. *Lancet* **369:** 2106-20.

Marshall GM, Gherardi S, Xu N, Neiron Z, Trahair T, Scarlett CJ *et al* (2010). Transcriptional upregulation of histone deacetylase 2 promotes Myc-induced oncogenic effects. *Oncogene*.

Mendell JT (2008). miRiad roles for the miR-17-92 cluster in development and disease. *Cell* **133:** 217-22.

Mestdagh P, Fredlund E, Pattyn F, Schulte JH, Muth D, Vermeulen J *et al* (2010). MYCN/c-MYC-induced microRNAs repress coding gene networks associated with poor outcome in MYCN/c-MYC-activated tumors. *Oncogene* **29:** 1394-404.

Miranda KC, Huynh T, Tay Y, Ang YS, Tam WL, Thomson AM *et al* (2006). A pattern-based method for the identification of MicroRNA binding sites and their corresponding heteroduplexes. *Cell* **126:** 1203-17.

Mizobuchi Y, Matsuzaki K, Kuwayama K, Kitazato K, Mure H, Kageji T *et al* (2008). REIC/Dkk-3 induces cell death in human malignant glioma. *Neuro Oncol* **10:** 244-53.

Muhlmann G, Untergasser G, Zitt M, Maier H, Mikuz G, Kronberger IE *et al* (2010). Immunohistochemically detectable dickkopf-3 expression in tumor vessels predicts survival in gastric cancer. *Virchows Arch* **456:** 635-46.

Murphy DM, Buckley PG, Bryan K, Das S, Alcock L, Foley NH *et al* (2009). Global MYCN transcription factor binding analysis in neuroblastoma reveals association with distinct E-box motifs and regions of DNA hypermethylation. *PLoS One* **4:** e8154.

Nakamura RE, Hackam AS (2010). Analysis of Dickkopf3 interactions with Wnt signaling receptors. *Growth Factors*.

Nakamura RE, Hunter DD, Yi H, Brunken WJ, Hackam AS (2007). Identification of two novel activities of the Wnt signaling regulator Dickkopf 3 and characterization of its expression in the mouse retina. *BMC Cell Biol* **8:** 52.

Nass D, Rosenwald S, Meiri E, Gilad S, Tabibian-Keissar H, Schlosberg A *et al* (2009). MiR-92b and miR-9/9* are specifically expressed in brain primary

tumors and can be used to differentiate primary from metastatic brain tumors. *Brain Pathol* **19:** 375-83.

Niehrs C (2006). Function and biological roles of the Dickkopf family of Wnt modulators. *Oncogene* **25:** 7469-81.

Pal S, Baiocchi RA, Byrd JC, Grever MR, Jacob ST, Sif S (2007). Low levels of miR-92b/96 induce PRMT5 translation and H3R8/H4R3 methylation in mantle cell lymphoma. *EMBO J* **26:** 3558-69.

Pei Y, Kano J, Iijima T, Morishita Y, Inadome Y, Noguchi M (2009). Overexpression of Dickkopf 3 in hepatoblastomas and hepatocellular carcinomas. *Virchows Arch* **454:** 639-46.

Revet I, Huizenga G, Koster J, Volckmann R, van Sluis P, Versteeg R *et al* (2009). MSX1 induces the Wnt pathway antagonist genes DKK1, DKK2, DKK3, and SFRP1 in neuroblastoma cells, but does not block Wnt3 and Wnt5A signalling to DVL3. *Cancer Lett*.

Saeb-Parsy K, Veerakumarasivam A, Wallard MJ, Thorne N, Kawano Y, Murphy G *et al* (2008). MT1-MMP regulates urothelial cell invasion via transcriptional regulation of Dickkopf-3. *Br J Cancer* **99:** 663-9.

Sakaguchi M, Kataoka K, Abarzua F, Tanimoto R, Watanabe M, Murata H *et al* (2009). Overexpression of REIC/Dkk-3 in normal fibroblasts suppresses tumor growth via induction of interleukin-7. *J Biol Chem* **284:** 14236-44.

Sato H, Suzuki H, Toyota M, Nojima M, Maruyama R, Sasaki S *et al* (2007). Frequent epigenetic inactivation of DICKKOPF family genes in human gastrointestinal tumors. *Carcinogenesis* **28:** 2459-66.

Schulte JH, Horn S, Otto T, Samans B, Heukamp LC, Eilers UC *et al* (2008). MYCN regulates oncogenic MicroRNAs in neuroblastoma. *Int J Cancer* **122:** 699-704.

Schwab M (2004). MYCN in neuronal tumours. *Cancer Lett* **204:** 179-87.

Schwab M, Alitalo K, Klempnauer KH, Varmus HE, Bishop JM, Gilbert F *et al* (1983). Amplified DNA with limited homology to myc cellular oncogene is shared by human neuroblastoma cell lines and a neuroblastoma tumour. *Nature* **305:** 245-8.

Sengupta S, Nie J, Wagner RJ, Yang C, Stewart R, Thomson JA (2009). MicroRNA 92b controls the G1/S checkpoint gene p57 in human embryonic stem cells. *Stem Cells* **27:** 1524-8.

Tanaka M, Oikawa K, Takanashi M, Kudo M, Ohyashiki J, Ohyashiki K *et al* (2009). Down-regulation of miR-92 in human plasma is a novel marker for acute leukemia patients. *PLoS One* **4:** e5532.

Untergasser G, Steurer M, Zimmermann M, Hermann M, Kern J, Amberger A *et al* (2008). The Dickkopf-homolog 3 is expressed in tumor endothelial cells and supports capillary formation. *Int J Cancer* **122:** 1539-47.

Veeck J, Bektas N, Hartmann A, Kristiansen G, Heindrichs U, Knuchel R *et al* (2008). Wnt signalling in human breast cancer: expression of the putative Wnt inhibitor Dickkopf-3 (DKK3) is frequently suppressed by promoter hypermethylation in mammary tumours. *Breast Cancer Res* **10:** R82.

Veeck J, Wild PJ, Fuchs T, Schuffler PJ, Hartmann A, Knuchel R *et al* (2009). Prognostic relevance of Wnt-inhibitory factor-1 (WIF1) and Dickkopf-3 (DKK3) promoter methylation in human breast cancer. *BMC Cancer* **9:** 217.

Vreugdenhil E, Verissimo CS, Mariman R, Kamphorst JT, Barbosa JS, Zweers T *et al* (2009). MicroRNA 18 and 124a down-regulate the glucocorticoid receptor: implications for glucocorticoid responsiveness in the brain. *Endocrinology* **150:** 2220-8.

Weber M, Hellmann I, Stadler MB, Ramos L, Paabo S, Rebhan M *et al* (2007). Distribution, silencing potential and evolutionary impact of promoter DNA methylation in the human genome. *Nat Genet* **39:** 457-66.

You A, Fokas E, Wang LF, He H, Kleb B, Niederacher D *et al* (2010). Expression of the Wnt antagonist DKK3 is frequently suppressed in sporadic epithelial ovarian cancer. *J Cancer Res Clin Oncol*.

Yue W, Sun Q, Dacic S, Landreneau RJ, Siegfried JM, Yu J *et al* (2008). Downregulation of Dkk3 activates beta-catenin/TCF-4 signaling in lung cancer. *Carcinogenesis* **29:** 84-92.

Zenzmaier C, Untergasser G, Hermann M, Dirnhofer S, Sampson N, Berger P (2008). Dysregulation of Dkk-3 expression in benign and malignant prostatic tissue. *Prostate* **68:** 540-7.

Figure Legends:

Figure 1: ***MYCN*** **knockdown increase** ***Dickkopf-3*** **(*DKK3*) mRNA and secreted protein in neuroblastoma cells - (A)** Real-time qRT-PCR measurements of *DKK3* mRNA levels in SK-N-BE(2) and Kelly cells induced to knock down *MYCN* expression. Secreted endogenous DKK3 proteins from **(B)** SK-N-BE(2) and **(C)** Kelly cells induced to knock down *MYCN* expression, and **(D)** SHEP Tet21N cells induced to repress exogenous *MYCN* overexpression were measured with ELISA.

Figure 2: ***DKK3*** **promoter methylation status in neuroblastoma tumors and cell lines -** Methylation-Specific PCR (MSP) was performed on bisulfite-treated DNA from neuroblastoma tumors and cell lines. Lanes labeled U and M contain PCR products amplified from primers recognizing unmethylated and methylated *DKK3* promoters, respectively. All neuroblastoma samples investigated were unmethylated. DNA from the breast cancer cell lines MDA-MB231 and HS578t were used as methylated and unmethylated controls, respectively (Veeck *et al.*, 2008). NTC represents the no template control. *MYCN*-amplified samples are marked with ▲.

Figure 3: **Luciferase assays for** ***mir-92a, mir-92b*** **and** ***let-7e*** **-** Luciferase activity of HEK293 cells cotransfected with the wild type (pMIR-DKK3 wt) or mutated *DKK3*-3'UTR luciferase vector and miRNA mimics of *mir-92a* **(A)**, *mir-92b* **(B)** or *let-7e* **(C)**. Mut mir-92 seed is mutated in the predicted *mir-92* seed sequence at position 28-

29 in *DKK3*-3'UTR. Similarly, mut let-7 seed1, mut let-7 seed2 and mut let-7 seed1+2 were mutated in the predicted *let-7* seed sequences at position 550-556, 180-185 and 550-556+180-185 in *DKK3*-3'UTR, respectively. A plasmid constitutively expressing Renilla luciferase was used for normalization of the data. Data shown are mean ± SD of the ratio of normalized luciferase activity in miRNA mimic and control transfections. *$P < 0.05$ vs. respective control.

Figure 4: DKK3 ELISA analyses of culture media from neuroblastoma cell lines treated with antagomirs and miRNA mimics - (A) MNA neuroblastoma cell lines SK-N-BE(2) and Kelly were transfected with antagomir-92a (antimir-92a), antagomir-92b (antimir-92b) or a negative control antagomir (antimir-NC). **(B)** Non-MNA neuroblastoma cell lines SH-SY-5Y and SK-N-AS were transfected with *mir-92a*, *mir-92b*, *let-7e* or negative control microRNA (mir-NC) mimics. Secretion of endogenous DKK3 proteins to the culture media was measured using an ELISA kit. Data shown are mean ± SD of the ratio of DKK3 proteins secreted to the culture media normalized to total protein in cell extracts of miRNA mimic/antagomir and control transfections. *$P < 0.05$ compared to antimir-NC or mir-NC.

Figure 5: Immunohistochemical staining of Dickkopf-3 (DKK3) in neuroblastoma tumors - (A) A human neuroblastoma tissue section stained with a red fluorescently labeled (Alexa 594) anti-DKK3 monoclonal antibody, together with a green fluorescently labeled (Alexa 488) anti-CD31 monoclonal antibody. The nuclei were stained with DAPI, which are represented in blue. The merge represents an

overlay view of the DKK3, CD31 and DAPI image; 600x magnification. **(B)** Immunohistochemical staining of DKK3 in neuroblastoma primary tumors and ganglioneuromas showing specific staining of DKK3 in tumor vasculature (left image, sample no. 8, Supplementary Table 2) and in differentiated ganglion cells of a benign ganglioneuroma (right image, sample no. 28, Supplementary Table 2); 600x magnification.

Supplementary Figure 1: MiRNA *in silico* analysis of *DKK3*-3'UTR - (A) Venn diagram displaying miRNAs computationally predicted to target the 3'UTR sequence of *DKK3* by Diana-microT3.0, TargetScan v5.1 and MicroCosm. **(B)** Schematic overview from TargetScan v5.1 of the *DKK3* 3'UTR with conserved miRNA binding sites. **(C)** TargetScan v5.1 predictions of miRNAs that bind to the seed sequences at positions 25-31 (Site-1) and 550-556 (Site-2) of the *DKK3* 3'UTR. The RNA22 miRNA software predicted *let-7e* to target *DKK3*-3'UTR at position 180-186 (Site-3).

Supplementary Figure 2: Luciferase reporter assay for mir-17-92 members - MicroRNA mimics of the individual members of the mir-17-92 cluster were cotransfected with the pMIR-DKK3 vector into HEK293 cells. A plasmid constitutively expressing Renilla luciferase was used for normalization of the data. Data shown are mean ± SD of the ratio of normalized luciferase activity in miRNA mimic and control transfections. $*P < 0.05$.

Supplementary Figure 3: ***Mir-92b*** **expression in SK-N-BE(2) and SH-SY-5Y cells treated with antagomir-92b and** ***mir-92b*** **mimic, respectively - (A)** Relative expression of *mir-92b* in SK-N-BE(2) cells transfected with *mir-92b* antagomirs (antimir-92b). Antimir-NC = negative control antagomir. **(B)** Relative expression of *mir-92b* in SH-SY-5Y cells transfected with miRNA mimics of *mir-92b*. *Mir-92b* was measured using a stem-loop qRT-PCR assay for *mir-92b*. **P* < 0.05.

Supplementary Figure 4: ***DKK3*** **mRNA levels in SH-SY-5Y cells treated with miRNA mimics of** ***mir-92a, mir-92b*** **and** ***let-7e*** **-** Relative expression of *DKK3* mRNA in SH-SY-5Y cells transfected with miRNA mimics of *mir-92b*. *Mir-92b* was measured using a stem-loop qRT-PCR assay for *mir-92b*. **P* < 0.05.

Supplementary Table 1: Overview of the oligonucleotide primers used in this study

Supplementary Table 2: Neuroblastoma tumor and ganglioneuroma samples used in this study - [a]Diagnosis, [b]INSS=International Neuroblastoma Staging System, [c]Patient fulfilling clinico-biological criteria to obtain high-risk therapy, [d]Neuroblastoma, [e]Ganglioneuroma, [f]Non-malignant adrenal gland, [g]Multifocal primary, [h]No evidence of disease, [i]Died from disease, [j]Alive with disease, [k]Died of surgical complications, *EC*: Endothelial cells, *GC*: Ganglion cells

Figure 1

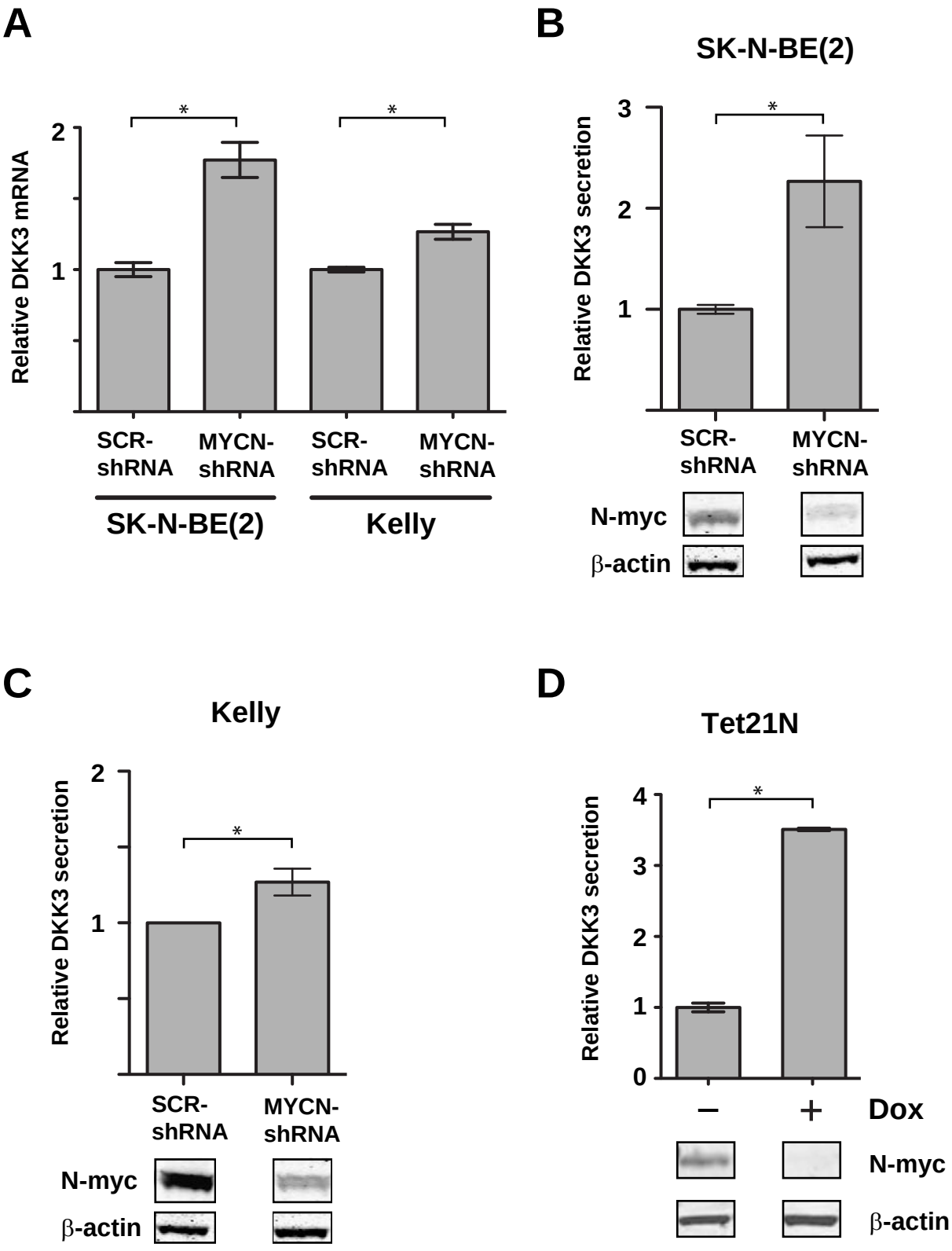
A
Relative DKK3 mRNA
2
1
*
*
SCR-shRNA
MYCN-shRNA
SCR-shRNA
MYCN-shRNA
SK-N-BE(2)
Kelly
B
SK-N-BE(2)
Relative DKK3 secretion
3
2
1
*
SCR-shRNA
MYCN-shRNA
N-myc
β-actin
C
Kelly
Relative DKK3 secretion
2
1
*
SCR-shRNA
MYCN-shRNA
N-myc
β-actin
D
Tet21N
Relative DKK3 secretion
4
3
2
1
0
*
–
+
Dox
N-myc
β-actin

Figure 2

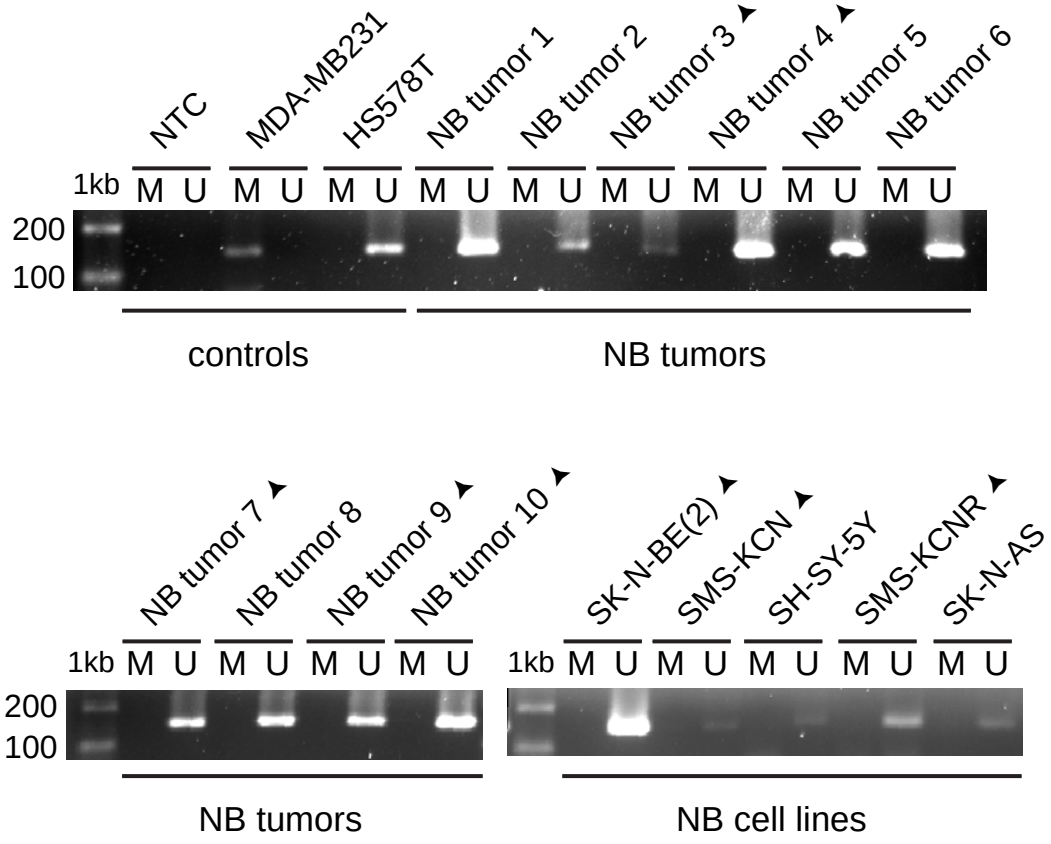
NTC
MDA-MB231
HS578T
NB tumor 1
NB tumor 2
NB tumor 3
NB tumor 4
NB tumor 5
NB tumor 6
1kb
M U M U M U M U M U M U M U M U M U M U
200
100
controls
NB tumors
NB tumor 7
NB tumor 8
NB tumor 9
NB tumor 10
SK-N-BE(2)
SMS-KCN
SH-SY-5Y
SMS-KCNR
SK-N-AS
1kb
M U M U M U M U
1kb
M U M U M U M U M U
200
100
NB tumors
NB cell lines

Figure 3

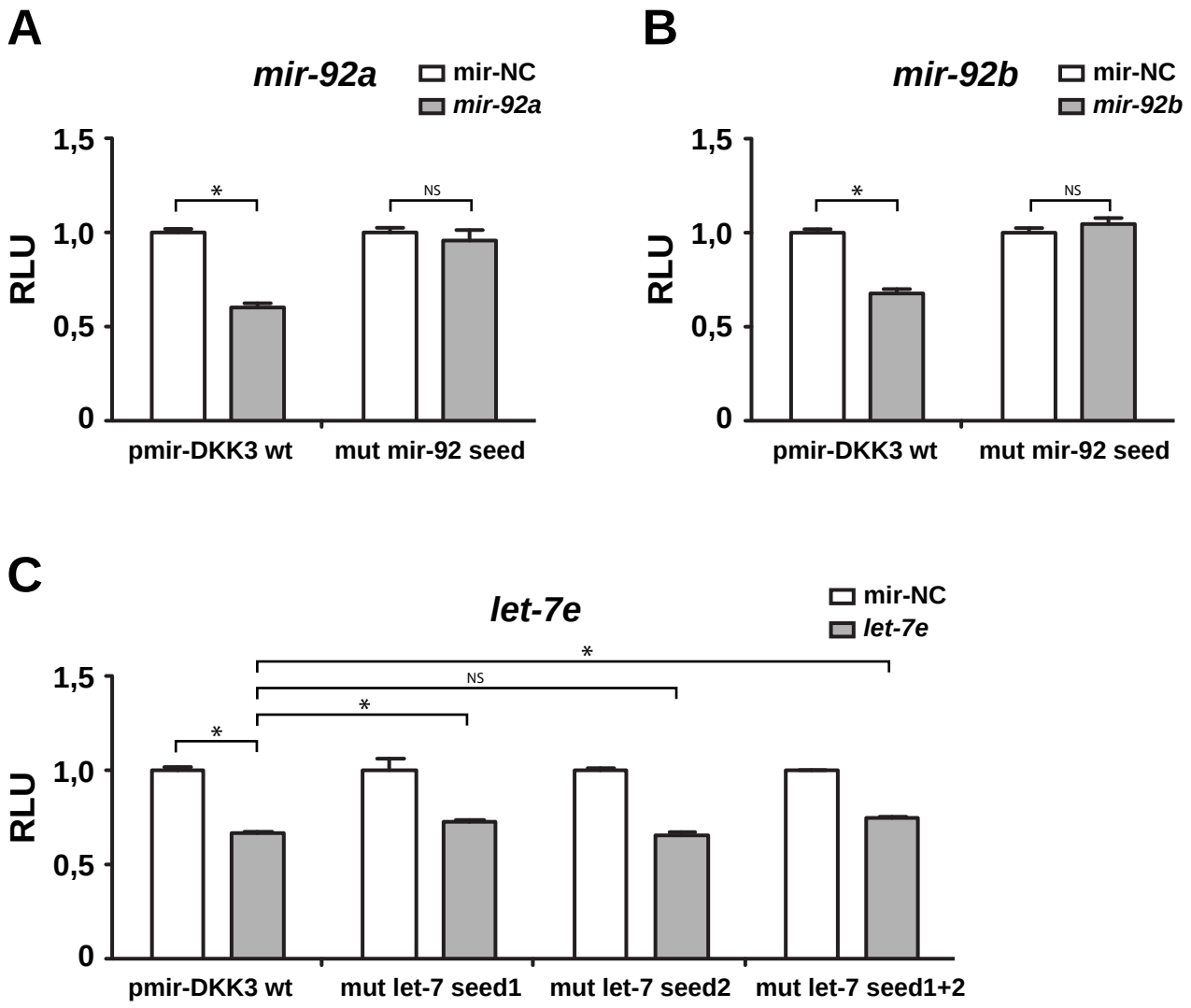
A
mir-92a
mir-NC
mir-92a
RLU
1,5
1,0
0,5
0
*
NS
pmir-DKK3 wt
mut mir-92 seed
B
mir-92b
mir-NC
mir-92b
RLU
1,5
1,0
0,5
0
*
NS
pmir-DKK3 wt
mut mir-92 seed
C
let-7e
mir-NC
let-7e
RLU
1,5
1,0
0,5
0
*
NS
*
*
pmir-DKK3 wt
mut let-7 seed1
mut let-7 seed2
mut let-7 seed1+2

Figure 4

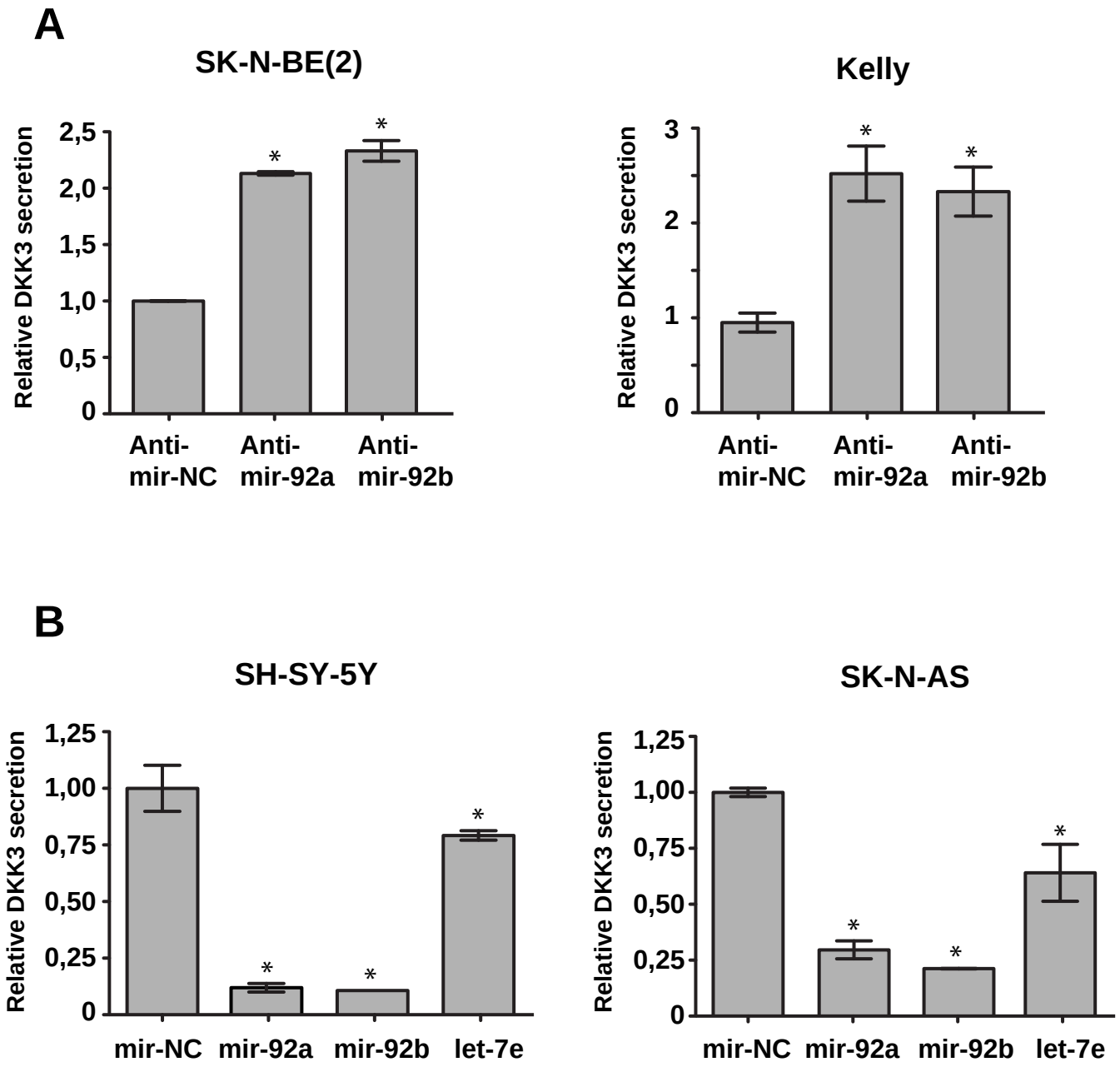
A
SK-N-BE(2)
Relative DKK3 secretion
2,5
2,0
1,5
1,0
0,5
0
*
*
Anti-mir-NC
Anti-mir-92a
Anti-mir-92b
Kelly
Relative DKK3 secretion
3
2
1
0
*
*
Anti-mir-NC
Anti-mir-92a
Anti-mir-92b
B
SH-SY-5Y
Relative DKK3 secretion
1,25
1,00
0,75
0,50
0,25
0
*
*
*
mir-NC
mir-92a
mir-92b
let-7e
SK-N-AS
Relative DKK3 secretion
1,25
1,00
0,75
0,50
0,25
0
*
*
*
mir-NC
mir-92a
mir-92b
let-7e

Figure 5

A

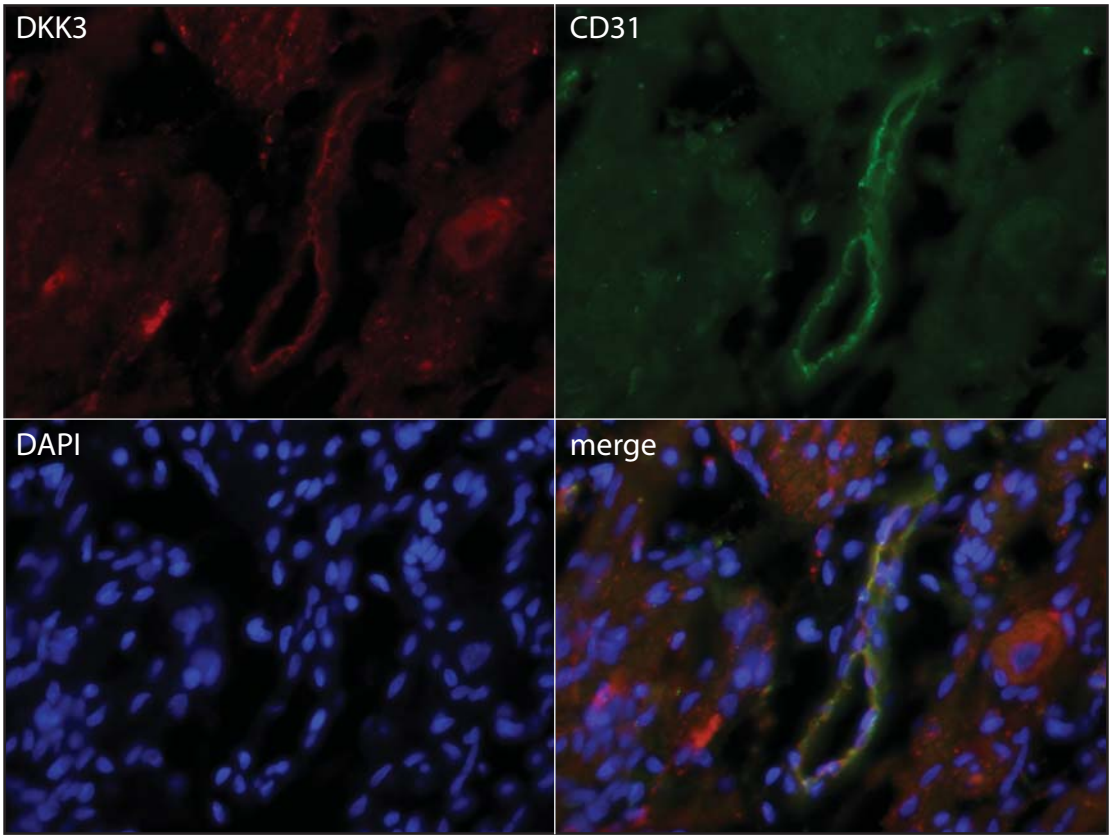

B

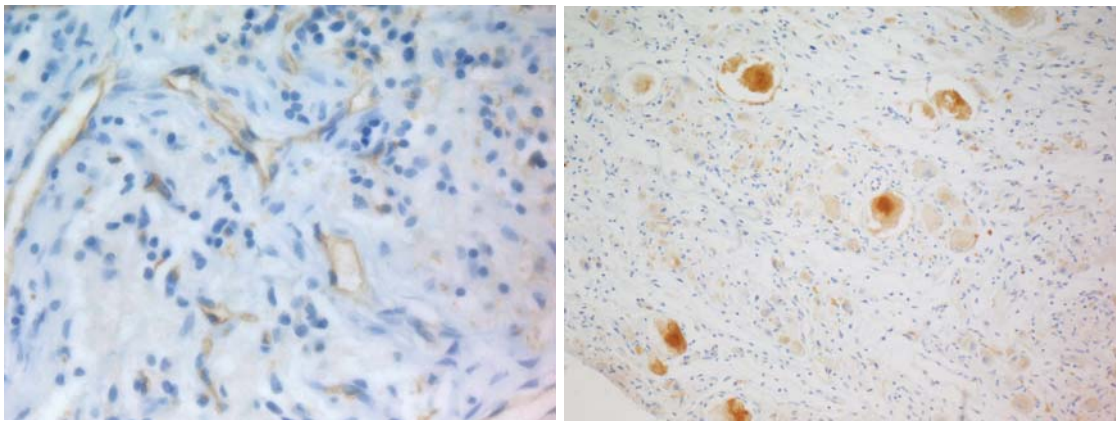

Supplementary figure 1

A

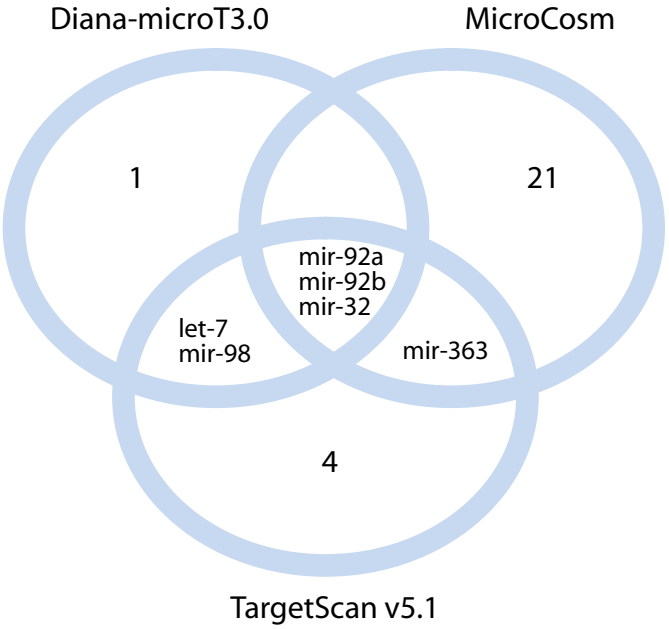

B

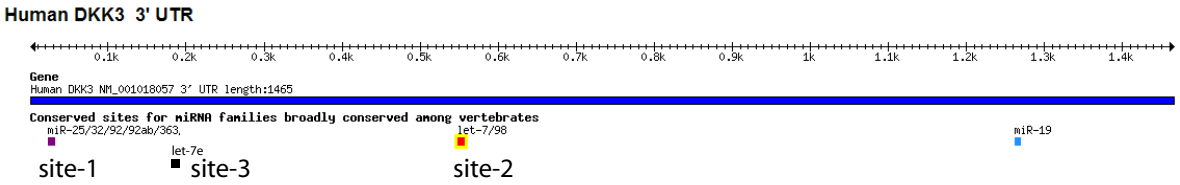

C

Site-1:

Position 25-31 of DKK3 3' UTR
hsa-miR-92a

```
5' ...AGGCUGUGGGUAGAUGUGCAAUA...
                |||      |||||||
3' ...UGUCCGGCCCUGUU-CACGUUAU...
```

Position 25-31 of DKK3 3' UTR
hsa-miR-92b

```
5' ...AGGCUGUGGGUAGAUGUGCAAUA...
                |||      |||||||
3' ...CCUCCGGCCCUGCU-CACGUUAU...
```

Position 25-31 of DKK3 3' UTR
hsa-miR-363

```
5' ...AGGCUGUGGGUAGAUGUGCAAUA...
                |||      |||||||
3' ...AUGUCUACCUAUGG-CACGUUAA...
```

Position 25-31 of DKK3 3' UTR
hsa-miR-32

```
5' ...AGGCUGUGGGUAGAU--GUGCAAUA...
                  |||    |||||||
3'    ...ACGUUGAAUCAUUACACGUUAU...
```

Site-2:

Position 550-556 of DKK3 3' UTR
hsa-let-7e

```
5'  ...AGUGUUGCUCAGCUCCUACCUCU...
                          |||||||
3'    ...UUGAUAUGUUGGAGGAUGGAGU...
```

Position 550-556 of DKK3 3' UTR
hsa-miR-98

```
5'  ...AGUGUUGCUCAGCUCCUACCUCU...
                          |||||||
3'    ...UUGUUAUGUUGAAUGAUGGAGU...
```

Site-3 (RNA22 predicted):

Position 180-185 of DKK3 3' UTR
hsa-let-7e

```
5' ...AGGCUGU----UCUCCAGGCUUCA...
      |||||||    |||||  |||||||
3' ...UUGAUAUGUUGGAGGA-UGGAGU...
```

Supplementary figure 2

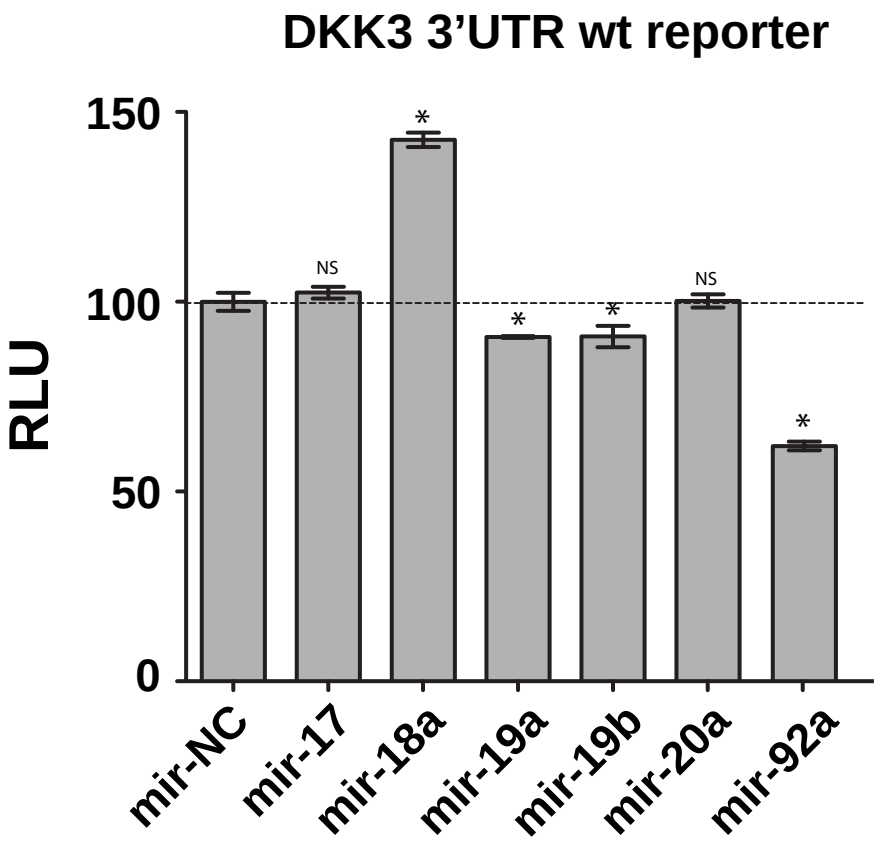

Supplementary figure 3

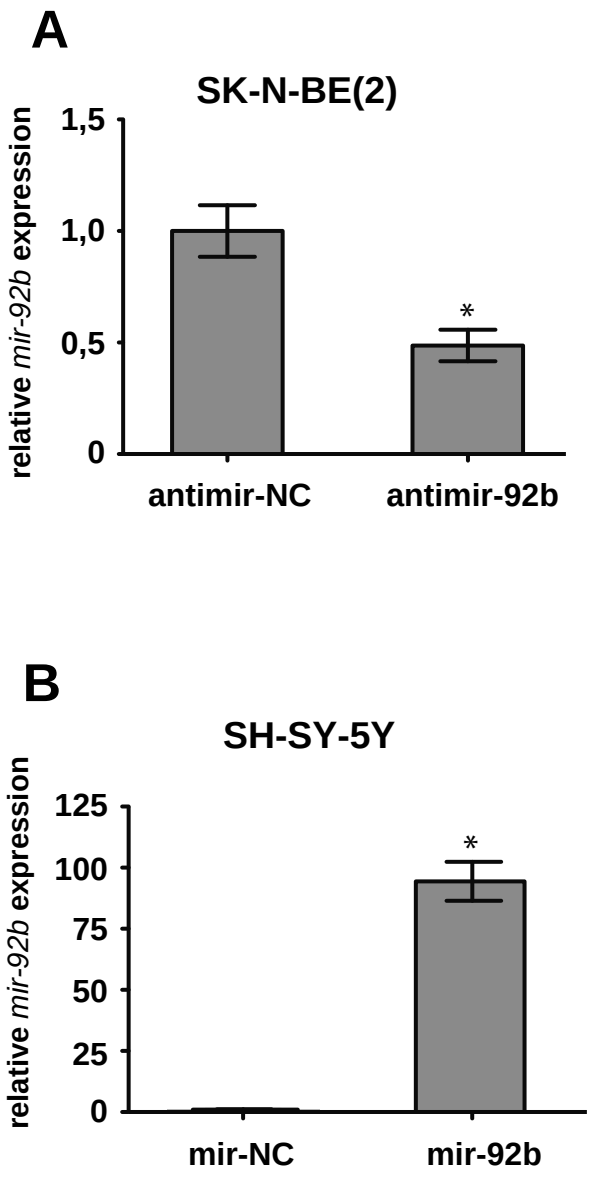

Supplementary figure 4

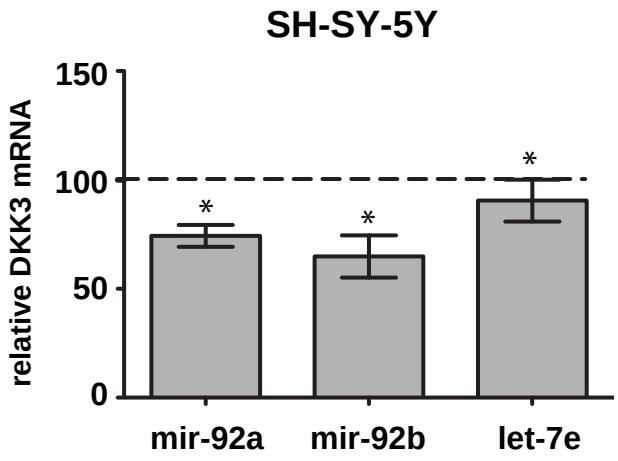

Supplementary Table 1.

Primer:	**Sequence (5'-3'):**	**Description:**
ON-005	ATGGGCGGTAGGCGTGTA	CMV sequencing primer
ON-056	ATTTGGGTCGCGGTTCTTG	qPCR UBC Forward
ON-057	TGCCTTGACATTCTCGATGGT	qPCR UBC Reverse
ON-176	TGACACTGGCAAAACAATGCA	qPCR HPRT1 Forward
ON-177	GGTCCTTTTCACCAGCAAGCT	qPCR HPRT1 Reverse
ON-327	GATCAAGCTTCTATGGAAGATTTTTAATACAGG	DKK3-3`UTR reverse
ON-342	GATGTTCCGCGAGGTTGAGG	qPCR DKK3 Forward
ON-343	CCAACCTTCGTGTCTGTGTTGG	qPCR DKK3 Reverse
ON-361	AAAGCTGCGCACTAGTATCTGGACCAGGCTGTGGGTAGA	Dkk3-3`UTR In-fusion cloning primer
ON-363	ATCCTCATAAAGGCCAAGAA	pMIR-report forward sequencing primer
ON-447	TGTGGGTAGATGTGGTATAGAAATAGCTAA	pMIR-report DKK3-mutagenesis 92a/b
ON-448	GCAGTGTTGCTCAGCTCCTACCAGTGTGCCAGGGCAGC	pMIR-report DKK3- mutagenesis let-7
ON-479	CGAGTAGATTTAGTTCGGTTCGTAGC	Methylated specific forward primer (DKK3)
ON-480	CTTAACGTCGAATCCTACTCGAACG	Methylated specific reverse primer
ON-481	GAGTGAGTAGATTTAGTTTGGTTTGTAGT	Unmethylated specific forward primer
ON-482	CCCCTTAACATCAAATCCTACTCAAACA	Unmethylated specific reverse primer

Supplementary Table 2.

Sample	*DIA*[a]	*AGE Mo*	*Gender*	*Stage INSS*[b]	*MYCN ampl.*	*1p del*	*DNA Ploidy*	*High-risk*[c]	*Outcome*	*DKK3 in EC*
1	NB[d]	21	M	1	no	no	4n	No	NED[h]	+++
2	NB	123	F	1	no	no	3n	No	NED	++
3	NB	7	F	1	yes	yes	2n	No	DOD[i]	-
4	NB	13	M	1	no	no		No	NED	+++
5	NB	18	F	1	no	no		No	NED	++
6	NB	31	M	2B	no	no	3n	No	NED	++
7	NB	33	F	2A	no	no	3n	No	NED	+
8	NB	8	F	2	no	no	3n	No	NED	+++
9	NB	110	M	2	no	no	2n	No	NED	+++
10	NB	5	F	2	no	no	3n	No	AWD[j]	(+)
11	NB	103	F	2B	no	no	2n	No	NED	++
12	NB	6	M	3	no	nd	3n	No	NED	++
13	NB	12	F	3	no	no	5n	No	NED	++
14	NB	0	M	3	no	no	3n	No	DOC[k]	+
15	NB	79	M	3	yes	yes	3n	Yes	NED	(+)
16	NB	136	M	4	yes	yes	2n	Yes	DOD	-
17	NB	39	F	4	yes	yes	2n	Yes	DOD	-
18	NB	35	F	4	no	yes		Yes	NED	-
19	NB	28	M	4	yes	yes	3n	Yes	NED	-
20a	NB	8	M	4_M[g]	no	no	3n	No	NED	+
20b	NB	8	M	4_M	no	no	4n/5n	No	NED	+
21	NB	22	M	4	yes	yes		Yes	DOD	(+)
22	NB	50	F	4	yes	yes		Yes	DOD	(+)
23	NB	0	M	4S	no	no	3n	No	NED	++
24	NB	10	M	4S	no	no	3n	No	NED	+++
25	NB	0	M	4S	no	nd	4n	No	NED	(+)
										DKK3 in GC
26	GN[e]	145	M						NED	+++
27	GN	30	F						AWD	++
28	GN	59	F						NED	+++
29	GN	137	M						NED	++

[a]Diagnosis, [b]INSS=International Neuroblastoma Staging System, [c]Patient fulfilling clinico-biological criteria to obtain high-risk therapy, [d]Neuroblastoma, [e]Ganglioneuroma, [f]Non-malignant adrenal gland, [g]Multifocal primary, [h]No evidence of disease, [i]Dead of disease, [j]Alive with disease, [k]Dead of surgical complications, *EC*: Endothelial cells, *GC*: Ganglion cells

APPENDIX

Inhibition of gene function in mammalian cells using shorthairpin RNA (shRNA)

Henriksen JR, Büchner J, Løkke C, Flægstad T, Einvik C.

Methods in Molecular Biology (2010) In Press, expected publishing date 22.12.2010

Inhibition of gene function in mammalian cells using short-hairpin RNA (shRNA)

Jørn Remi Henriksen[1], Jochen Büchner[1], Cecilie Løkke[2], Trond Flægstad[1,2] and Christer Einvik[1].

[1.] Department of Pediatrics, University Hospital of North-Norway, 9038 Tromsø, Norway
[2.] Department of Pediatrics, Institute of Clinical Medicine, University of Tromsø, 9037 Tromsø, Norway

Corresponding author:
Christer Einvik - christer@fagmed.uit.no

Keywords: RNAi, short-hairpin RNA, gene silencing, target knockdown validation, MYCN, neuroblastoma

Summary

RNAi is now the preferred method for silencing gene expression in a variety of systems. In this chapter we describe the procedure for applying short-hairpin RNA (shRNA) to study gene function. Detailed descriptions of target site selection, shRNA construction, shRNA transfection and target knockdown validation are included.

1 Introduction:

Gene silencing by antisense technology is now being used as a powerful molecular tool to study gene functions in living organisms. The antisense agents bind to target messenger RNA (mRNA), thus inactivating the target gene expression. The inhibitory effects on protein production from the corresponding gene may result in phenotypic changes. Thereby, the function of the gene can be understood. To date, there are a number of antisense molecules that can affect efficient post-transcriptional gene silencing. They include antisense oligonucleotides (ON), antisense 'third-generation' nucleic acid analogues (peptide nucleic acid -PNA, locked nucleic acid - LNA or morpholinos), ribozymes, small-interfering RNAs (siRNAs), short-hairpin RNAs (shRNAs) and microRNAs (miRNAs). These antisense molecules cause specific gene inhibitory effects through different mechanisms. In this chapter, we demonstrate the characteristics of gene silencing using RNAi-based short-hairpin RNA (shRNA) technology.

RNAi is a highly conserved gene silencing mechanism that plays an important role in regulation of gene expression. In addition, the RNAi system is important in protecting the host cell from viral infections and invasion by mobile genetic elements (Obbard *et al.*, 2008).

The RNAi pathway takes place in the cytoplasm and can be subdivided into two phases; an initiation and an effector phase. In the initiation phase, long dsRNAs are cleaved by the RNase III-like nuclease Dicer to produce 21-23 nt duplex RNAs, called small interfering RNAs (siRNAs). During the effector phase, the siRNA molecule is incorporated into the RNA-induced silencing complex (RISC), where an ATP-dependent RNA helicase activity unwinds the duplex. The siRNA strand which is antisense to the target RNA (guide strand) is incorporated into RISC, while the complementary passenger strand is destroyed. The guide strand permits highly sequence-specific recognition of the complementary mRNA, which is then cleaved by Argonaute 2, a component of RISC. This results in inhibition of protein synthesis from the mRNA (Shrivastava and Srivastava, 2008).

Unlike miRNA and other long dsRNAs, shRNAs transcribed from exogenously introduced DNA do not require Drosha processing in the nucleus. These tight hairpin turn RNA structures are transported directly to the cytoplasm via exportin-5 were they are cleaved by Dicer into siRNA molecules, which then follow the RNAi pathway for gene silencing (Yi *et al.*, 2003).

RNAi is now a well-established method for high-throughput analysis as well as for functional studies in vitro, including mammalian cells (Scherr and Eder, 2007). Two different methods are commonly used to deliver siRNA molecules for gene silencing in mammalian cell lines; 1) synthetic siRNAs (Watts *et al.*, 2008) and 2) RNA polymerase III transcribed shRNAs from plasmids or viral vectors (Wang *et al.*, 2008;Walchli and Sioud, 2008).

Plasmid vector based shRNA expression is a low-cost and easy-to-perform method for studying gene function in mammalian cells. In addition, this strategy offers the advantage of inducible siRNA expression in the case where gene silencing is expected to have deleterious effects on the target cell (Henriksen *et al.*, 2007).

2 Materials

2.1 Oligonucleotides and plasmids used for cloning

1 Oligonucleotides:

Name:	Sequence (5'-3'):	Description:
ON 3	GTTTTCCCAGTCACGACGTTGTA	M13 forward sequencing primer
ON10	CGGGATCCAAAAAAGGTCTGGGTCCTTGCAGACCACG CCCGACCAAGCTTCGCCGGGCATGATCTGCAAGAACC CAGACCGGTGTTTCGTCCTTTCCACAA	Reverse antiMYCN-27 shRNA cloning primer. Contain BamHI
ON11	CGGGATCCAAAAAAGCTAGTGCTCCTCGGCCTAGAAG GAGTAGCAAGCTTCCCACTCCCTCCAGGCCGAGGAGC ACCAGCGGTGTTTCGTCCTTTCCACAA	Reverse antiMYCN-1291 shRNA cloning primer. Contain BamHI
ON19	CGGGATCCAAAAAAGAATCACTCAGAGTGTCCCCTCC GGAAGTGAAGCTTGACCTCCGGAGAGGACACCCTGA GCGATTCGGTGTTTCGTCCTTTCCACAA	Reverse antiMYCN-760 shRNA cloning primer. Contain BamHI
ON20	CGGGATCCAAAAAAGTTCTTGAGACACACAGCGATGG TAAATGGAAGCTTGCATTCACCATCACTGTGCGTCCC AAGAACGGTGTTTCGTCCTTTCCACAA	Reverse antiMYCN-887 shRNA cloning primer. Contain BamHI
ON22	ATAAGAATGCGGCCGCAAGGTCGGGCAGGAAGAGGG CC	U6 forward primer. Contain NotI.
ON51	CGGGATCCAAAAAAGAGCGTTCGGAGCTGATGGCCAT AAATACGAAGCTTGGTACTTATGACCACCAACTCCGA ACGCTCGGTGTTTCGTCCTTTCCACAA	Reverse cloning primer for SCR shRNA. Contain BamHI
ON 56	ATTTGGGTCGCGGTTCTTG	UBC forward QPCR primer
ON 57	TGCCTTGACATTCTCGATGGT	UBC reverse QPCR primer
ON 87	CACCCTGAGCGATTCAGATGA	MYCN forward QPCR primer
ON 89	CCGGGACCCAGGGCT	MYCN reverse QPCR primer
ON 58	GCAGCTACTCCTCCAGCTCT	NFL forward QPCR primer
ON 59	ACTTGAGGTCGTTGCTGATG	NFL reverse QPCR primer
ON 60	TCCAGCCCAGAGACACTGATT	NPY forward QPCR primer
ON 61	AGGGTCTTCAAGCCGAGTTCT	NPY reverse QPCR primer
ON 96	AAGTTCTACGGTGACGAGGAG	CRT forward QPCR primer
ON 97	GTCGATGTTCTGCTCATGTTTC	CRT reverse QPCR primer
ON 100	AGATCCCGGAGTTGGAAAAC	c-MYC forward QPCR primer
ON 101	AGCTTTTGCTCCTCTGCTTG	c-MYC reverse QPCR primer
ON 170	TCACCCACACTGTGCCCATCTACGA	β-actin forward QPCR primer
ON 171	CAGCGGAACCGCTCATTGCCAATGG	β-actin reverse QPCR primer
ON 176	TGACACTGGCAAAACAATGCA	HPRT1 forward QPCR primer
ON 177	GGTCCTTTTCACCAGCAAGCT	HPRT1 reverse QPCR primer
ON 304	CGAGAGCGAGCGGATGA	CHGB forward QPCR primer
ON 305	GGCGTGTCTTCACTTCTTCAGA	CHGB reverse QPCR primer

.

2 Plasmids:

pSHAG-Ff1 (Paddison *et al.*, 2002) encodes an U6-driven anti-luciferase (anti-luc) shRNA homologous to nucleotides 1340-1368 of the coding sequence of the firefly luciferase gene (NCBI accession number U47296).

2.2 Cell culture and transfection

1 Neuroblastoma cell line SK-N-BE(2) – MYCN amplified.

2 6-well multiwell culture plates (Falcon)

3 RPMI-1640 supplemented with 10% fetal bovine serum (FBS).

4 Phosphate-buffered saline (PBS)

5 Trypsin solution – 0,25 % trypsin and 0,05% ethylenediamine tetraacetic acid (EDTA) in PBS , pH 7,5

6 Cells were maintained in a humidified 37^{o}C incubator with 5% CO_2, supplied with fresh complete medium every 3 days, and subcultured before confluence was reached.

7 Lipofectamin2000 (Invitrogen)

2.3 Cellular protein isolation and Western blot analysis

1 Tropix lysis buffer, Protease inhibitor (Roche), DTT

2 XCell SureLock^{TM} Mini-Cell (Invitrogen)

3 NuPAGE Novex 4-12% Bis-Tris Gel – 1,0mm x 10 well (Invitrogen)

4 NuPAGE LDS Sample Buffer (4x) (Invitrogen)

5 Markers. MagicMarkTMXP Western standard (Invitrogen) as a protein size marker. Kaleidoscope Prestained Standard (Bio-RAD) for visualisation of size during electrophoresis and protein transfer efficiency from gel to membrane during blotting.

6 Methanol

7 Running buffer; NuPAGE MOPS SDS Running Buffer (20x) (Invitrogen)

8 XCell II^{TM} Blot Module (Invitrogen)

9 Immobilon-FL PVDF transfer membrane (Millipore)

10 Whatman 3MM chromatography paper

11 Transfer buffer: NuPAGE Transfer Buffer (20x) (Invitrogen)

12 Blocking buffer: Odyssey$^{®}$ Blocking buffer (LI-COR Biosciences)

13 Primary Ab:
anti-N-myc mouse mAb (Calbiochem)
anti-actin rabbit pAb (Sigma)

14 Secondary Ab.
Alexa Fluor® 680 conjugated goat anti-mouse IgG (Invitrogen)
IRDye800CW conjugated goat anti-rabbit IgG (Rockland)

15 PBST ; PBS containing 0,1 % Tween-20

16 Odyssey Infrared Imaging System (LI-COR)

2.4 Total RNA isolation and cDNA synthesis

1 RNeasy Plus Mini Kit (Qiagen)

2 QIAshredder™ (Qiagen)

3 Superscript™ III reverse transcriptase (Invitrogen)

4 Oligo-dT_{20} primer

5 dNTPs

6 RNase inhibitor

7 Thermocycler

2.5 Real-time RT-PCR analysis

1 Power SYBR Green PCR Master Mix (Applied Biosystems)

2 MicroAmp Optical 96-well Reaction Plate (Applied Biosystems)

3 MicroAmp Optical Adhesive Film (Applied Biosystems)

4 7300 Real Time PCR System (Applied Biosystems)

5 7300 System Sequence Detection Software v1.4 (Applied Biosystems)

6 qBase (http://medgen.ugent.be/qbase/)

3 Methods

This section gives a detailed description of the design and cloning of anti-MYCN shRNA constructs. A detailed procedure for cell transfection and evaluation of shRNA treated neuroblastoma cells, using confocal microscopy, Western blot and real-time RT-PCR analysis, is also described.

3.1 Selection of anti-MYCN shRNA target sites

There are many factors affecting shRNA efficiency. Among the most important factors are both shRNA and target mRNA structures. Several software programmes for siRNA target prediction have been developed, but no single standard exists for predicting the best siRNA target sequence (Li and Cha, 2007). Functional studies are required to evaluate the efficiencies of any shRNA constructed.

We chose 4 different target sites in the MYCN cDNA (GeneBank accession NM_005378) sequence (figure 1A). Two sites (antiMYCN-27 and antiMYCN- 1291) were picked at random. The other two target sites (antiMYCN-760 and antiMYCN-887) and a scrambled shRNA sequence were picked using Genescript siRNA Target Finder and Genescript siRNA Sequence Scrambler (http://www.genscript.com/tools.html), respectively (Wang and Mu, 2004).

All antiMYCN shRNA sequence candidates were BLASTed (NCBI database) to ensure that only the MYCN mRNA was targeted.

3.2 Designing reverse primers for anti-MYCN shRNA cloning

The PCR-based cloning strategy used to construct the U6 expressed shRNAs from the pSHAG plasmid, requires a reverse primer containing the complete shRNA sequence.

The following steps describe how ON-20, the reverse primer for amplifying antiMYCN-887, was designed:

1 Pick a 29 nt target sequence which ends with a C from the MYCN cDNA sequence:

5'–**CATTCACCATCACTGTGCGTCCCAAGAAC**–3'

2 Reverse complement the target sequence to create the 'antisense' strand:

5'–**GTTCTTGGGACGCACAGTGATGGTGAATG**–3'

3 Add a HindIII-containing 'loop' sequence to the 3'end:

5'–GTTCTTGGGACGCACAGTGATGGTGAATG**CAAGCUUC**–3'

4 Add the reverse complement of the 'antisense' sequence to the 3'end of the 'loop' sequence:

5'–GTTCTTGGGACGCACAGTGATGGTGAATGCAAGCUUC**CATTCACCATCACTGTGCGTCCCAAGAAC**–3'

This sequence represents the shRNA molecule (see figure 1b).

5 Change 4 nucleotides in the 'sense' strand to create G-U basepairs in the shRNA stem sequence. **Note 1**:

5' -GTTCTTGGGACGCACAGTGATGGTGAATGCAAGCUUCCATT**T**ACCATC**G**CTGTG**T**GTC**T**CAAGAAC – 3'

6 Add 6 thymidines to create the RNA polymerase III transcription termination sequence:

5’ – GTTCTTGGGACGCACAGTGATGG /……../CCATCGCTGTGTGTCTCAAGAAC**TTTTTT** – 3’

7 Reverse complement the sequence:

5’ –**AAAAAAGTTCTTGAGACACACAGCGATGG**/……../**CCATCACTGTGCGTCCCAAGAAC** – 3’

8 Add a 21 nt downstream U6 promoter binding sequence (GGTGTTTCGTCCTTTCCACAA) to the 3’ end:

5’ –AAAAAAGTTCTTGAGAC/……../CCATCACTGTGCGTCCCAAGAAC**GGTGTTTCGTCCTTTCCACAA** – 3’

9 Add a BamHI restriction enzyme site to the 5’ end for cloning purposes to finish the reverse cloning primer ON-20 (see section 2.1):

5’ –**CGGGATCC**AAAAAAGTTCTTGAGAC/……../CCATCACTGTGCGTCCCAAGAACGGTGTTTCGTCCTTTCCACAA – 3’

3.3 Construction of anti-MYCN shRNA expressing plasmids

Plasmids containing different anti-MYCN shRNA sequences, expressed from a U6 promoter, are made using a PCR-based strategy. In this strategy, 272 bp of the U6 promoter from pSHAG-Ff1 is amplified using a NotI-containing U6 forward primer (ON22) in combination with different BamHI-containing reverse primers including the complete anti-MYCN shRNA sequences. **Note 2**.

PCR products are digested with NotI/BamHI and purified from agarose gels, before ligation into NotI/BamHI digested pSHAG-Ff1 plasmids. Reverse primers ON10, ON11, ON19, ON20 and ON51 are used to construct plasmids pantiMYCN-27, pantiMYCN-1291, pantiMYCN-760, pantiMYCN-887 and pScr-shRNA, respectively. Numbers in plasmid names indicates the first position of the shRNA target recognition site in the MYCN cDNA sequence. All plasmid constructs are verified by DNA sequencing using ON-3.

3.4 Transient transfection of anti-MYCN shRNAs into a MYCN-amplified neuroblastoma cell line

1 Day 1: Seed $1.3x10^5$ SK-N-BE(2) cells into each well of a 6-well tissue culture plate.

2 Day 2: Cells are transfected with 3 μg plasmids pantiMYCN-27, pantiMYCN-1291, pantiMYCN-760, pantiMYCN-887 or pScr-shRNA using Lipofectamin2000 (4 μl) in a total of 2 ml media in each well according to the manufacturers protocol.

3 Day 5: Isolate total cellular RNA and protein extracts.

Transfection efficiencies typically vary between 50-80%.

3.5 Total cellular protein isolation

1 Wash cells with 2 ml PBS, make sure to remove all supernatant.

2 Add trypsin solution.

3 When cells detach from the culture dish (few minutes at room temperature), add 1,0 ml RPMI1640 with 10% serum, resuspend and transfer to 1,5 ml Eppendorf tubes.

4 Wash cells once in 0,5 ml PBS.

5 Resuspend cells in 40 µl Tropix lysis buffer containing protease inhibitor and 1 mM DTT **Note 3**.

6 Leave on ice for 5 minutes. Sentrifuge at top speed for 5 minutes. Collect the supernatants containing total cellular proteins in fresh tubes.

7 Measure total protein concentrations.

3.6 Western immunoblot analysis

To investigate the effect of anti-MYCN shRNA knockdown at the protein level, we use western immunoblot analysis. The XCell SureLock^{TM} Mini-Cell and XCell II^{TM} Blot Module (Invitrogen) is used to resolve the proteins by Bis-Tris polyacrylamide gel electrophoresis and to transfer the resolved proteins from the gel to a membrane support, respectively. The protocols were done according to the specifications of the producer and briefly include the following steps:

Separation of proteins by Bis-Tris polyacrylamide gel electrophoresis:

1 Assemble the electrophoresis chamber with a 4-12 % Bis-Tris Gel and running buffer.

2 Load 25 µg total protein in sample buffer preheated for 10 min at 70^{o}C to each sample well (total 20 µl). Include MagicMark (1 µl) and Kaleidoscope (7µl) markers in separate wells.

3 Run the gel at constant 200 volt for 1 hour.

Transfer of resolved protein from the gel to a membrane support:

4 Prepare the membrane by briefly soaking it for 10 sec in 100% methanol, 5 sec in water and store it in transfer buffer until used

5 Assemble the gel/blot sandwich from the cathode core in the following order: 2x blotting pads, 1 Whatman 3MM filter paper, gel, membrane, 1x Whatman 3MM filter paper and 3x blotting pads. **Note 4.**

6 Assemble the Mini-Cell Blot Module with the gel/blot sandwich.

7 Electroblot at 30 volts for 1 hour. The kaleidoscope marker colours should be transferred to the membrane.

Processing of the blot for detection of specific proteins with an antibody:

8 Wash membrane in PBS for 5 min.

9 Block membrane in blocking buffer for 1 hour.

10 Add primary antibodies anti-N-myc (1:400) and anti-actin (1:1000) diluted in blocking buffer containing 0,01% SDS and 0,01% Tween-20. Incubate over night at 4^{o}C. **Note 5.**

11 Wash membrane 4 x 5 min at room temperature in PBST.

12 Add secondary antibodies diluted 1:5000 in blocking buffer containing 0,01% SDS and 0,01% Tween-20. Incubate 1 hour at room temperature. Cover in aluminium to protect from light.

13 Wash membrane 4 x 5 min at room temperature in PBST. Protect membrane from light.

14 Scan membrane on an infrared imaging system to develop the final western immunoblott.

Results:
Western immunoblot analysis was used to evaluate the effect of different anti-MYCN shRNA constructs. As can be seen from figure 2, the MYCN protein levels are reduced to different degrees with the tested shRNAs. aMN-887 is the most efficient anti-MYCN shRNA. β-actin protein levels remain unaffected by the different transfections.
These results show that the knockdown effect by shRNAs at the RNA level is reflected at the MYCN protein level.

3.7 Total RNA isolation

We use the RNeasy Plus Mini Kit to isolate total RNA samples. This kit includes gDNA Eliminator Mini Spin Columns for efficient DNA removal and do not require additional DNase treatment. Procedures are according to that recommended by the manufacturer; and include the following steps:

1 Cells from one transfected well of a 6-well culture dish are disrupted by addition of 350 µl of Buffer RLT Plus

2 Homogenize cell lysates using QIAshredder^{TM}. **Note 6.**

3 Closely follow steps 4-12 in the Qiagen protocol for purification of total RNA from animal cells. Samples are usually eluted in 35 µl RNase-free water both in step 11 and 12.

3.8 cDNA synthesis

Superscript^{TM} III reverse transcriptase is used to reverse transcribe total RNA to cDNA.

1 For each RNA sample prepare the following in a 0,5 µl microcentrifuge tube;

Component:	Volume:
Oligo-dT_{20} primer (50 µM) **Note 7.**	1 µl
dNTP (2,5 mM each)	1 µl
$MgCl_2$ (25 mM)	1 µl
1,4-2,0 µg total RNA **Note 8.**	x µl
RNase-free water	(13 – x) µl
TOTAL:	13 µl

2 Incubate at 65 ^{o}C for 5 minutes, then on ice for 1 minute.

3 Add the following to RNA-containing solution from step 1.

Component:	Volume:
(RNA-containing solution from step1)	(13 µl)
5 x First Strand buffer	4 µl
DTT (0,1 M)	1 µl
RNase inhibitor	1 µl
SuperScript™ III **Note 9.**	1 µl
TOTAL:	20 µl

4 Incubate in a thermocycler;

Temperature:	Time (minutes):
50 ^{o}C	60
70 ^{o}C	15
4 ^{o}C	until PCR setup is ready

3.9 Real-time PCR analysis

1 Prepare stocks of master reaction mixes. Each reaction includes the following:

Component:	Volume:
Nuclease-free water	6,5 µl
2 x SYBR Green Master Mix	12,5 µl
cDNA template (30 x diluted)	5,0 µl
Primer mix (5 µm each primer) **Note 10.**	1,0 µl
TOTAL:	25 µl

2 Add 25 µl of the reaction mix to each well of an optical 96-well reaction plate.

3 Seal the plate with adhesive film. Make sure all edges are properly sealed.

4 Spin the reaction plate at 1600 rpm for 1 minute.

5 Start the PCR software on the real-time PCR system and assign each well with the correct sample / control

6 Insert the reaction plate and execute the PCR with the following program:

Pre-incubation:

Temperature:	Time:
50 °C	2 min.
95 °C	10 min.

Amplification (40 cycles):

Temperature:	Time:
95 °C	15 sec.
60 °C	1 min.

Melting curve:

Temperature:	Time:
95 °C	15 sec.
60 °C	1 min.
95 °C	15 sec..
60 °C	15 sec.

7 Calculate relative gene expressions. **Note 11**.

Results:

To measure the direct effect of different anti-MYCN shRNAs on MYCN mRNA, we use real-time RT-PCR analysis. Figure 3a shows relative expression levels of MYCN mRNA. The reductions in MYCN mRNA levels are consistent with the decrease of MYCN protein observed on western immunoblots. aMN-887 is the most efficient shRNA showing a 70 % reduction of MYCN mRNA in transient transfection experiments. To support the observed MYCN knockdown effects, we quantified c-MYC mRNA levels in the transfected cells using quantitative real-time RT-PCR. Previous studies have shown that there is a reverse correlation of MYCN and c-MYC expression in neuroblastoma cells (Breit and Schwab, 1989;Westermann *et al.*, 2008). Figure 3b shows a close reverse correlation between MYCN mRNA and c-MYC mRNA expression, supporting the knockdown efficiencies of the tested anti-MYCN shRNAs. Based on the measured CT values in these experiments, MYCN mRNA levels exceed c-MYC mRNA levels by a factor of 10^4 in the MYCN-amplified neuroblastoma cell line SK-N-BE(2).

In addition, to indirectly verify MYCN downregulation upon anti-MYCN shRNA treatment, we used real-time RT-PCR to confirm neuronal differentiation observed by immunostaining confocal microscopy (data not shown). We chose a panel of 4 neuronal differentiation markers, Neuropeptid Y –NPY (Jalava *et al.*, 1992), Calreticulin - CRT (Johnson *et al.*, 1998; Hsu *et al.*,

2005), Chromogranin B – CHGB (Jogi *et al.*, 2004), Neurofilament L – NFL (Breen and Anderton, 1991) and investigated mRNA levels in aMN-887 treated neuroblastoma cells. All markers were significantly increased in anti-MYCN shRNA treated cells (figure 4), confirming the observed neuronal differentiation.
Hypoxanthine phosphoribosyltransferase 1 (HPRT1), β-actin and Ubiquitin C (UBC) were used as housekeeping genes in all real-time PCR experiments. **Note 12.**

4 Notes

1 The G-U basepairs added are not central for the efficiency of the shRNA, but they are thought to stabilize the shRNA molecule (Paddison *et al.*, 2004). Furthermore, the wobble basepairs aid sequencing the shRNA construct and is also believed to reduce unwanted immunostimulation.

2 When using very long primers (the reverse primer including the entire shRNA construct) in PCR, it is recommended to add DMSO to the PCR reaction mix. We use 2 µl DMSO in a 50 µl PCR reaction mix.

3 Lysis of cells can be done directly in the well, but this requires larger volume of lysis buffer, and thus results in lower concentration of protein in the final solution. This might cause problems since there is only room for ca 20 µl sample in each well of the western gel.

4 Blotting pads, Whatman paper and membrane should be soaked thoroughly in transfer buffer before assemble. Avoid air bubbles.

5 We perform primary antibody staining in 50 ml centrifuge tubes to reduce the amounts of blocking buffer and antibody (total 5 ml). Membranes are rolled in oven mesh sheets to ensure complete exposure to the antibody solution.

6 Passing cell lysates 5 times through a RNase-free 20-gauge needle works as well.

7 Random hexamer primer works as well.

8 If RNA concentration is below the amount required to get 1,4 µg in 10 µl, we use Microcon Ultracel YM-100 filters (Millipore) to up-concentrate the RNA.

9 A No-RT control reaction, lacking reverse transcriptase, is always used as a control for DNA removal. Using primer sets located within an exon sequence (ex: UBC) will give PCR amplification whenever DNA is present in this reaction.

10 If the same cDNA template is being analyzed for multiple genes, it is more efficient to add primers separately. Mix the other components of the master reaction mix in the desired magnitude (number of paralleles multiplied with number of genes being analyzed) Apply 1 µl of primer mix to the well intended for its respective genes. Then add 24 µl of the reaction mix to the wells.

11 We use qBase v1.3.5 to calculate relative expression levels with 2-3 housekeeping genes (Hellemans *et al.*, 2007).

12 There is not one single housekeeping gene suitable for all experiments. It is recommended to test the consistency of expression of several housekeeping genes in your

own experiments. We have used the Human Endogenous Control Gene Panel (tataa Biocenter) to find the housekeeping genes most suitable for our experimental setup. We always use 2-4 different housekeeping genes in each real-time PCR experiment.

5 Reference List

Breen,K.C. and Anderton,B.H. (1991). Temporal expression of neurofilament polypeptides in differentiating neuroblastoma cells. Neuroreport *2*, 21-24.

Breit,S. and Schwab,M. (1989). Suppression of MYC by high expression of NMYC in human neuroblastoma cells. J. Neurosci. Res. *24*, 21-28.

Hellemans,J., Mortier,G., De,P.A., Speleman,F., and Vandesompele,J. (2007). qBase relative quantification framework and software for management and automated analysis of real-time quantitative PCR data. Genome Biol. *8*, R19.

Henriksen,J.R., Lokke,C., Hammero,M., Geerts,D., Versteeg,R., Flaegstad,T., and Einvik,C. (2007). Comparison of RNAi efficiency mediated by tetracycline-responsive H1 and U6 promoter variants in mammalian cell lines. Nucleic Acids Res. *35*, e67.

Hsu,W.M. *et al.* (2005). Calreticulin expression in neuroblastoma--a novel independent prognostic factor. Ann. Oncol. *16*, 314-321.

Jalava,A., Heikkila,J., Lintunen,M., Akerman,K., and Pahlman,S. (1992). Staurosporine induces a neuronal phenotype in SH-SY5Y human neuroblastoma cells that resembles that induced by the phorbol ester 12-O-tetradecanoyl phorbol-13 acetate (TPA). FEBS Lett. *300*, 114-118.

Jogi,A., Vallon-Christersson,J., Holmquist,L., Axelson,H., Borg,A., and Pahlman,S. (2004). Human neuroblastoma cells exposed to hypoxia: induction of genes associated with growth, survival, and aggressive behavior. Exp. Cell Res. *295*, 469-487.

Johnson,R.J., Liu,N., Shanmugaratnam,J., and Fine,R.E. (1998). Increased calreticulin stability in differentiated NG-108-15 cells correlates with resistance to apoptosis induced by antisense treatment. Brain Res. Mol. Brain Res. *53*, 104-111.

Li,W. and Cha,L. (2007). Predicting siRNA efficiency. Cell Mol. Life Sci. *64*, 1785-1792.

Obbard,D.J., Gordon,K.H., Buck,A.H., and Jiggins,F.M. (2008). Review. The evolution of RNAi as a defence against viruses and transposable elements. Philos. Trans. R. Soc. Lond B Biol. Sci.

Paddison,P.J., Caudy,A.A., Bernstein,E., Hannon,G.J., and Conklin,D.S. (2002). Short hairpin RNAs (shRNAs) induce sequence-specific silencing in mammalian cells. Genes Dev. *16*, 948-958.

Paddison,P.J., Caudy,A.A., Sachidanandam,R., and Hannon,G.J. (2004). Short hairpin activated gene silencing in mammalian cells. Methods Mol. Biol. *265*, 85-100.

Scherr,M. and Eder,M. (2007). Gene silencing by small regulatory RNAs in mammalian cells. Cell Cycle *6*, 444-449.

Shrivastava,N. and Srivastava,A. (2008). RNA interference: an emerging generation of biologicals. Biotechnol. J. *3*, 339-353.

Walchli,S. and Sioud,M. (2008). Vector-based delivery of siRNAs: in vitro and in vivo challenges. Front Biosci. *13*, 3488-3493.

Wang,L. and Mu,F.Y. (2004). A Web-based design center for vector-based siRNA and siRNA cassette. Bioinformatics. *20*, 1818-1820.

Wang,Q.Z., Lv,Y.H., Diao,Y., and Xu,R. (2008). The design of vectors for RNAi delivery system. Curr. Pharm. Des *14*, 1327-1340.

Watts,J.K., Deleavey,G.F., and Damha,M.J. (2008). Chemically modified siRNA: tools and applications. Drug Discov. Today *13*, 842-855.

Westermann,F. *et al.* (2008). Distinct transcriptional MYCN/c-MYC activities are associated with spontaneous regression or malignant progression in neuroblastomas. Genome Biol. *9*, R150.

Yi,R., Qin,Y., Macara,I.G., and Cullen,B.R. (2003). Exportin-5 mediates the nuclear export of pre-microRNAs and short hairpin RNAs. Genes Dev. *17*, 3011-3016.

Legends to figures:

Figure 1. A. Schematic representation of MYCN cDNA. Exons are shown as grey arrows. Localization of antiMYCN shRNA target-sites are indicated by black arrowheads. **B.** Sequence and secondary structure representation of antiMYCN-887 (aMN-887) shRNA.

Figure 2. Western immunoblotting analysis of MYCN in antiMYCN shRNA transfected SK-N-BE(2) cells. Knockdown effects from 4 different antiMYCN shRNAs (aMN-27, aMN-760, aMN-887 and aMN-1291) were compared. aMN-887 is the most efficient antiMYCN shRNA.

Figure 3. Real-time RT-PCR analysis of MYCN (**A**) and c-myc (**B**) mRNA levels in shRNA transfected SK-N-BE(2) cells. Knockdown effects from 4 different antiMYCN shRNAs (aMN-27, aMN-760, aMN-887 and aMN-1291) were compared. aMN-887 is the most efficient antiMYCN shRNA, showing approximately 70 % reduction in MYCN mRNA compared to the scrambled control (SCR). A close reverse correlation is observed between MYCN mRNA and c-MYC mRNA expression levels.

Figure 4. Real-time RT-PCR analysis of known neuronal differentiation markers, neuropeptid Y, neurofilament L, chromogranin B and calreticulin, in shRNA transfected SK-N-BE(2) cells. All markers show increased expression when transfected with an antiMYCN shRNA (aMN-887) compared to a scrambled control shRNA (SCR).

A

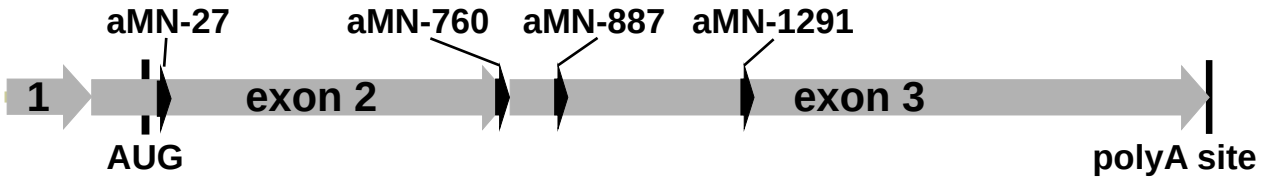

MYCN cDNA (NM005378)

B

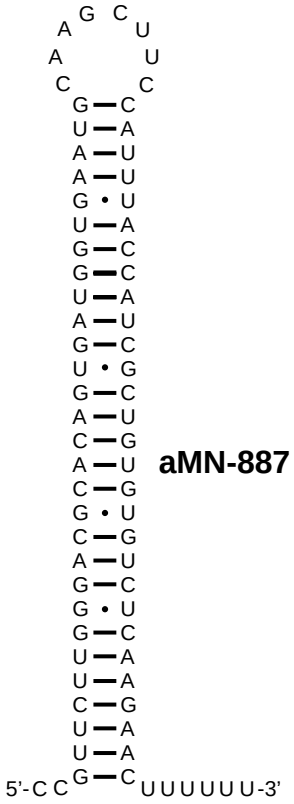

figure 1

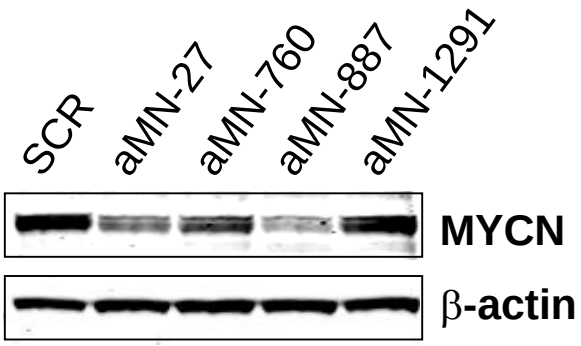

figure 2

A

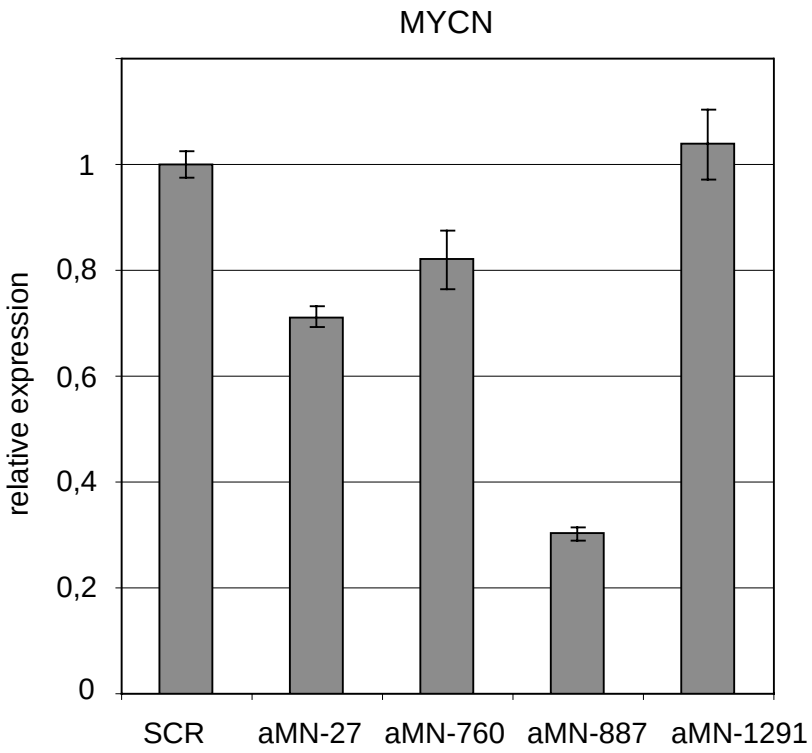
MYCN
relative expression
1
0,8
0,6
0,4
0,2
0
SCR
aMN-27
aMN-760
aMN-887
aMN-1291

B

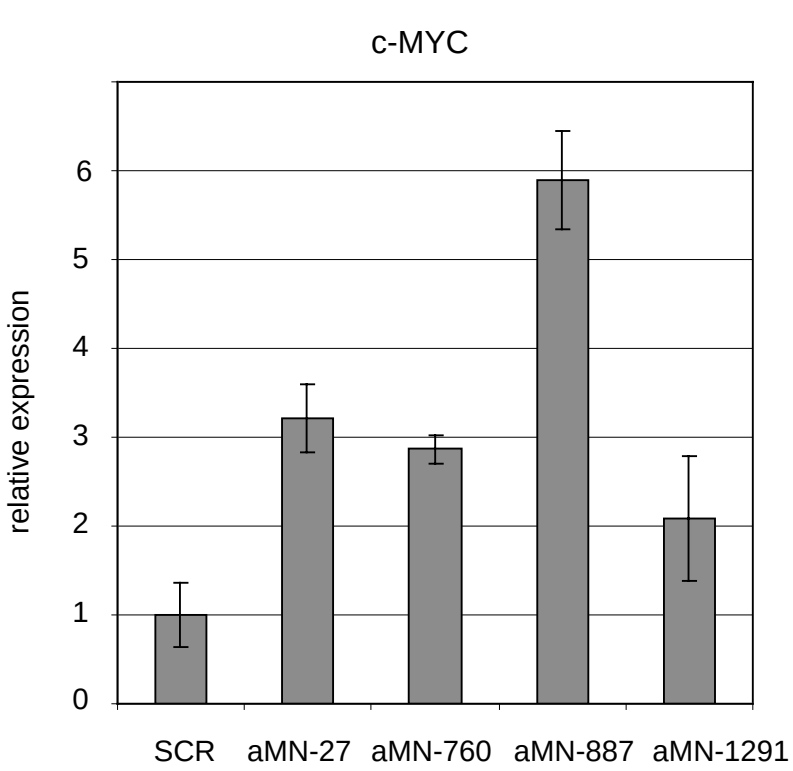
c-MYC
relative expression
6
5
4
3
2
1
0
SCR
aMN-27
aMN-760
aMN-887
aMN-1291

figure 3

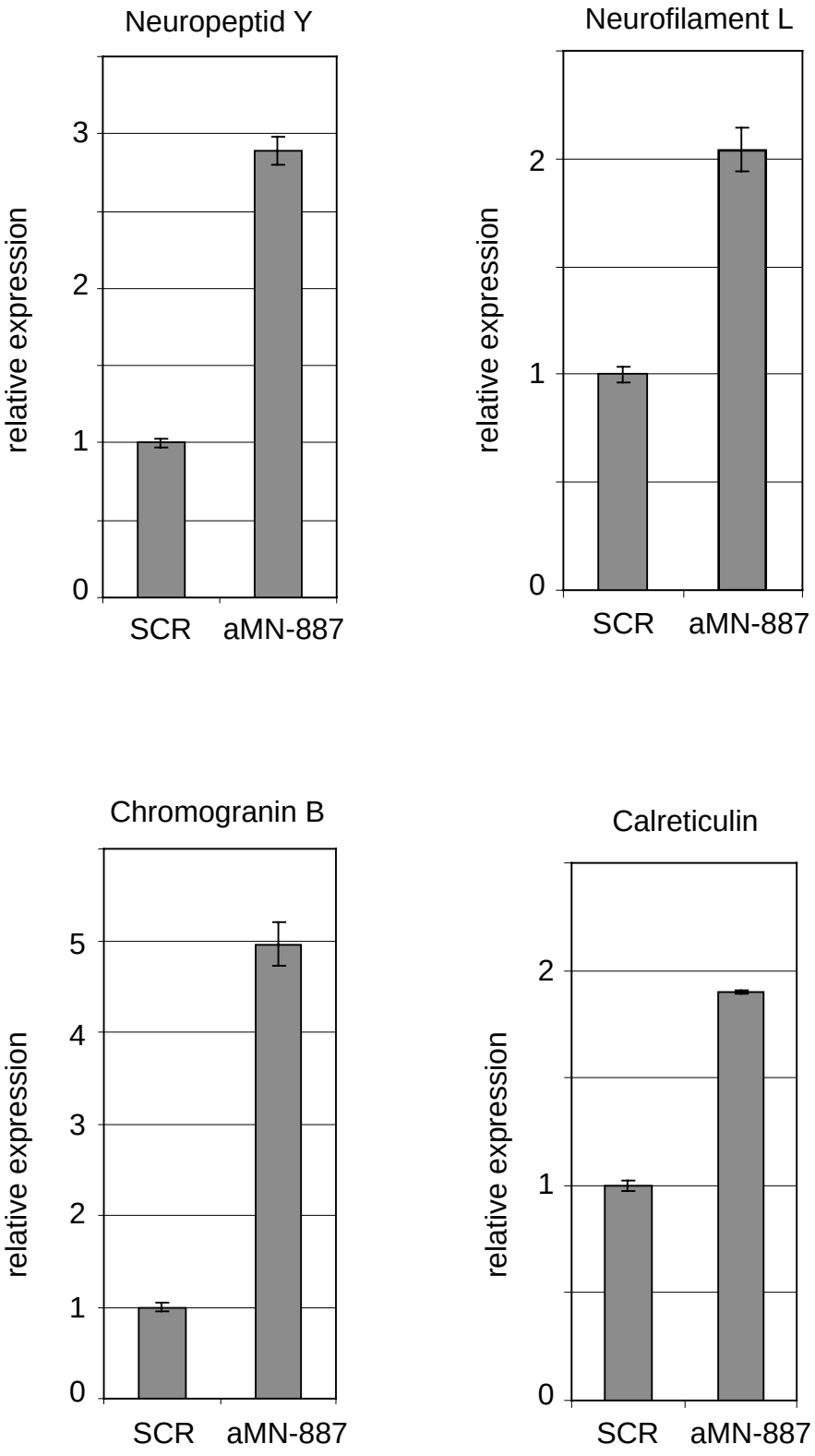
Neuropeptid Y
relative expression
0
1
2
3
SCR
aMN-887
Neurofilament L
relative expression
0
1
2
SCR
aMN-887
Chromogranin B
relative expression
0
1
2
3
4
5
SCR
aMN-887
Calreticulin
relative expression
0
1
2
SCR
aMN-887

figure 4

ISBN 978-82-7589-285-8
Print: Tromsprodukt • 40 00 72 00